Fracture toughness investigation of an indigenous limestone rock formation.

Khaqan Khan

Civil Engineering

April 1998

Abstract

Hydrofracturing is a well known technique used to create fractures in a rock formation in order to enhance the oil or gas recovery from a reservoir of low permeability. Results of various analytical appraoches to understand this technique are very sensitive to the fracture toughness of the rock material. Fracture toughness is a strength parameter in terms of ease of initiation and propagation of a preexisting rack subjected to some externally applied stress field. Due to high cost involved in field scale testing, laboratory based testing under reservoir simulated conditions of temperature and pressure using small core specimens remains the only alternative to have a representative value of fracture toughness of a rock formation. Nevertheless, poor quality in some cases and most of the time limited amount of core based specimens from a deep-seated formation still remains a big hurdle in a comprehensive experimental investigation. However, the problem could be addressed if the outcrop specimens, instead of reservoir, from the same geological formation could be used for fracture toughness investigation.

An experimental fracture toughness investigation was carried out using specimens collected from Khuff formation in the Ghawar region, the largest oilfield in the world producing oil and gas from multi-reservoir zones. The study was focused on reservoir specimens formm a depth of 3.5 km as well as form outcrop under both ambient and reservoir simulated temperature and pressure. Notched Brazilian disk specimens under diametral compression and notched semicircular disk and circular rod specimens under three point bending were used for this purpose.

The results reveal that outcrop specimens can be successfully used to predict the fracture behavior at in-situ conditions. Furthermore, the effect of confining pressure on fracture toughness was more pronounced than the temperature. The fracture toughness showed an increase of 100 to 250% over the ambient value under effective reservoir confining pressure of 28 Mpa (4000 psi); whereas an increase of only 20 to 50% under reservoir temperature of 116 oC was observed. Experimental results were in good agreement with the theoretical fracture criterion based on maximum tangential stress. Moreover, it was observed that the experimental crack propagation trajectories follow a path which is high in tensile stresses.

Fracture Toughness Investigation of an Indigenous Limestone Rock Formation

by

Khaqan Khan

A Thesis Presented to the

FACULTY OF THE COLLEGE OF GRADUATE STUDIES

KING FAHD UNIVERSITY OF PETROLEUM & MINERALS

DHAHRAN, SAUDI ARABIA

In Partial Fulfillment of the
Requirements for the Degree of

MASTER OF SCIENCE

In

CIVIL ENGINEERING

April, 1998

INFORMATION TO USERS

This manuscript has been reproduced from the microfilm master. UMI films the text directly from the original or copy submitted. Thus, some thesis and dissertation copies are in typewriter face, while others may be from any type of computer printer.

The quality of this reproduction is dependent upon the quality of the copy submitted. Broken or indistinct print, colored or poor quality illustrations and photographs, print bleedthrough, substandard margins, and improper alignment can adversely affect reproduction.

In the unlikely event that the author did not send UMI a complete manuscript and there are missing pages, these will be noted. Also, if unauthorized copyright material had to be removed, a note will indicate the deletion.

Oversize materials (e.g., maps, drawings, charts) are reproduced by sectioning the original, beginning at the upper left-hand corner and continuing from left to right in equal sections with small overlaps. Each original is also photographed in one exposure and is included in reduced form at the back of the book.

Photographs included in the original manuscript have been reproduced xerographically in this copy. Higher quality 6" x 9" black and white photographic prints are available for any photographs or illustrations appearing in this copy for an additional charge. Contact UMI directly to order.

UMI

A Bell & Howell Information Company
300 North Zeeb Road, Ann Arbor MI 48106-1346 USA
313/761-4700 800/521-0600

FRACTURE TOUGHNESS INVESTIGATION OF AN INDIGENOUS LIMESTONE ROCK FORMATION

BY

KHAQAN KHAN

A Thesis Presented to the

FACULTY OF THE COLLEGE OF GRADUATE STUDIES

KING FAHD UNIVERSITY OF PETROLEUM & MINERALS

DHAHRAN, SAUDI ARABIA

In Partial Fulfillment of the
Requirements for the Degree of

MASTER OF SCIENCE

In

CIVIL ENGINEERING

APRIL, 1998

UMI
300 North Zeeb Road
Ann Arbor, MI 48103

بسم الله الرحمن الرحيم

KING FAHD UNIVERSITY OF PETROLEUM AND MINERALS
DHAHARAN, SAUDI ARABIA

COLLEGE OF GRADUATE STUDIES

This Thesis, written by

Khaqan Khan

under the direction of his Thesis Advisor, and approved by his Thesis Committee, has been presented and accepted by the Dean of the College of Graduate Studies, in partial fulfillment of the requirements for the degree of

Master of Science in Civil Engineering (Geotechnical)

Thesis Committee

Dr. Naser Al-Shayea (Chairman)

Dr. S.N. Abduljauwad (Co-Chairman)

Dr. Abdulazeez Abduraheem (Member)

Dr. Saad A. Aiban (Member)

Dr. Omar S.B. Al-Amoudi (Member)

Dr. S.N. Abduljauwad
Chairman, Dept. of Civil Engineering

Dr. Abdallah M. Al-Shehri
Dean, College of Graduate Studies

2/6/98
Dated

This Humble work is Dedicated to:

My Parents and Brothers

Acknowledgments

All praise and thanks be to Allah, the Most Gracious, the Most merciful; and peace be upon His Prophet.

I pay my sincere gratitude to my thesis advisor Dr. Naser Al-Shayea for his valuable guidance, support and encouragement throughout this research work. I highly acknowledge the cooperation, encouragement and useful suggestions from thesis co-advisor Dr. Sahel N. Abduljauwad and thesis committee members Dr. Abdulazeez Abduraheem, Dr. Saad A. Aiban, and Dr. Omar S.B. Al-Amoudi.

I am highly thankful to Petroleum Engineering Section of the Research Institute for providing rock material as well as financial and technical support for this research work. My special thanks are due to Mr. Hassan Zakariya, the technician in the geotechnical lab of the Civil Engineering Department, for designing the experimental setup and solving many technical problems during the experimental work of my thesis. I am grateful to all those who helped me during the course of this research work including the faculty and staff members of the Dept. of Civil Engineering and people in the central research workshop.

Last, but not the least, I extend my thanks to all my family members for their moral support, patience, encouragement, and prayers throughout my studies. I wish to express my thanks to my friends Shahid Azam, Rashid, Imtiaz, Saleem, Shareef, and Rizwan for their encouragement. I thank all those who were actively involved in arranging cricket on regular basis which made my stay at KFUPM enjoyable.

Contents

Acknowledgments i

List of Tables vi

List of Figures vii

Abstract (English) xiii

Abstract (Arabic) xiv

Chapter 1 Introduction

1.1 Problem Definition 2

1.2 Objectives 4

1.3 Thesis Organization 5

Chapter 2 Literature Review

2.1 General 6

2.2 Fracture Mechanics 9

2.3 Linear Elastic Fracture Mechanics (LEFM) 10

2.4 Stress Distribution At A Crack Tip 11

2.4.1 Mode-I 14

2.4.2 Mode-II 15

2.4.3 Mode-III 15

2.4.4 Mixed Mode 16

2.5 Failure Theories 18

2.5.1 Maximum Stress ($\sigma_{\theta max}$) Criterion 19

2.5.2 Minimum Strain Energy Density (S_{min}) Criterion 19

2.5.3 Maximum Energy Release (G_{max}) Criterion 20

Chapter 3 Background

3.1 Fracture Toughness Testing 22
3.1.1 Mode-I Testing Technique 22
3.1.2 Mixed-Mode I-II Testing Techniques 25
3.1.2.1 Notched Brazilian Disk Specimen 25
3.1.2.2 Stress Distribution in Uncracked Brazilian Disk 28
3.1.2.3 Stress Intensity Factor for Notched Brazilian Disk 33
3.1.2.4 Notched Semicircular Disk Specimen 37
3.2 Factors Affecting Fracture Toughness 41
3.2.1 Scale Effect 41
3.2.2 Fracture Process Zone (FPZ) 43
3.2.3 Specimen size 46
3.2.4 Confining Pressure 47
3.2.5 Temperature 49
3.3 Crack Propagation 50
3.4 Fracture Toughness Envelope 53
3.5 Indirect Tensile Strength Testing 55
3.6 Mineralogical Composition 55
3.7 Fractured Surface Study 57

Chapter 4 Experimental Program

4.1 Geology and Material Description 60
4.2 Mineralogical Composition 63
4.3 Selection of the Specimen Shape 63
4.4 Sample Preparation 64
4.5 Notches 68
4.5.1 Straight Notch 71
4.5.2 Chevron Notch 71

4.6 Fracture Toughness Testing under Ambient Conditions 75
4.6.1 Testing Equipment 75
4.6.2 Crack Extensometers 76
4.6.3 Mode -I Fracture Toughness Testing 78
4.6.4 Mixed Mode I-II Fracture Toughness Testing 78
4.6.4.1 Notched Brazilian Disk Specimens 80
4.6.4.2 Notched Semicircular Disk Specimens 80
4.7 Fracture Toughness Testing under *In-situ* Conditions 82
4.7.1 Simulation of *In-situ* Confining Pressure 84
4.7.1.1 Mode-I Fracture Toughness Testing 88
4.7.1.2 Mixed Mode I-II Fracture Toughness Testing 88
4.7.2 Simulation of *In-situ* Temperature Condition 89
4.7.2.1 Mode-I Fracture Toughness Testing 91
4.7.3 Mixed Mode I-II Fracture Toughness Testing 91
4.8 Indirect Tensile Strength 91
4.9 Microscopic Studies 92

Chapter 5 Results and Discussions

5.1 XRD Results 94
5.2 Indirect Tensile Strength 94
5.3 Fracture Toughness Results 94
5.3.1 Ambient Conditions 99
5.3.1.1 Mode-I Results 99
5.3.1.2 Mixed Mode I-II Results 113
5.3.2 *In-situ* Conditions 135
5.3.2.1 Effect of Confining Pressure 135
5.3.2.2 Effect of Temperature 159
5.4 Crack Opening 165
5.5 Crack Propagation 171

5.5.1 Crack Initiation Point and Angle 171
5.5.2 Crack Propagation Path 175
5.6 Fracture Toughness Envelope 181
5.7 SEM Results of Fractured Surfaces 186

Chapter 6 Summary, Conclusions and Recommendations

6.1 Summary 193
6.2 Conclusions 195
6.3 Recommendations 197

Nomenclature 199

References 201

Vita 209

List of Tables

Table 3.1: A comparison of Minimum Crack Length (a_m) for Valid Fracture Toughness Testing [after Lim *et al.*, 1994-c] 48

Table 4.1: Summary of Specimen Dimensions Used in This Study. 70

Table 5.1: Summary of Results for the Tensile Strength of Outcrop and Reservoir Specimens 98

Table 5.2: Table 5.2: Summary of Results for the Effect of Strain Rate on Mode-I Fracture Toughness. 102

Table 5.3: Summary of Results for the Effect of Notch Length on Mode-I Fracture Toughness. 105

Table 5.4 Summary of Results for the Effect of Specimen Thickness on Mode-I Fracture Toughness. 109

Table 5.5 Table 5.5: Summary of Results for the Effect of Specimen Diameter on Mixed Mode I-II Fracture Toughness 115

Table 5.6: Summary of Results for the Effect of Notch Length on Mixed Mode I-II Fracture Toughness. 119

Table 5.7: Table 5.7: Summary of the Results for the Effect of Notch Type on Mixed Mode I-II Fracture Toughness. 122

Table 5.8: Summary of Mixed Mode I-II Fracture Toughness Results for Semicircular Specimens 127

Table 5.9: Summary of Mixed Mode I-II Fracture Toughness Results for Reservoir Specimens at Ambient Conditions 130

Table 5.10: Summary of Mixed Mode Fracture Toughness Results for Outcrop Specimens at Ambient and under Confining Pressure: 146

Table 5.11: Table 5.11: Summary of Mixed mode I-II Fracture Toughness Results for Reservoir Specimens under Reservoir Confining Pressure of 28 MPa. 151

List of Figures

Figure 2.1: Basic Crack Extension Modes, [after Twiss and Moores, 1992]. 7

Figure 2.2: Representation of the Fracture Process Zone [after Whittaker *et al.*, 1`992]. 12

Figure 2.3: Stress State at a Crack Tip Expressed in Polar Coordinates [after Ashmavi, 1990]. 13

Figure 2.4: An Inclined Crack Subjected to Tension [after Whittaker *et al.*, 1992]. 17

Figure 3.1: Single-Edge Cracked Round Bar Bend (SECRBB) Specimen [after Ouchterlony, 1981].. 24

Figure 3.2: Notched Brazilian Disk Specimens: (a) Loading Fixture, (b) Section A-A for the Straight Notch, (c) Section A-A for the Chevron Notch [after Fowell and Xu, 1994]..... 26

Figure 3.3: Uncracked Brazilian Disk Specimen under Diametral Compression..... 29

Figure 3.4: Figure 3.4: Normalized Stresses in a Uncracked Brazilian Disk under Diametral Compression: (a) Tangential Stresses, (b) Shear Stresses, (c) Radial Dresses..... 32

Figure 3.5: Variation of Normalized Coefficients N_I and N_{II} for a Notched Brazilian Disk..... 36

Figure 3.6: Semicircular Disk Specimen under Three Point Bending [after Lim *et al.*, 1994-c]..... 38

Figure 3.7: Variation of Normalized Stress Intensity Factor for a Semicircular Specimen [after Lim *et al.*, 1994-c]..... 40

Figure 3.8: Normalized Intensity Factor for a Semicircular Specimen Used in the Present Study..... 42

Figure 3.9: Fracture Process Zone for a Typical Rock [after Whittaker *et al.*, 1992]. 44

Figure 3.10: Variation of Crack Initiation Angle with Crack Inclination Angle for Specimens Subjected to Compressive Loads [after Tirosh and Catz, 1981]..... 52

Figure 4.1: Summary of Various Laboratory Tests Used in the Present Study..... 59

Figure 4.2: Vicinity Map of the Samples Collection Area. 61

Figure 4.3: A Trend of Sedimentary Rock Formation Showing Outcrop and Deep-seated Rocks in the Same Formation. 62

Figure 4.4: Rock Anchoring Mechanism with the Coring Machine Fixed Above. 66

Figure 4.5: Sliced Disk and Circular Rod Specimens. 67

Figure 4.6: Leveled Disks Ready to be Notched. 69

Figure 4.7: Wire Saw Used for Making Straight-edge Notches in Rock Specimens 72

Figure 4.8: Notched Disks: (a) Brazilian Disks, (b) Semicircular Disks. 73

Figure 4.9: Slow Speed Circular Saw Used for Making Chevron Notches in Rock Specimens. 74

Figure 4.10: Crack Extension Measurement Assembly. 77

Figure 4.11: A Schematic of the Experimental Setup used for Mode-I Fracture Toughness Testing. 79

Figure 4.12: (a) A Schematic of the Notched Brazilian Disk Testing Setup, (b) Crack Extensometer Attached with the Disk. 81

Figure 4.13: (a) A Schematic of the Semicircular Disk Testing Setup under Three Point Bend Loading Configuration, (b) Crack Extensometer Attachment. 83

Figure 4.14: A Schematic of the Triaxial Cell used for the Testing under Simulated *In-situ* Confining Pressure 85

Figure 4.15: Specimen Fixed to the Base of Triaxial Cell for Testing under Confining pressure. 86

Figure 4.16: Equipment Used to Apply Confining Pressure. 87

Figure 4.17: A Schematic of the Setup used for Simulating the *In-situ* Temperature Condition 90

Figure 5.1: Mineralogical Analysis for a Outcrop Specimen. 95

Figure 5.2: Mineralogical Analysis for a Reservoir Specimen from Lithology A and B 96

Figure 5.3: (a) Mineralogical Analysis for a Reservoir Specimen from Lithology C; (b) Specimens Showing the presence of Anhydrite as an Impurity. 97

Figure 5.4: Load-Displacement Curves for Straight Notched Circular Rod Specimens under Mode-I Loading Condition for Different Strain Rates. 101

Figure 5.5: Effect of Strain Rate on Mode-I Fracture Toughness. 103

Figure 5.6: Effect of Notch Length on Mode-I Fracture Toughness. 106

Figure 5.7: Effect of Specimen Thickness on Mode-I Fracture Toughness. 110

Figure 5.8: Effect of Diameter on Mode-I Fracture Toughness 112

Figure 5.9: Effect of Specimen Diameter on Mixed Mode I-II Fracture Toughness for Straight Notched Brazilian Disks at Ambient Conditions. 116

Figure 5.10: Normalized Mode-I and Mode-II Fracture Toughness for Straight Notched Outcrop Brazilian Disk Specimens at Ambient Conditions. 117

Figure 5.11: Effect of Notch Length on Mixed Mode I-II Fracture Toughness for Straight Notched Brazilian Disk Specimens at Ambient Conditions. 120

Figure 5.12: Effect of Notch Length on Normalized Mode-I and Mode-II Fracture Toughness of Straight Notched Outcrop Brazilian Disk Specimens at Ambient Conditions..... 121

Figure 5.13: Comparison of Mixed Mode I-II Fracture Toughness for Straight and Chevron Notched Brazilian Disk Specimens at Ambient Conditions. 123

Figure 5.14: Normalized Mode-I and Mode-II Fracture Toughness of Straight and Chevron Notched Brazilian Disk Specimens at Ambient Conditions.. 125

Figure 5.15: Comparison of Mixed Mode I-II Fracture Toughness for Straight Notched Brazilian and Semicircular Disk Specimens at Ambient Conditions. 128

Figure 5.16: Mixed Mode I-II Fracture Toughness Variation for Straight Notched Reservoir Brazilian Disk Specimens at Ambient Conditions. 131

Figure 5.17: Comparison of Mixed Mode I-II Fracture toughness for Straight Notched Outcrop and Reservoir Brazilian Disk Specimens at Ambient Conditions. 133

Figure 5.18: Normalized Mixed Mode I-II Fracture Toughness Variation for Straight Notched Outcrop and Reservoir Specimens at Ambient Conditions. 134

Figure 5.19: Load-Displacement response of Straight Notched Brazilian Disk Specimens under Different Confining Pressures ($\beta = 0$). 137

Figure 5.20: Effect of Confining Pressure on Mode-I Fracture Toughness. 138

Figure 5.21: Effect of Confining Pressure on Mode-I Fracture Toughness for Reservoir Specimens. 139

Figure 5.22: Effect of Specimen Diameter of Mode-I Fracture Toughness at Ambient and under Confining Pressure Conditions for Straight Notched Brazilian Disks. 142

Figure 5.23: Load-Displacement Curves for Straight Notched Brazilian Disk Specimens for Mixed Mode I-II Loading under Confining Pressure. 143

Figure 5.24: Mixed Mode I-II Fracture Toughness Variation for Outcrop Straight Notched Brazilian Disk Specimens under Confining Pressure. 145

Figure 5.25: Comparison of Mixed Mode I-II Fracture Toughness Variation for Outcrop Straight Notched Brazilian Disk Specimens at Ambient and under Confining Pressure. 147

Figure 5.26: Effect of Specimen Size on Mixed Mode I-II Fracture Toughness for Straight Notched Brazilian Disks under Confining Pressure. 149

Figure 5.27: Mixed Mode I-II Fracture Toughness Variation for Straight Notched Reservoir Brazilian Disk Specimens under Confining Pressure. 150

Figure 5.28: Comparison of Mixed Mode I-II Fracture Toughness Variation for Straight Notched Reservoir Brazilian Disk Specimens at Ambient and under Confining Pressure 152

Figure 5.29: Comparison of Mixed Mode I-II Fracture Toughness Variation for Outcrop and Reservoir Straight Notched Brazilian Disk Specimens under Confining Pressure..... 154

Figure 5.30: Comparison of Normalized Mode-I Fracture Toughness for Outcrop and Reservoir Straight Notched Brazilian Disk Specimens under Confining Pressure..... 155

Figure 5.31: Comparison of Normalized Mode-II Fracture Toughness for Outcrop and Reservoir Straight Notched Brazilian Disk Specimens under Confining Pressure..... 156

Figure 5.32: Comparison of Normalized Mode-I Fracture Toughness at Ambient and under Confining Pressure for Straight Notched Outcrop and Reservoir Brazilian Disk Specimens. 157

Figure 5.33: Comparison of Normalized Mode-II Fracture Toughness at Ambient and under Confining Pressure for Straight Notched Outcrop and Reservoir Brazilian Disk Specimens. 158

Figure 5.34: Comparison of Load-Displacement Response of Straight Notched Brazilian Disk Specimens under Different Temperatures. 160

Figure 5.35: Effect of Temperature on Mode-I Fracture Toughness for Straight Notched Brazilian Disk Specimens. 161

Figure 5.36: Load-Displacement Curves for Straight Notched Brazilian Disk Specimens under Mixed Mode I-II Loading at Reservoir Temperature..... 163

Figure 5.37: Comparison of Mixed Mode I-II Fracture Toughness for Straight Notched Outcrop Brazilian Disk Specimens at Ambient and Reservoir Temperature Conditions..... 164

Figure 5.38: Comparison of Load-Displacement Response of Straight Notched Brazilian Disk Specimens at Ambient and Simulated Reservoir Temperature and Confining Pressure Conditions..... 166

Figure 5.39: Crack Extension in Mixed Mode I-II Loading for Straight Notched Brazilian Disk Specimens at Ambient Conditions. 167

Figure 5.40: Crack Extension in Mixed Mode I-II Loading for Straight Notched Semicircular Disk Specimens at Ambient Conditions. 169

Figure 5.41: Comparison of Maximum Crack Extension under Mixed Mode I-II Loading for Straight Notched Brazilian and Semicircular Disk Specimens at Ambient Conditions 170

Figure 5.42: Rock Specimens after Failure: (a) Notched Brazilian Disks, (b) Semicircular Disks..... 172

Figure 5.43: Variation of Crack Initiation Angle as a Function of Crack Inclination Angle under Mixed Mode I-II Loading for Straight Notched Brazilian Disk Specimens..... 174

Figure 5.44: Experimental Failure Trajectories for Straight Notched Brazilian Disk Specimens under Mixed Mode I-II Loading. 176

Figure 5.45: Combined Failure Trajectories for Straight Notched Brazilian Disk Specimens under Mixed Mode I-II Loading..... 177

Figure 5.46: Failure Trajectories Superimposed on Normalized Tangential Stress Contours..... 178

Figure 5.47: Failure Trajectories Superimposed on Normalized Shear Stress Contours..... 180

Figure 5.48:Comparison of Mixed Mode I-II Fracture Toughness Results for Notched Brazilian Disk Specimens With Theoretical Fracture Toughness Envelopes..... 182

Figure 5.49: Proposed Mixed Mode I-II Fracture Toughness Envelope for Notched Brazilian Disk Specimens for Positive Fracture Toughness Values..... 184

Figure 5.50: A Comparison of Mixed Mode I-II Fracture Toughness Envelope under Different Testing Conditions for Notched Outcrop and Reservoir Brazilian Disk Specimens. 185

Figure 5.51: Mixed Mode I-II Fracture Toughness Envelope for Notched Outcrop and Reservoir Brazilian Disk Specimens at Ambient Conditions. 187

Figure 5.52: Mixed Mode I-II Fracture Toughness Envelope for Notched Outcrop and Reservoir Brazilian Disk Specimens under Reservoir Confining Pressure..... 188

Figure 5.53: Scanning Electron Microscopic (SEM) Image of the Fractured Surface for Specimens Tested at (a) $\beta = 0^\circ$, (b) $\beta = 15^\circ$..... 190

Figure 5.54: Scanning Electron Microscopic (SEM) Image of the Fractured Surface for Specimens Tested at (a) $\beta = 30^\circ$, (b) $\beta = 45^\circ$..... 191

Figure 5.55: Scanning Electron Microscopic (SEM) Image of Fractured Surface for Specimens Tested at (a) $\beta = 60^\circ$, (b) $\beta = 75^\circ$..... 192

Abstract

Name: **Khaqan Khan**
Title: **Fracture Toughness Investigation of an Indigenous Limestone Rock Formation**
Major Field: **Civil Engineering (Geotechnical)**
Date of Degree: **April 1998**

Hydrofracturing is a well known technique used to create fractures in a rock formation in order to enhance the oil or gas recovery from a reservoir of low permeability. Results of various analytical approaches to understand this technique are very sensitive to the fracture toughness of the rock material. Fracture toughness is a strength parameter in terms of ease of initiation and propagation of a preexisting crack subjected to some externally applied stress field. Due to high cost involved in field scale testing, laboratory based testing under reservoir simulated conditions of temperature and pressure using small core specimens remains the only alternative to have a representative value of fracture toughness of a rock formation. Nevertheless, poor quality in some cases and most of the time limited amount of core based specimens from a deep-seated formation still remains a big hurdle in a comprehensive experimental investigation. However, the problem could be addressed if the outcrop specimens, instead of reservoir, from the same geological formation could be used for fracture toughness investigation.

An experimental fracture toughness investigation was carried out using specimens collected from Khuff formation in the Ghawar region, the largest oilfield in the world producing oil and gas from multi-reservoir zones. The study was focused on reservoir specimens form a depth of 3.5 km as well as form outcrop under both ambient and reservoir simulated temperature and pressure. Notched Brazilian disk specimens under diametral compression and notched semicircular disk and circular rod specimens under three point bending were used for this purpose.

The results reveal that outcrop specimens can be successfully used to predict the fracture behavior at *in-situ* conditions. Furthermore, the effect of confining pressure on fracture toughness was more pronounced than the temperature. The fracture toughness showed an increase of 100 to 250% over the ambient value under effective reservoir confining pressure of 28 MPa (4000 psi); whereas an increase of only 20 to 50% under reservoir temperature of 116 °C was observed. Experimental results were in good agreement with the theoretical fracture criterion based on maximum tangential stress. Moreover, it was observed that the experimental crack propagation trajectories follow a path which is high in tensile stresses.

Master of Science Degree
Department of Civil Engineering
King Fahd University of Petroleum and Minerals
Dhahran, Saudi Arabia
April 1998

الخلاصة

إسم الطالب: خاقان خان

عنوان الدراسة: دراسة عسر التفتيت لصخور من التكوينات الجيرية المحلية

التخصص: هندسة المدنية

تاريخ الشهادة: أبريل ١٩٩٨م

إشتهر إستعمال تقنية التفتيت الهيدروليكي لإحداث تشققات في التكوينات الصخرية وذلك لتعزيز إستخراج الزيت والغاز من المكامن ذات النفاذية المتدنية. نتائج الدراسات التحليلية لفهم هذه التقنية تتأثر جداً بقيمة معامل عسر التفتيت للمواد الصخرية. معامل عسر التفتيت هو عبارة عن معيار لقياس سهولة إبتداء وإنتشار الشقوق الموجـــودة في المادة الصخرية عندما تتعرض لضغوط خارجية. وبسبب التكاليف الباهضة للتجارب الحقلية، تبقى الإختبارات المعملية لعينات من الصخور هي الخيار الوحيد لإيجاد قيمة صحيحة لمعامل عسر التفتيت لأي تكوين صخري، بشرط أن تُعمل هذه الإختبارات تحت ضغط ودرجة حرارة تحاكيان ما هو موجود في المكمن. وأيضاً فإن عدم جودة عينات الصخـــور المستخرجة من المكمن ومحدودية كميتها، تشكلان عقبات في طريق الدراسة المعملية الشاملة. لكن هذه المشكلة يمكـــن حلها، وذلك بإستخدام عينات من الصخور النائتة فوق سطح الأرض لنفس التكوين بدلا من صخور المكمن، وذلـــك لدراسة معامل عسر التفتيت.

لقد عملت دراسة معملية لإيجاد عسر التفتيت بإستخدام عينات من تكوين "خف" في منطقة "الغوار" الذي يعتبر أكـــبر حقل في العالم لإنتاج البترول والغاز وذلك من مكمن متعدد المناطق. ركزت هذه الدراسة على عينات مـــن المكمـــن اخذت من عمق ٣,٥ كم وكذلك على عينات من نتوءات التكوين نفسه، إختبرت تحت الظروف العاديـــة وكذلـــك تحت الظروف الحرارية والضغطية للمكمن نفسه. لهذا الغرض إستخدمت الأشكال التالية للعينات: القـــرص الـــبرازيلي المحزوز تحت الضغط القطري، والقضيب الدائري تحت الثني بواسطة ثلاث نقاط تحميل.

من الممكن إستخدام نتائج الدراسة على عينات من الصخور النائتة فوق سطح الأرض للتنبؤ بسلوك التفتيت للصخـــــر تحت ظروف المكمن. تأثير الضغط المحيط على معامل عسر التفتيت أكبر من تأثير الحرارة. فمعامل عسر التفتيت تحـــت ضغط المكمن المقدر بـــ ٤٠٠٠ باوند/بوصة مربعة (٢٨ مليون باسكال) زاد بمقدار ١٠٠ إلى ٢٥٠ % عنـــه تحـــت الظروف العادية، بينما زاد معامل عسر التفتيت تحت الظروف الحرارية للمكمن المقدر بـــ ١١٦ درجة مئوية بمقـــدار ٢٠ إلى ٥٠ % فقط عنه تحت الظروف العادية. وبمقارنة نتائج التجارب المعملية بمعايير نظريات التفتيت، وجد تقارب كبير خاصة مع معيار الضغط المماسي الأكبر. كما لوحظ أن مسار إنتشار الشق في العينات المخبرية يتبع طريقا يكـــون فيه الشد كبيرا.

درجة الماجستير في العلوم الهندسية

جامعة الملك فهد للبترول والمعادن

الظهران - المملكة العربية السعودية

أبريل ١٩٩٨م

Chapter 1

Introduction

Fracture toughness, an intrinsic material property, is measured by the *Stress Intensity Factor* (SIF). The stress intensity factor is a measure of the energy required to create a new surface in a material containing a crack and subjected to an externally applied stress field. Due to the presence of crack, stress concentrates at the crack tip. The magnitude of this concentrated stress is much higher than the externally applied stress depending upon the degree of the sharpness of crack tip. Fracture is presumed to initiate when the stress intensity in the region of a crack tip is greater than or equal to the critical value known as the critical stress intensity factor of the material . The fracture will continue to propagate until the local stress intensity becomes equal to or less than the critical SIF value [Guo *et al.*, 1993].

Fracture properties of rocks are determined by their fracture toughness, which is actually a measure of the resistance of rock against crack initiation and propagation. For isotropic materials under a given loading system, failure initiates when the stress intensity factor reaches its critical value. However, for anisotropic materials, the fracture toughness is not a uniform material property; rather it depends on the crack orientation with respect to the layers or bedding planes.

Understanding the fracture mechanism of rocks is considered a fundamental tool for solving many rock mechanics problems. The subject has got its applications in a variety of fields dealing with rocks directly or indirectly; for example, tunnel boring and excavation, hydraulic fracturing, explosive fracturing, fragmentation control, etc. Some of these applications are further utilized to study certain rock behaviors or characteristics. A good example of these applications is the hydraulic fracturing which is not only used to enhance the oil recovery from a reservoir, but also the determination of *in-situ* stresses in a rock mass [Hefny *et al.*, 1992]. The determination of *in-situ* stresses in a rock formation is considered an important parameter for designing underground structures made for different purposes.

In recent years, the disposal of hazardous and radioactive waste in underground cavities in rocks has become a common practice in many parts of the developed world. Ground water flow and contaminant transport in fractured media is a field which also requires the knowledge of rock fracture behavior.

1.1 Problem Definition

As far as the Kingdom of Saudi Arabia is concerned, most of the research work done in the area of geotechnical engineering, has been dealt with the characterization and the determination of solutions of problems related to different soils types. However, large extent of the surface and subsurface formation in the Arabian Peninsula is composed of rocks. These rocks need to be characterized and classified according to their strength. Rock strength determination will be a valuable information not only for the expanding petroleum industry in the Kingdom, but will also open a new research area which has not

yet been explored. Moreover, it is equally important for many other civil engineering applications, such as designing and construction of tunnels, rock excavation, power stations, rock slopes, foundations on rocks, and subsurface structures.

To enhance the oil or gas from a reservoir of low permeability, deliberately cracks or fractures are created in the rock formation by a well known technique called "Hydrofracturing". In this technique, a high pressurized fluid is injected in the formation which creates fractures by mobilizing the fracture strength of the rock material present therein. Therefore, fracture toughness study of the rock formation becomes very important for designing various aspects of a hydrofracturing process.

Due to the fact that field-scale testing is very expensive, studying fracture toughness behavior of a rock formation in a laboratory using small core based specimens remains the only alternative to have a representative value of the fracture toughness. Nevertheless, obtaining samples from deep-seated rock formations via boreholes is not only very expensive but also requires extreme care in sample handling which makes the process very slow and tedious. Moreover, the quality of collected samples is also questionable in some cases. However, this problem could be partially resolved by considering outcrop specimens having the same composition as that of the reservoir rock mass (i.e. from the same lithology of the geologic formation). By studying the behavior of outcrop specimens and comparing the results with those obtained from the reservoir, a correlation between the two results can be obtained.

Since there is a lack of information on this issue, therefore, this research program is focused on the determination of fracture toughness for both outcrop and reservoir specimens, and to envisage if the outcrop specimens could be a successful candidate to

represent the fracture toughness of deep-seated rocks. Samples from both outcrop and reservoir of a limestone formation are studied for its fracture toughness behavior. Moreover, fracture toughness and fracture propagation and their dependence on the physical parameters such as temperature and confining pressure are investigated.

1.2 Objectives

The literature search indicates that most of the work concerning the fracture toughness determination of limestone has been devoted to mode-I loading condition (failure in pure tension). Little attention is often paid to the mix-mode (failure caused by combination of tensile and shear action) failure condition [Whittaker *at al.*, 1992]. In addition, almost all pervious studies have utilized a specimen geometry other than the notched disk. Furthermore, during the laboratory experiments, no study has incorporated the effect of temperature and pressure for the mixed mode loading conditions which are necessary to simulate the field conditions. Therefore, this experimental investigation is formulated to determine the fracture toughness of a selected limestone formation using a methodology which takes into consideration the above-mentioned parameters. Accordingly, the objectives of this study are briefly summarized as follows:

1) To determine the fracture toughness for a selected rock formation for both the outcrop and the reservoir samples under ambient and *in-situ* conditions of temperature and confining pressure.
2) To determine the fracture toughness envelope of the formation under mixed mode I-II failure conditions

3 To monitor the crack propagation during testing, and to study the fractured surface using Scanning Electron Microscopy (SEM) in order to investigate whether the crack propagates along the boundary of the grains or through their bodies

4) To study the mineralogy of the material used by X-ray diffraction (XRD)analysis.

1 .3 Thesis Organization

To accomplish the above-mentioned objectives, published literature related to the fracture toughness testing of rocks is thoroughly surveyed. Chapter 2 is devoted to the literature review of the research work in the area of fracture toughness determination of rocks. Mathematical formulation for different modes of loading and failure theories is also presented. Background and description of different methods used in this research work to determine the fracture toughness is presented in Chapter 3. Description of the material, sample preparation, and experimental setup for the fracture toughness determination used in this study are discussed in Chapter 4. Chapter 5 presents the results and discussion of the results. The main conclusions derived from the findings of this research work are presented in Chapter 6. The Thesis is complemented by a comprehensive list of references used throughout in various chapters.

Chapter 2

Literature Review

2.1 General

Rock fracture toughness, being an intrinsic material property, is studied by making use of one or more of the three types of crack extension modes, namely, the crack opening mode (mode-I), the crack sliding mode (mode-II), and the anti-plane shear mode (mode-III). Schematic representations of these loading conditions are shown in Figure 2.1. In mode-I, the crack propagates under the action of a tensile force acting normal to the failure surface. In mode-II, the crack extends under a shearing (i.e. sliding) action acting parallel to the crack plane. Mode-III is caused by a tensile and shearing action both acting simultaneously.

Irwin (1957) was the first to develop a basis for the fracture mechanics applications to practical problems in terms of the above-mentioned crack opening modes. He presented an equivalent formulation to the energy approach proposed by Griffith (1921), which was based on the stress concentration ahead of the crack tip. The material property governing the fracture initiation and propagation is referred to

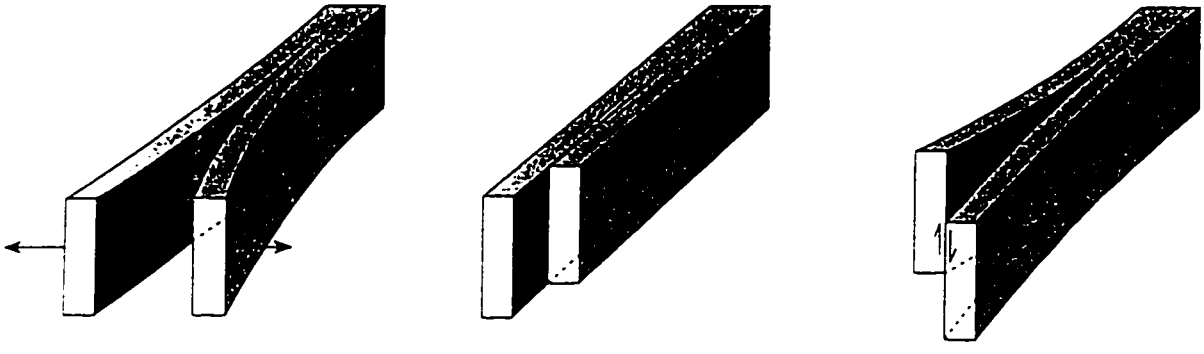

Figure 2.1: Basic Crack Extension Modes [after Twiss and Moores, 1992].

as the critical stress intensity factor, K_c, or in terms of energy as a critical strain energy release rate, G_c, [Shah *et al.*, 1971].

A large number of studies have been conducted in linear elastic fracture mechanics (LEFM) using mode-I failure condition, in which the crack extends in a direction normal to that of the externally applied load. Crack instability occurs when the stress intensity factor reaches a critical value, called the critical stress intensity factor for mode-I, K_{IC}. However, the fracture of a brittle material occurs at a shear stress approximately equal to the tensile fracture stress [Awaji and Sato, 1978]. Also, due to the boundary conditions and/or field stresses encountered in various applications involving rock fracture, the induced fracture may tend to propagate in a curvilinear (mixed-mode) fashion [Lim *et al.*, 1994-a]. For this reason, in addition to mode-I, mode-II, mode-III as shown in Figure 2.1, it is necessary to study the fracture toughness of a rock material and its behavior under a combined action of such loading modes.

The application of fracture mechanics principles to study the fracture behavior of rock is not very old. About two decades back, Schmidt (1976) conducted fracture toughness testing of rocks using a method originally developed for metallic materials. He studied the fracture toughness of Indiana limestone using three point bend specimens of rectangular cross-section. Afterwards, numerous test methods and techniques have been developed for fracture toughness determination under both mode-I and mixed mode I-II loading configurations. Based on several studies, the International Society for Rock Mechanics (ISRM) succeeded in standardizing the

specimen configuration for the study of fracture toughness under mode-I loading condition. However, no consensus has so far been made on the specimen geometry which can be used for mixed mode I-II fracture studies. Therefore, many test configurations have been reported in the literature.

2.2 Fracture Mechanics

Fracture mechanics is an engineering discipline, which focuses on the quantitative description of the transformation of an intact structural component into broken ones by crack propagation. In its most basic form, it relates the maximum permissible stress to the size and location of a crack in a body subjected to some externally applied stress field. It can also predict the rate at which cracks grow to a critical size, by environmental influences or by repeated loads (fatigue) or a combination. Further, it can determine the conditions of rapid propagation and arrest of moving cracks [Kanninen and Popelar, 1985].

Initially, fracture mechanics principles were used to predict and avoid catastrophic and sudden failure of various structures of man-made materials such as metals, plastics, and ceramics. It has also been successively used to predict the cracking phenomenon in concrete. Another application is in the area of geophysics, where an earthquake fault movement is studied by making use of fracture mechanics principles. In the field of rock engineering, fracture mechanics has got applications in areas where cracks can be initiated in the rock mass like hydraulic fracturing, rock excavation, tunnel boring and rock cutting. Furthermore, it is applied in areas where

the purpose is the determination of the strength of rock against external structural loading such as foundation design, rock slope stability and handling of nuclear waste in rock cavities [ISRM, 1988].

Fracture mechanics has been developed using the strength of materials approach whereby stress in a structure is compared with some material strength value in order to decide whether failure will occur or not. The basic material parameter in fracture mechanics is called the fracture toughness [ISRM, 1988]. Since fracture mechanics specifically describes the effect of cracks, fracture toughness tests differ from ordinary strength tests by requiring specimens with well defined cracks to be used.

2.3 Linear Elastic Fracture Mechanics (LEFM)

The problem of crack propagation through rocks is studied using the theory of fracture mechanics and, in particular, Linear Elastic Fracture Mechanics (LEFM). LEFM is basically concerned with the determination of the magnitude of the singularity at the crack tip in an elastic body. This value is called the stress intensity factor and is usually denoted by K. The stress intensity factor (K) is a function of the mode of load applied, the crack and body geometry, and the stress in the vicinity of the crack tip induced due to externally applied load. If the stress intensity is larger than a critical stress intensity factor, K_c, the crack will propagate. This stress intensity factor is a property of the intact material and is a measure of the material's resistance to fracture initiation and propagation.

The inability of the rock (as well as other materials) to remain elastic throughout the loading stage, poses significant problem to the application of LEFM to such materials. Because of the concentration of high magnitude stresses at the crack tip, rocks tend to yield locally and a crack tip yield zone is formed. This yield zone is schematically shown in Figure 2.2 with λ being the radius of the crack tip yield zone. The shape and size of this yield zone has significant effect on the performance of the cracked specimens. If the yield zone is small compared to the size of the specimen, the effect of the yield zone is also small and the specimen may be considered as behaving in an elastic manner. On the other hand, as the yield zone size increases compared to that of the specimen, much of the specimen will be in the inelastic zone and the application of LEFM becomes questionable.

The implications of the large size of the yield zone appear in the form of dependence of fracture toughness on the specimen size. Therefore, the test specimen should be sufficiently large so that elastic behavior is ensured and reasonably constant fracture toughness is obtained [Haberfield *et al.*, 1990].

2.4 Stress Distribution At A Crack Tip

When a cracked body is subjected to external loading, stresses develop within the body. The type and magnitude of stresses developed at the crack tip are function of many parameters such as type of loading, crack orientation and crack geometric features. Consider a body containing a crack in the middle and subjected to an externally applied arbitrary state of stress as shown in Figure 2.3. Due to the presence

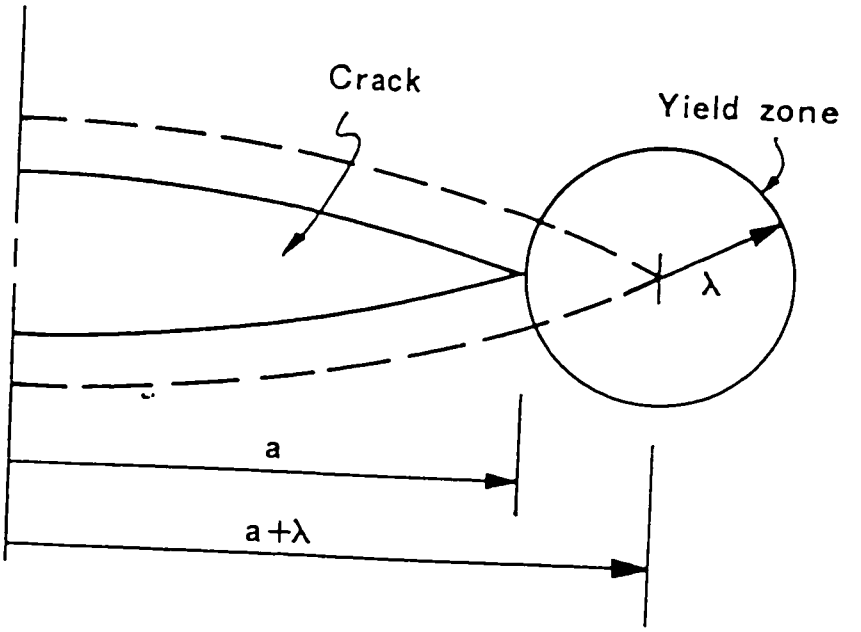

Figure 2.2: Representation of Fracture Process Zone (FPZ) [after Haberfield *et al.*, 1990].

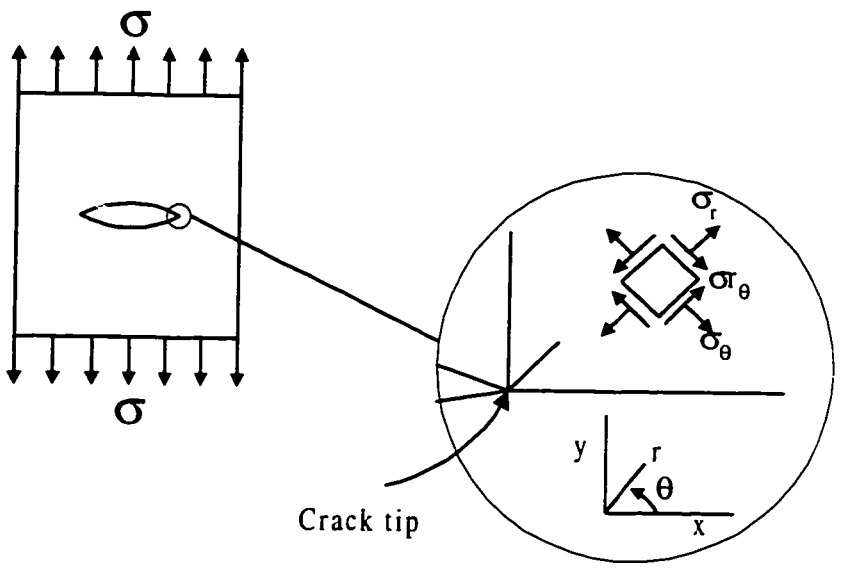

Figure 2.3: Stress State at a Crack Tip Expressed in Polar Coordinates [after Ashmawi, 1990].

of crack, stresses concentrate at the tip. These concentrated stresses expressed in polar coordinates are also shown in Figure 2.3. The stress concentration at the crack tip is a major point of interest as far as stability of rock against crack initiation and its subsequent propagation is concerned. The stress distribution at the crack tip for each of the three modes of loading (shown in Figure 2.1) is described below.

2.4.1 Mode-I

In mode-I loading condition, the stress at the crack tip acts normal to the crack propagation direction, and the crack opening takes place normal to the crack plane. This mode is also called opening or splitting mode. The stresses at the crack tip expressed in polar coordinates (Figure 2.3) are given as follows [Whittaker *et al.*, 1992]:

$$\begin{Bmatrix} \sigma_r \\ \sigma_\theta \\ \sigma_{r\theta} \end{Bmatrix} = \frac{K_I}{\sqrt{2\pi r}} \cos\frac{\theta}{2} \begin{Bmatrix} 1+\sin^2\frac{\theta}{2} \\ \cos^2\frac{\theta}{2} \\ \sin\frac{\theta}{2}\cos\frac{\theta}{2} \end{Bmatrix} \qquad (2.1)$$

Where,

K_I = mode-I stress intensity factor;

r = radial distance from crack tip;

θ = angular distance from the crack tip;

σ_r, σ_θ = radial and tangential stresses, respectively; and,

$\sigma_{r\theta}$ = radial shear stress.

2.4.2 Mode-II

Mode-II loading condition, also called sliding or shearing mode, causes the crack to propagate under the action of an in-plane shear force. The stresses at the crack tip are expressed as follows [Whittaker *et al.*, 1992]:

$$\begin{Bmatrix} \sigma_r \\ \sigma_\theta \\ \sigma_{r\theta} \end{Bmatrix} = \frac{K_{II}}{\sqrt{2\pi r}} \cos\frac{\theta}{2} \begin{Bmatrix} \sin\frac{\theta}{2}\left(1-3\sin^2\frac{\theta}{2}\right) \\ -3\sin\frac{\theta}{2}\cos^2\frac{\theta}{2} \\ \cos\frac{\theta}{2}\left(1-3\sin^2\frac{\theta}{2}\right) \end{Bmatrix} \tag{2.2}$$

Where,

K_{II} = mode-II stress intensity factor.

2.4.3 Mode-III

Mode-III, also called tearing mode, causes crack extension under an out of plane shear stress. The crack faces move relative to each other and the displacement of crack surfaces are in the crack plane. Stresses at the crack tip are given by the following mathematical expression [Whittaker *et al.*, 1992]:

$$\begin{Bmatrix} \sigma_{rz} \\ \sigma_{\theta z} \end{Bmatrix} = \frac{K_{III}}{\sqrt{2\pi r}} \begin{Bmatrix} \sin\frac{\theta}{2} \\ \cos\frac{\theta}{2} \end{Bmatrix} \tag{2.3}$$

Where,

K_{III} = mode-III stress intensity factor; and,

σ_{rz} , $\sigma_{\theta z}$ = radial and tangential shear stresses, respectively.

2 .4 .4 Mixed Mode

Mixed-mode loading condition is created by combining any two of the three previously described loading conditions. For example, the combination of mode-I and mode-II loading conditions causes mixed mode I-II. Similarly, mode-I and mode-III acting simultaneously cause mixed mode I-III; and mode-II and mode-III cause mixed mode II-III loading condition. More commonly, fracturing of rock structures may occur under mixed mode I-II loading, since in reality, a crack in a rock structure may be oriented in an arbitrary manner with respect to the applied load and it will, quite possibly, extend under mixed mode I-II loading [Whittaker *et al.*, 1992]. Therefore, the main focus of this study was the investigation of fracture toughness under mode-I as well as mixed mode I-II loading conditions.

To achieve a mixed mode I-II loading condition at the crack tip, consider an infinite thin plate with an inclined crack subjected to a remote tensile loading as shown in Figure 2.4. If the normal and shear stresses acting on the crack plane are σ_n and τ_n, respectively, then:

$$\sigma_n = \sigma \sin^2 \beta \tag{2.4}$$

$$\tau_n = \sigma \sin \beta \cos \beta \tag{2.5}$$

Where,

β = orientation of the crack with respect to the applied load.

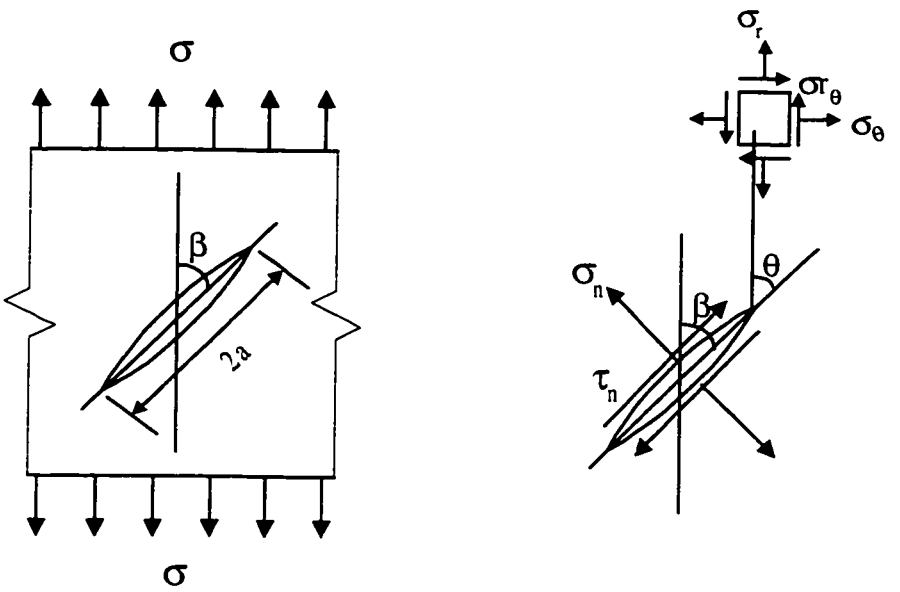

Figure 2.4: An Inclined Crack Subjected to Tension [after Whittaker *et al.*, 1992].

Using the superimposition principle, the crack tip stresses can be expressed in the following form [Whittaker *et al.*, 1992].

$$\begin{Bmatrix}\sigma_r\\ \sigma_\theta\\ \sigma_{r\theta}\end{Bmatrix}=\frac{K_I}{\sqrt{2\pi r}}\cos\frac{\theta}{2}\begin{Bmatrix}1+\sin^2\frac{\theta}{2}\\ \cos^2\frac{\theta}{2}\\ \sin\frac{\theta}{2}\cos\frac{\theta}{2}\end{Bmatrix}+\frac{K_{II}}{\sqrt{2\pi r}}\begin{Bmatrix}\sin\frac{\theta}{2}\left(1-3\sin^2\frac{\theta}{2}\right)\\ -3\sin\frac{\theta}{2}\cos^2\frac{\theta}{2}\\ \cos\frac{\theta}{2}\left(1-3\sin^2\frac{\theta}{2}\right)\end{Bmatrix} \tag{2.6}$$

Where,

$K_I=\sigma_n\sqrt{\pi a}=\sigma\sqrt{\pi a}\sin^2\beta$;

$K_{II}=\tau_n\sqrt{\pi a}=\sigma\sqrt{\pi a}\sin\beta\cos\beta$;

a = half of the crack length;

r = radial distance from the crack tip; and,

θ = direction of crack propagation with respect to crack original plane.

2 .5 Failure Theories

For a cracked body under mixed mode I-II loading, the following three criteria of fracture have been advanced [Awaji and Sato, 1978].

1) The maximum stress ($\sigma_{\theta max}$) criterion

2) The minimum strain energy density (S_{min}) criterion

3) The maximum energy release (G_{max}) criterion

2.5.1 Maximum Stress ($\sigma_{\theta max}$) Criterion

This failure criterion, first developed by Erdogan and Sih (1963), assumes that the fracture propagates under the influence of maximum tangential stress at the crack tip. The stress distribution in the vicinity of the crack tip under mixed mode-I-II is expressed in polar coordinates by Equation 2.6. The σ_{max}-criterion states the following conditions for crack initiation and propagation :

1) Crack extension starts at the crack tip in a radial direction.
2) The crack extension takes place in a plane perpendicular to the direction θ of greatest tension, i.e. such that the tangential stress σ_θ is maximum (or $\sigma_{r\theta} = 0$).
3) The crack extension occurs when $\sigma_{\theta max}$ reaches a critical value which is a material constant.

2.5.2 Minimum Strain Energy Density (S_{min}) Criterion

The strain energy density criterion was introduced by Sih (1974). It states that the variation of strain energy density around a circular region surrounding the crack tip determines the direction of fracture initiation. The strain energy density, S_{min}, is defined as:

$$S = a_{11}K_I^2 + 2a_{12}K_I K_{II} + a_{22}K_{II}^2 \qquad (2.7)$$

Where,

$$a_{11} = \frac{1}{16G}[(1+\cos\theta)(k-\cos\theta)];$$

$$a_{12} = \frac{1}{16G}\sin\theta[2\cos\theta-(k-1)];$$

$$a_{22} = \frac{1}{16G}[(k+1)(1-\cos\theta)+(1+\cos\theta)(3\cos\theta-1)];$$

G = shear modulus;

ν = Poisson's ratio; and,

k = (3-ν)/(1+ν) for plane stress; and k = 3-4ν for plane strain and axisymmetry.

Crack propagation is postulated to occur in the direction θ of the local minima given by $\partial S/\partial\theta = 0$ and $\partial^2 S/\partial\theta^2 > 0$. Should more than one minimum occur, the minimum with the greatest S would be the point of fracture initiation [Sih and Cha, 1974]. The critical strain energy density, S, is given by

$$S_c = \frac{k-1}{8G}K_{Ic}^2 \qquad (2.8)$$

Where,

K_{IC} = critical mode-I stress intensity factor

2 .5 .3 Maximum Energy Release (G_{max}) Criterion

The Griffth theory of fracture, Griffith (1921), has been applied in many rock mechanics problems with some success. Basically, the theory is based on equating the release of the strain energy associated with incremental crack growth to the energy required to create the new surface, i.e., surface energy. Griffth applied his theory to the fracture of glass and obtained a crude agreement. Since the theory neglected all

forms of energy dissipation other than the surface energy, Orowan (1952) modified the theory slightly to account for the small scale of plastic flow at the crack tip. The theory was further modified by Irwin (1957) who introduced the concept of stress intensity factor, K, which is basically the stress singularity at a crack tip and is directly related to the strain energy release rate (G) [Schmidt, 1976].

The maximum energy release rate criterion assumes that the direction of crack propagation is governed by the maximum elastic energy release rate. The crack extension takes place when the energy release rate exceeds a certain critical value termed as a material constant. This criterion has been formulated in many forms, but the expression proposed by Hussain *et al.* (1974) is described here. According to them, the energy release rate (G) in terms of K_I, K_{II} and θ is given by following expression.

$$G = \frac{4}{E}\left(\frac{1}{3+\cos^2\theta}\right)^2\left(\frac{1+\theta/\pi}{1-\theta/\pi}\right)^{-\theta/\pi} * \\ *\left[\left(1+3\cos^2\theta\right)K_I^2 - 8\sin\theta\cos\theta K_I K_{II} + \left(9-5\cos^2\theta\right)K_{II}^2\right] \qquad (2.9)$$

Where E represents the Young's modulus. The direction of maximum energy release rate is found from $\partial G/\partial\theta = 0$ and, $\partial^2 G/\partial\theta^2 < 0$.

Chapter 3

Background

3.1 Fracture Toughness Testing

There is a large number of factors that control the choice of a particular method for the determination of rock fracture toughness. Such factors include the strength of the rock, the availability of testing equipment, and the ease of sample preparation. Two types of experimental techniques were used in this research work to study the fracture toughness: (1) Diametral compression of circular disk specimens containing an inclined crack in the middle; (2) Semicircular disk specimens containing an inclined crack and circular rod specimens containing a crack in the middle subjected to three point bending. The background of theses methods is described in the following sections.

3.1.1 Mode-I Testing Technique

For mode-I fracture toughness testing, Single-Edge Cracked Round Bar Bend (SECRBB) was used. This technique was first developed by Ouchterlony (1981).

Haberfield and Johnston (1990) employed this method for fracture toughness study of a synthetic rock. Figure 3.1 shows the schematic representation of the technique. Ouchterlony (1981) developed the following expression for mode-I fracture determination for this geometry.

$$K_I = 0.25\left(S/D\right)\left(P/D^{1.5}\right)Y_I' \tag{3.1}$$

Where,

$$Y_I' = \frac{2(D/S)\left[450.8531\rho^2(a/D)^{1.5}\right]^{0.5}}{\left[(a/D)-(a/D)^2\right]^{0.25}} \tag{3.2}$$

$\rho = \left(S/D\right)/3.33$; and,

P = load at failure.

and the other variables are depicted in Figure 3.1. The dimensionless stress intensity factor Y_I' varies slightly with the span to diameter ratio (*S/D*) as given above. This technique has been found to provide results similar to the single edge cracked beam under three point bending technique (SECB). Consequently, it is considered as an excellent candidate for computing mode-I fracture toughness. In addition, it also serves as a useful tool for validating other techniques for the determination of mode-I fracture toughness such as a semicircular disk specimen under three point bending.

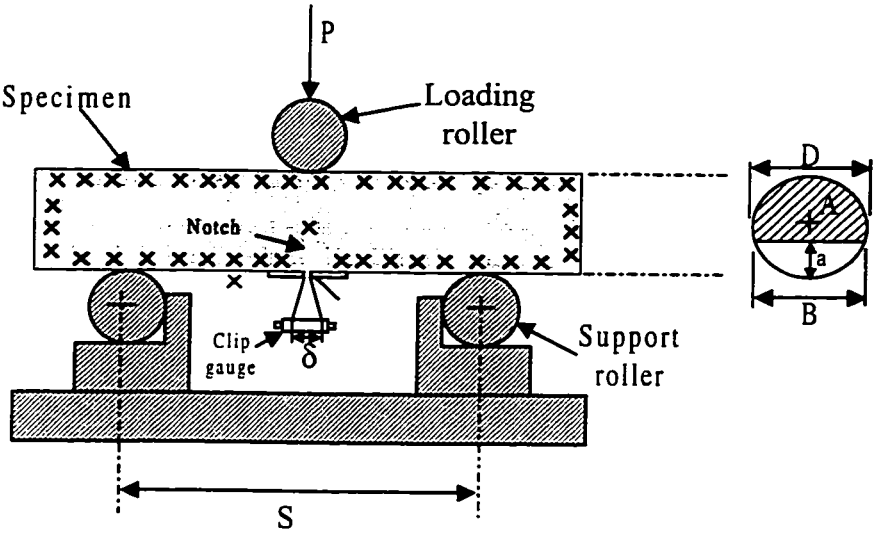

a = maximum notch depth
D = diameter of rock core
S= support span
A = reduced cross-sectional area
B = crack front length
P = load on specimen at failure
β = crack inclination angle
δ = crack mouth opening displacement

Figure 3.1: Single-Edge Cracked Round Bar Bend (SECRBB) Specimen [after Ouchterlony, 1981].

3 .1 .2 Mixed-Mode I-II Testing Techniques

Mixed mode I-II fracture toughness was studied using notched circular and semicircular disk specimens. Circular disks were tested under diametral compression whereas semicircular disk specimens were tested under three point bending.

3 .1 .2 .1 Notched Brazilian Disk Specimen

The ISRM recommended mode-I rock fracture toughness determination methods, Chevron Bend (CB) and Short Rod (SR), have a number of practical disadvantages associated with their applicability. These drawbacks include the small load level at which fracture will initiate, the relatively large amount of intact rock sample required to be used for testing, the complicated loading fixtures, and the complex sample preparation for Short Rod (SR) specimens [Fowell and Xu, 1994]. Cracked Chevron Notched Brazilian Disk (CCNBD) and Cracked Straight Through Brazilian Disk (CSTBD) specimen geometry, (Figure 3.2), have solved the problems related to these disadvantages. The methods are equally applicable for mode-I as well as mode-II and mixed mode-I-II loading conditions.

CSTBD was independently proposed by Awaji and Sato (1978) and Sanchez (1979) based on the early work of Yareman and Krestin (1966). This testing technique makes use of circular disk geometry with a central straight through notch. CCNBD differs from the CSTBD only in the shape of the central notch. Both specimens have

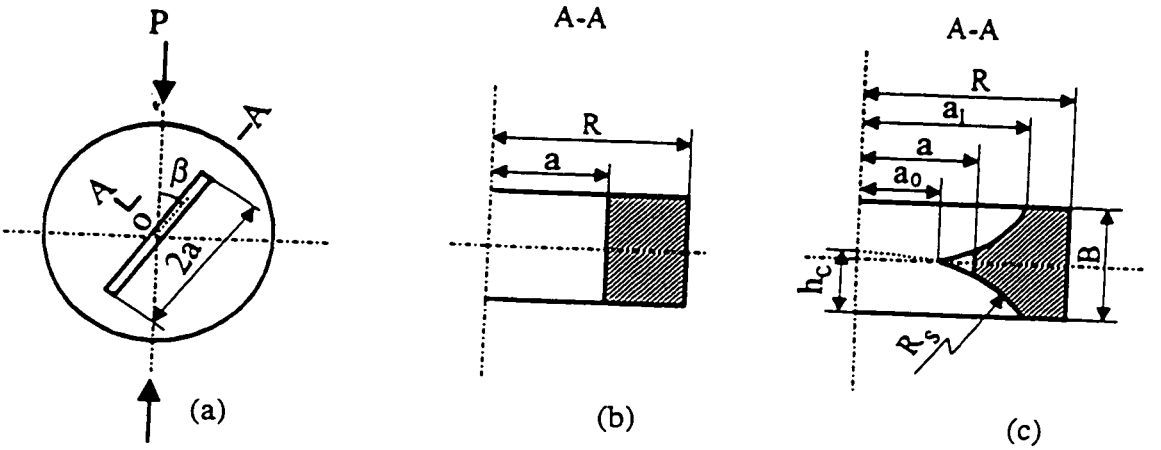

Figure 3.2: Notched Brazilian Disk Specimens: (a) Loading Fixture, (b) Section A-A for the Straight Notch, (c) Section A-A for the Chevron Notch [after Fowell and Xu, 1994].

the same loading arrangement in which a diametral compressive load is applied whose line of action passes through the center of the disk (Figure 3.2).

By aligning the crack at some angle β, relative to the loading plane, a variety of mixed mode-I-II failure patterns are possible to study. For $\beta = 0$, i.e., the loading direction is parallel to the crack orientation, pure mode-I stress field is achieved. This test has a practical advantage of using only one specimen geometry for a wide range of mixed mode-I-II failure mechanism. The actual ratio of mode-I/mode-II is a function of crack length and its orientation with respect to the line of action of load. For CSTBD, a variety of failure mechanisms have been reported in the literature as a function of (a/R) ratio, where "a" is half the crack length and R is the radius of the disk. However, only few studies show the long crack effects (i.e. $a/R > 0.7$). Most of the studies were made on short crack cases so that the interaction between the crack and the boundary was negligible. Fowell (1994) has recently reported that such approximation can only be valid for the case of $a/R < 0.6$. Based on his findings, he suggested that the cracked Brazilian disk with a short crack length will be difficult to machine and proposed a range of a/R between 0.65 and 0.80) for practical purposes. For a CCNBD specimen geometry, pure Mode-II can be obtained by having a certain combination of (a/R) and the crack orientation, β. However, a slight deviation from the crack length and/or orientation may change the stress field thereby introducing some mode-I component. This variation in the stress intensity factor was determined numerically by Awaji and Sato (1978). Subsequently, Atkinson *et al.* (1982) presented an explicit formula for K_I and K_{II} variation.

When fatigue precracking is required, CSTBD is not considered an advantageous tool for fracture toughness study because the specimen will be susceptible to fracture during precracking. In such circumstances, a CCNBD specimen is considered a second alternative. Studies made by Singh and Shetty (1989) and Shetty and Rosenfield (1987) used CCNBD to measure the mixed mode I-II fracture properties of ceramics. Some other researchers also used this specimen geometry to investigate the mode-I fracture toughness of rock [Lim *et al.*, 1994-a]. A few studies have also been made to study the fracture toughness of weak sandstone rock under mixed mode I-II loading conditions using CSTBD geometry. However, only few studies have been reported in the literature which may focus on the behavior of hard rocks for mixed mode I-II failure case.

3 .1 .2 .2 Stress Distribution in Uncracked Brazilian Disk

The determination of stress field in a specimen subjected to externally applied forces is the initial point in the fracture analysis. Assuming a homogeneous, isotropic, and linearly elastic material, a stress solution for an uncracked disk under diametral compression as shown in Figure 3.3 was formulated by Timoshinko and Goodier (1960). The results have been reported by Andreev (1995) in the form of following mathematical formulas expressed in Cartesian coordinates:

$$\sigma_x = \frac{2P}{\pi B}\left[\frac{(R-y)x^2}{r_1^4} + \frac{(R+y)x^2}{r_2^4} - \frac{1}{D}\right] \tag{3.3}$$

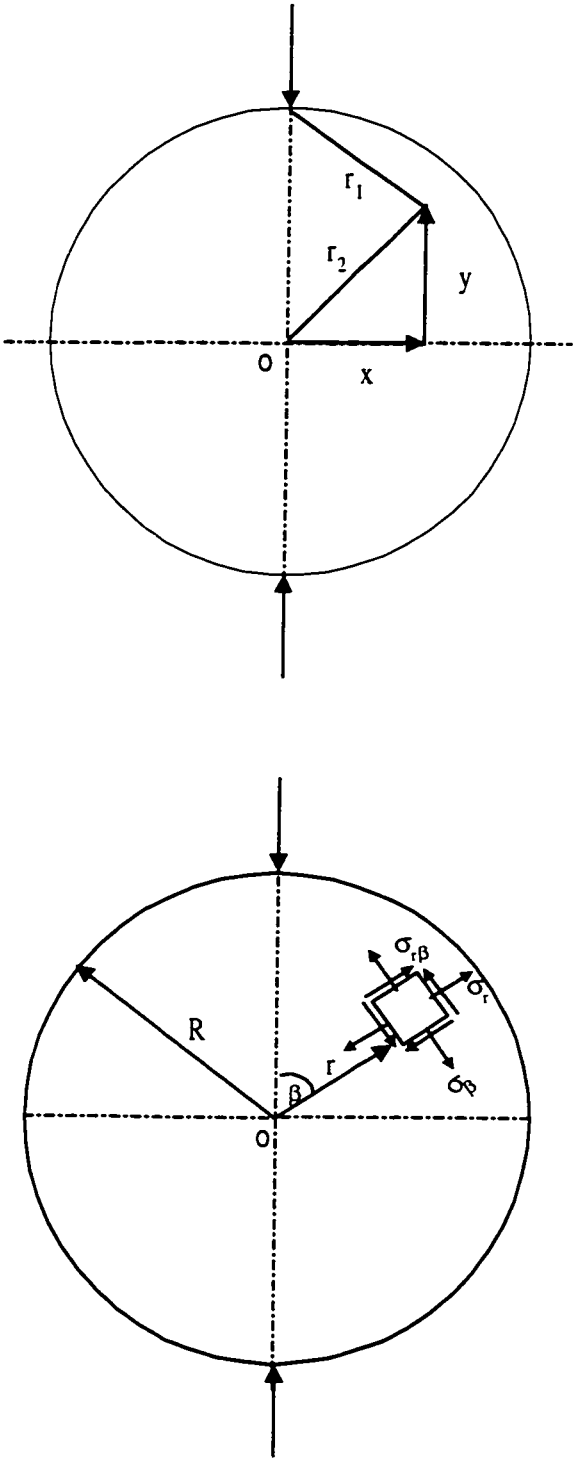

Figure 3.3: Uncracked Brazilian Disk Specimen under Diametral Compression.

$$\sigma_y = \frac{2P}{\pi B}\left[\frac{(R-y)^3}{r_1^4} + \frac{(R+y)^3}{r_2^4} - \frac{1}{D}\right] \tag{3.4}$$

$$\sigma_{xy} = -\frac{2P}{\pi B}\left[\frac{(R-y)^2 x}{r_1^4} + \frac{(R+y)^2 x}{r_2^4}\right] \tag{3.5}$$

where,

B = thickness of the disk;

R = radius of the disk;

D = diameter of the disk;

P = compressive load applied; and,

x, y = Cartesian coordinates of a point from center of the disk.

Due to the fact that among the various theoretical fracture criteria, the crack initiation as well as its subsequent propagation in mixed mode I-II loading is more realistically predicted by the tangential stress (σ_β) criterion, stress distribution in the disk in polar coordinates is of major interest. The stress distribution in polar coordinates, as proposed by Atkinson *et al.* (1982), has the following form:

$$\sigma_\beta = \frac{2P}{\pi RB}\left[\frac{1}{2} - \frac{\left(1-\frac{r}{R}\cos\beta\right)\sin^2\beta}{\left(1+\frac{r^2}{R^2}-2\frac{r}{R}\cos\beta\right)^2} - \frac{\left(1+\frac{r}{R}c\cos\beta\right)\sin^2\beta}{\left(1+\frac{r^2}{R^2}+2\frac{r}{R}\cos\beta\right)^2}\right] \tag{3.6}$$

$$\sigma_r = \frac{2P}{\pi RB}\left[\frac{1}{2} - \frac{\left(1-\frac{r}{R}\cos\beta\right)\left(\cos\beta-\frac{r}{R}\right)^2}{\left(1+\frac{r^2}{R^2}-2\frac{r}{R}\cos\beta\right)^2} - \frac{\left(1+\frac{r}{R}\cos\beta\right)\left(\cos\beta+\frac{r}{R}\right)^2}{\left(1+\frac{r^2}{R^2}+2\frac{r}{R}\cos\beta\right)^2}\right] \tag{3.7}$$

$$\sigma_{r\beta} = \frac{2P}{\pi RB}\left[\frac{\left(1-\frac{r}{R}\cos\beta\right)\left(\cos\beta-\frac{r}{R}\right)\sin\beta}{\left(1+\frac{r^2}{R^2}-2\frac{r}{R}\cos\beta\right)^2}+\frac{\left(1+\frac{r}{R}\cos\beta\right)\left(\cos\beta+\frac{r}{R}\right)\sin\beta}{\left(1+\frac{r^2}{R^2}+2\frac{r}{R}\cos\beta\right)^2}\right] \quad (3.8)$$

When a centrally notched disk with a crack inclined at an angle β with respect to the loading direction is loaded diametrally as in the case of mixed mode I-II fracture toughness determination, the radial stress (σ_r) is acting parallel to the crack and has no influence on the crack propagation. On the other hand, the stress components (σ_β) and ($\sigma_{r\beta}$) are used not only for mixed mode I-II fracture toughness calculation, but are also used for predicting the direction of crack propagation originating from the crack tip.

To have a detailed idea about the stress distribution in an uncracked disk under diametrical compression, the above-mentioned mathematical expressions were solved computationally. The normalized stresses (σ_β/σ_o), (σ_r/σ_o), and ($\sigma_{r\beta}/\sigma_o$) where $\sigma_o = P/\pi RB$, are presented in terms of the stress contours shown in Figure 3.4. Stresses were computed along the lines of constant orientation and constant normalized radius (r/R). Orientations of 0 to 90 degrees with an increment of 5 degrees were chosen. Normalized radius for the analysis was varied from 0.1 to 0.99. Radius of the disk was chosen as 50 mm which is mainly used for fracture toughness study in the present experimental work. Making use of symmetry, only a quarter of the disk was used in the analysis. Lines of constant inclination from 0 to 90 degrees with an increment of 15 degrees and lines of constant normalized radius (r/R) from 0.1 to 1 with an increment of 0.1 have also been superimposed on the stress contours so that stress variation could be more easily investigated.

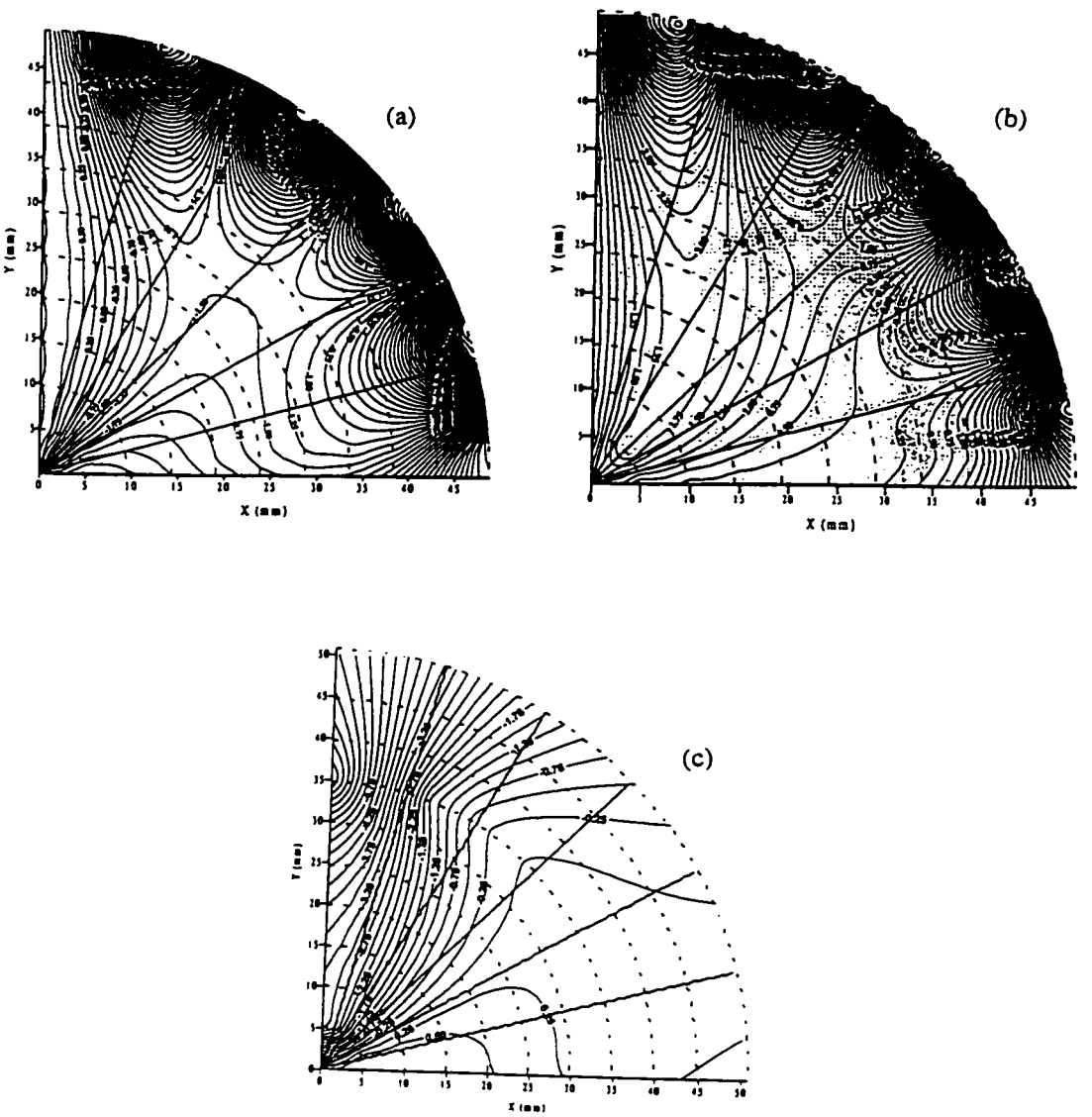

Figure 3.4: Stress Distribution for Uncracked Brazilian Disk under Diametral Compression: (a) Tangential Stresses, (b) Shear Stresses, (c) Radial Stresses.

As can be seen in Figure 3.4-a, σ_β is maximum (positive values for contours) along the diameter of the disk coinciding with the loading direction and then reduces gradually from a tensile zone along the loading direction at low orientations (i.e., 0 to 27 degrees) to a compression zone (negative contour values) at higher orientations. The orientation for which σ_β is zero is a function of r/R and cannot be achieved at an inclination of about more than 30 degrees. Variation of shear stresses ($\sigma_{r\beta}$) along various orientations and normalized radius (r/R) is shown in Figure 3.4-b. Contrary to tangential stress, $\sigma_{r\beta}$ is zero along the loading direction and then increases till it becomes maximum between 30 and 45 degrees and then decreases but remains positive even for higher inclinations lying symmetrical about its maximum value. Variation of normalized radial stresses is shown in Figure 3.4-c.

3 .1 .2 .3 Stress Intensity Factor for Notched Brazilian Disk

When a centrally notched Brazilian disk with crack inclined with respect to the loading direction is loaded along the diametral axis, the tangential and shear stresses discussed in the Section 3.1.2.2 do not vary in a smoother way but concentrate at the notch tip. When the externally applied load exceeds a certain limit, the crack initiates and propagates till it reaches the two loading points resulting in the failure of the specimen. For such a situation, a stress intensity or stress concentration rather than the usual stress distribution is considered to be more valuable. For the Brazilian disk with a central straight notch, Atkinson *et al.* (1982) has proposed a mathematical expression for the stress intensity factor in the following form:

$$K_I = \frac{P\sqrt{a}}{\sqrt{\pi}RB} N_I \tag{3.9}$$

$$K_{II} = \frac{P\sqrt{a}}{\sqrt{\pi}RB} N_{II} \tag{3.10}$$

Where,

R = radius of the Brazilian disk;

B = thickness of the disk;

P = compressive load at failure;

a = half crack length; and

N_I *and* N_{II} are non-dimensional coefficients which depend on (a/R) and the orientation angle (β) of the notch with the direction of loading.

Atkinson *et al.* (1982) proposed the following expression for N_I and N_{II}:

$$N_I = \sum_{i=1}^{n} T_i \left(\frac{a}{R}\right)^{2i-2} A_{i\beta} \tag{3.11}$$

$$N_{II} = 2\sin 2\beta \sum_{i=1}^{n} S_i \left(\frac{a}{R}\right)^{2i-2} B_{i\beta} \tag{3.12}$$

Where,

T_i, S_i = numerical constants; and

$A_{i\beta}$, $B_{i\beta}$ = angular constants.

For the LEFM to be applicable for the fracture toughness study, it was mentioned earlier that fracture process zone (FPZ) should be as small as possible. This is achieved partly by using a specimen of larger dimensions, and partly by limiting the notch size to a minimum but a practical value. To achieve this goal, small crack

approximation proposed by Atkinson *et al.* (1982) is utilized here. According to them, for half crack to radius ratio ($a/R \leq 3$), the following formulation is valid for the above-mentioned non-dimensional coefficients N_I, and N_{II}:

$$N_I = 1 - a\sin^2\beta + \sin^2\beta\left(1 - 4\cos^2\beta\right)\left(\frac{a}{R}\right)^2 \tag{3.13}$$

$$N_{II} = \left[2 + \left(8\cos^2\beta - 5\right)\left(\frac{a}{R}\right)\right]\sin 2\beta \tag{3.14}$$

The variation of N_I and N_{II} obtained from above two equations and using the numerical-based results of Atkinson *et al.* (1982), after analyzing computationally, are shown in Figure 3.5. It can be seen from the Figure that their variation is in the same order as was observed for normalized tangential and shear stresses in an uncracked disk. For $\beta = 0$ (i.e. mode-I), $N_{II} = 0$ and N_I is function of relative crack size (a/R). Shetty and Rosenfield (1985) derived the following third order polynomial for N_I by fitting the numerical results of Atkinson *et al.* (1982).

$$N_I = 0.99 + 0.141\left(a/R\right) + 0.863\left(a/R\right)^2 + 0.886\left(a/R\right)^3 \tag{3.15}$$

The above-mentioned formulation for stress intensity factor under mixed mode I-II fracture toughness study has originally been developed for straight notched Brazilian disk geometry. When the crack or opening in the specimen is a Chevron type (Figure 3.2), the formulation is still valid but the specimens before testing in mixed mode I-II are recommended to be precracked under mode-I to achieve a sharp crack tip [Shetty and Rosenfield, 1985]. However, the method of precracking is tedious and needs sophisticated instruments for carefully monitoring the crack

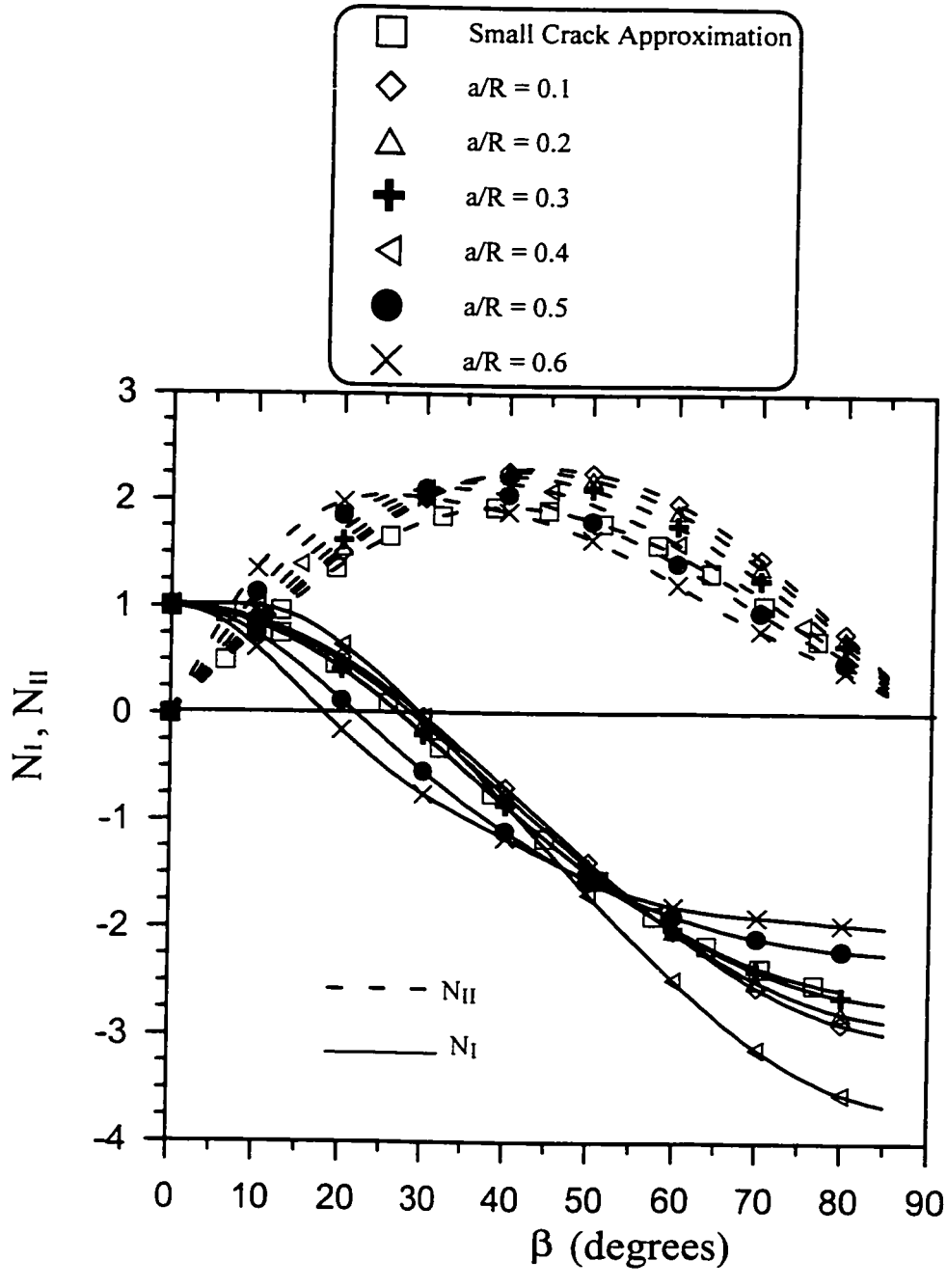

Figure 3.5: Variation of Normalized Coefficients N_I and N_{II} for a Notched Brazilian Disk.

extension so that crack does not propagate behind, a_l, (see Figure 3.2). If the crack extends behind this point, unstable crack propagation takes place and the specimen is lost and the purpose is not fulfilled [whittaker *et al.*, 1992]. Moreover, brittle nature of the material as is the case in this research work, makes the problem of precracking difficult. Keeping in mind that the purpose of precracking is only to achieve a sharp crack tip, and recognizing the difficulty of precracking, it was decided to use the Chevron notch without precracking. The mathematical formulation described above for stress intensity calculation is also used for the specimens with Chevron notch. It is expected that the difference in results will not be considerable. Moreover, in order to compare the results with the straight notched specimens, crack to radius ratio (a_o/R) for Chevron notched specimens was chosen as 0.3.

3.1.2.4 Notched Semicircular Disk Specimen

In this type of testing scheme, a notched semicircular disk specimen is centrally loaded using three point loading arrangement as shown in Figure 3.6. Originally, this arrangement was used for mode-I fracture toughness study, and lately used for mixed I-II fracture toughness study using different crack orientations. Depending upon the crack length, its orientation with respect to the loading direction, and the distance between the supports, a variety of mixed-mode failure patterns are achieved. For pure mode-I, the crack is aligned parallel to the direction of load and lies below the loading point. However, for pure mode-II, only a slight misalignment of the specimen and/or

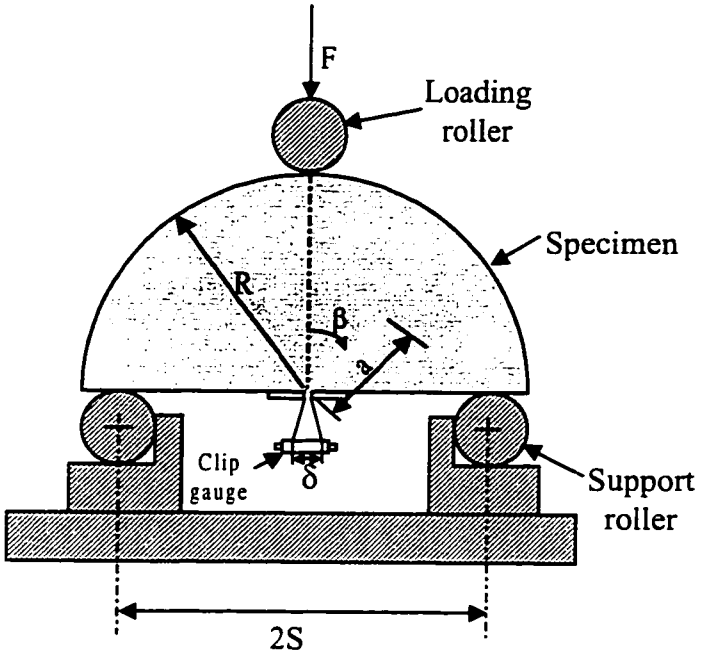

a= crack length
R= radius of specimen
2S = support span
β = crack inclination angle
δ = crack mouth opening displacement

Figure 3.6: Semicircular Disk Specimen under Three Point Bending [after Lim *et al.*, 1994-c].

crack orientation may induce a component of mode-I loading and pure mode-II can not be achieved.

Semicircular disk specimen has been used for a number of mode-I fracture toughness determination tests and the results have been found comparable to other techniques [Lim, *et al.*, 1994-b]. Lim, *et al.* (1994-c) have also conducted some mixed mode I-II tests using this specimen geometry and the results were found sufficiently promising. Stress intensity factor is determined by the following expressions:

$$K_I = \sigma_o \sqrt{\pi a} Y_I, \quad \text{for } \beta \geq 0 \tag{3.16}$$

$$K_{II} = \sigma_o \sqrt{\pi a} Y_{II}, \quad \text{for } \beta > 0 \tag{3.17}$$

Where,

β = crack orientation with respect to loading direction.

K_I, K_{II} = Mode-I and Mode-II stress intensity factors, respectively;

a = notch or crack length;

$\sigma_o = P/2RB$

P = failure load;

R = specimen radius;

B = specimen thickness; and

Y_I, Y_{II} = normalized stress intensity factors for mode-I and mode-II, respectively.

Figure 3.7 represents the variation of Y_I and Y_{II} for the range of notch lengths and inclination angles for a half span to radius ratio (S/R) of 0.5. From Figure 3.7, it is obvious that pure mode-II loading can be obtained without β exceeding 60° only if

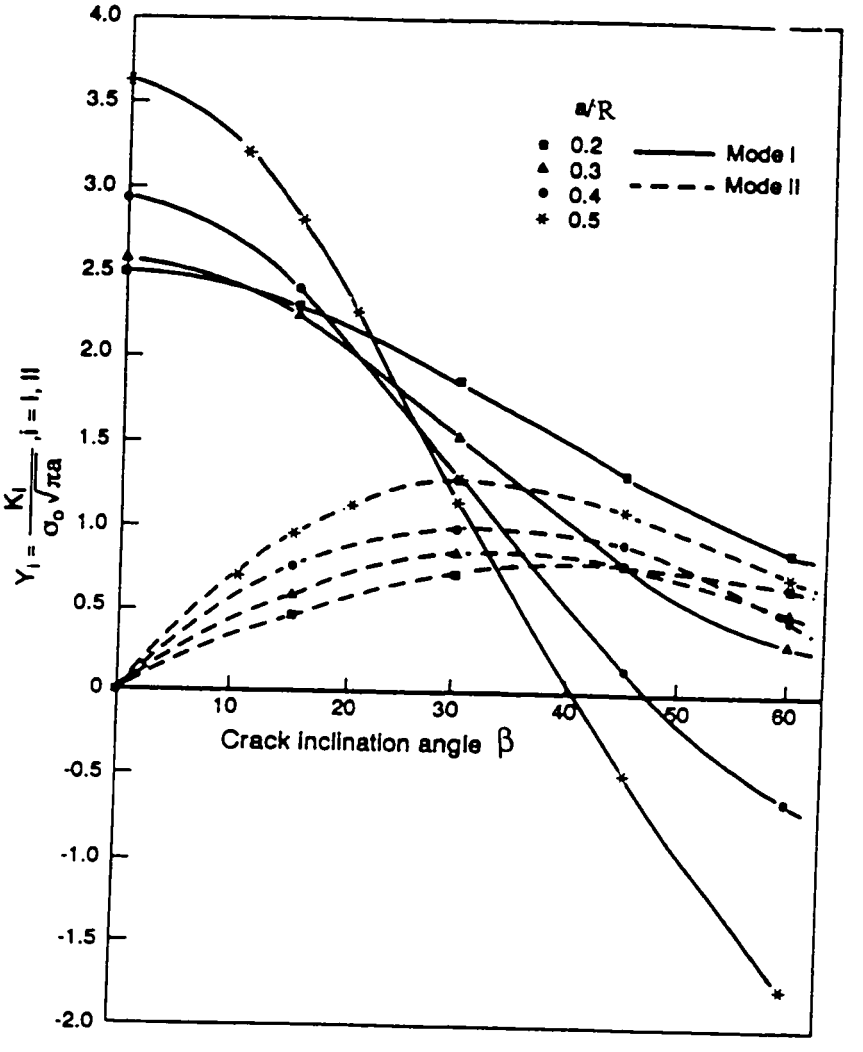

Figure 3.7: Variation of Normalized Stress Intensity Factor for a Semicircular Disk Specimen [after Lim *et al.*, 1994-c].

(a/R) > 0.34. However, the use of large a/R values may render the calculated Y more sensitive to errors in measuring. Consequently, the shortest possible a/R should be used [lim *et al.*, 1994-c]. Pure mode-I can also be achieved using Y value corresponding to $\beta = 0$.

For comparison purpose with the notched Brazilian disk results, the crack to radius (a/R) ratio of 0.3 will be used in this study. Moreover, half span to radius (S/R) ratio was restricted by the size of the crack extension measurement assembly and was chosen as 0.8. Numerical results obtained by Lim *et al.* (1993) have been plotted in Figure 3.8 and approximated by the following polynomials.

$$Y_I = 4.83 - 0.005\beta - 0.002\beta^2 + 1.18 \times 10\beta^3 \tag{3.18}$$

$$Y_{II} = 0.01 + 0.06\beta - 0.0007\beta^2 \tag{3.19}$$

Where, β is in degrees.

3 .2 Factors Affecting Fracture Toughness

3 .2 .1 Scale Effect

Rock samples that are tested in the laboratory are generally homogeneous and free of flaws. However, in nature, both the geometrical (i.e., joints, faults, etc.) and compositional heterogeneities are a characteristic feature of rocks. Thus, it is expected that the results obtained in the laboratory based on the flawless specimens might not be representative of large rock bodies. In jointed rocks, for example, fracture behavior may be governed more by the properties of the joints rather than by the rock mass

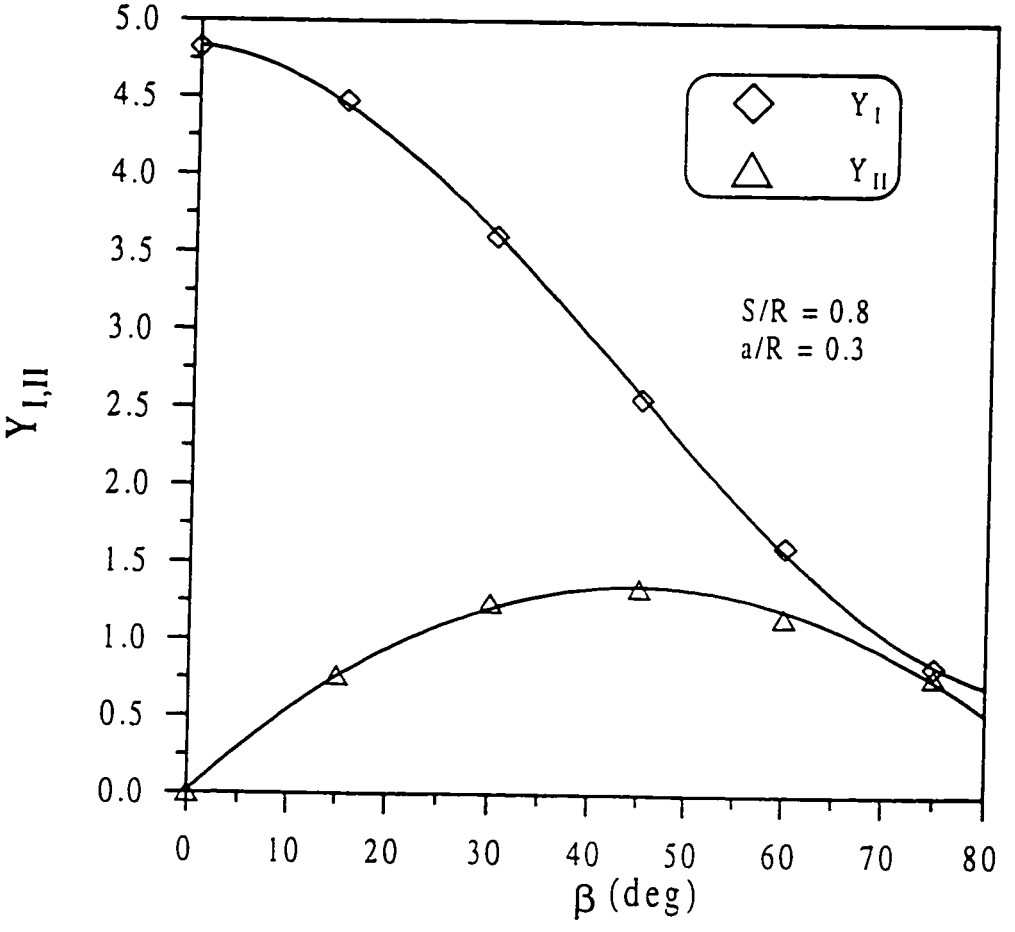

Figure 3.8: Normalized Intensity Factor for a Semicircular Specimen Used in the Present Study.

between them. In fact, experiments have demonstrated that as the scale of the test specimen increases, the measured strength decreases [Twiss and Moores, 1992]. The fracture strength of the earth's brittle crust, therefore, is expected to be less than that obtained from the laboratory measurements.

3.2.2 Fracture Process Zone (FPZ)

In fracture toughness testing of rocks, precracked specimens are subjected to externally applied load. This loading causes stresses to concentrate in the vicinity of the crack tip. Due to high stress concentration, microcracks develop and rock material yields locally ahead of the crack tip resulting in a zone of fine fractures called Fracture Process Zone (FPZ). The shape of this yield zone is still unknown and a simple representation is in the form of a circle with a radius λ as discussed in Chapter 2 (see Figure 2.2). Since the formulations available for rock fracture toughness study have been adopted assuming that the LEFM approach is applicable, consideration of FPZ becomes important for valid fracture toughness study.

Schmidt (1980) suggested a maximum normal stress criterion to describe the shape of the FPZ for rock. This criterion assumes that the formation of FPZ takes place when the local maximum principle stress in the vicinity of the crack tip reaches the ultimate tensile strength of the rock The shape of the FPZ is shown in Figure 3.9 and the governing mathematical expression is as follows:

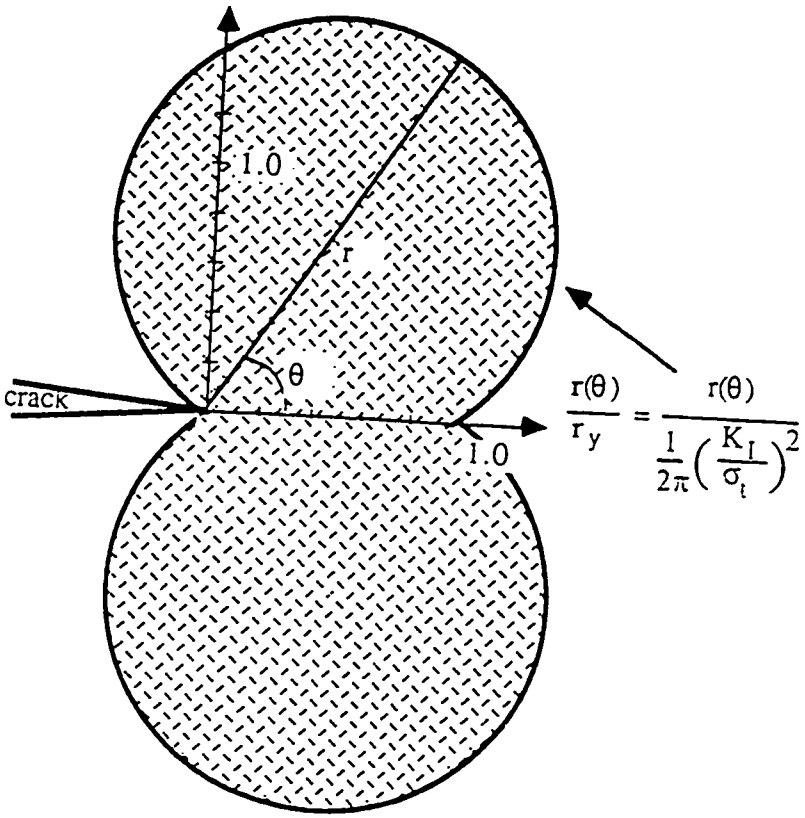

Figure 3.9: Fracture Process Zone for a Typical Rock [after whittaker *et al.*, 1992].

$$r(\theta)=\frac{1}{2\pi}\left(\frac{K_I}{\sigma_t}\right)^2\cos^2\frac{\theta}{2}\left(1+\left|\sin\frac{\theta}{2}\right|\right)^2 \tag{3.20}$$

From Equation (3.20) the maximum extension of FPZ, r_{mc}, can be calculated to take place at $\theta = 60^\circ$ at which the magnitude of r_m is

$$r_{mc}=\frac{27}{32\pi}\left(\frac{K_{IC}}{\sigma_t}\right)^2 \tag{3.21}$$

Where,

r_{mc} = maximum size of FPZ (radial distance from crack tip);

K_{IC} = pure mode-I critical stress intensity factor; and,

σ_t = tensile strength.

Specimens tested under mode-I are more sensitive to the size of FPZ. For the specimens tested under mixed mode I-II, stresses in the vicinity of crack tip are a combination of shear and normal stresses. For notched Brazilian disk specimens normal stresses change from tensile to compressive as the crack inclination with respect to loading direction increases (i.e. $\beta > 30^\circ$). Due to this compressive nature of the stress, the crack tip tends to close. As a result, the associated microcracking and, hence, the FPZ is less likely to develop. A similar situation occurs when the specimens are tested under a confining pressure. Confining pressure induces compression at the crack tip and, therefore, tries to inhibit the development of microcracks in the vicinity of crack tip.

3.2.3 Specimen size

The specimen size requirement for a valid and representative fracture toughness value of a material has been a matter of controversy among the researchers. The criterion of size requirement for rock material has been adopted from what was proposed initially for metals and was introduced by Schmidt (1976) in the form of the following mathematical expression:

$$\left.\begin{matrix} a \\ (D-2a) \end{matrix}\right\} \geq 2.5\left(\frac{K_{IC}}{\sigma_t}\right)^2 \tag{3.22}$$

and,

$$B \geq r_{mc} = 0.269\left(\frac{K_{IC}}{\sigma_t}\right)^2 \tag{3.23}$$

where,

a = crack length (2a for Brazilian disk);

D = diameter of the specimen;

B = thickness of the specimen;

r_{mc} = critical FPZ (radial distance from the notch tip)

σ_t = tensile strength; and,

K_{IC} = pure mode-I stress intensity factor.

More recent studies on fracture toughness has confirmed that the above-mentioned criterion of minimum crack length vary from case to case and is not strictly valid for all rocks and test methods [Lim *et al.*, 1994-c]. It has been proved by a number of researchers that the factor of 2.5 in the above expression of minimum crack

length (Equation 3.22) is somewhat conservative and a factor of less than 2.5 has been reported for most rocks. A summary of the minimum crack length studies provided by Whittaker *et al.* (1992) suggested that the multiplication factor in the above equation could range between 1.5 and 2. A more recent study on the subject of minimum crack length for valid fracture toughness value has been conducted by Lim *et al.* (1994-b). They documented a comprehensive list of a minimum crack length required for valid fracture toughness testing for different rocks. The results are presented in Table 3.1. It can be seen that the minimum crack length depends on both the type of material and the testing technique. The crack length is varying over a large range, however, a crack length between 3 and 10 mm is seen to be more common. Contrary to the effect of crack length, the effect of specimen thickness (B) seems to be less sensitive [Whittaker *et al.*, 1992].

In practice, a minimum required specimen dimension (thickness or crack length say H) for plain strain fracture toughness testing can be found by measuring the apparent fracture toughness for specimens with constant other dimensions but with different H values and plotting the fracture toughness results against H to determine the point from which fracture toughness is independent of H [Whittaker *et al.*, 1992].

3.2.4 Confining Pressure

Fracture toughness behavior of a deep-seated rock formation requires the testing to be conducted in a manner that is simulating the important *in-situ* conditions such as confining pressure. Estimates based on field data have indicated representative

Table 3.1: A comparison of Minimum Crack Length (a_m) for Valid Fracture Toughness Testing [after Lim *et al.*, 1994-c].

Rock Type	K_{IC} MPa $\sqrt{mm}$	σ_t MPa	a_m (mm)	$\frac{a_m}{\left(\frac{K_{IC}}{\sigma_t}\right)^2}$	Test Method
Westerly granite	85.40	13.64	50	1.28	CT
Stripa granite	55.00	10.00	10	0.33	SECRBB
Colorado oil shale	32.24	13.56	10.77	< 1.89	SCB
Indiana limestone	30.67	8.49	50	1.54	SECB
Welsh limestone	26.88	2.87	25	2.50	SCB
Fine grained sandstone	19.44	2.65	10	<0.22	CSTBD
Coarse grained	11.07	3.34	10	0.57	SCB
Fine grained sandstone	8.70	0.42	10	1.47	SCB
Johnstone (w = 18%)	1.6	0.42	6	< 0.41	SECB
Johnstone (w = 18%)	1.95	0.42	3	0.14	SCB

CT Compact Tension specimen.
SECRBB Straight-Edge Cracked Round Bar Bend under three point bending.
SCB Semi-Circular specimen under three point Bending.
CSTBD Cracked Straight Through Brazilian Disk under diametral compression.
SECB Straight Edge Cracked Round Bar Bend under three point bending.

hydrofracture toughness parameters of one to two orders of magnitude higher than the values determined at ambient conditions [Shlyapobersky, 1985]. Several studies on quarried rocks have showed a significant increase in mode-I fracture toughness with an increase in the confining pressure. The measured data show a considerable scatter, but an increase which is roughly linear with the confining pressure has been observed [Thallak *et al.*, 1993].

The literature shows that most of the studies related to fracture toughness under confining pressure have been limited to mode-I condition. Moreover, a specimen type other than the Brazilian disk has been used in such investigations. Due to the fact that the actual crack propagation in rock is under a force field of mode-I and mode-II (i.e., Mixed mode I-II) and since the only way to obtain samples from a deep-seated rock formation (i.e., reservoir) is through coring cylindrical specimens, it is a matter of potential interest to investigate the fracture toughness for mixed mode I-II loading condition using a disk type specimen.

3 .2 .5 Temperature

The study of temperature effects on the fracture toughness of rock is valuable from practical applications point of view. Rock formations at larger depths have temperatures considerably higher than the ambient which is generally used during laboratory based study. Many studies have been focused on the mechanical and transport properties of the rocks at elevated temperature. However, little attention has been paid to the fracture toughness and in particularly mixed mode I-II fracture

toughness under simulated reservoir temperature conditions. Studying fracture toughness behavior at elevated temperatures is valuable for a number of practical situations such as hydraulic fracturing used to enhance oil and gas recovery from a reservoir and the disposal or safe storage of radioactive wastes in underground cavities.

3 .3 Crack Propagation

Propagation of a crack in engineering materials including rocks can cause failure. Knowledge of the stress state under which a crack propagates and the trajectory along which it follows during its growth, is thus very important for the design of structures. During the last two decades, much theoretical and experimental work has been applied to predict the initial crack growth angle and the crack propagation path. So far, significant progress has been made in this field and various theories, based on Linear Elastic Fracture Mechanics (LEFM), have been developed for engineering materials. However, the application of (LEFM) to materials like rocks, concrete and ceramics, is still under development [Degiorgi *et al.*, 1995].

When a specimen with a pre-existing crack is subjected to a compressive force, stresses concentrate at the vicinity of the crack tip. When the externally applied stress exceeds a certain value, the crack at the tip starts propagating until it reaches the boundaries of the specimen resulting in the breaking of specimens into two halves. Two types of crack growth patterns are recognized in the materials. The crack growth which is under load or displacement control is called stable crack growth. The other

type is called the unstable crack growth and is almost instantaneous and out of control. Generally, it has been found that the crack propagation depends upon a combined effect of loading type, material properties, and the geometry of the specimen [Xedakis *et al.*, 1997].

Several theories regarding crack propagation have been formulated in the past. Among them, the theory of maximum tangential stress is considered to be more reasonable (Section 2.5.1). It assumes that crack propagates along a path normal to which the tangential stress is maximum. Apart from the nature of the stresses at the crack tip, the crack propagation also depends upon the degree of the sharpness of the crack tip. Tirosh and Catz (1981) analyzed the problem of crack propagation in a body with a preexisting crack and subjected to compressive forces taking into consideration the effect of the crack tip radius. Figure 3.10 shows a relationship between the crack inclination angle with respect to the loading direction and the crack initiation angle for different conditions of normalized crack tip radius (ρ/a), in which ρ and a represent the crack tip radius and crack length, respectively.

Brazilian disk geometry with central straight through crack was used in the present work for mixed mode I-II fracture toughness study. The disk with a symmetrically oriented central inclined crack was subjected to a diametrical compression till failure occurred. Usually the crack starts extending from the tip and follows a curvilinear path until it reaches the two loading points. This results in the breaking of the disk into two halves. The direction of crack initiation, θ, is easily measured from the broken pieces. In this study, the crack initiation angle was plotted

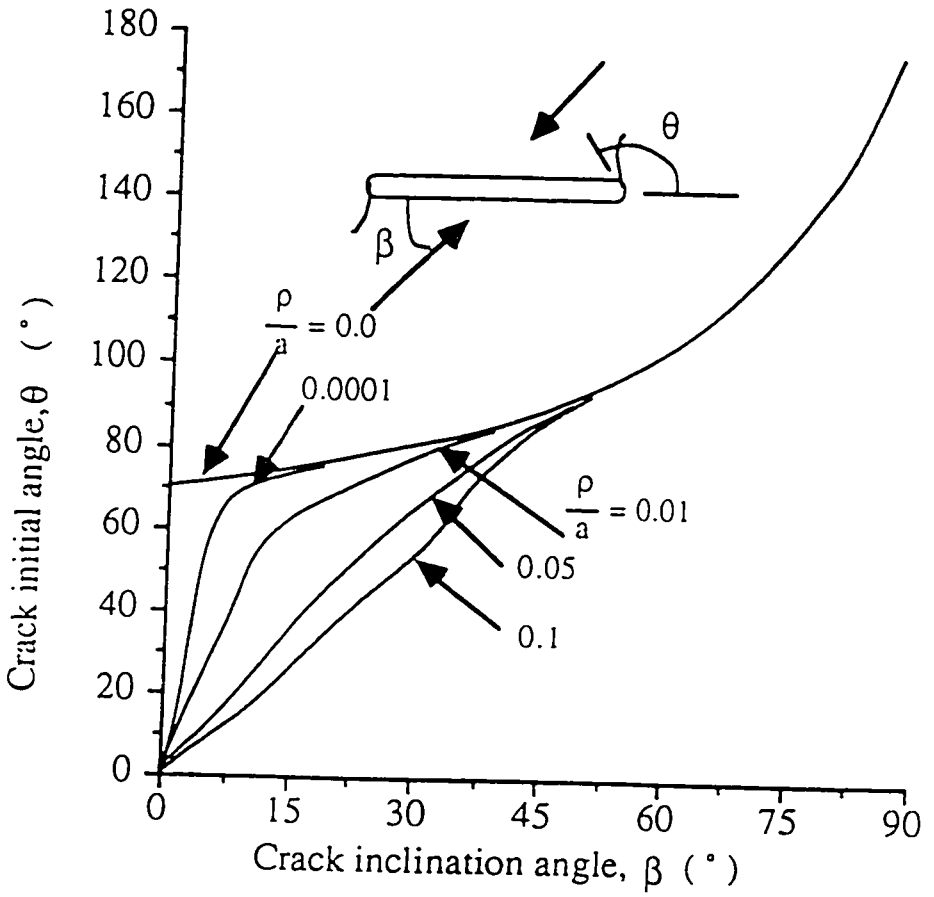

Figure 3.10: Variation of Crack Initiation Angle with Crack inclination Angle for Specimens Subjected to Compressive Loads [after Tirosh and Catz, 1981].

against the crack inclination angle, β, and the results were compared with the theoretical predictions.

3 .4 Fracture Toughness Envelope

Numerous theoretical approaches have been made to best represent the fracture toughness results under mixed mode I-II loading condition. However, among all of them, the following three have been extensively reported in the literature:

(i) The maximum tangential stress ($\sigma_{\theta max}$) criterion

(ii) The maximum energy release rate (G_{max}) criterion

(iii) The minimum strain energy density (S_{min}) criterion

Many researchers have performed experimental work to see how well the above-mentioned theoretical fracture loci predict the experimental results. Ingrafea (1981) conducted mixed mode I-II fracture toughness testing using four point bend geometry for westerly granite and determined the fracture toughness envelope. He concluded that the S_{min}-criterion was the best to fit the experimental data. Kenner *et al.*, (1982) determined the fracture locus of an anisotropic rock of shale also using four point bending loading configuration and came to the conclusion that the G_{max}-criterion was a good representation of the experimental results.

The available experimental data shows that no distinct theoretical failure criterion is applicable to all cases. Moreover, due to the fact that the above-mentioned failure criteria were developed based on the tensile loading rather than the

compressive, many researchers have recommended to rely on empirical relations for practical applications.

Huang and Wang (1985) and Sun (1985) have used three empirically based equations of straight line, ellipse, and homogenous quadratic to fit the experimental fracture toughness data. It was concluded that the homogenous quadratic fitted the results well in all cases. The forms of the empirical relations are as follows:

$$\frac{K_I}{K_{IC}} + \frac{K_{II}}{K_{IIC}} = 1 \tag{3.24}$$

$$\left(\frac{K_I}{K_{IC}}\right)^2 + C\left(\frac{K_{II}}{K_{IIC}}\right)^2 = 1 \tag{3.25}$$

$$\left(\frac{K_I}{K_{IC}}\right)^2 + C\frac{K_I K_{II}}{K_{IC} K_{IIC}} + \left(\frac{K_{II}}{K_{IIC}}\right)^2 = 1 \tag{3.26}$$

Where, C is a constant.

Equations 3.24, 3.25, and 3.26 represent a straight line, ellipse, and a quadric, respectively. Apart from the above-mentioned empirical relations, the following form has also been used.

$$\left(\frac{K_I}{K_{IC}}\right)^\alpha + \left(\frac{K_{II}}{K_{IIC}}\right)^\alpha = 1 \tag{3.27}$$

A value of 1.6 for α was reported by Awaji and Sato (1978) for graphite and plaster, and 2 for marble. Lim *et al.* (1994-b) used a semicircular specimen under three point bending for mixed mode I-II fracture toughness study of a synthetic saturated soft rock. They reported the value of 2.55 for α.

3.5 Indirect Tensile Strength Testing

Indirect tensile strength of rock can be determined by testing uncracked Brazilian disk under uniaxial compression. Because of its relative simplicity and steadiness of the results obtained, this test is the most widely used to determine the tensile strength of rocks and rock-like materials [Andreev, 1995]. The disk is loaded along a diametrical line till failure occurs. The governing expression for indirect tensile strength is in the from:

$$\sigma_t = 2P/\pi BD \tag{3.28}$$

Where,

σ_t = tensile strength;

P = load at failure;

B = thickness of the specimen; and,

D = diameter of the specimen.

3.6 Mineralogical Composition

Mineralogical composition plays an important role towards the strength behavior of a material. The strength and fracture properties of a rock material are dependent both on the relative amount of different minerals present and the interaction among themselves. The most widely used technique for mineralogical identification is the X-ray diffraction (XRD) analysis.

In the XRD analysis, a beam of X-rays is directed towards a representative specimen of the material whose mineralogical composition is required to be analysed. Upon striking the surface of a crystal, X-rays are partly absorbed and partly reflected or scattered at specific inclinations depending upon the type of material present. The absorbed portion of the incident beam by individual atoms at each atomic plane oscillates as dipoles and radiates in all directions. Some of these radiations are in phase and emerge as a coherent beam that can be detected on a photographic film. The orientations of parallel atomic planes, relative to the direction of the incident beam, at which the radiations are in phase, depends on the wavelength (λ) of X-rays and the spacing (d) between the atomic planes. The relationship between the wavelength and atomic spacing is expressed by the following equation proposed by Bragg.

$$n\lambda = 2d\sin\theta \tag{3.29}$$

where,

n = any whole number (i.e. 1, 2, 3, 4,.....etc.) and,

θ = angle between the incident beam and atomic planes.

Since the inter-atomic spacing for each mineral is unique in a three dimensional space, the atomic spacing calculated from the above expression can be used for the identification of minerals. The phase identification involves calculating the 'most likely' for a given phase on the peak intensity when compared to a database of standard phases while the weight fraction is calculated by comparing the intensity of the most intense peaks of that phase with those of standard ones.

3.7 Fractured Surface Study

When Brazilian disks with central notch are subjected to diametral compression with crack inclined with respect to the loading direction, tangential stresses at the crack tip may be tensile or compressive depending upon the crack inclination angle. This tangential stress in combination with varying shear stresses at the crack tip could cause a crack to propagate in a variety of mixed mode I-II fashions resulting in an abrasive action along the failure surface. This abrasion could cause damage or crush the grains along the failure path depending upon the relative amount of each of the two stresses. Microscopic study using Scanning Electron Microscope (SEM) can be conducted in order to investigate the nature of the cracked surface. The fractured surface of the specimens for different crack orientations could be studied to investigate whether or not the crack orientation has any influence on the grain crushing along the failure surface.

Chapter 4

Experimental Program

A comprehensive laboratory testing program was carried out to investigate the variation of fracture toughness as a function of geological and environmental factors, specimen shape, and type of artificially-created cracks. This Chapter describes in detail the material used, specimen preparation, equipment used for specimen preparation and testing procedure employed for various tests. Figure 4.1 shows schematically the various laboratory tests used in this research work.

The experiments can be divided into two main categories: (1) Fracture toughness testing, and (2) Mineralogical and microscopic study using XRD and SEM. The bulk of the experimental work focuses on the fracture toughness determination for both mode-I and mixed mode I-II conditions. Different parameters considered are outcrop vs. reservoir samples, laboratory vs. *in-situ* conditions, effect of notch and specimen shapes and dimensions.

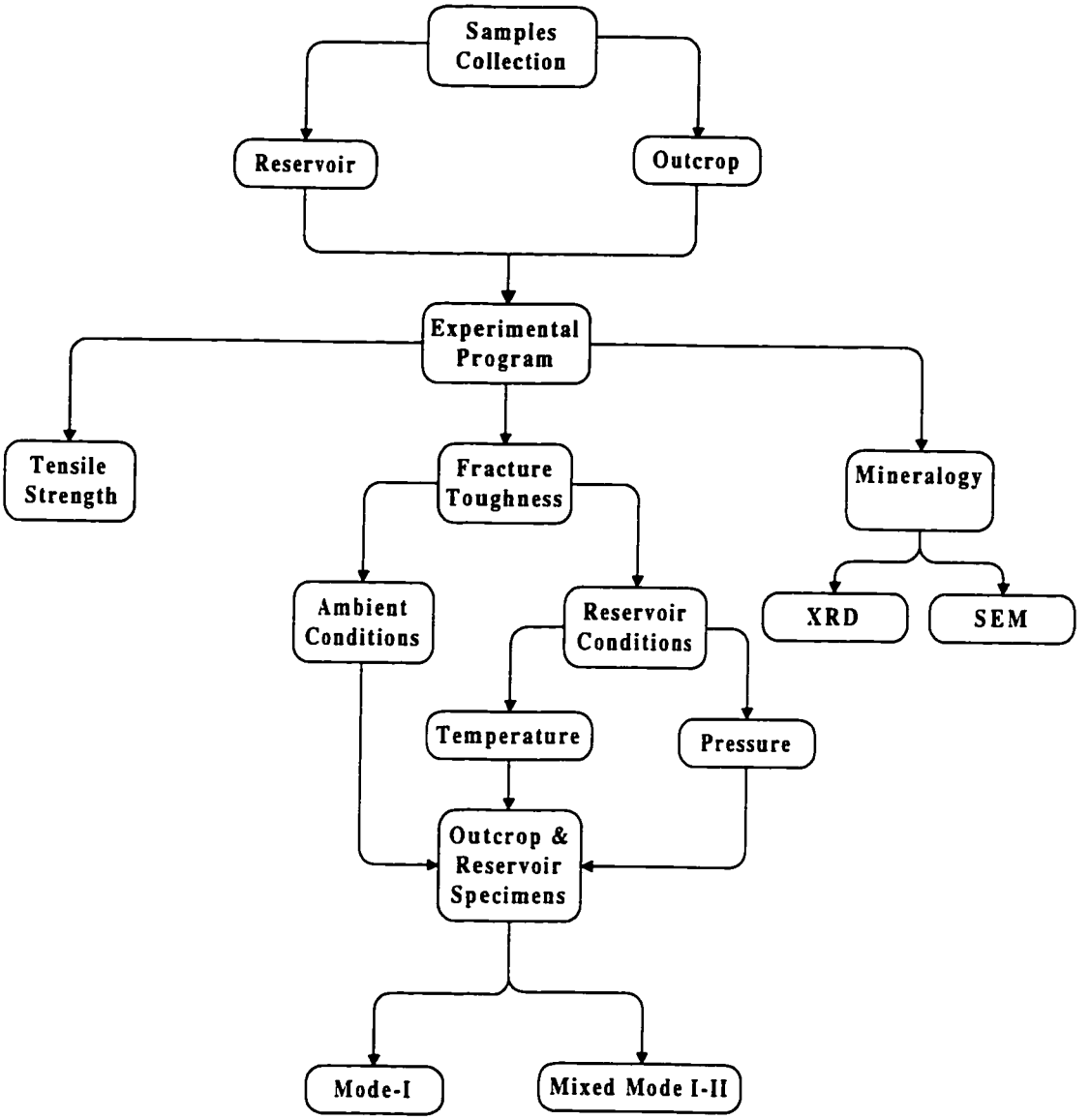

Figure 4.1: Summary of Various Laboratory Tests Used in the Present Study.

4 .1 Geology and Material Description

The Ghawar is the largest oilfield in the world producing oil and gas from multi-reservoir zones from the Khuff formation. The structure of Ghawar oilfield is 280 km in length and 25 km in width, extending north-south in the Eastern Province of Saudi Arabia. These fields from south to north are Haradh, Hawiyah, Uthmaniya, Shedgum, Ain Dar, and Fazran. Figure 4.2 shows the vicinity map of the Ghawar oilfields and those oil fields from where reservoir samples were collected. Outcrop samples were collected in the form of large rock blocks from the same formation when it outcrops in Qassim area. A general trend of the sedimentary rock formation in the region is shown in Figure 4.3. As can be seen, the formation which is about 1000 m deep at one location is outcropping in the form of mountains at other location about 1000 km away.

The Khuff formation in the subsurface of Central and Eastern Saudi Arabia, consists of alternating limestone, dolomite, and anhydrite sequences. The thickness of the Khuff formation increases basinward (from west to east and northeast) from 1,377 to 2,947 ft. In the Ghawar field, its thickness is around 1500 ft. The Khuff formation unconformably overlies the Unayzah formation of Permian age and is conformably overlain by Sudair formation of Triassic age. A siliciclastic basal unit at the bottom of the Khuff formation is called the "Basal Khuff Siliciclastics." Carbonate and anhydrite sequence upward is subdivided to alternating four anhydrite and four carbonate intervals. From top to bottom anhydrite-carbonate pairs are called Khuff A,

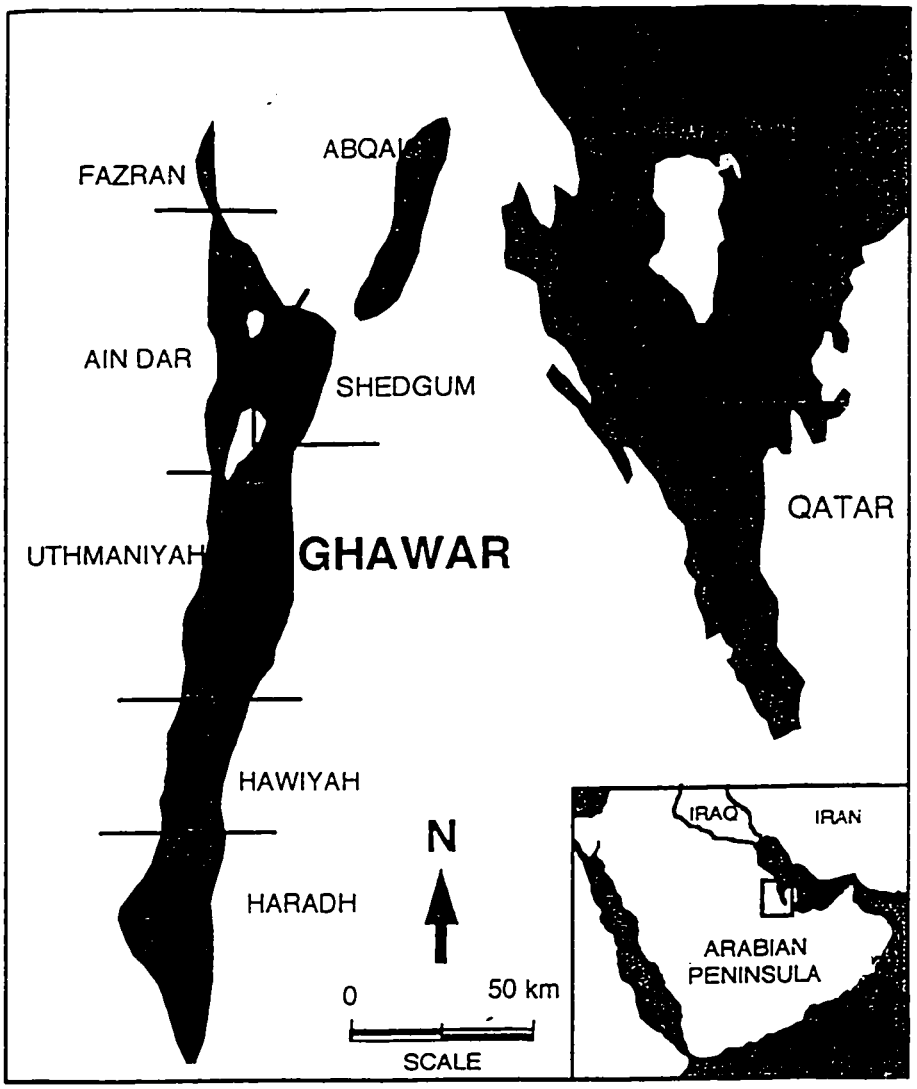

Figure 4.2: Vicinity Map of the Samples Collection Area.

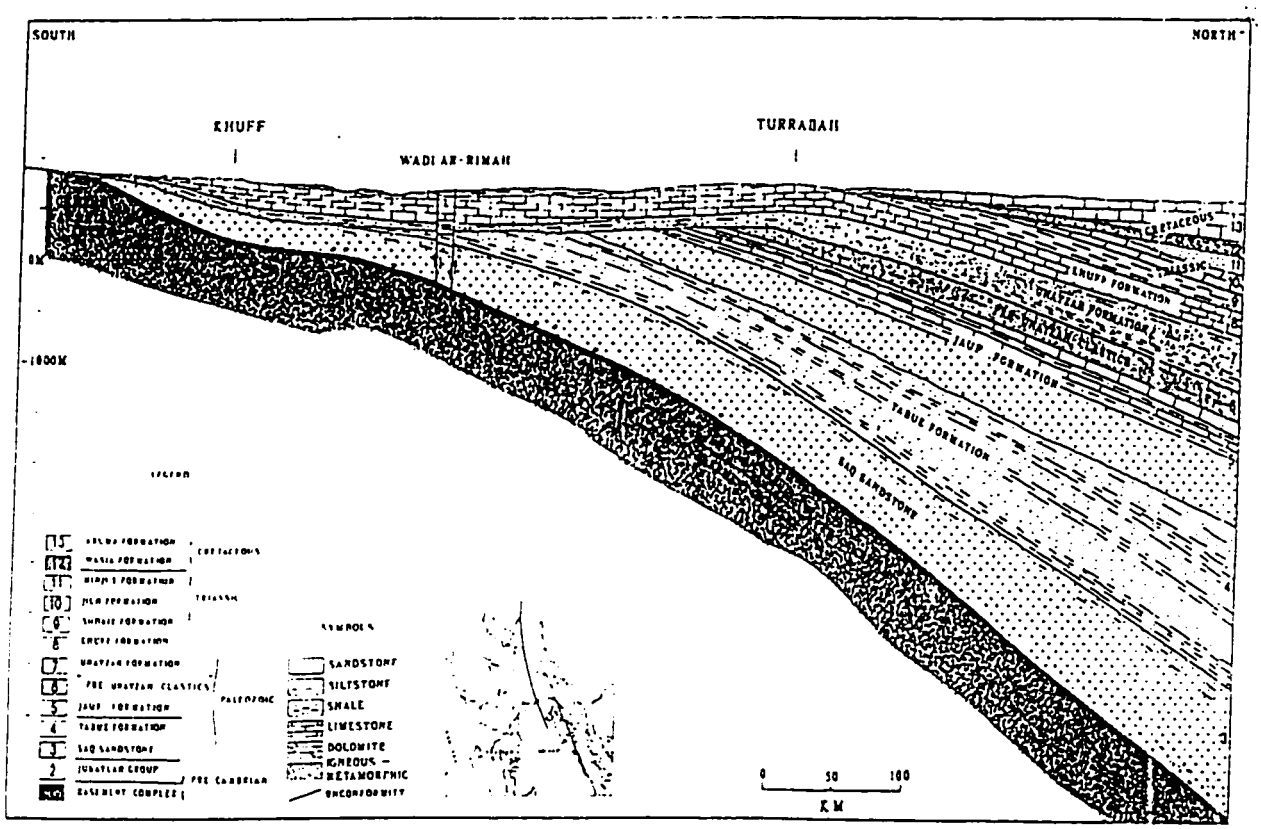

Figure 4.3: A Trend of Sedimentary Rock Formation Showing Outcrop and Deep Seated Rocks in the Same Formation. .

B, C, and D. Khuff A, B, and C are gas reservoir zones. The overlying anhydrite intervals serve as seals.

The reservoir samples were obtained by Saudi Aramco in the form of cores from different depths and their lithology was found to be varying. Moreover, many samples were containing impurities such as anhydrite. To avoid the sample inhomogenuity, the samples from one lithology were selected for which much of the material was available. These samples were mainly chosen from two lithologies namely A, B, and to some extent from lithology C.

4.2 Mineralogical Composition

Mineralogical composition of the outcrop and reservoir specimens was determined by XRD technique. The samples were prepared by crushing the rock material first under the compression machine and then finely grinding the crushed pieces into powder form. Apart from the mineral identification, semi-quantitative analysis of the minerals present was carried out. The analysis was made in the Research Institute (RI) at KFUPM.

4.3 Selection of the Specimen Shape

The choice of a particular specimen geometry for the determination of the fracture toughness is restricted by the amount of the sample available, specimen preparation ease, and the availability of loading system, etc. Since reservoir specimens are obtained from the boreholes using 4 inch diameter coring bits, it is more easy and

practical to use a disk shape specimen geometry. Further, disk shape specimen geometry is suitable for both mode-I and mixed-mode I-II testing. Moreover, it involves less machining required for sample preparation and resists the loads more efficiently thus requiring higher load level to cause failure.

Apart from the circular disk specimens, semicircular disk specimens were also used for the fracture toughness study. The semicircular disk specimen geometry requires half the material required for the full disk specimen geometry. The semicircular specimens can also be used for mode-I and mixed mode I-II fracture toughness study. Therefore, it is more advantageous to use such a specimen geometry. The results of the semicircular specimens used for fracture toughness study were compared with those obtained for the notched Brazilian disk specimens.

For the determination of pure mode-I fracture toughness, a Straight Edge Cracked Round Bar Bend (SECRBB) was used. This testing technique requires less amount of material for sample preparation and the results so obtained are close to those obtained by the ISRM recommended methods [Haberfield and Johnston, 1990].

4.4 Sample Preparation

For the disk shape specimen geometry, the reservoir rock cores of 4 inch (100 mm) diameter were obtained from the Research Institute at KFUPM. For the outcrop samples, 98 mm diameter cores were firstly drilled from large blocks of rock. Although most of the specimens were 98 mm in diameter, some specimens of 3.3 inch (84 mm) were also cored. To have a good quality of cores, the vibrations during

coring process must be avoided. For this purpose, a rock anchoring mechanism was designed and fabricated at KFUPM. The setup involves anchoring of the rock block inside a square box 700 mm in length and 600 mm in height by four vices attached to the sides of the box. Figure 4.4 shows the photograph of the anchoring setup. The coring machine is rigidly screwed to a platform above the box. After properly securing the rock inside the box, the coring bit is lowered and cores are drilled from the rock block.

In the preparation of the round bar bend specimens, circular rods were cored using a 25 mm coring bit. The length of the specimens was restricted by the height of the rock block available for coring typically, 150 mm. Furthermore, such specimens were available only for the outcrop samples. Reservoir specimens were collected in the from of 100 mm diameter cylindrical cores. Coring small size rods from such cores was both difficult and involved loss of material. To remain consistent with the orientation of reservoir specimens, outcrop samples collected from the field were marked for their vertical orientation and cores were obtained parallel to the marked vertical direction. Both the outcrop and reservoir cores were sliced into 24 $\pm$ 2 mm thick disks using a high speed saw. In addition, some specimens were sliced with thickness ranging from 11 to 22 mm to study the effect of specimen thickness on fracture toughness. A diamond impregnated 2 mm thick saw blade was used for slicing the cores. Figure 4.5 shows the sliced disks and the circular rod specimens cored from the outcrop samples. The sliced disks were then leveled using a rough sand paper to have a uniform thickness. The disks were further rubbed against a relatively

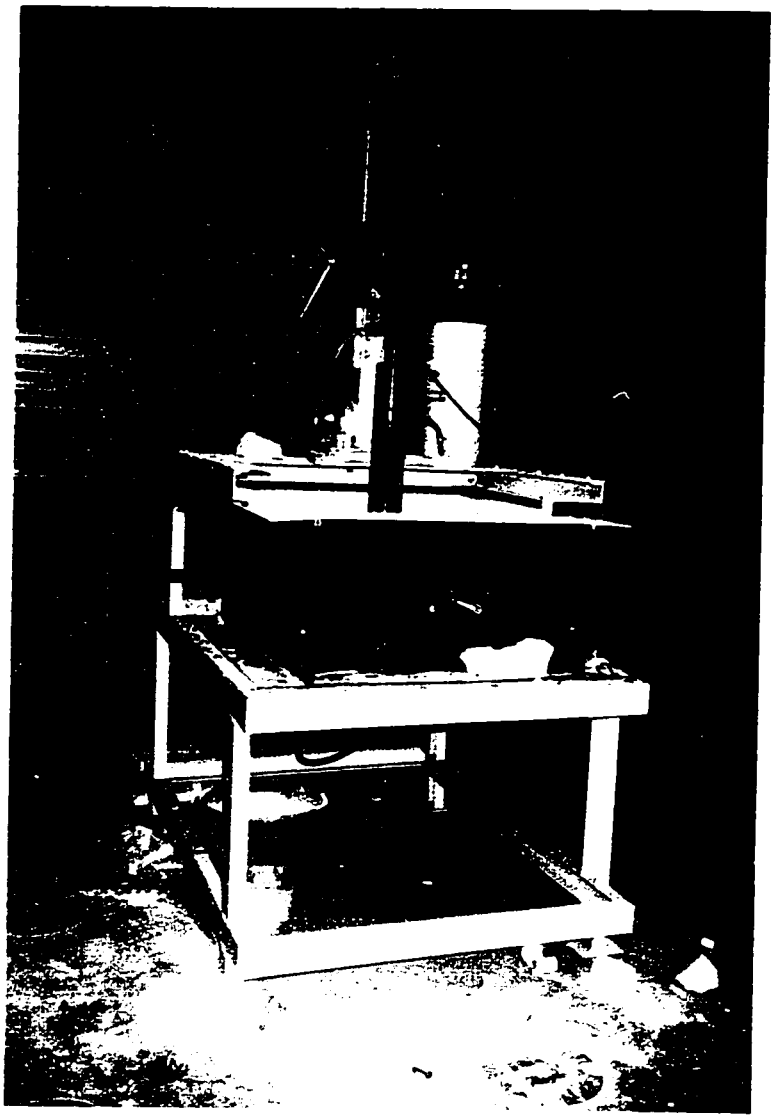

Figure 4.4: Rock Anchoring Mechanism with the Coring Machine Fixed Above.

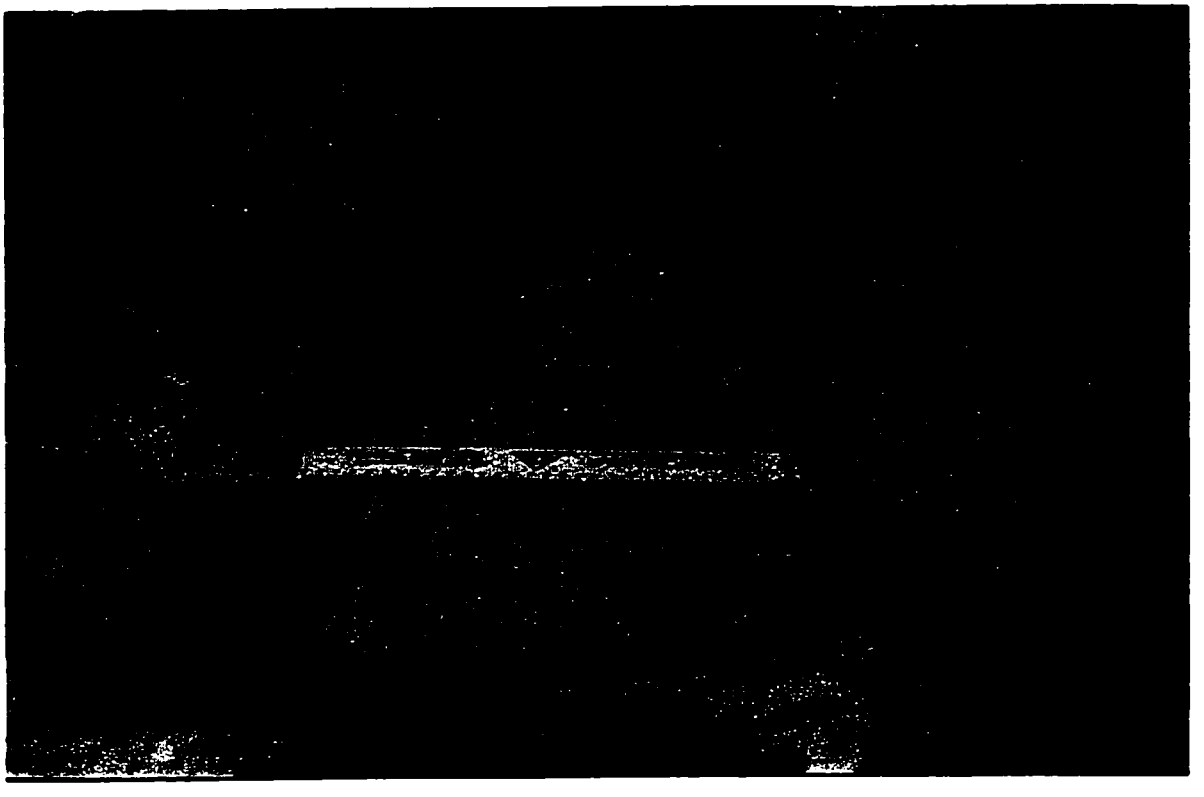

Figure 4.5: Sliced Disk and Circular Rod Specimens.

smoother sand paper to make their surfaces level and smoother to facilitate the attachment of the crack extensometers. Leveled disks, ready for making notches are shown in Figure 4.6.

For the preparation of the semicircular specimens, sliced full disks were cut into two pieces along the diameter. The two halves obtained were a bit smaller than the exact semicircular shape. However, it has been reported by [Lim *et al.*, 1994-c] that this small difference does not affect the estimated stress intensity factor appreciably.

4 .5 Notches

After slicing the disks, the next step was to make notches through them. Two types of notches, namely straight and Chevron notches, were used. As mentioned earlier, most of the mathematical expressions used for the determination of fracture toughness are based on the assumption that the Linear Elastic Fracture Mechanics (LEFM) is applicable. To ensure the applicability of the LEFM, fracture process zone should be as small as possible. This can be achieved partly using the larger specimen size (i.e. 100 mm) and partly using the small notch length. The crack length used in the present study was restricted by the size of the crack extensometers. Keeping in mind this fact, notch length was kept to a smaller value (a/R = 0.1 to 0.4). The dimensions of specimens and other related parameters are summarized in Tables 4.1.

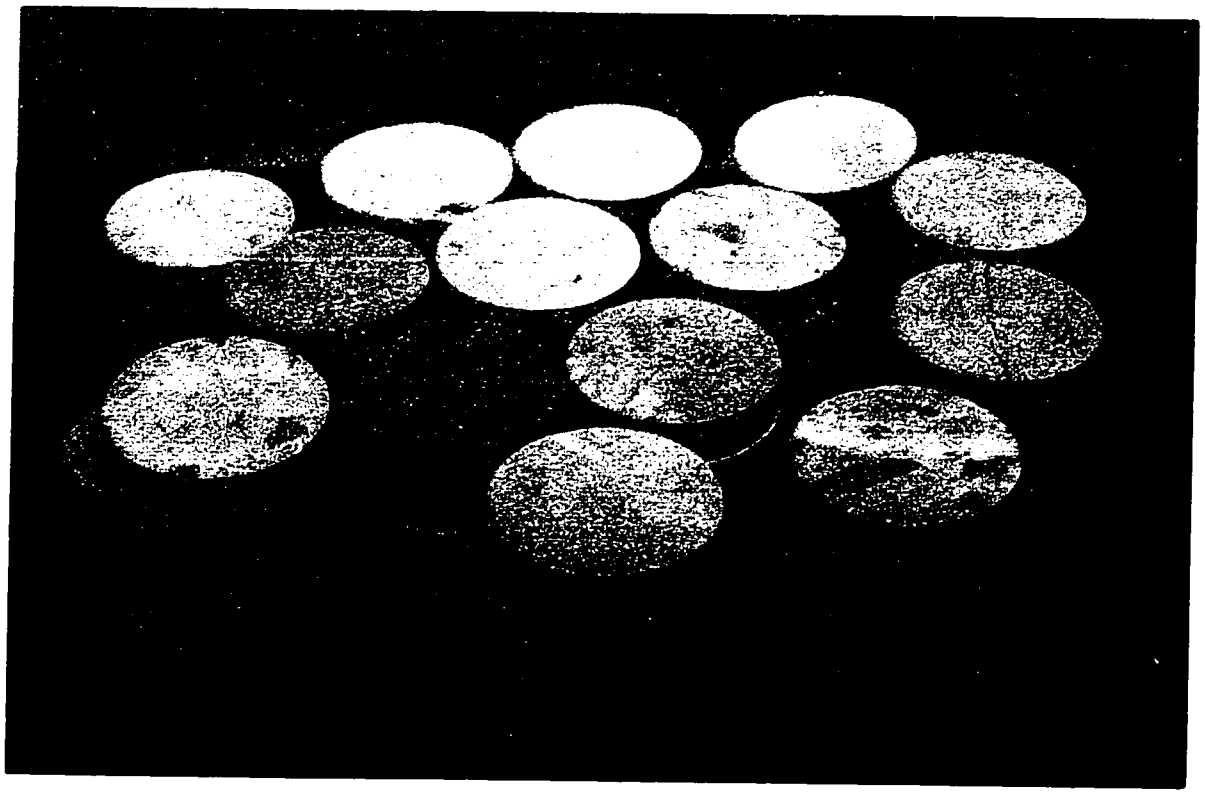

Figure 4.6: Leveled Disks Ready to be Notched.

Table 4.1: Summary of Specimen Dimensions Used in This Study.

Specimen Type	Radius (mm)	Crack ratio (a/R)	Thickness (mm)	Span (mm)
Circular disk	42-52	0.1-0.5	11-26	-
Semicircular disk	49-52	0.3	22-26	80
Circular rod	12	0.1-0.5	-	108

4 .5 .1 Straight Notch

Straight notches were made using a wire saw. A photograph of the saw is shown in Figure 4.7. A diamond coated wire of 0.25 mm diameter was used to make the notch. In order to make the notch through the disk, a through hole was first drilled in the center of the disk using a 3 mm bit. In this process, disk was fixed in the rotating lathe machine and the drilling bit was moved in the horizontal plane to strike the disk in the center. For making a notch, the diamond coated wire of the wire saw was then passed through the central hole and the saw was started to make notch of desired length along a prescribed line. Notch of any length was possible to machine and the difficulty associated with machining small notches in Brazilian disks, as reported by Fowell and Xu (1994), was overcome.

For the semicircular specimens, disks were first cut into two halves using a high speed saw. The semicircular disks were marked for the required orientation and length of the notch. The notches were then machined using the wire saw. Notched Brazilian and semicircular disks are shown in Figure 4.8.

4 .5 .2 Chevron Notch

The Chevron notches were made using a slow speed circular saw (Figure 4.9). Rock disks were first marked on both sides along the diameter of the disk for the two extreme points upto which the crack was supposed to be cut. The marked disk was then pressed against the circular rotating disk of 80 mm (3 inch) diameter and 2 mm

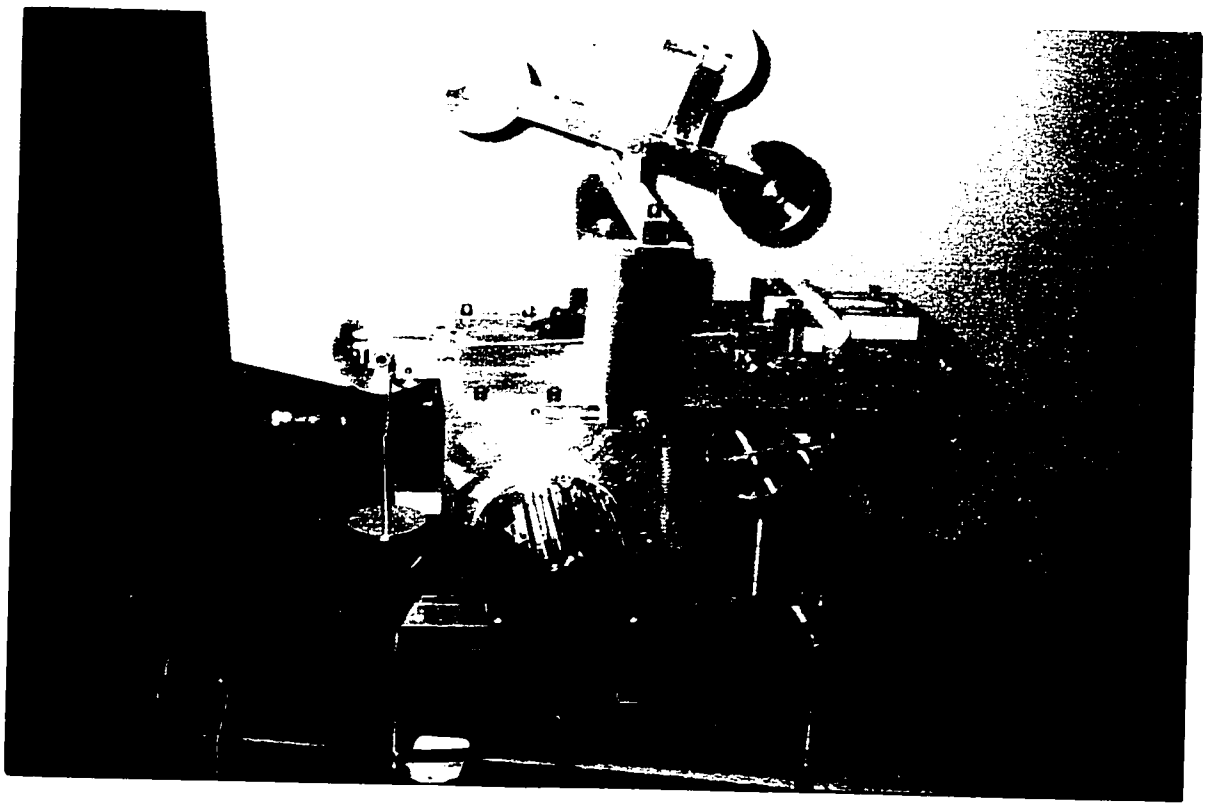

4.7: Wire Saw Used for Making Straight-edge Notches in Rock Specimens.

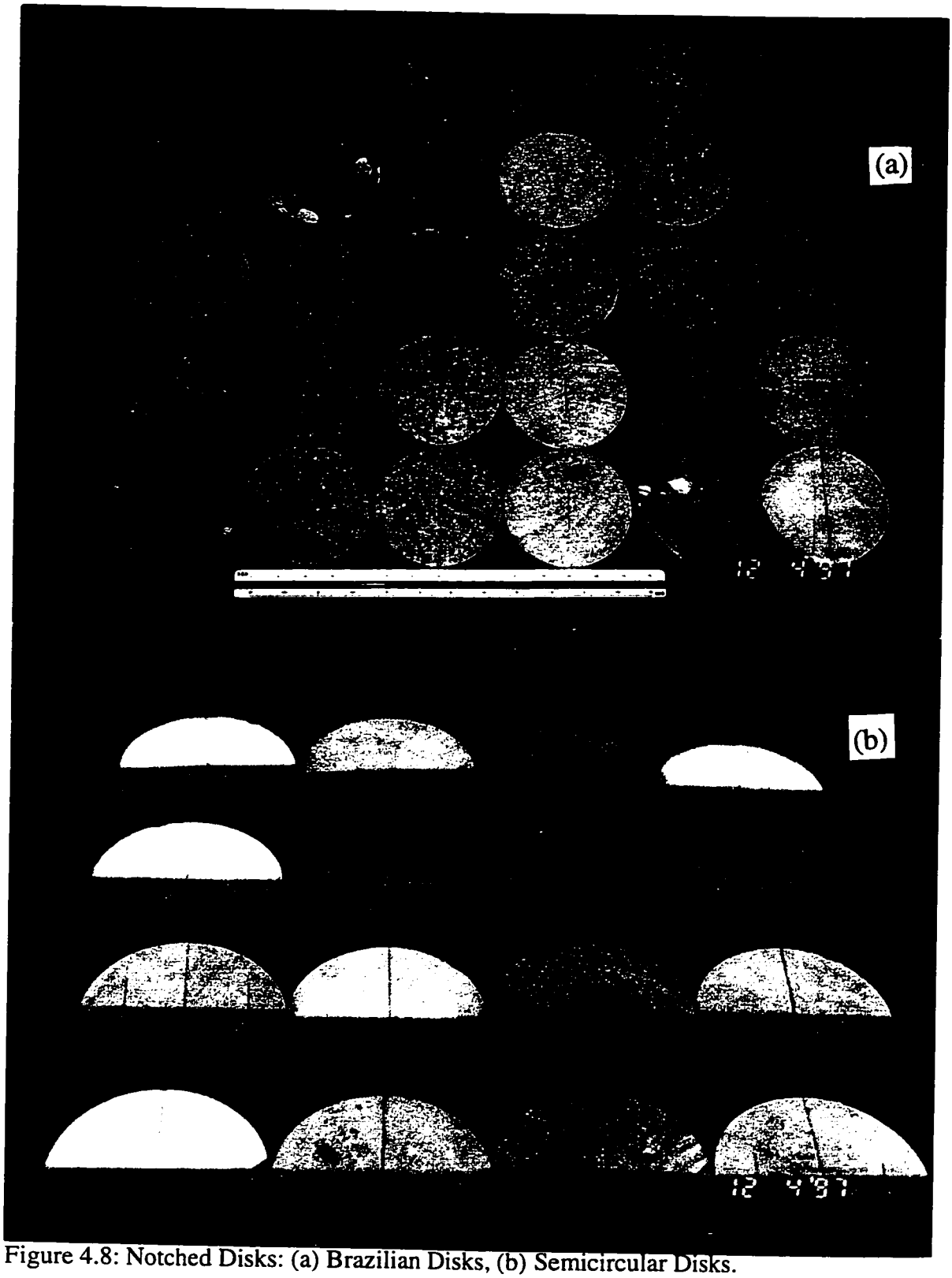

Figure 4.8: Notched Disks: (a) Brazilian Disks, (b) Semicircular Disks.

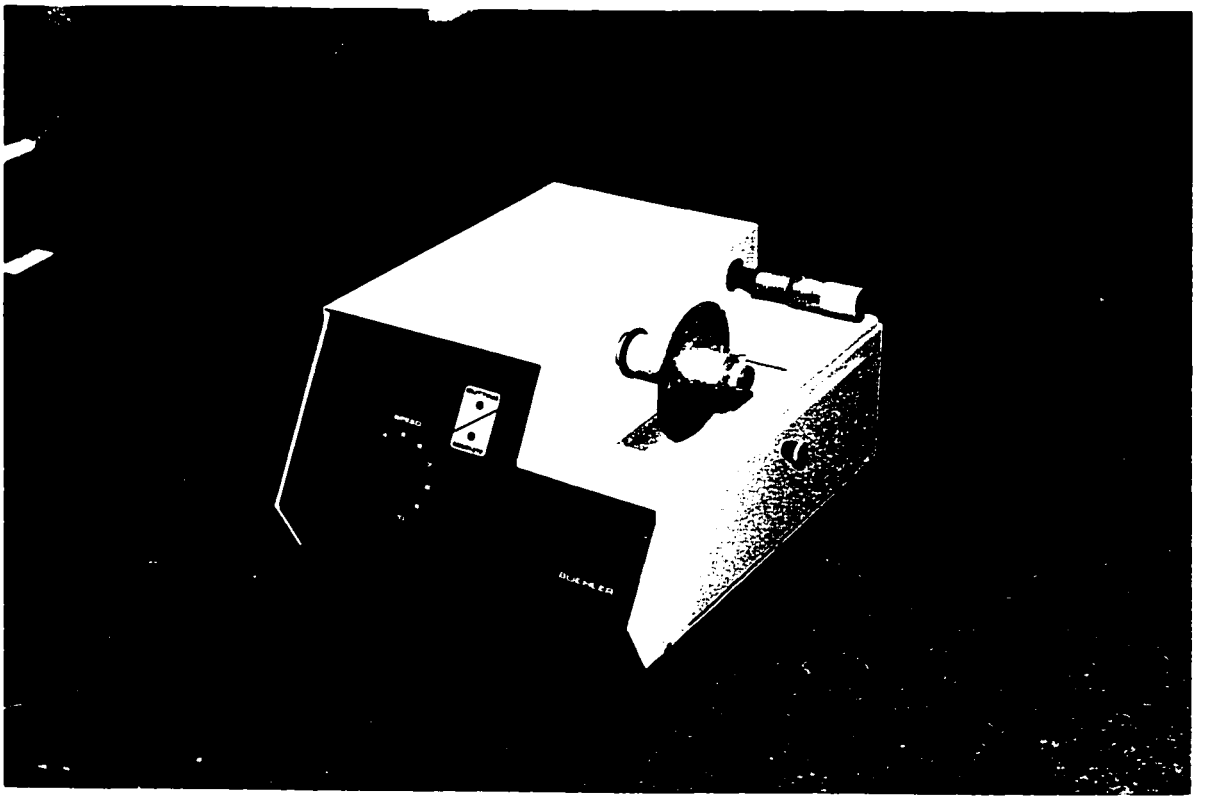

Figure 4.9: Slow Speed Circular Saw Used for Making Chevron Notches in Rock Specimens.

thickness. When the saw reached the two marked extreme points, the disk was removed against the rotating saw. The disk was then rotated and the same procedure was repeated from the other side of the disk. This left a central opening of 15 mm. The length of the extreme point on each side from the center along the diameter of the disk was 30 mm. During the notch-making process, disks were held manually against the saw. Therefore, the dimensions and the crack geometry was difficult to control precisely. However, it is assumed that such errors were negligible and did not effect the fracture toughness measurements appreciably.

4 .6 Fracture Toughness Testing under Ambient Conditions

4 .6 .1 Testing Equipment

A strain-controlled loading frame having a capacity of 100 kN was used for the load application. Brazilian disks were placed on a smooth steel base and a small (8 mm in diameter) circular rod was placed on top of the disk. A solid circular steel piece having a longitudinal groove was placed over the rod so that the rod fits into the groove. Initially, circular rod specimens were tested under three point bending over a range of strain rate varying from 0.005 mm/min to 0.1 mm/min. After that, a strain rate, viz., 0.08 mm/min, was chosen for which no variation in fracture toughness was observed. The applied load, load point displacement, and crack opening were acquired using a data logger and recorded in a personal computer.

During testing, the recorded deformation is composed of two parts, namely, the deformation of the specimen and longitudinal extension of the studs used to support the loading frame. The axial deformation or extension of the studs depends upon both their rigidity and as well as on the strength of the specimen being tested. To investigate how appreciably the deformation of the loading system is contributing to the total recorded deformation during testing, the platform was loaded using steel blocks instead of the rock specimen and the deformation was recorded for the maximum anticipated load during specimen testing (i.e., 3000 kg). It was found that the deformation of the system was in the range of 3 to 7% of the total deformation recorded during the testing of a rock specimen. Because of its small magnitude compared to the total deformation and the fact that the recorded deformation was not used anywhere in the fracture toughness determination, total deformation recorded during sample testing was assumed as the deformation of the specimen.

4.6.2 Crack Extensometers

U-shaped crack extensometers capable of measuring crack extension to the nearest of 0.0001 mm were used in this study to measure crack extension during mixed mode I-II loading under ambient condition. To facilitate the attachment of extensometers to the specimen surface close to the crack boundary, an auxiliary L-shaped assembly was fabricated from stainless steel. This epoxy coated assembly was attached to the specimen on both sides of the crack boundary. The extensometer was then screwed to the assembly. Figure 4.10 shows the crack extensometrs along with the L-shaped

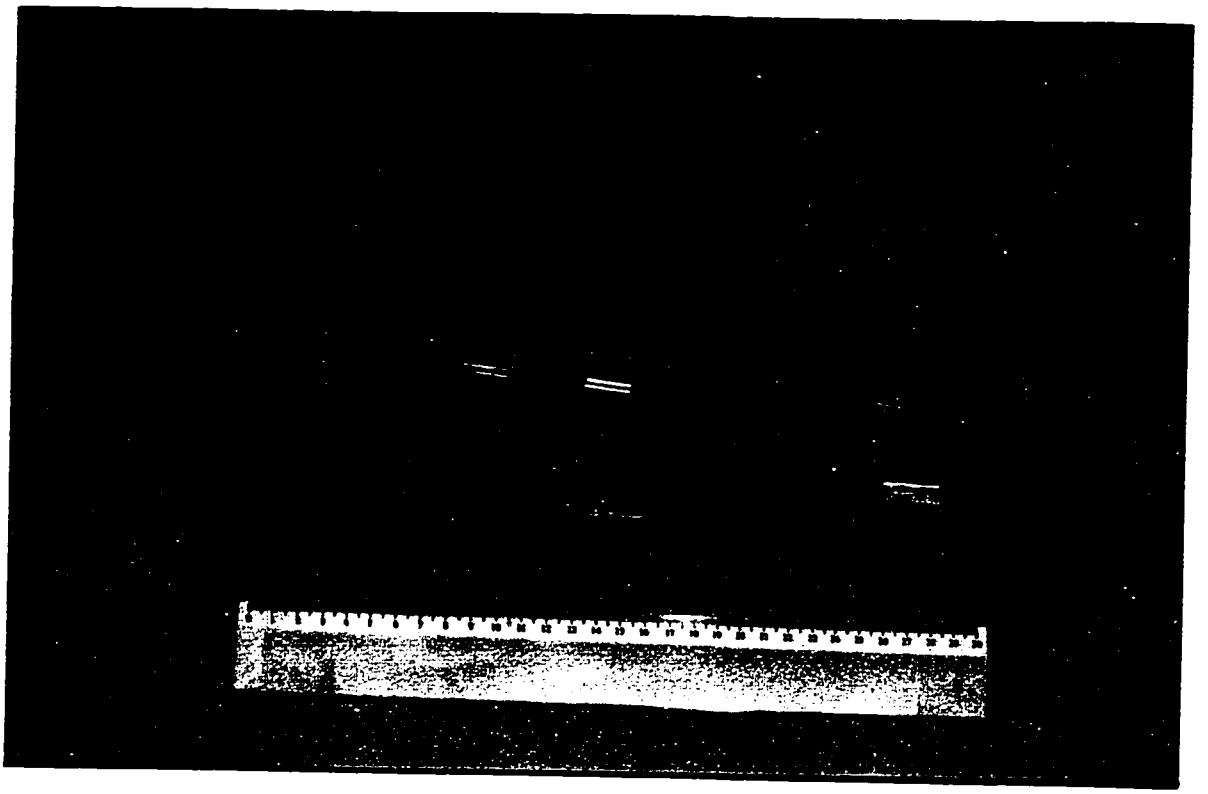

Figure 4.10: Crack Extension Measurement Assembly.

attachment assembly. The extensometers were first calibrated before being used in this experimental program. The extensometers were so sensitive that an opening or closure of 1 mm was reflected by 2040 divisions on the extensometer. This corresponds to a coefficient of 5×10^{-5} which on multiplying with the recorded crack opening divisions, yields crack extension in mm.

4.6.3 Mode -I Fracture Toughness Testing

Under mode-I loading condition, a total of 6 circular rod specimens under three point bending were tested over a range of strain rate varying from 0.005 to 0.1 mm/min. The specimens were 23 mm in diameter and the center to center distance between the supports was maintained at 108 mm. Any span length smaller than this value was restricted by the size of the crack extensometer. The crack to diameter ratio (a/D) was kept at 0.3. Apart from this, some samples were tested using crack to diameter ratio of 0.1 to 0.5 (2 specimens for each case) at a constant strain rate of 0.08 mm/min. A schematic of the experimental setup is shown in Figure 4.11.

4.6.4 Mixed Mode I-II Fracture Toughness Testing

For mixed mode I-II fracture toughness testing, notched circular disks under diametral compression and semicircular specimens under three point bending were used. The details of the testing is describe in the following sections.

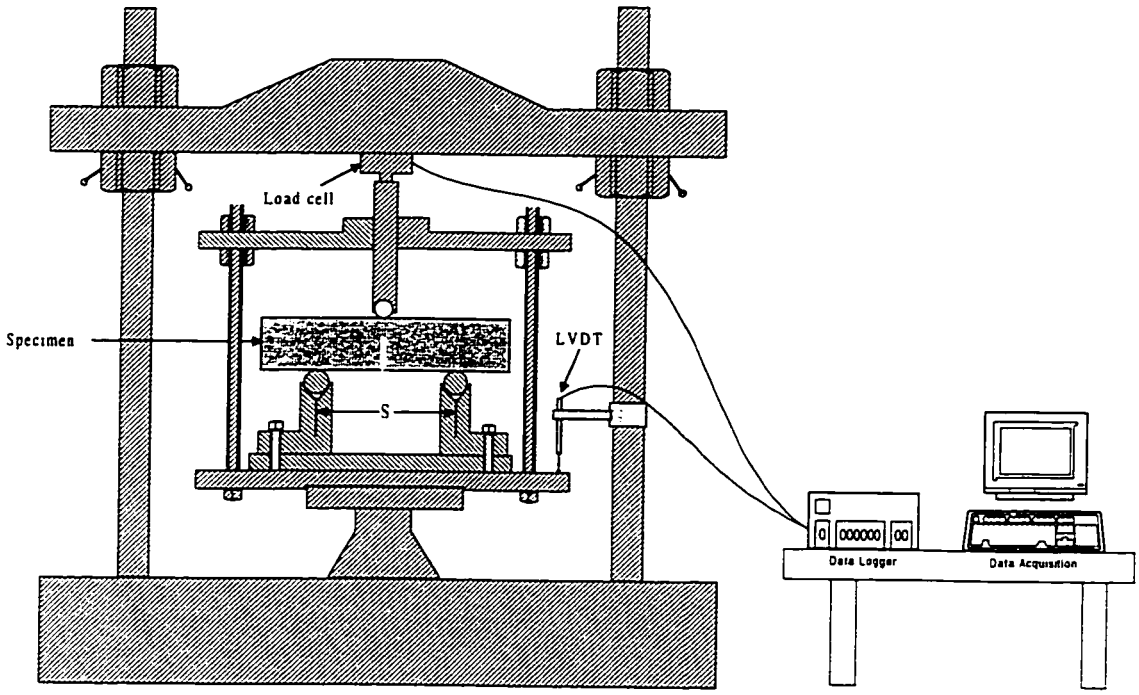

Figure 4.11: A Schematic of the Experimental Setup used for Mode-I Fracture Toughness Testing.

4.6.4.1 Notched Brazilian Disk Specimens

Brazilian disks with both Chevron and straight notches were tested for the mixed mode I-II loading condition. The specimens from outcrop were tested to study the effect of notch type on mixed mode I-II fracture toughness. Reservoir specimens were tested using a straight notch so as to compare them with the same type of specimens from outcrop. A crack length to diameter ratio (a/R) was again maintained as 0.3. Disks were tested with the orientation of the crack with respect to the loading direction varying from 0 to 75 degrees with two specimens for each crack inclination for straight notch and one for Chevron notch. The crack opening and load point displacement were recorded during the testing. Schematic representation of the experimental setup is shown in Figure 4.12.

4.6.4.2 Notched Semicircular Disk Specimens

Semicircular disk specimens were tested under three point bending. Mixed mode loading at the crack tip was achieved by varying the crack inclination from 0 to 60 degrees with respect to the loading direction. Span to diameter ratio (S/R) was maintained at 0.8. Any value smaller than 0.8 was restricted by the presence of the crack extensometer used to measure the crack extension whereas larger span length was restricted by the size of the specimen. To compare the results of the semicircular specimens with the Brazilian disk specimens, straight notch with the crack to radius ratio (a/R) of 0.3 was used. Pure mode-II was not achievable for the semicircular

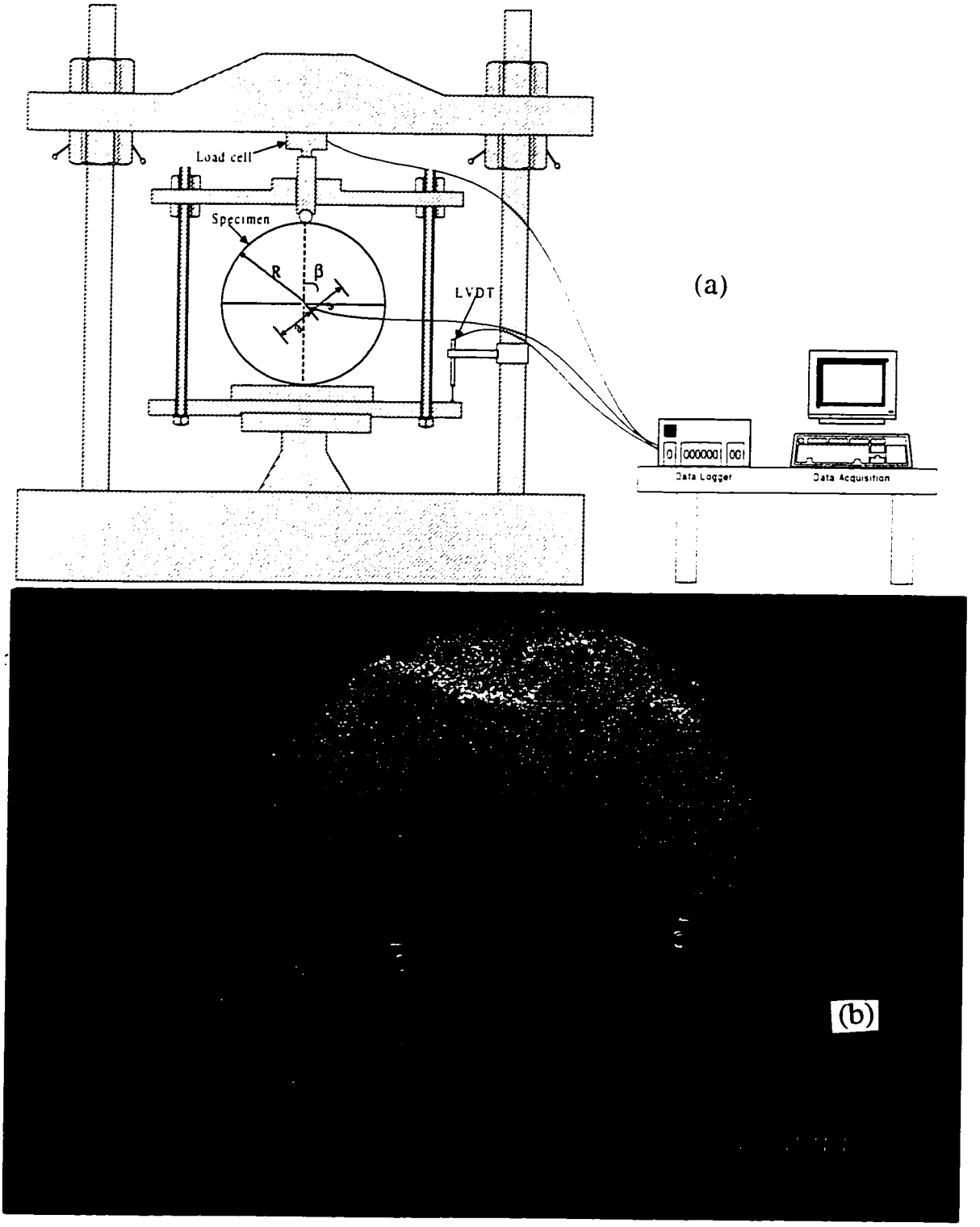

Figure 4.12: (a) A Schematic of the Notched Brazilian Disk Testing Setup, (b) Crack Extensometer Attached with the Disk.

specimens using crack to radius ratio adopted in this study. The load point displacement and crack opening were measured during the testing. Two specimens were tested for each crack inclination. Figure 4.13 shows the schematic view of the loading arrangement.

4.7 Fracture Toughness Testing under *In-situ* Conditions

The fracture toughness behavior of rocks at simulated borehole *in-situ* conditions of temperature and confining pressure was also investigated in this study. The average temperature of the reservoir from which the samples were extracted, is 116 °C. The total confining pressure is 70 MPa (10,000 psi) and the pore pressure is around 49 MPa. Assuming that the usual relation between total and effective stresses exits, a value of around 21 MPa is obtained for the effective confining pressure. However, the samples were tested using an effective confining pressure of 28 MPa to be on the safe side for practical purposes. For the *in-situ* conditions of temperature and confining pressure testing, Brazilian disks with straight through notch were used. Fracture toughness testing under simulated reservoir temperature and confining pressure was achieved using the apparatus fabricated at KFUPM. The methodology of simulating *in-situ* conditions is explained in the following sections.

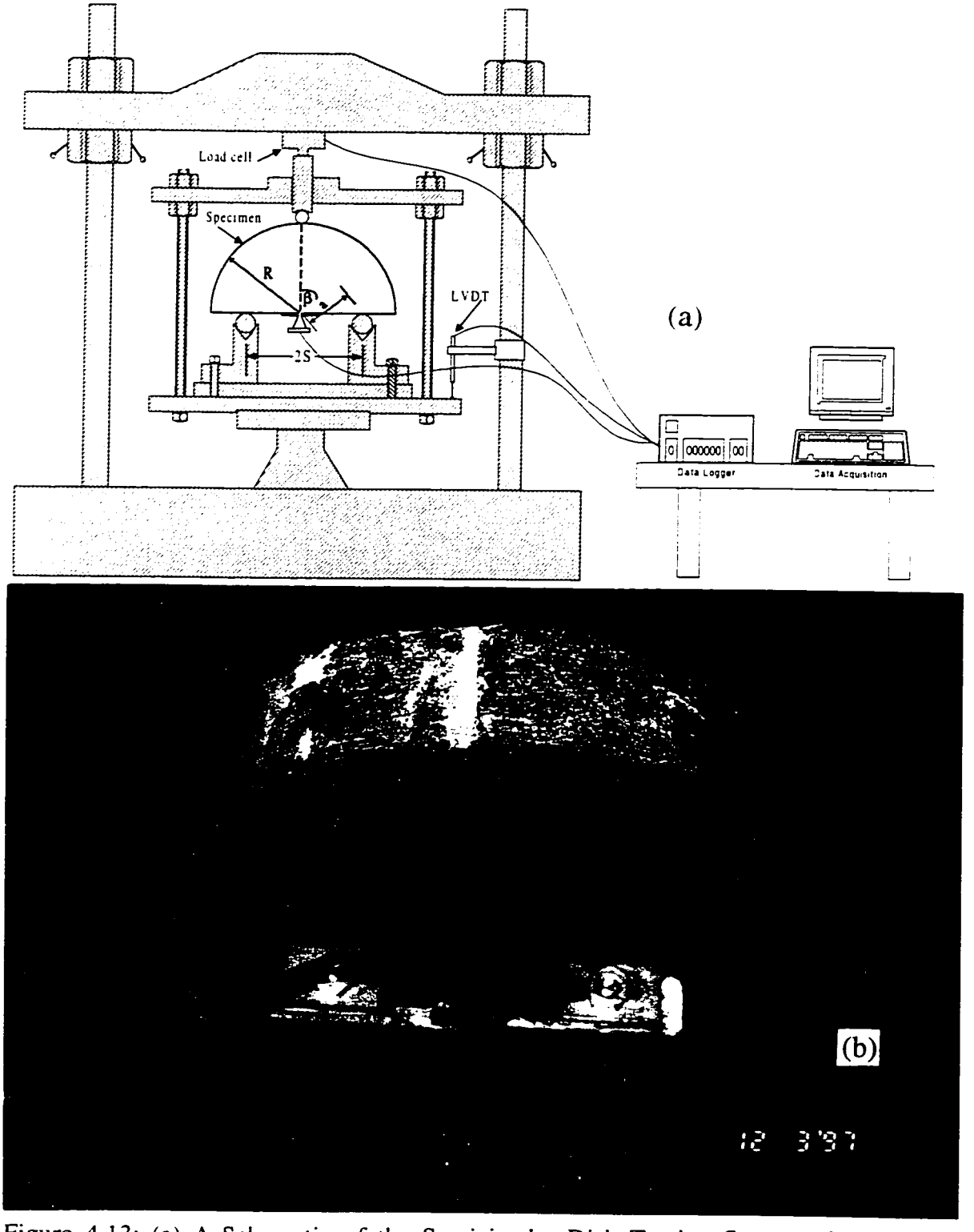

Figure 4.13: (a) A Schematic of the Semicircular Disk Testing Setup under Three Point Bend Loading Configuration, (b) Crack Extensometer Attachment.

4.7.1 Simulation of *In-situ* Confining Pressure

For the fracture toughness testing simulating the *in-situ* conditions of confining pressure and temperature, the compression machine used for the ambient condition was also used here. To achieve the simulated reservoir confining pressure around the specimen, a triaxial cell made of stainless steel was fabricated at KFUPM. Schematic representation of the cell is shown in Figure 4.14.

The disk was first mounted on the prefabricated base at the desired inclination of crack with respect to loading direction. The disk was laterally supported by screws to ensure proper crack orientation during the entire process of sample installation and testing. To avoid saturation of the specimen with oil due to high confining pressure, the specimen was coated with a spray paint. After the specimen was properly secured in position on the base, a circular rod grooved under a flat circular stainless steel piece was fixed at the top of the specimen using a quick setting glue. The circular base over the rod was able to rotate and was able to adjust itself in the horizontal position when the loading piston from the top is made in contact with it. The whole assembly was then placed on the base of the cell as shown in Figure 4.15. The cylindrical cell was placed over the base and the assembly is tightly closed. The entire cell assembly was then moved on to the loading platform and the cell was filled with a light oil. The oil was obtained from the oil research lab at KFUPM. The confining pressure was applied through a hydraulic pump capable of applying a pressure of 70 MPa. The hydraulic pump used for applying the confining pressure is shown in Figure 4.16. The

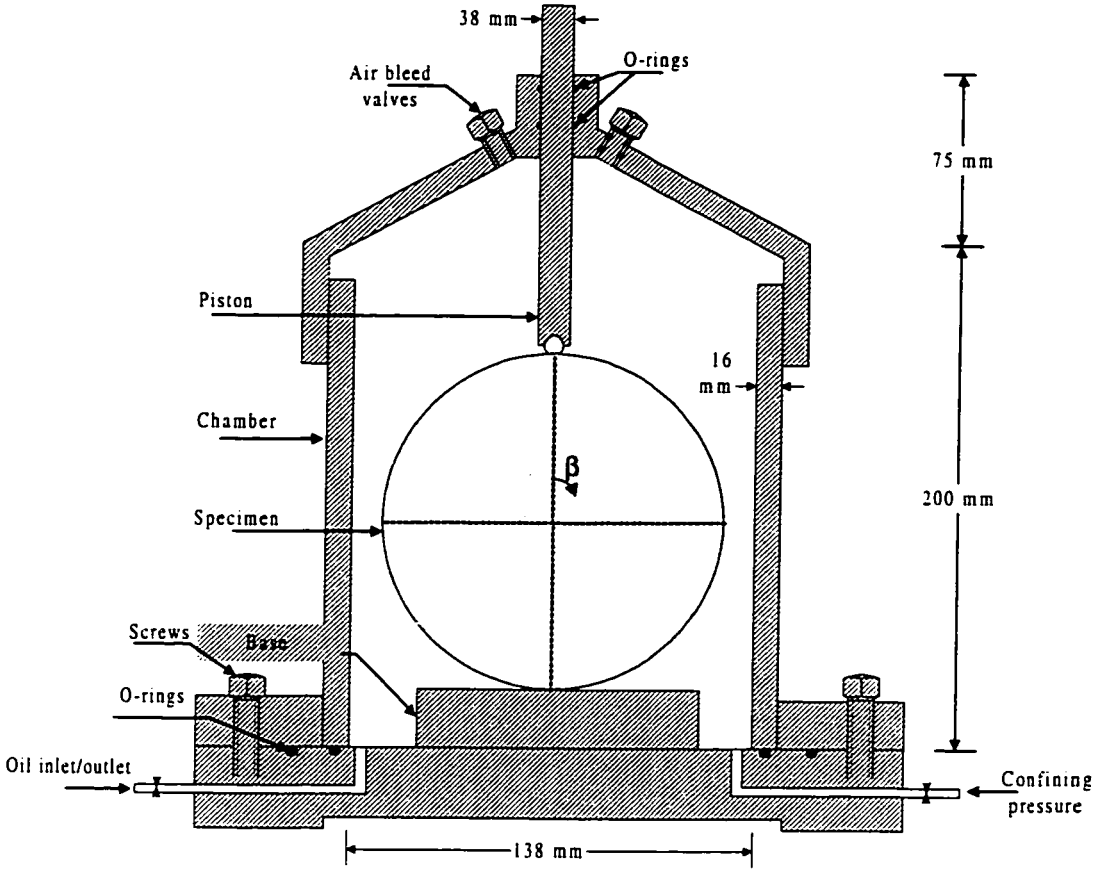

Figure 4.14: A Schematic of the Triaxial Cell used for the Testing under Simulated *In-situ* Confining Pressure.

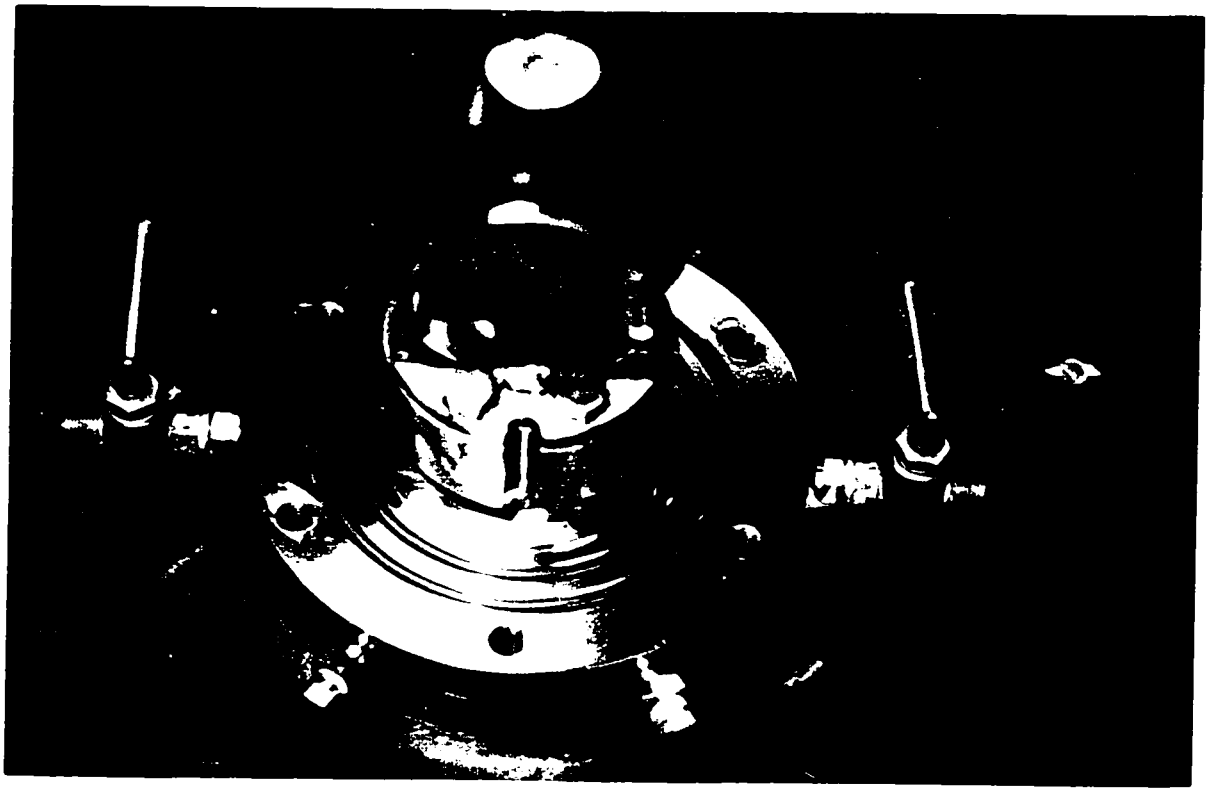

Figure 4.15: Specimen Fixed to the Base of Triaxial Cell for Testing under Confining Pressure.

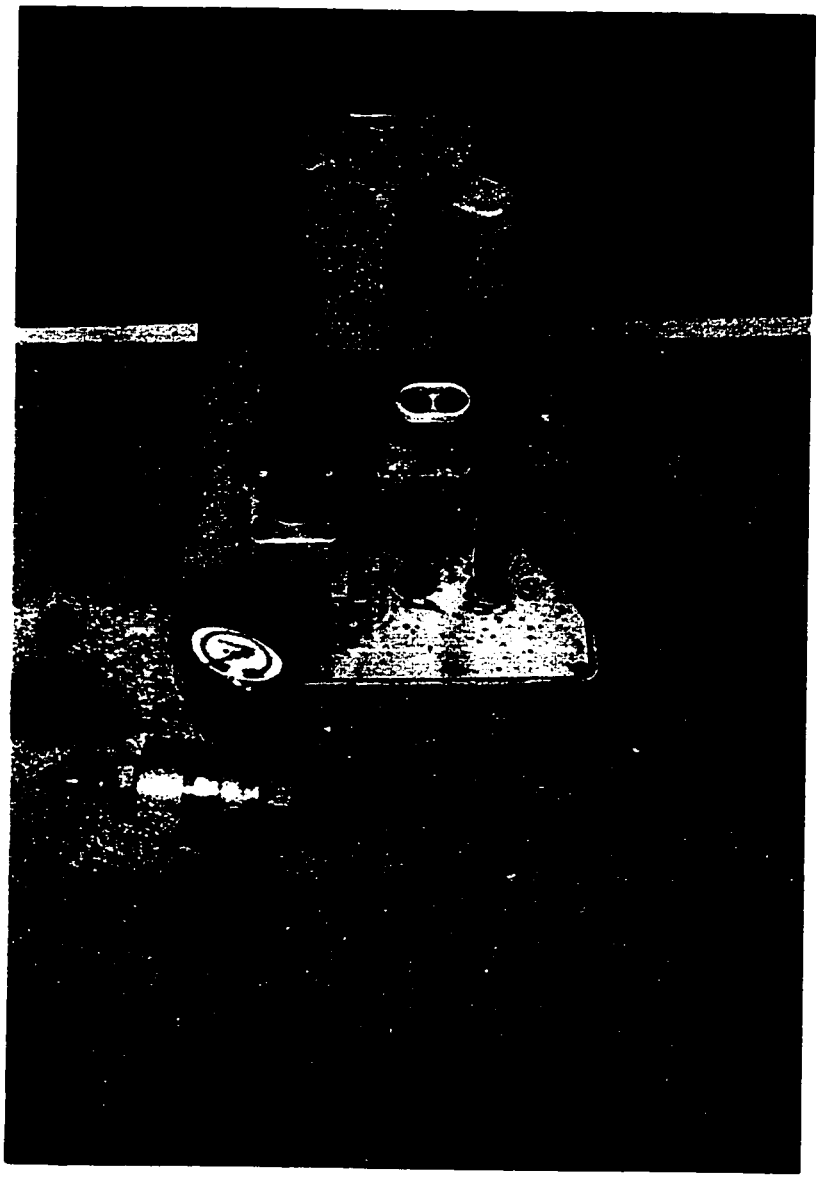

Figure 4.16: Equipment used to Apply Confining Pressure.

hydrostatically confined specimen was then loaded diametrally until failure occurs. No variation in the confining pressure was observed during the whole testing process. Load point displacement was measured using a LVDT during testing.

4.7.1.1 Mode-I Fracture Toughness Testing

Brazilian disks with straight notch prepared from outcrop and reservoir specimens were tested in Mode-I. To investigate the variation in mode-I fracture toughness with confining pressure, outcrop specimens were tested (one specimen for each case) under confining pressure ranging from 7 MPa to 28 MPa. Reservoir specimens were tested only under a confining pressure of 28 MPa due to their limited availability.

4.7.1.2 Mixed Mode I-II Fracture Toughness Testing

Mixed mode I-II fracture toughness was determined under an effective reservoir confining pressure of 28 MPa (4000 psi). To investigate whether or not the outcrop specimens could be used for fracture toughness study as representative of the reservoir specimens from the same formation, straight notched Brazilian disk specimens from both outcrop and reservoir were tested. The crack inclination was varied between 0 and 75 degrees with two specimens for each inclination. The reservoir specimens used in this investigation were from lithology A and B.

4.7.2 Simulation of *In-situ* Temperature Condition

Although some studies have been made on the effect of temperature on mode-I fracture toughness, little or no attention has so far been focused on the mixed mode I-II. In field, however, mode-I may not be dominant. Mode-II, and in particular mixed mode I-II, are frequently encountered in the field [whittaker *et al.*, 1982]. Therefore, studying mixed mode fracture toughness behavior at elevated temperature becomes a matter of prime importance. To study the fracture toughness behavior at a temperature simulating field conditions, a rectangular box was fabricated from a heat resistant material. Figure 4.17 shows the schematic representation of the box. The box is 200 mm x 300 mm from inside and its height is 200 mm. The sample was placed inside the box with a known inclination of crack with respect to the loading direction. The sample was precisely secured in position by two lateral screws. The box was then filled with coarse sand in a loose state. The cap was then placed on top of the box and the whole assembly was put in an oven to bring the system to the desired temperature. After the sample reached the required temperature, the box was then taken out of the oven and the sample was tested in diametral compression. Load point displacement was recorded during testing. Due to the long time required for the sample to reach to a uniform temperature, testing of only two samples per day was possible. The samples were tested both in mode-I and mixed mode I-II loading conditions as explained in the following sections.

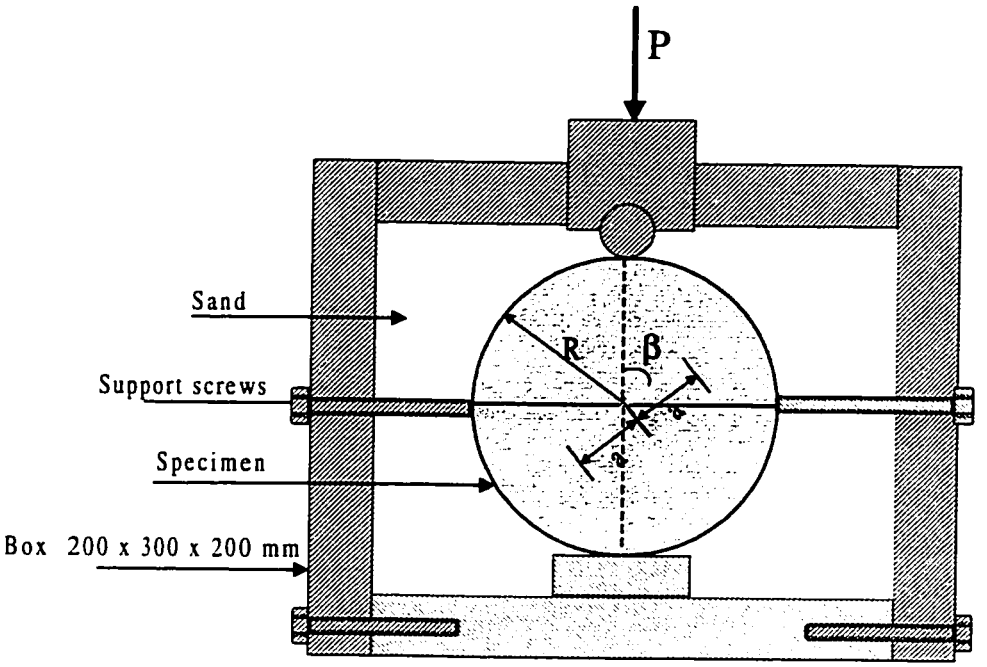

Figure 4.17: A Schematic of the Setup used for Simulating the *In-situ* Temperature Condition.

4.7.2.1 Mode-I Fracture Toughness Testing

The effect of temperature on mode-I fracture toughness was studied using straight notched Brazilian disk specimens from outcrop. The specimens were tested under a temperature of 50 °C and 116 °C (reservoir temperature); and only one sample for each condition was tested.

4.7.3 Mixed Mode I-II Fracture Toughness Testing

Straight notched Brazilian disk specimens were tested under a temperature of 116 °C. Outcrop specimens were tested for this purpose with a crack inclination of 0 to 75 degrees with two specimens for each inclination. Due to limited number of reservoir specimens, testing was conducted only for pure mode-I and pure mode-II loading condition.

4.8 Indirect Tensile Strength

The indirect method of measuring the tensile strength of rock material was achieved by loading the uncracked Brazilian disk along the diametral axis. The testing setup was the same as that used for fracture toughness testing under ambient conditions. During the testing, the vertical load and load point displacement were recorded.

4.9 Microscopic Studies

The effect of mixed mode I-II loading condition on the nature of the broken surface was investigated using SEM analysis. The specimens tested at a crack inclination of 0, 15, 30, 45, 60, and 75 degrees were used for this purpose.

Chapter 5

Results and Discussions

The results of the experimental work accomplished according to the methodology and procedures outlined in Chapter 3 and 4 are presented here. The results for the mineralogical study of the rock material used in this study are presented in terms of XRD analysis. Much of this Chapter is concerned with the fracture toughness results obtained for both outcrop and reservoir specimens under mode-I as well as mixed mode I-II loading conditions. The results of tests conducted under ambient and simulated reservoir conditions of temperature and pressure are presented. The effect of other factors such as the type and size of the specimen and the strain rate on fracture toughness is investigated. Crack propagation under mixed mode I-II and fracture locus (fracture toughness envelope) are studied experimentally and the results are compared with the theoretical predictions. Finally, SEM results of the fractured surface under mixed mode I-II are summarized. Apart from fracture toughness, the specimens from outcrop and reservoir were studied for their tensile strength. These tensile strength results are required in a formulation used to assess the specimen size requirement for valid fracture toughness study.

5.1 XRD Results

Figure 5.1 shows the XRD analysis for the outcrop specimens. Analysis for the reservoir specimens is shown in Figure 5.2 and 5.3. As can be seen from these Figures both types of specimens comprise predominantly of calcite with some traces of dolomite and iron. However, the samples from lithology C contain about 52% anhydrite. The anhydrite in these specimens was present as a localized impurity.

5.2 Indirect Tensile Strength

Indirect tensile strength of both outcrop and reservoir specimens was determined using uncracked Brazilian disk in diametral compression. The disks were chosen to have a diameter of 99 ± 1 mm, and 23 ± 1 mm in thickness, so as to be consistent with the specimens tested for fracture toughness. Tensile strength was calculated using Equation (3.28) and results along with the failure loads and specimen dimensions are summarized in Table 5.1. The average values of tensile strength were found to be 2.31 and 2.14 MPa for outcrop and reservoir specimens, respectively.

5.3 Fracture Toughness Results

Fracture toughness of outcrop and reservoir samples was determined at both the ambient and reservoir conditions of temperature and pressure. Brazilian disk specimens with central straight notch were mainly used in this investigation.

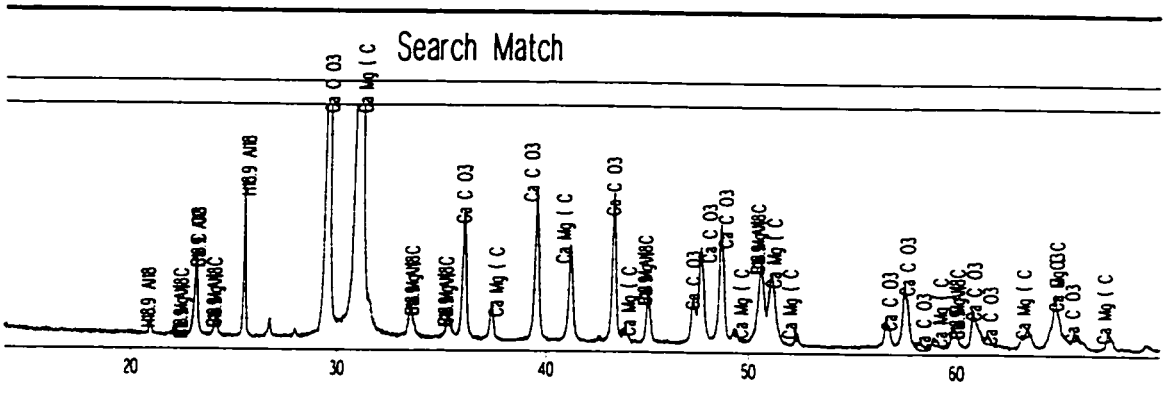

Figure 5.1: Mineralogical Analysis for an Outcrop Specimen.

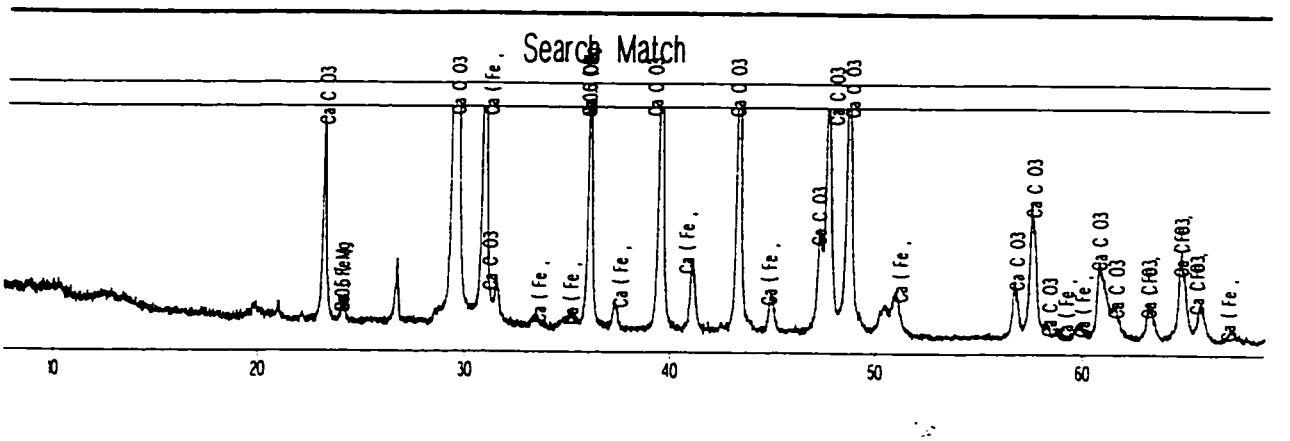

Figure 5.2: Mineralogical Analysis for a Reservoir Specimen from Lithology A and B.

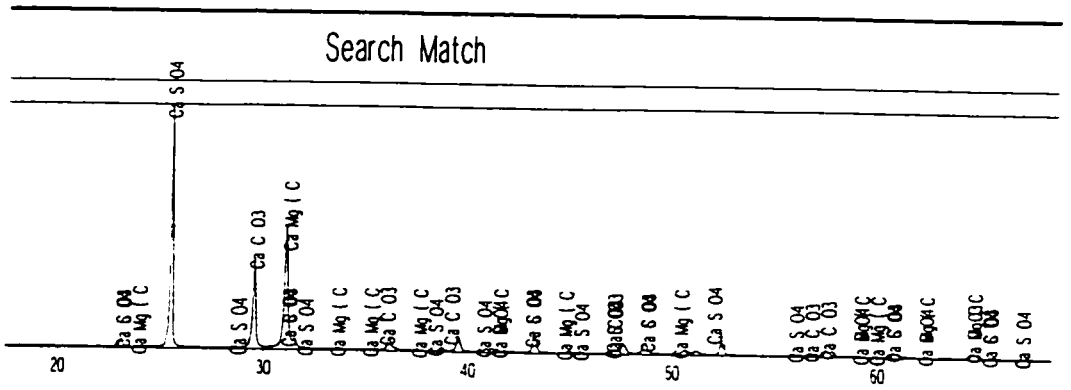

(a)

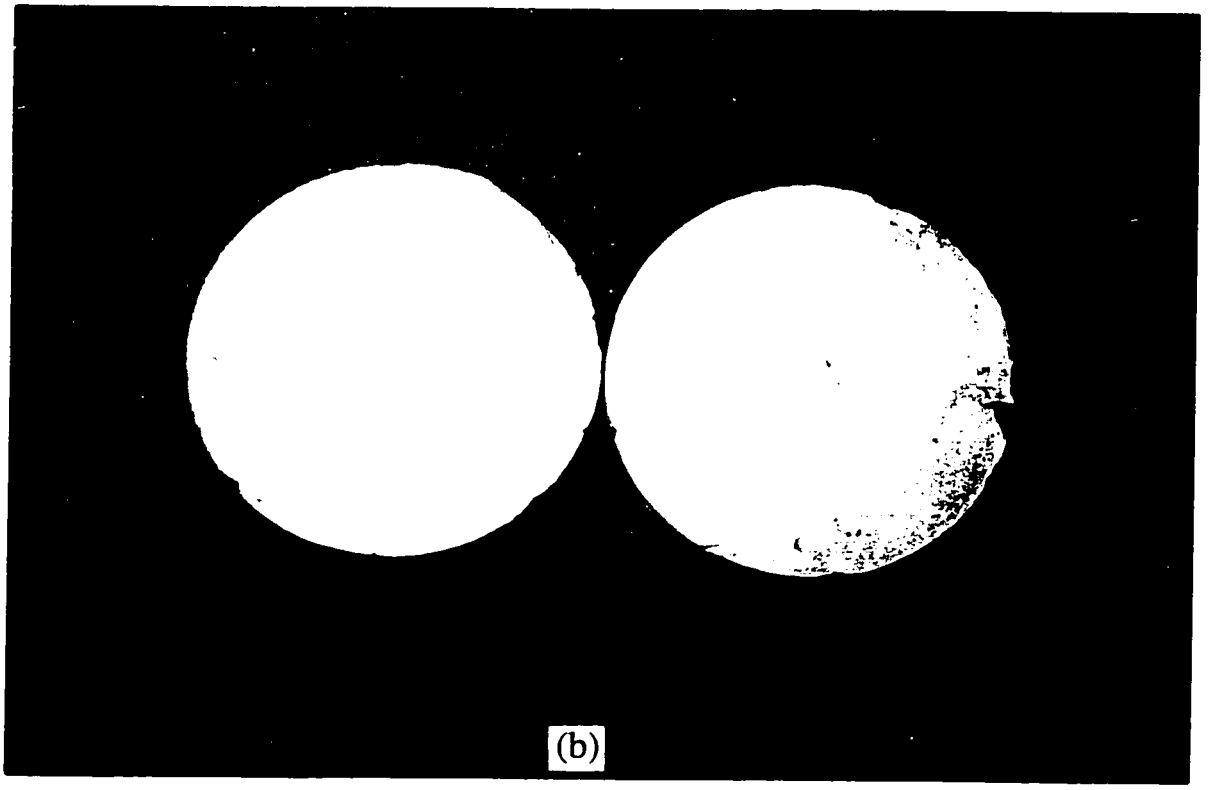

Figure 5.3: (a) Mineralogical Analysis for a Reservoir Specimen from Lithology C, (b) Specimens Showing the Presence of Anhydrite as an Impurity.

Table 5.1: Summary of Results for the Tensile Strength of Outcrop and Reservoir Specimens.

B (mm)	D (mm)	P (kg)	σ_t (Mpa)	Specimens
22	98	721	2.13	Outcrop
22	98	783	2.31	Outcrop
22	98	810	2.39	Outcrop
24	101	742	1.95	Reservoir
26	101	769	1.86	Reservoir
24	100	752	1.99	Reservoir
24	101	891	2.34	Reservoir
22	100	812	2.35	Reservoir
23	100	843	2.33	Reservoir

However, few specimens of Brazilian disk with Chevron notch under diametral compression and straight notched circular rod and semicircular disk specimens under three point bending were also used for comparison purposes. Brazilian disks were about 99 ± 1 mm in diameter. Some samples, with a diameter of 83 ± 1 mm, were used to investigate the variation in fracture toughness with specimen size. Crack extension and failure trajectory under mixed mode I-II were also investigated. For all notched Brazilian disk specimens, fracture toughness values were calculated using Equations (3.9) and (3.10). For semicircular specimens Equations (3.16) and (3.17) were used. For notched circular rod specimens under three point bending, Equation (3.1) was used to calculate the fracture toughness values.

5.3.1 Ambient Conditions

Fracture toughness under ambient conditions was studied both in mode-I and mixed mode I-II loading conditions. Notched Brazilian disk and notched round bar specimens under three point bending were used in this investigation. The effect of strain rate, specimen size, specimen type and specimen origin on fracture toughness was studied. Further, the effect of notch type was also investigated.

5.3.1.1 Mode-I Results

Effect of Strain Rate

To study the effect of strain rate, circular rods 23 mm in diameter from outcrop samples were tested under three point bend load loading arrangement. Notch depth of

7 mm (i.e., a/D = 0.3) was maintained for all the specimens tested. The specimens were tested for strain rates of 0.005, 0.01, 0.1 mm/min. Figure 5.4 shows the plot of load point displacement and the vertical load applied on the specimen. The failure load for all the samples falls within a range of 19 to 25 kg. Moreover, brittle failure was observed for the specimens tested. The brittle failure of the specimens is attributed to the stiff nature of the rock.

Table 5.2 summarizes the fracture toughness results along with the failure loads and dimensions of the specimen tested. Figure 5.5 shows the variation of mode-I stress intensity factor as a function of the strain rate. The Fracture toughness was found to be in the range of 0.36 to 0.42 MPa $m^{1/2}$. It is observed that there is no significant variation in the stress intensity factor value for the strain rate levels used in this study. As a comparison, Haberfield and Johnston (1990) and Lim *et al.* (1994-b) studied the mode-I fracture toughness variation of a saturated soft rock over a range of strain rate (i.e., 0.05-1.00 mm/min). They concluded that at low strain rates, fracture toughness variation was negligible. However, an increase in the fracture toughness value was observed at a higher strain level (i.e., 0.1-1.0 mm/min). This increase in fracture toughness at higher strain rates was attributed to the development of negative pore water pressure at the crack tip of water saturated samples caused by high tensile stresses developed at the crack tip. Contrary to that, the rock material used in this study was dry and, consequently, increase in fracture toughness at high strain rates is not expected. Depending on the results, it was decided to use a strain rate of 0.08 mm/min for the rest of the experimental work in this study.

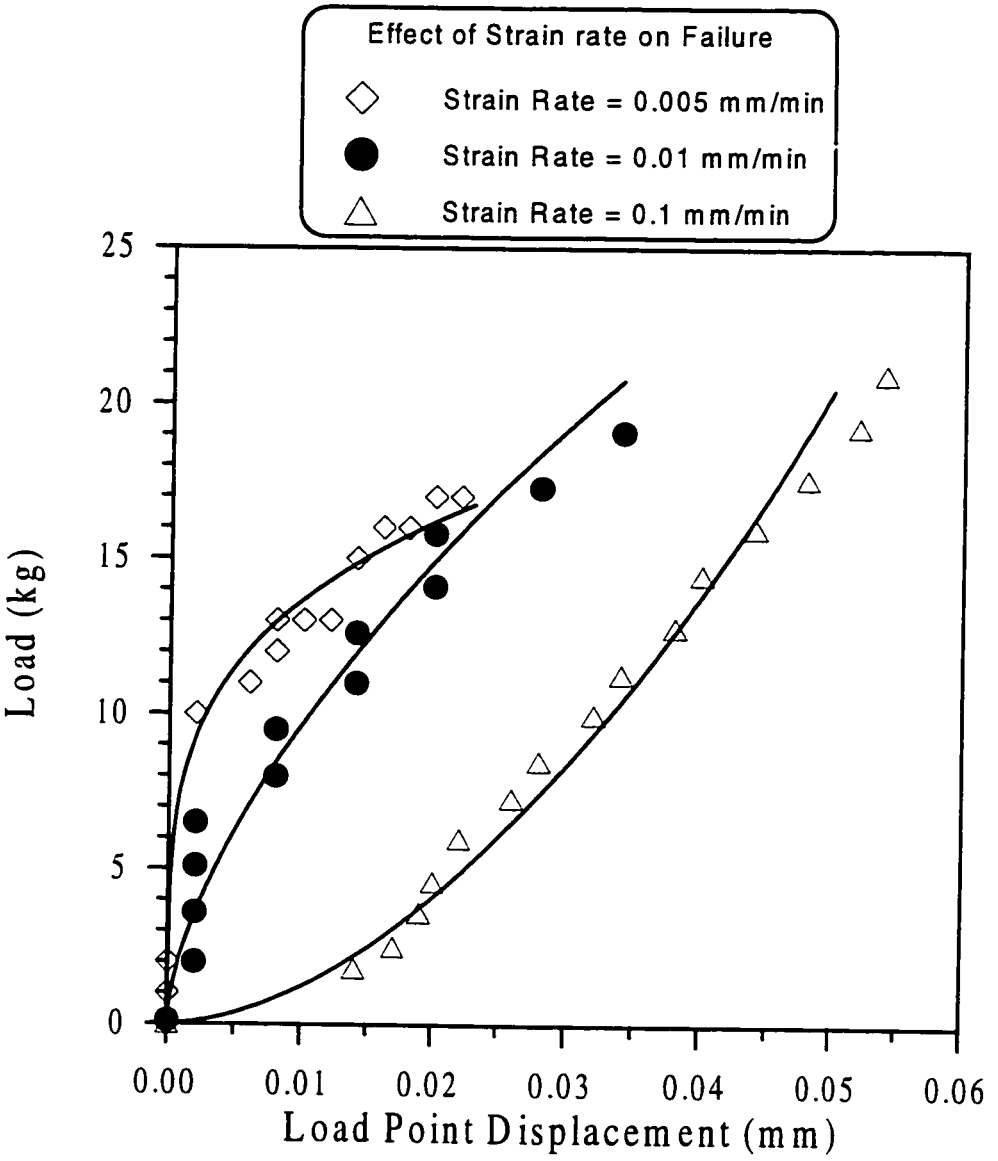

Figure 5.4: Load-Displacement Curves for Notched Circular Rod Specimens under Mode-I Loading Condition for Different Strain Rates.

Table 5.2: Summary of Results for the Effect of Strain Rate on Mode-I Fracture Toughness.

Strain Rtae (mm/min.)	P (kg)	a (mm)	a/D	K_I Mpa $(m)^{1/2}$
0.005	23	7.5	0.31	0.42
0.005	19	8	0.33	0.36
0.01	22	7	0.29	0.39
0.01	23	7	0.29	0.41
0.1	20	8	0.33	0.38
0.1	23	7.5	0.31	0.42

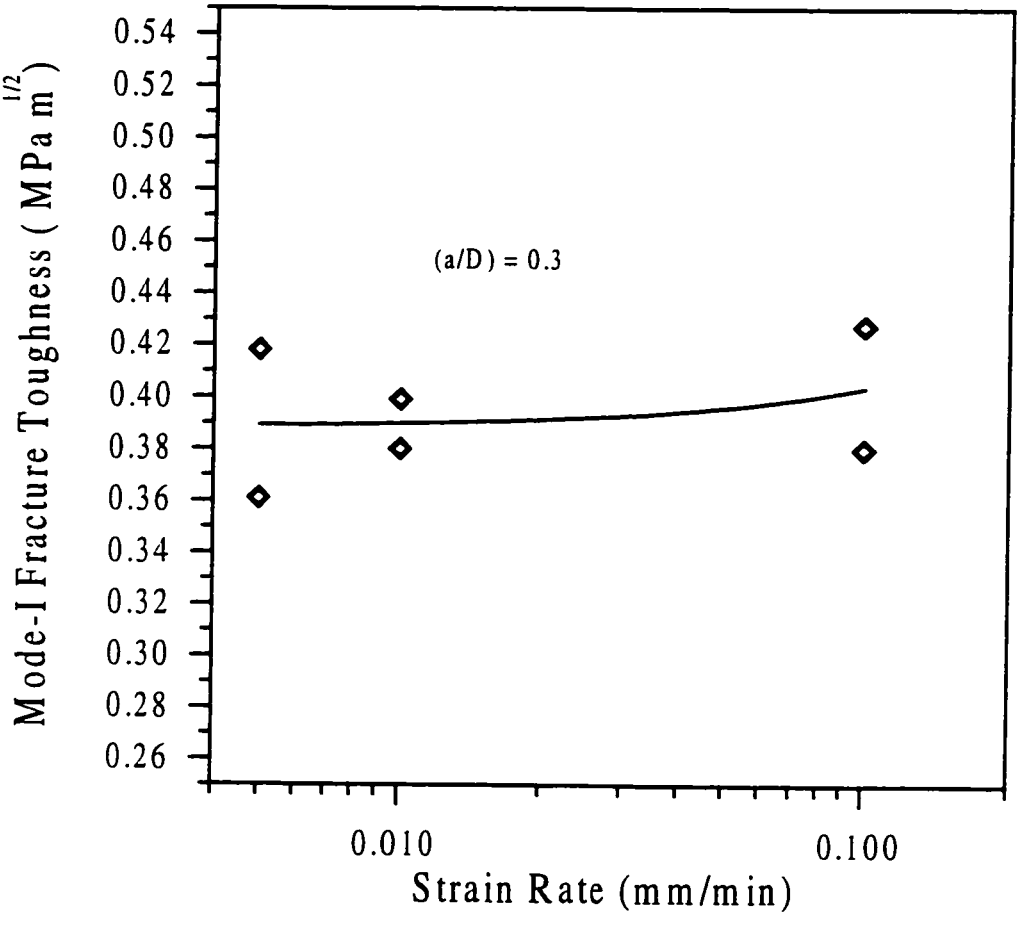

Figure 5.5: Effect of Strain Rate on Mode-I Fracture Toughness.

Effect of Notch Length

The effect of notch length on mode-I fracture toughness was investigated using centrally notched Brazilian disks in diametrical compression and notched circular rods under three point bend loading configuration. The disks from outcrop specimens used for this purpose were 99 ± 1mm in diameter. The thickness of all the disks was kept invariant as 22 mm. Straight notches of length 10 to 58 mm (i.e. a/R = 0.1 to 0.6) were used. For the circular rod specimens, the diameter was kept constant at 24 mm and crack length was varied from 3 to 14 mm (i.e., a/D = 0.13 to 0.58). Fracture toughness for each notch length was calculated and the results are summarized in Table 5.3 and shown in the graphical form in Figure 5.6.

As can be seen from the plot, the fracture toughness for the Brazilian disk specimens is almost unaffected by the crack length. However, the results for the notched circular rod specimens show an initial increase in the fracture toughness value till a normalized crack length (a/D) is 0.4 and then becomes constant for the normalized crack length of 0.4 to 0.6. Interestingly, a minimum crack length after which fracture toughness does not show any variation, was same for both methods (i.e., 10 mm for disk specimens and 9.6 mm for rod specimens). Based on the minimum crack length criterion, the ratio of minimum crack length ($2a$ for disk specimens and a for rod specimens, respectively) to (K_{IC}/σ_t) was found to be 0.3 which is very close to 0.22 and 0.33, respectively, for the Brazilian disk and single edge cracked round bar beam specimens as reported in Table 3.1.

Table 5.3: Summary of Results for the Effect of Notch Length on Mode-I Fracture Toughness.

Brazilian Disk Specimens

B (mm)	D (mm)	$2a$ (mm)	$2a/D$	P (kg)	K_I Mpa $(m)^{1/2}$
23	98	11	0.11	1034	0.38
23	98	10	0.10	1087	0.39
23	98	11	0.11	983	0.36
23	98	21	0.21	821	0.44
22	98	21	0.21	765	0.43
23	98	20	0.20	743	0.40
23	98	31	0.32	574	0.41
23	98	31	0.31	608	0.42
22	98	49	0.50	352	0.39
22	98	50	0.51	378	0.43

Circular Rod Specimens under Three Point Bending

D (mm)	a (mm)	a/D	P (kg)	K_I Mpa $(m)^{1/2}$
24	4	0.17	34	0.44
24	7	0.29	25	0.44
24	11.5	0.48	18	0.44
24	13	0.54	16	0.43
24	3	0.13	38	0.42
24	7	0.29	22	0.39
24	11	0.46	20	0.47

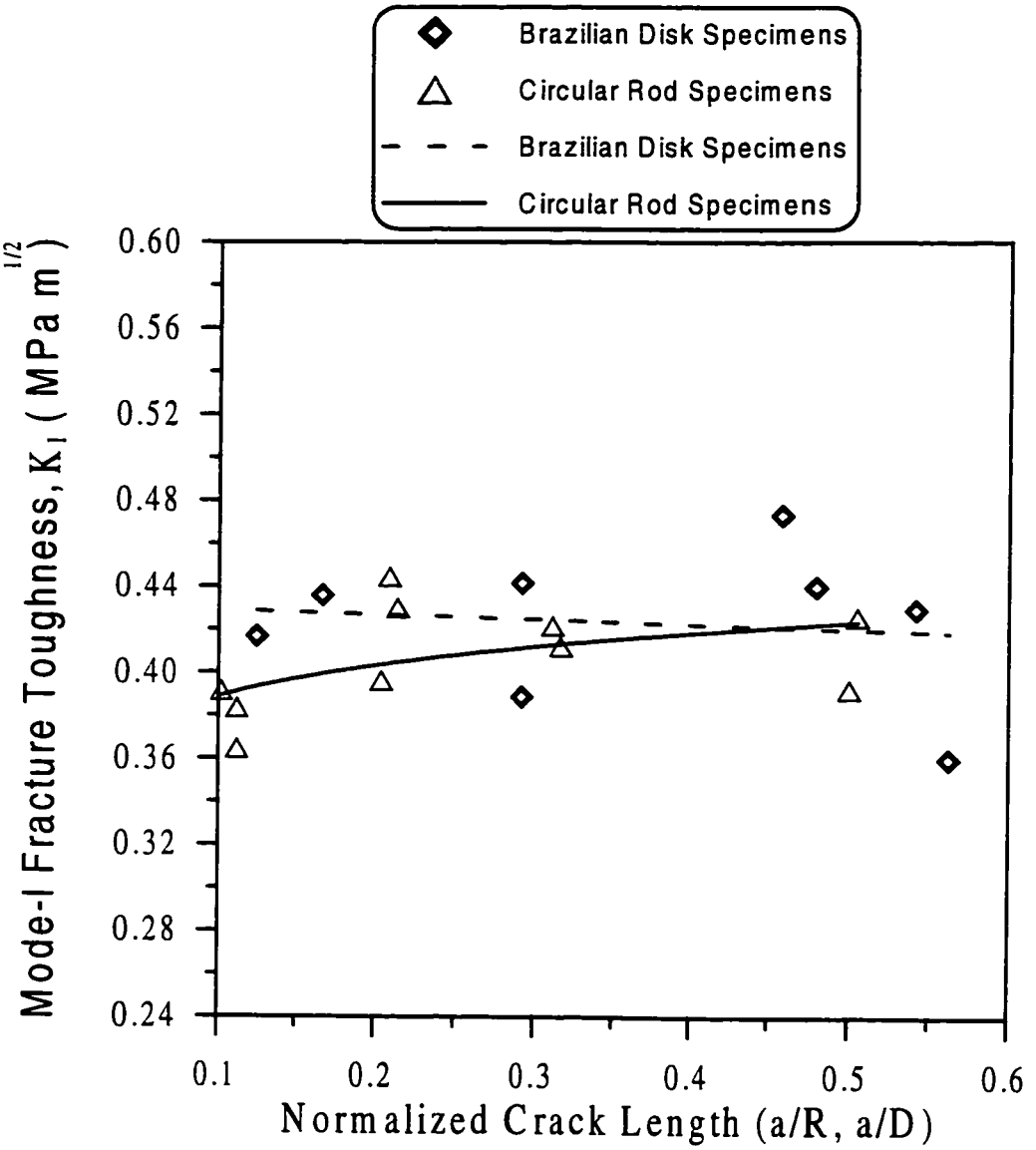

Figure 5.6: Effect of Notch Length on Mode-I Fracture Toughness.

Based on the LEFM theory, the valid mode-I fracture toughness value can be obtained only if the fracture process zone is small (i.e. a few percent) with respect to the dimensions of the specimens such as crack or notch length. As a result, the present study suggests that the process zone for the limestone employed in this study must be smaller than 10 mm. As a comparison, Singh and Pathan (1988) studied the fracture toughness behavior of five different rocks using the diametrical compression of disks. The minimum notch lengths used for Ryfield sandstone, siltstone, basalt, granite and coal were approximately 2.5, 4, 2, 2, and 3 mm, respectively. No decrease in fracture toughness was observed even with such a small crack length. This led them to conclude that fracture toughness of those rocks was independent of the notch length. In contrast, Labuz *et al.* (1987) used wedge-loaded, double cantilever beam specimens and came up with a process zone of approximately 40 and 90 mm for Charcoal Granite and Rockville granite, respectively. On the other hand, Laqueche *et al.* (1986) also used double cantilever beam specimens for mode-I fracture toughness of slate and reported almost no variation in the fracture toughness value over the normalized notch length of 0.2 to 0.6.

It is important to note that tensile loads were used for the double cantilever beam configuration in the work conducted by Laqueche *et al.* (1986) whereas for Singh and Pathan (1988) and in the present work, compressive loads were used. According to Thiercelin and Roegiers (1986), it is likely that the application of compressive loads tends to induce non-singular compressive stresses normal to the crack face which result in a smaller process zone. On the other hand, non-singular

tensile stresses will be created normal to the crack face in case of the double cantilever specimens. It is more likely for the process zone to be enlarged in the case of tensile loads.

Based on the above-mentioned results and those presented in Table 3.1, it can be concluded that Equation (3.21) for the size of fracture process zone, originally developed for materials other than rocks (i.e., metals), may not be representative of the actual process zone size for rocks and the required notch length can be considerably small. Similar remarks have also been made by Lim *et al.* (1994-b) regarding the applicability of Equation (3.21) for rocks. Moreover, it is believed that the mode-I fracture toughness dependence on the crack size could be material dependent rather than the testing technique. However, more detailed study would be necessary to better understand this phenomenon using the specimens from the same material and conducting tests on a variety of available test methods.

Effect of Specimen Thickness

Brazilian disks, 98 mm in diameter with a central straight notch of 33 mm (i.e. a/R = 0.30), were employed to investigate the effect of specimen thickness on mode-I fracture toughness. Specimens with thickness ranging between 11 and 25 mm were used in this investigation. The fracture toughness was calculated for all the specimens and the results are summarized in Table 5.4 and plotted in Figure 5.7. Fracture toughness ranging from 0.39 to 0.42 MPa $(m)^{1/2}$ over the range of specimen thickness does not show any significant variation. Haberfield and Johnston (1990) conducted a large number of tests using rectangular beams under three point bend loading and

Table 5.4: Summary of Results for the Effect of Specimen Thickness on Mode-I Fracture Toughness.

B (mm)	D (mm)	$2a$ (mm)	$2a/D$	P (kg)	K_I Mpa $(m)^{1/2}$
25	98	33	0.34	595	0.40
24.5	98	33	0.34	580	0.40
14	98	34	0.35	337	0.42
15	98	34	0.35	333	0.39
12	98	33.5	0.34	277	0.40
11	98	33.5	0.34	258	0.40
18	98	33	0.34	432	0.41
19	98	33.5	0.34	469	0.42

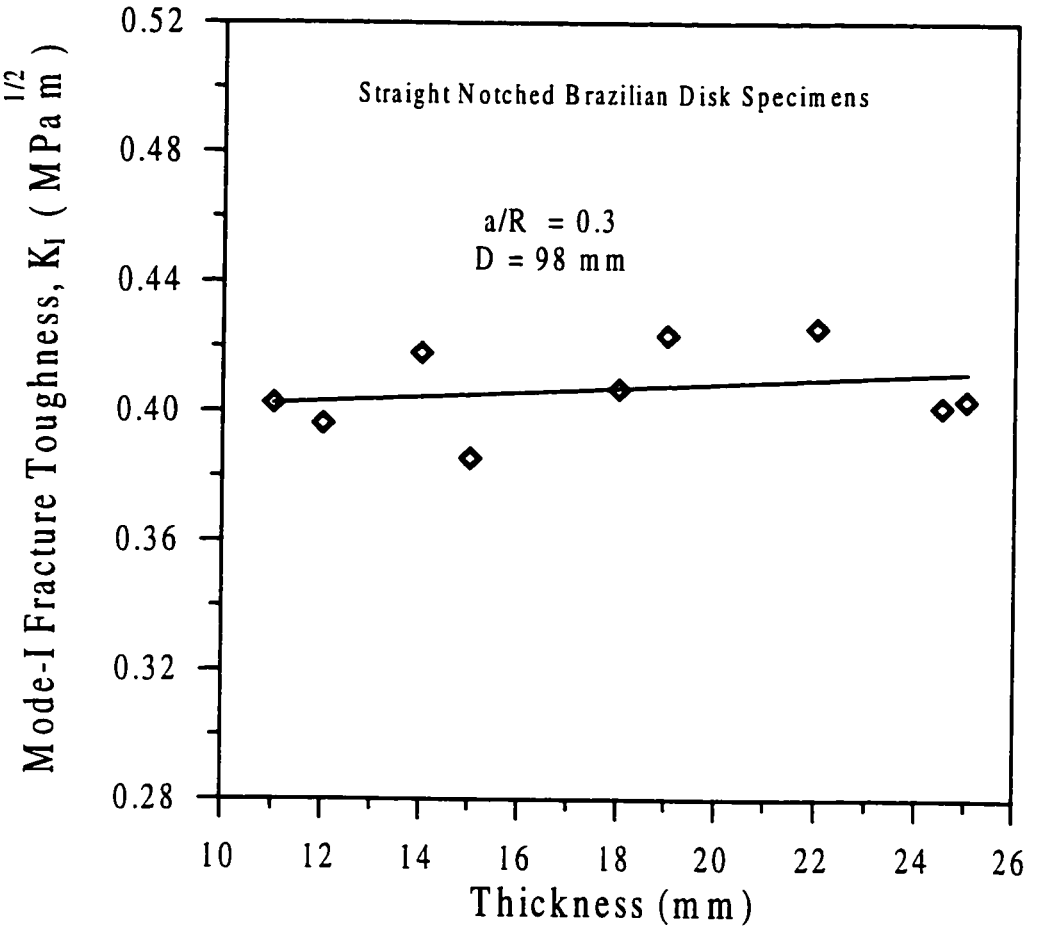

Figure 5.7: Effect of Specimen Thickness on Mode-I Fracture Toughness.

reached at the same conclusion. Similar findings have been reported in the literature Schmidt and Lutz (1979) for westerly granite, Fowell and Chen (1990) using fine grained sandstone, Chong *et al.* (1987) for Colorado oil Shale, Singh and Sun (1990) using Welsh Limestone, Kobayashi *et al.* (1986) using Ogino tuff, and Laqueche *et al.* (1986) making use of slate schist in double cantilever beam loading configuration. Although different testing techniques were used in the above-mentioned studies, yet the results are comparable.

In the explanation of the effect of specimen thickness on mode-I fracture toughness, Schmidt and Lutz (1979) reasoned that the maximum principal stress was responsible for the crack tip yield zone. It follows that the crack tip yield zone is independent of the out-of-plane stress. This implies that the size of the crack tip yield zone is also independent of the thickness of the specimen.

Based on the consideration of the fracture process zone at the crack tip, the critical fracture process zone size (r_{mc}) comes out to be 8.88 mm with the values of 0.42 MPa $m^{1/2}$ and 2.31 MPa for mode-I fracture toughness and tensile strength, respectively. This dictates a specimen thickness of around 18 mm. To be on the safer side, thickness of the specimens was kept in the range of 22-26 mm.

Effect of Specimen Size

The specimen size effect on mode-I fracture toughness was investigated by conducing tests on the outcrop specimens. Brazilian disk specimens were 98 mm and 84 mm in diameter. The crack to radius ratio (a/R) was kept same for both types of specimens at 0.3. Two specimens were tested for each size. The results are presented in Figure 5.8.

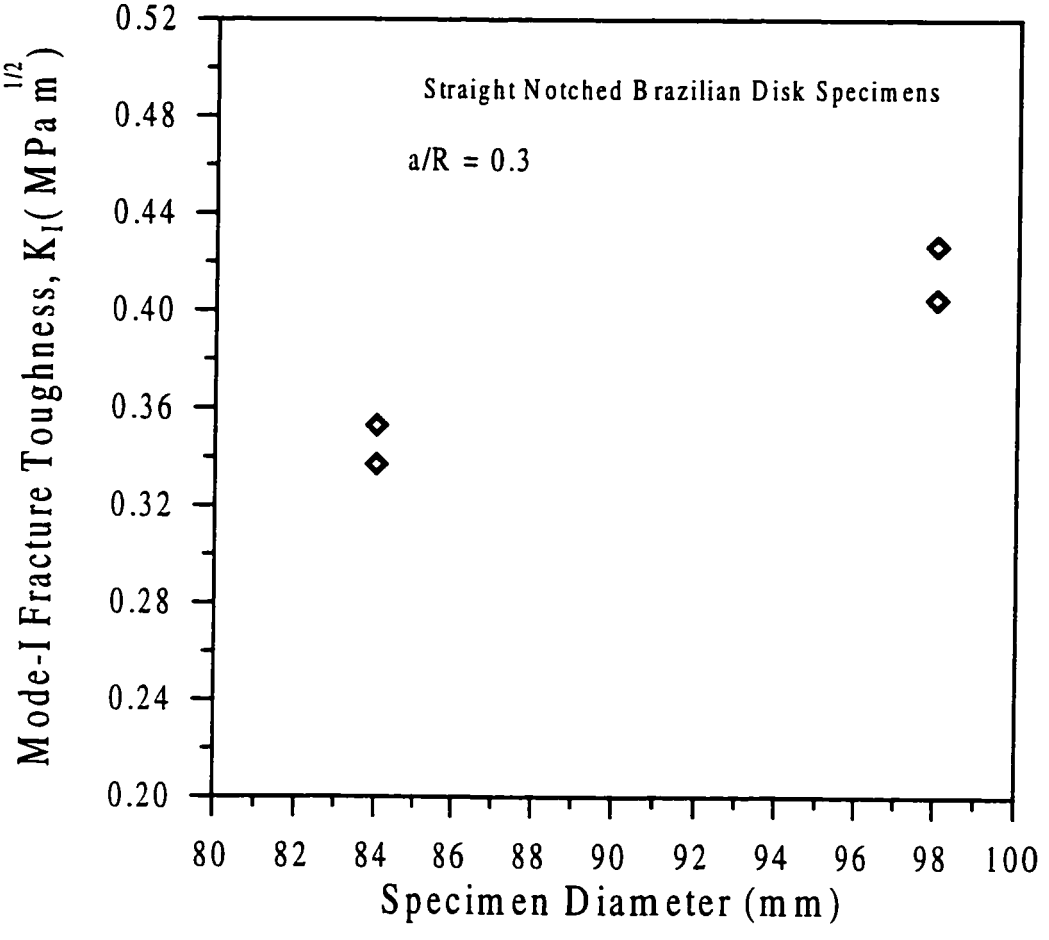

Figure 5.8: Effect of Specimen Diameter on Mode-I Fracture Toughness.

The fracture toughness value of 0.35 and 0.43 MPa $m^{1/2}$ was observed for 84 and 98 mm diameter disks, respectively. It was observed that there was an increase of about 23% in the fracture toughness when the diameter was increased by 17%. No consensus has so far been found in the literature regarding the mode-I fracture toughness variation with specimen diameter. Matsuki *et al.* (1988) has reported a trend of increasing fracture toughness with increasing the specimen diameter; whereas the results by Barker (1977), Sun (1983) and Yi (1987) suggest that the mode-I fracture toughness is independent of the specimen diameter. In all of the above-mentioned references, specimens other than the centrally notched Brazilian disk were used.

5.3.1.2 Mixed Mode I-II Results

Mixed mode fracture toughness study at the ambient conditions was made using Brazilian disks as well as semicircular specimens. Brazilian disks were tested with crack orientation ranging between 0 to 75 degrees. Semicircular specimens were tested with notch orientations between 0 to 60 degrees. It was difficult to machine a crack at an angle greater than 60 degrees for the semicircular specimens. The notch to radius ratio (a/R) of 0.3 was used for both types of specimens. Load point displacement and crack extension were recorded during the test. Apart from this, the effect of crack length and specimen size on mixed mode I-II fracture toughness was investigated.

Effect of Specimen Size

The effect of specimen size on mixed mode I-II fracture toughness was investigated by conducting diametrical compression tests on centrally straight notched Brazilian disks. Outcrop specimens with a diameter of 98 mm and 84 mm were used for this purpose. The crack to radius (a/R) ratio and thickness to diameter (B/D) ratio were chosen as 0.3 and 0.2, respectively. Summary of the results is presented in Table 5.5 and the fracture toughness variations for the two types of specimens are shown in Figure 5.9 in terms of K_I and K_{II} for various crack inclination angles. It was observed that the fracture toughness results for the smaller disks were not compatible with that of the bigger ones in terms of quantitative comparison. Pure mode-I (K_{IC}) and pure mode-II (K_{IIC}) values for the 84 mm diameter disks were 0.35 and 0.65 MPa $m^{1/2}$, respectively compared to the corresponding values of 0.43 and 0.92 MPa $m^{1/2}$ for 98 mm notched disk specimens. K_{IC} decreased by an amount of 19% and K_{IIC} showed a reduction of around 29%. The ratio of pure mode-II to pure mode-I (K_{IIC}/K_{IC}) was obtained as 1.86 for 84 mm disks compared to a value of 2.14 for 98 mm disks which means a reduction of about 13%. Normalized mode-I and Mode-II fracture toughness variation is shown in Figure 5.10. Contrary to fracture toughness results described above, normalized results for two types of specimens are very close. The normalized fracture toughness results of 98 mm disks are within 10 to 15% of the 84 mm disks.

Effect of Notch Length

Straight notched Brazilian disks from outcrop specimens were used to study the effect of crack size on mixed mode I-II fracture toughness. The diameter and thickness of

Table 5.5: Summary of Results for the Effect of Specimen Diameter on Mixed Mode I-II Fracture Toughness.

β (deg)	B (mm)	D (mm)	$2a$ (mm)	$2a/D$	P (kg)	K_I Mpa $(m)^{1/2}$	K_{II} Mpa $(m)^{1/2}$	K_I/K_{IC}	K_{II}/K_{IIC}
0	22	98	30	0	680	0.43	0.00	1.00	0.00
15	22	98	30	0	675	0.30	0.47	0.71	0.51
27	22	98	30	0	902	0.08	0.97	0.18	1.06
30	22	98	30	0	935	-0.03	1.06	-0.06	1.15
45	22	98	30	0	913	-0.60	1.09	-1.40	1.19
60	22	98	30	0	852	-1.07	0.80	-2.51	0.87
75	22	98	30	0	751	-1.26	0.38	-2.95	0.41
0	22	98	30	0	645	0.41	0.00	0.95	0.00
15	22	98	30	0	618	0.28	0.43	0.65	0.47
27	22	98	30	0	820	0.07	0.88	0.16	0.96
30	22	98	30	0	856	-0.02	0.97	-0.06	1.06
45	22	98	30	0	873	-0.57	1.05	-1.34	1.14
60	22	98	30	0	920	-1.16	0.87	-2.71	0.94
75	22	98	30	0	810	-1.36	0.41	-3.18	0.44
0	19	84	26	0	421	0.34	0.00	1.00	0.00
15	20	84	26	0	337	0.17	0.34	0.52	0.52
30	20	83	26	0	528	-0.08	0.84	-0.22	1.29
45	20	84	26	0	378	-0.33	0.63	-0.99	0.96
60	20	84	26	0	500	-0.75	0.67	-2.23	1.02
75	20	83	26	0	406	-0.80	0.31	-2.38	0.47
0	20	84	26	0	463	0.35	0.00	1.04	0.00
15	19	84	26	0	299	0.16	0.31	0.47	0.47
30	20	84	26	0	496	-0.07	0.78	-0.21	1.19
45	20	84	26	0	363	-0.32	0.60	-0.95	0.93
60	19	83	26	0	473	-0.76	0.67	-2.25	1.03
75	19	84	26	0	516	-1.03	0.40	-3.06	0.61

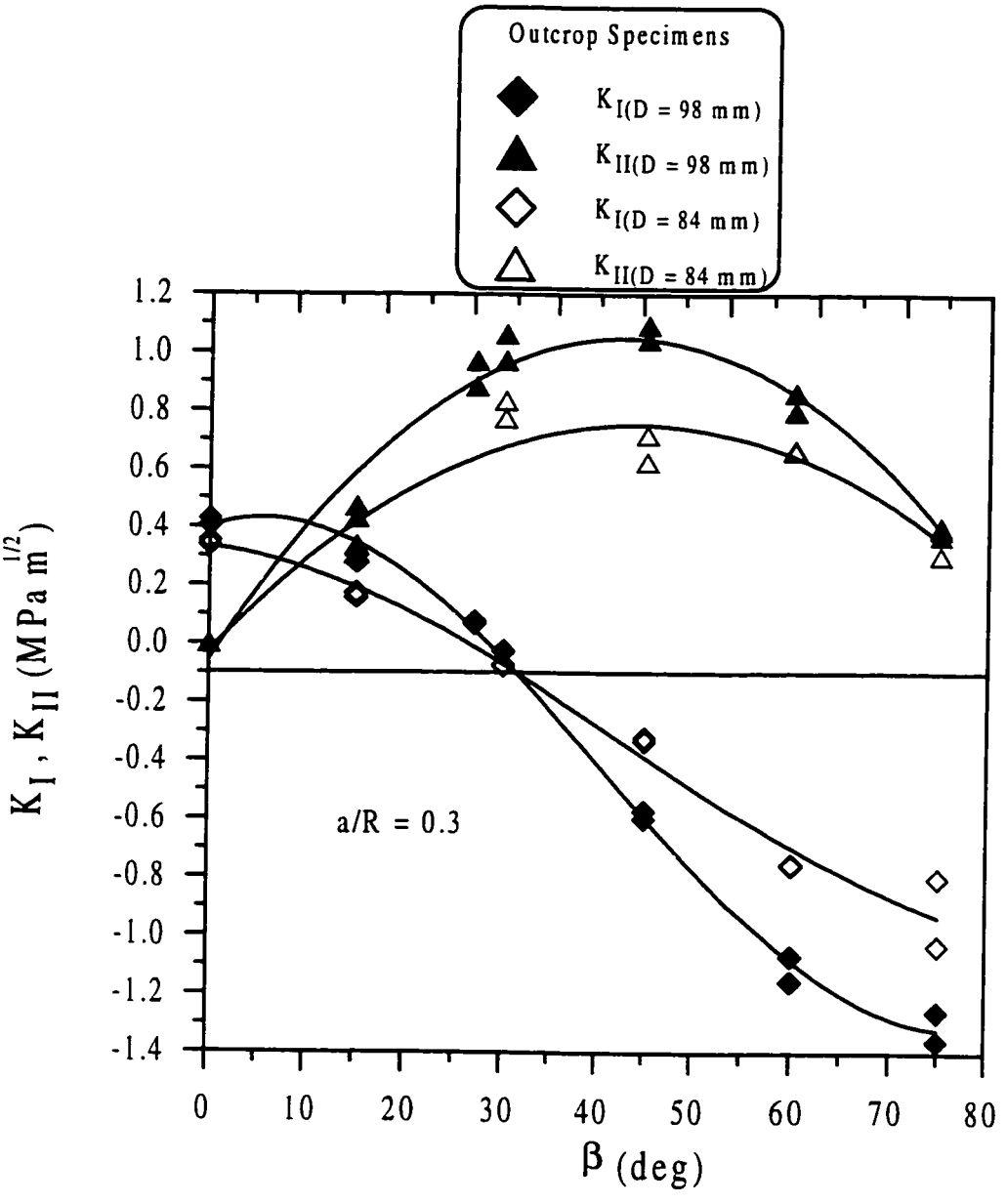

Figure 5.9: Effect of Specimen Diameter on Mixed Mode I-II Fracture Toughness for Straight Notched Brazilian Disks at Ambient Conditions.

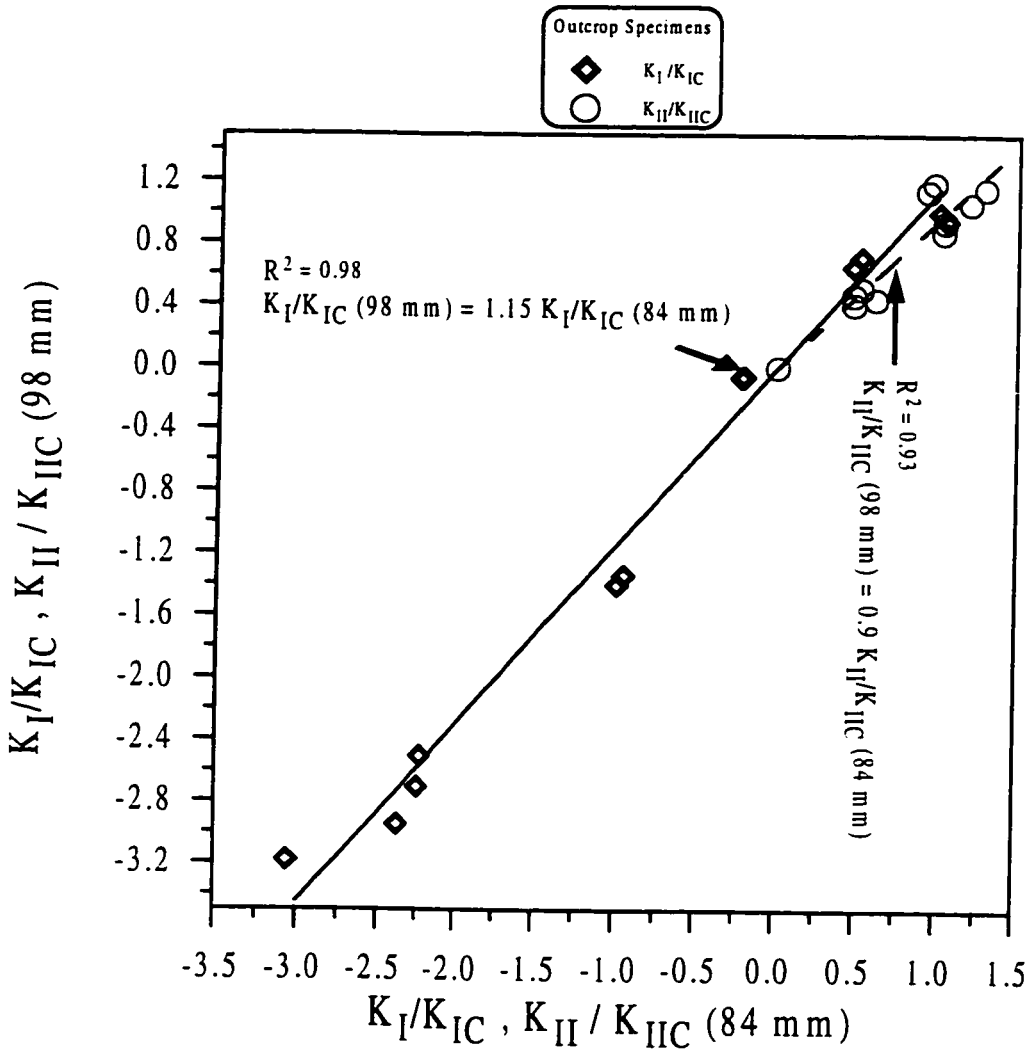

Figure 5.10: Effect of Specimen Diameter on Normalized Mode-I and Mode-II Fracture Toughness for Straight Notched Brazilian Disks at Ambient Conditions.

disks were 84 and 17 mm, respectively. The two normalized crack sizes (i.e., a/R) used in this investigation were 0.3 and 0.4. The fracture toughness results along with load at failure and specimen dimensions are presented in Table 5.6 and the fracture toughness variations are shown in Figure 5.11. It is clear from the plot that mixed mode I-II fracture toughness variation is negligible at least for the range of the crack size used in this study. Pure mode-I (K_{IC}) and pure mode-II (K_{IIC}) values for $a/R = 0.4$, were found to be 0.37 and 0.68 MPa $m^{1/2}$, respectively. This can be compared with the corresponding values of 0.35 and 0.65 MPa $m^{1/2}$ for the same specimens (a/R= 0.3), respectively, for pure mode-I (K_{IC}) and Pure mode-II(K_{IIC}). The results differ only by about 5%. The ratio of pure mode-II to pure mode-I (K_{IIC}/K_{IC}) for the larger crack length differs only by 1% from the corresponding value of 1.86 for the smaller crack length (a/R= 0.3) and was obtained as 1.84. The normalized mode-I and mode-II fracture toughness is shown in Figure 5.12. Again, compatibility of results for the two cases is clear as a value of 0.97 was obtained for the coefficient of determination (R^2).

Effect of Notch Type

The effect of notch type was investigated using Brazilian disks with straight and Chevron notches. The specimens were selected from outcrop samples and the crack to radius ratio was maintained at 0.3. The diameter and thickness of specimens were chosen as 98 mm and 22 mm, respectively. A summary of the results is presented in Table 5.7. Figure 5.13 shows the variations of the mixed mode fracture toughness for both types of notches over the range of inclination angles. The results for both notch

Table 5.6: Summary of Results for the Effect of Notch Length on Mixed Mode I-II Fracture Toughness.

β (deg)	B (mm)	D (mm)	2a (mm)	$2a/D$	P (kg)	K_I Mpa $(m)^{1/2}$	K_{II} Mpa $(m)^{1/2}$	K_I/K_{IC}	K_{II}/K_{IIC}
0	19	84	34	0	309	0.35	0.00	0.87	0.00
15	18	84	35	0	327	0.29	0.44	0.71	0.65
30	18	83	34	0	391	-0.01	0.80	-0.02	1.17
45	18	84	35	0	337	-0.41	0.68	-1.03	1.00
60	19	84	34	0	335	-0.75	0.49	-1.88	0.71
75	18	83	35	0	350	-1.15	0.29	-2.89	0.43
0	17	84	34	0	318	0.40	0.00	1.00	0.00
15	19	84	34	0	310	0.26	0.41	0.65	0.60
30	17	84	34	0	422	-0.01	0.90	-0.02	1.33
45	18	84	34	0	317	-0.39	0.65	-0.99	0.96
60	17	83	34	0	324	-0.82	0.53	-2.06	0.78
75	18	84	34	0	372	-1.20	0.30	-2.99	0.45
0	19	84	26	0	421	0.34	0.00	1.00	0.00
15	20	84	26	0	337	0.17	0.34	0.52	0.52
30	20	83	26	0	528	-0.08	0.84	-0.22	1.29
45	20	84	26	0	378	-0.33	0.63	-0.99	0.96
60	20	84	26	0	500	-0.75	0.67	-2.23	1.02
75	20	83	26	0	406	-0.80	0.31	-2.38	0.47
0	20	84	26	0	463	0.35	0.00	1.04	0.00
15	19	84	26	0	299	0.16	0.31	0.47	0.47
30	20	84	26	0	496	-0.07	0.78	-0.21	1.19
45	20	84	26	0	363	-0.32	0.60	-0.95	0.93
60	19	83	26	0	473	-0.76	0.67	-2.25	1.03
75	19	84	26	0	516	-1.03	0.40	-3.06	0.61

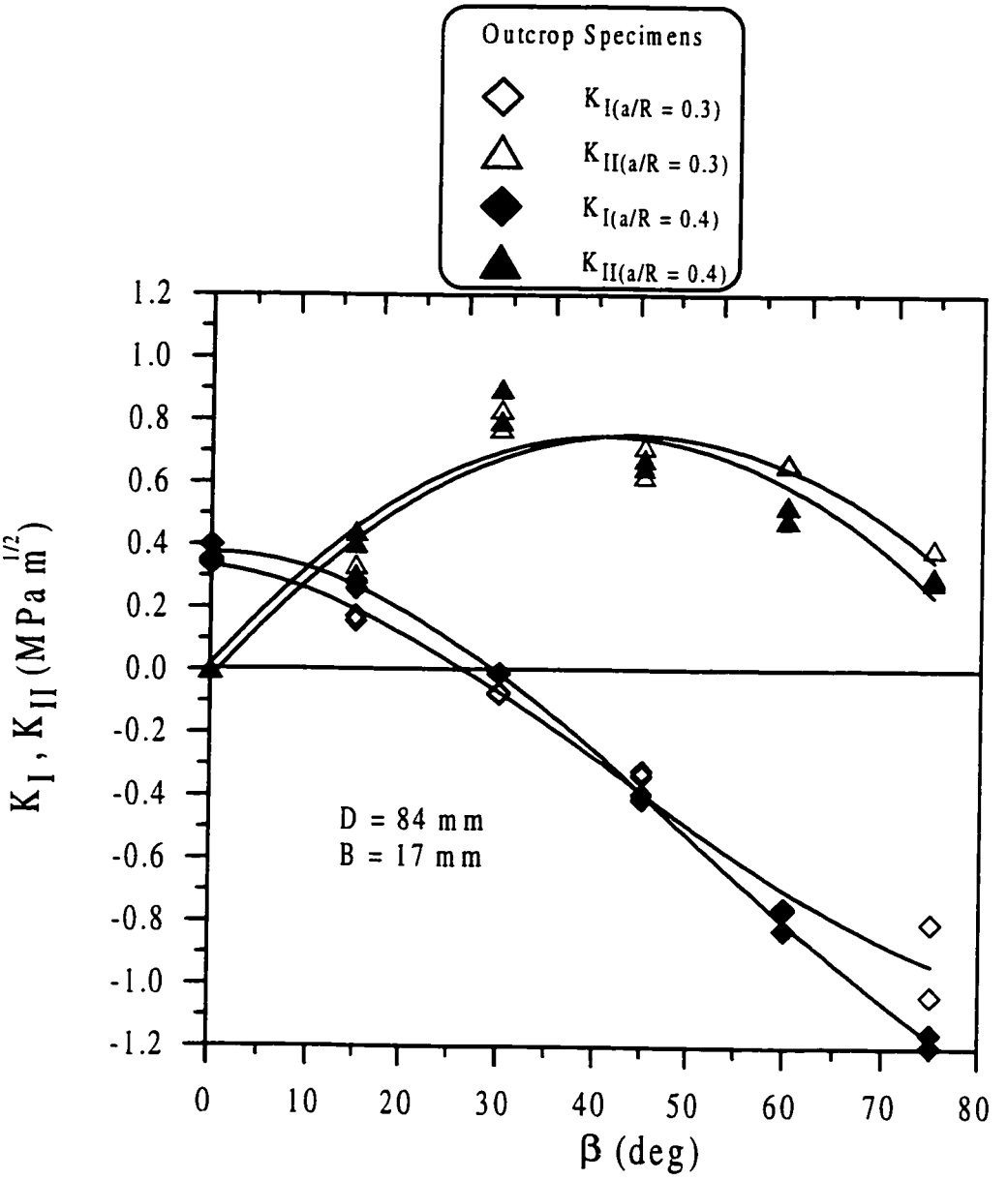

Figure 5.11: Effect of Notch Length on Mixed Mode I-II Fracture Toughness for Straight Notched Brazilian Disk Specimens at Ambient Conditions.

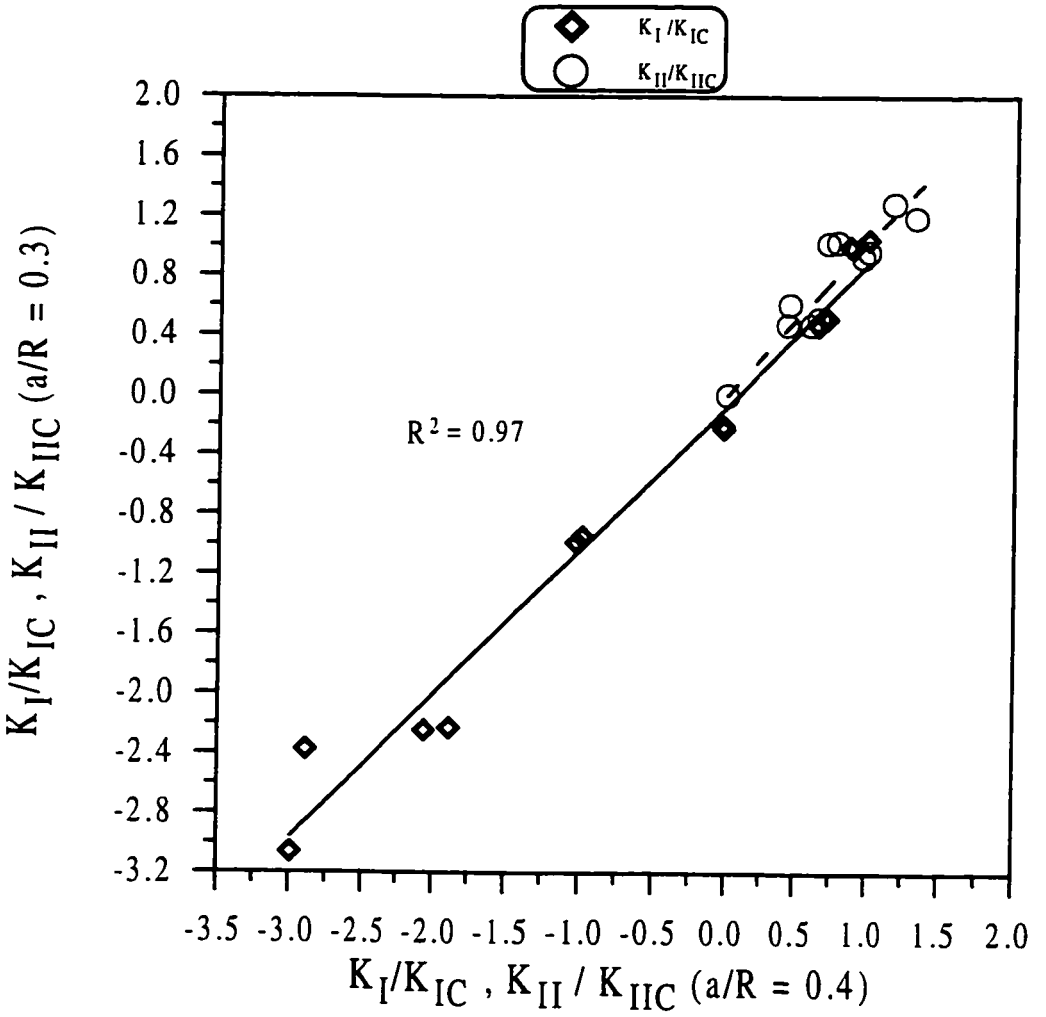

Figure 5.12: Effect of Notch Length on Normalized Mode-I and Mode-II Fracture Toughness of Straight Notched Outcrop Brazilian Disk Specimens at Ambient Conditions.

Table 5.7: Summary of the Results for the Effect of Notch Type on Mixed Mode I-II Fracture Toughness.

Straight Notch

β (deg)	B (mm)	D (mm)	*2a* (mm)	*2a/D*	P (kg)	K_I Mpa $(m)^{1/2}$	K_{II} Mpa $(m)^{1/2}$	K_I/K_{IC}	K_{II}/K_{IIC}
0	19	84	34	0	309	0.35	0.00	0.87	0.00
15	18	84	35	0	327	0.29	0.44	0.71	0.65
30	18	83	34	0	391	-0.01	0.80	-0.02	1.17
45	18	84	35	0	337	-0.41	0.68	-1.03	1.00
60	19	84	34	0	335	-0.75	0.49	-1.88	0.71
75	18	83	35	0	350	-1.15	0.29	-2.89	0.43
0	17	84	34	0	318	0.40	0.00	1.00	0.00
15	19	84	34	0	310	0.26	0.41	0.65	0.60
30	17	84	34	0	422	-0.01	0.90	-0.02	1.33
45	18	84	34	0	317	-0.39	0.65	-0.99	0.96
60	17	83	34	0	324	-0.82	0.53	-2.06	0.78
75	18	84	34	0	372	-1.20	0.30	-2.99	0.45

Chevron Notch

β (deg)	B (mm)	D (mm)	*2a* (mm)	*2a/D*	P (kg)	K_I Mpa $(m)^{1/2}$	K_{II} Mpa $(m)^{1/2}$	K_I/K_{IC}	K_{II}/K_{IIC}
0	22	98	28	0	970	0.61	0.00	1.00	0.00
15	22	98	29	0	975	0.44	0.68	0.72	0.79
27	22	98	29	0	764	0.07	0.83	0.11	0.96
30	22	98	28	0	745	-0.02	0.85	-0.03	0.99
45	22	98	30	0	764	-0.50	0.92	-0.82	1.07
60	22	98	30	0	932	-1.17	0.88	-1.92	1.02
75	22	98	29	0	1189	-2.00	0.60	-3.27	0.70

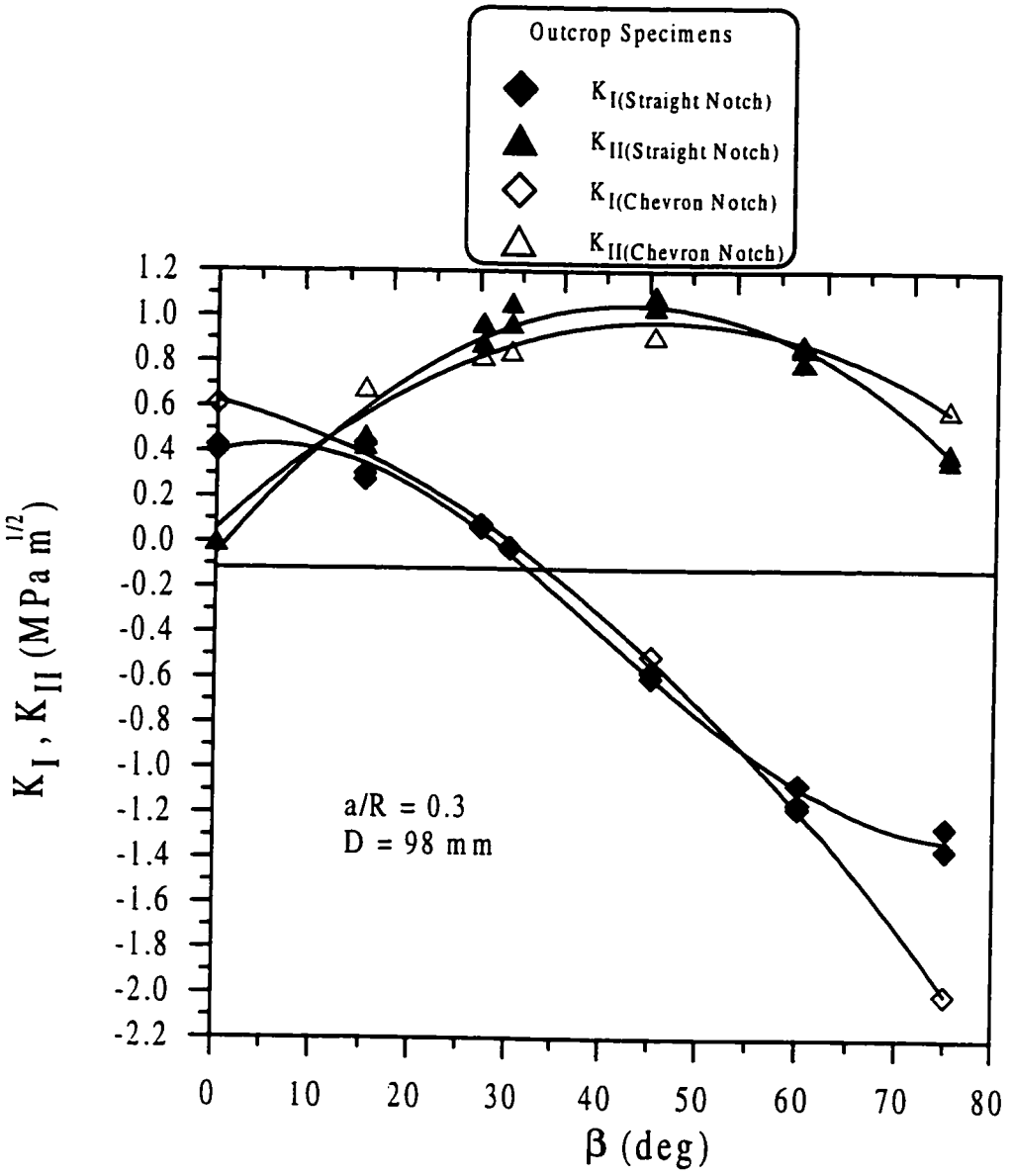

Figure 5.13: Comparison of Mixed Mode I-II Fracture Toughness for Straight and Chevron Notched Brazilian Disk Specimens at Ambient Conditions.

types are in good agreement except for pure mode-I. The fracture toughness values under pure mode-I (K_{IC}) and mode-II (K_{IIC}) for Chevron notched specimens are 0.61 and 0.86 MPa $m^{1/2}$, respectively. The corresponding values for the straight notch were 0.43 and 0.92 MPa $m^{1/2}$. The ratio of pure mode-II to pure mode-I (K_{IIC}/K_{IC}) was found to be 1.41 for Chevron notch, as compared to a value of 2.14 for straight notch. Normalized mode-I and mode-II fracture toughness results are presented in Figure 5.14.

The Chevron notched specimens resulted in fracture toughness values comparable to the straight notched ones. However, due to the fact that the straight notch was very sharp (0.25 mm) compared to about 1.5 mm thick Chevron notch and because crack boundaries and alignment of crack along the diameter of the specimen was difficult to control while machining a Chevron notch, it was decided to use only the straight notch for the rest of the samples used in this study for fracture toughness investigation.

Effect of Specimen Type

Fracture toughness results under mixed mode I-II for straight notched semicircular and Brazilian disk specimens are compared herein to investigate whether or not semicircular specimens could be an alternative to the Brazilian disk specimens. Outcrop specimens with 98 mm diameter and 22 mm thickness were chosen for this purpose. To compare the results, thickness, diameter and crack length were kept invariant for both types of specimens. The Normalized crack ratio (a/R) was chosen to be 0.3. The semicircular specimens were tested under three point bend loading

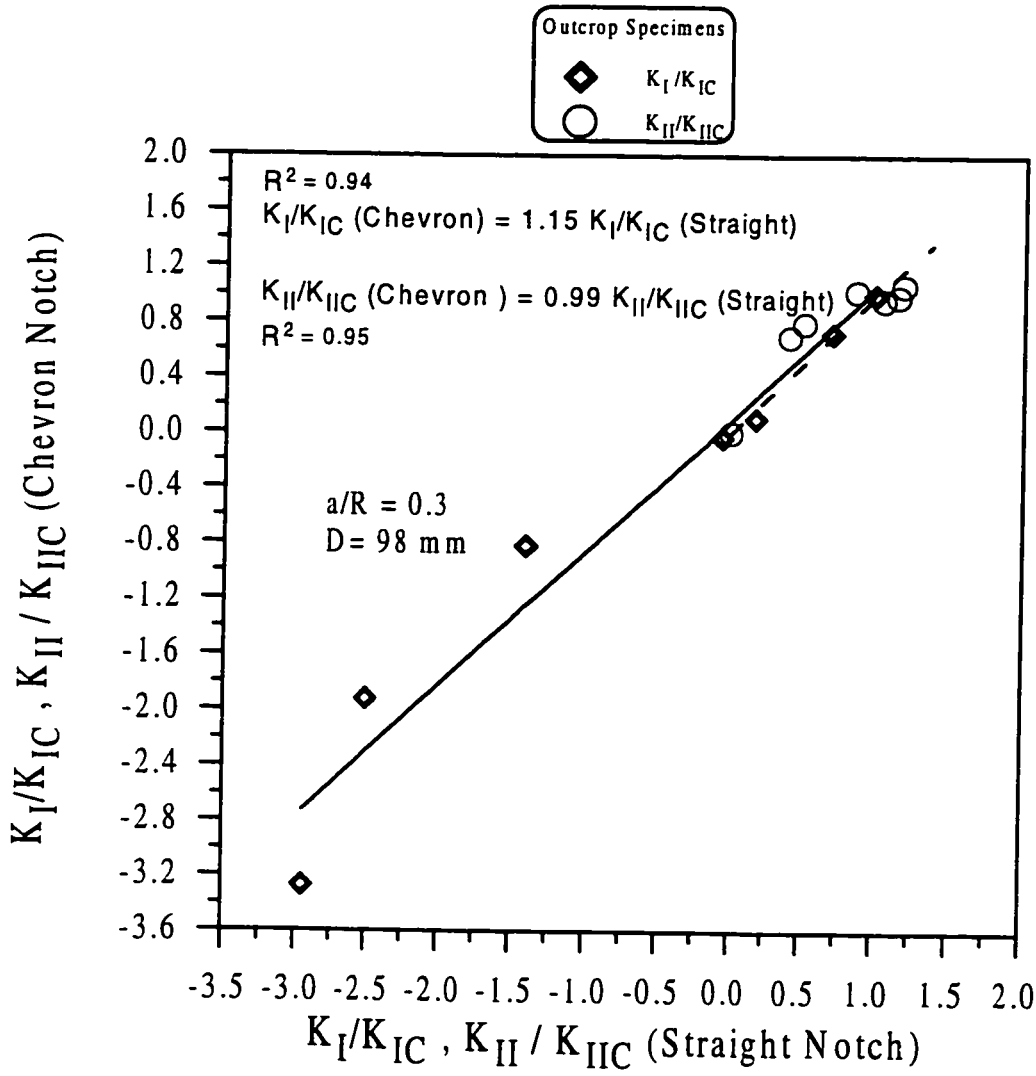

Figure 5.14: Normalized Mode-I and Mode-II Fracture Toughness for Straight and Chevron Notched Brazilian Disk Specimens at Ambient Conditions.

configuration with a span ratio (*S/R*) of 0.8 (see Figure 3.6). Any other span ratio was restricted by the size of both the specimen and the crack extensometer attached to the specimen to measure the crack extension during testing as described earlier. The specimens were tested with a crack inclination with respect to the loading direction varying from 0 to 60 degrees. The fracture toughness results for semicircular specimens are summarized in Table 5.8.

Comparison of the mixed mode I-II results for semicircular and Brazilian disk specimens is shown in Figure 5.15. It was observed that pure mode-I fracture toughness (K_{IC}) for semicircular specimens is about 0.40 MPa $m^{1/2}$ which is well within the range of being compared with the average value of 0.43 MPa $m^{1/2}$ for the Brazilian disk specimens. The pure mode-II fracture toughness (K_{IIC}) value obtained by extrapolating the existing results occurs at a crack inclination of approximately 72 degrees as compared to a value of 29 degrees for the Brazilian disks. K_{IIC} for the semicircular specimens was 0.17 MPa $m^{1/2}$ whereas for the notched Brazilian disk it was 0.92 MPa $m^{1/2}$. K_{IIC}/K_{IC} for the Brazilian and the semicircular specimens was 2.14 and 0.43, respectively. Since the load at failure, and hence, the fracture toughness value as well, is dependent on the radius to span ratio (i.e. *S/R*) for semicircular specimens, keeping all other parameters the same, no unique solution is obtainable for this type of specimen geometry. For smaller crack lengths, pure mode-II is possible to be achieved at larger crack inclinations. However, crack machining becomes almost impossible for the inclinations larger than 60 degrees.

Table 5.8: Summary of Mixed Mode I-II Fracture Toughness Results for Semicircular Specimens.

β (deg)	B (mm)	D (mm)	a (mm)	a/R	P (kg)	K_I Mpa $(m)^{1/2}$	K_{II} Mpa $(m)^{1/2}$	K_I/K_{IC}	K_{II}/K_{IIC}
0	22	96	15	0.31	140	0.39	0	1	0
8	22.5	97	16	0.33	220	0.58	0.06	1.53	0.34
13	23	98	15	0.31	195	0.49	0.08	1.31	0.46
15	23	98	15	0.31	249	0.62	0.11	1.64	0.65
22	22	98	15.5	0.32	219	0.50	0.13	1.33	0.75
30	22	98	16	0.33	250	0.51	0.17	1.34	1.02
37	22	98	15	0.31	234	0.41	0.17	1.09	1.02
45	22	98	15	0.31	281	0.41	0.21	1.08	1.25
52	22	98	15	0.31	232	0.27	0.17	0.72	1.00
60	22	98	15	0.31	310	0.28	0.21	0.73	1.22

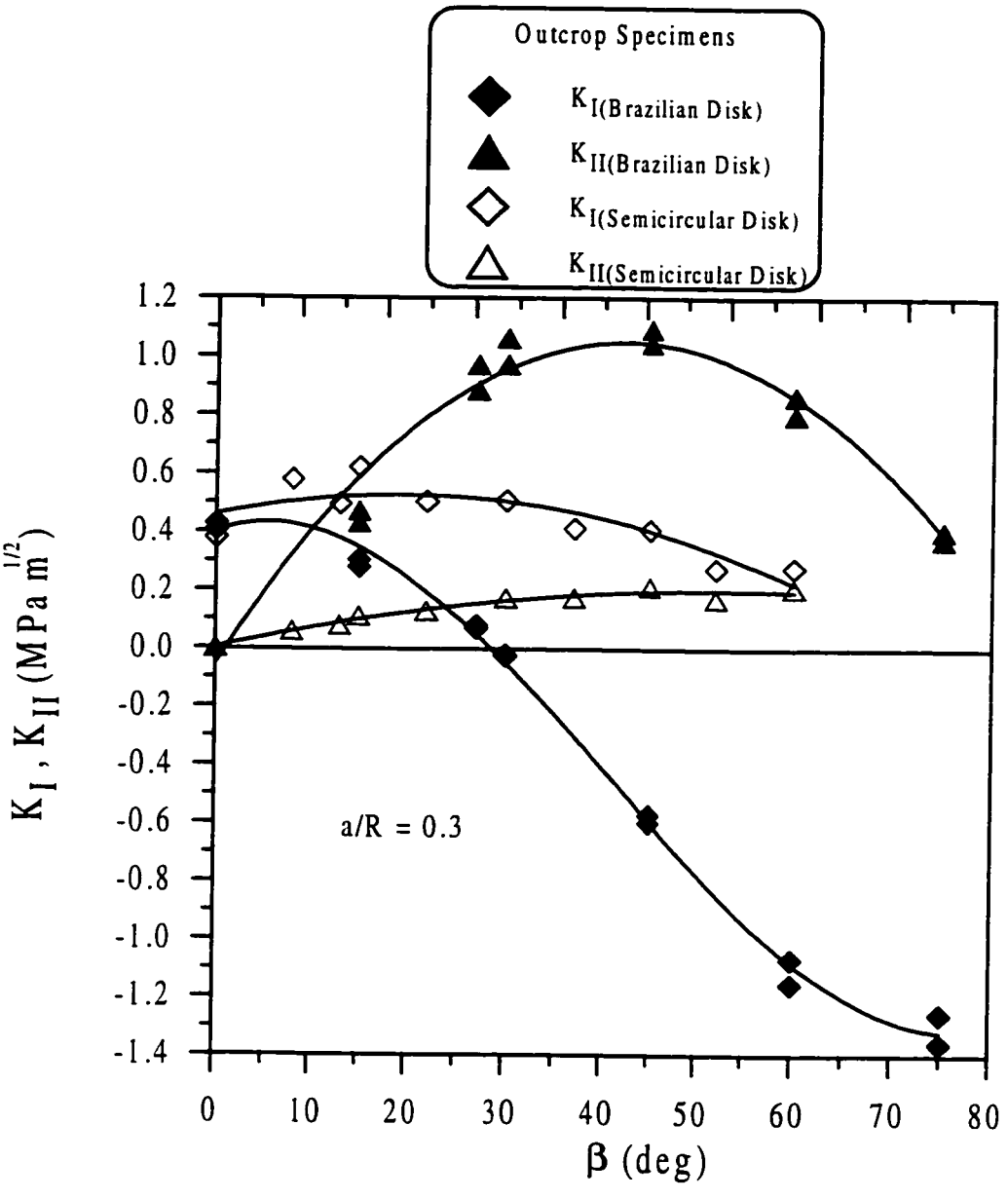

Figure 5.15: Comparison of Mixed Mode I-II Fracture Toughness for Straight Notched Brazilian and Semicircular Disk Specimens at Ambient Conditions.

On other hand, for larger crack lengths which facilitate the pure mode-II to be obtained at smaller crack inclination angles, the size of Fracture Process Zone (FPZ) limits the Linear Elastic Fracture Mechanics (LEFM) to be applicable. Therefore, it can be concluded that the results for the semicircular specimen geometry are not comparable to the notched Brazilian disk for mixed mode I-II as long as all the geometrical parameters are kept the same for both types of specimens. However, for studying pure mode-I fracture toughness, semicircular specimen shape can be a good candidate. The above findings encourage to neglect the semicircular specimens and rely on the notched Brazilian disk geometry for further detailed studies of mixed mode I-II fracture toughness in the course of this experimental work.

Effect of Specimen Origin

Notched Brazilian disks from the outcrop and reservoir samples were tested for mixed mode I-II fracture toughness to compare the variation with respect to the origin of the samples. Brazilian disks with straight notch were tested for this purpose. The specimens were 99 ± 1 mm in diameter and 23 ± 1 in thickness, and the crack to radius ratio (a/R) was kept at 0.3. The fracture toughness results for reservoir specimens are summarized in Table 5.9. Figure 5.16 shows the mixed mode fracture toughness variation for the reservoir specimens. Pure mode-I and mode-II fracture toughness values were 0.41 and 0.50 MPa $m^{1/2}$, respectively. It was observed that the reservoir samples had some inherent microcracks. Some of the samples even failed along those inherent flaws. The presence of such microcracks was thought to be

Table 5.9: Summary of Mixed Mode I-II Fracture Toughness Results for Reservoir Specimens at Ambient Conditions.

β (deg)	B (mm)	D (mm)	2a (mm)	$2a/D$	P (kg)	K_I Mpa $(m)^{1/2}$	K_{II} Mpa $(m)^{1/2}$	K_I/K_{IC}	K_{II}/K_{IIC}
0	25	100.5	16	0.32	736	0.41	0.00	1.00	0.00
15	23	100	16	0.32	444	0.19	0.30	0.47	0.74
27	24	101	16	0.32	430	0.03	0.43	0.08	1.05
30	23	100	16.5	0.33	379	-0.01	0.43	-0.03	1.04
45	25	100	17	0.34	582	-0.36	0.63	-0.87	1.54
60	24	100	16	0.32	666	-0.78	0.57	-1.89	1.39
75	24	100	16	0.32	680	-1.06	0.31	-2.57	0.75
0	24	100	16	0.32	695	0.41	0.00	0.99	0.00
15	23	101	16	0.32	420	0.18	0.28	0.44	0.69
30	24	100.5	16	0.32	561	-0.02	0.59	-0.04	1.45
60	23	100.5	16	0.32	588	-0.71	0.52	-1.74	1.28

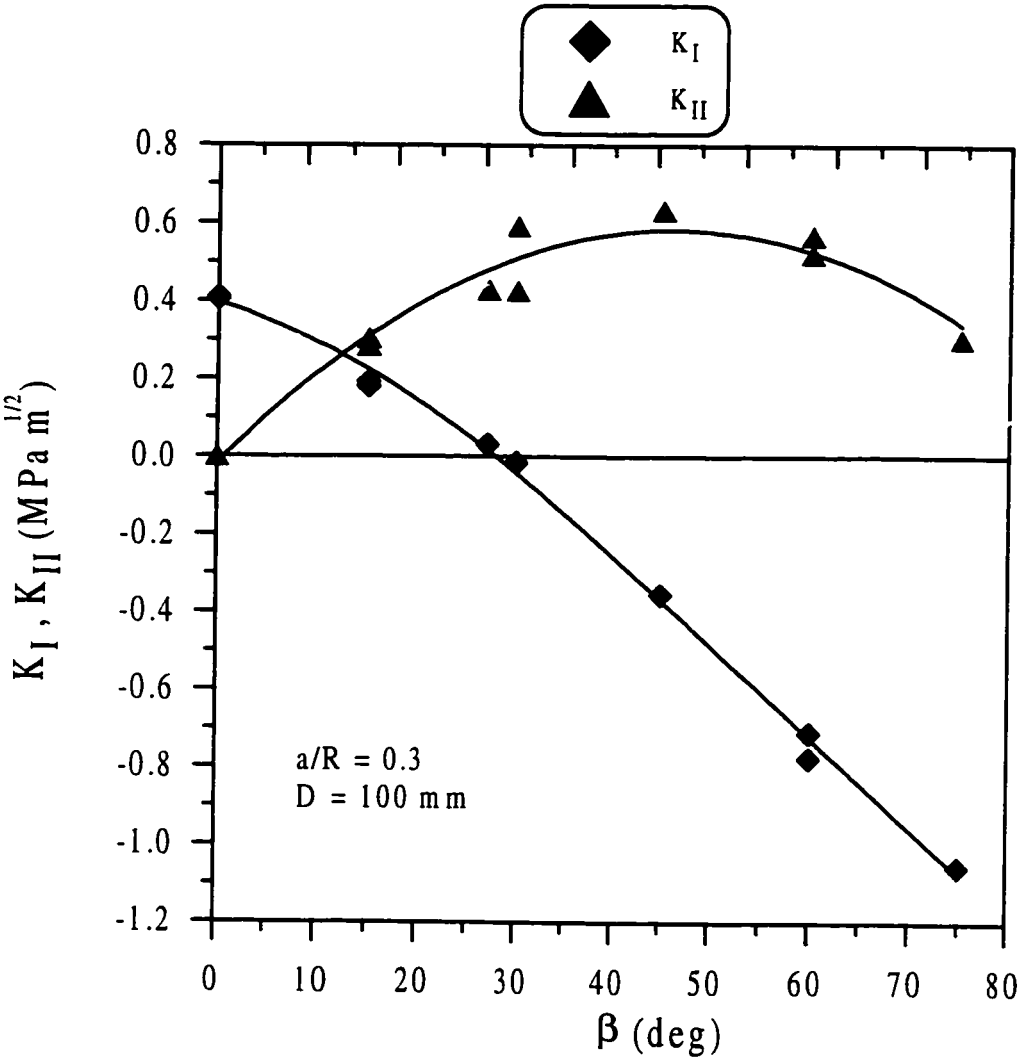

Figure 5.16: Mixed Mode I-II Fracture Toughness Variation for Straight Notched Reservoir Brazilian Disk Specimens at Ambient Conditions.

responsible for the reduced shearing action along the failure surface resulting in the decrease of mode-II component of fracture toughness.

Figure 5.17 gives a comparison between the outcrop and reservoir specimens. It was observed that both types of samples have the same value for mode-I fracture toughness. However, the reservoir specimens were seen to be weaker in shear as the mode-II component of fracture toughness for reservoir samples lies well below that of the outcrop specimens for the crack inclination range of 15 to 60 degrees. It is clear from Figure 5.17 that both types of specimens have almost the same angle of crack inclination for pure mode-II which is around 29-30 degrees. This revealed that the angle at which pure mode-II can be achieved is dependent on the specimen geometry and is not a function of material properties. Moreover, the ratio of pure mode-II to pure mode-I (K_{IIC}/K_{IC}) for reservoir specimens was 1.22 compared to 2.14 for outcrop specimens. Although, both specimens were collected from the same formation and have almost the same mineralogical composition, the fracture toughness behavior is very diverse. Normalized mode-I and mode-II results are plotted in Figure 5.18. Difference of fracture toughness values for the two types of specimens is clear. When reservoir specimens are cored from large depths, microcrcaks develop due to removal of the confinement. The induced microcracks make the specimens weaker and, consequently, a lower fracture toughness was observed.

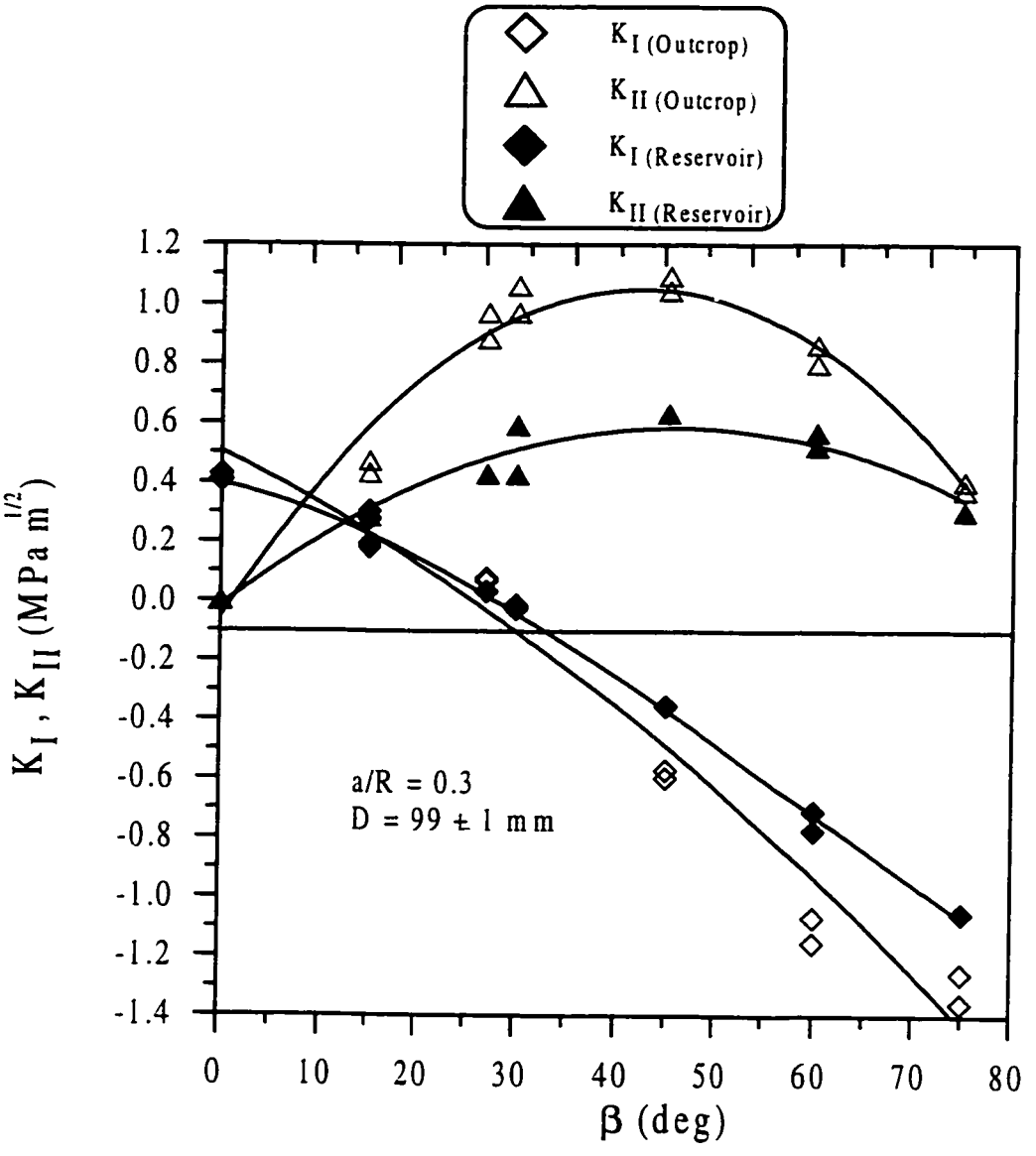

Figure 5.17: Comparison of Mixed Mode I-II Fracture Toughness for Straight Notched Outcrop and Reservoir Brazilian Disk Specimens at Ambient Conditions.

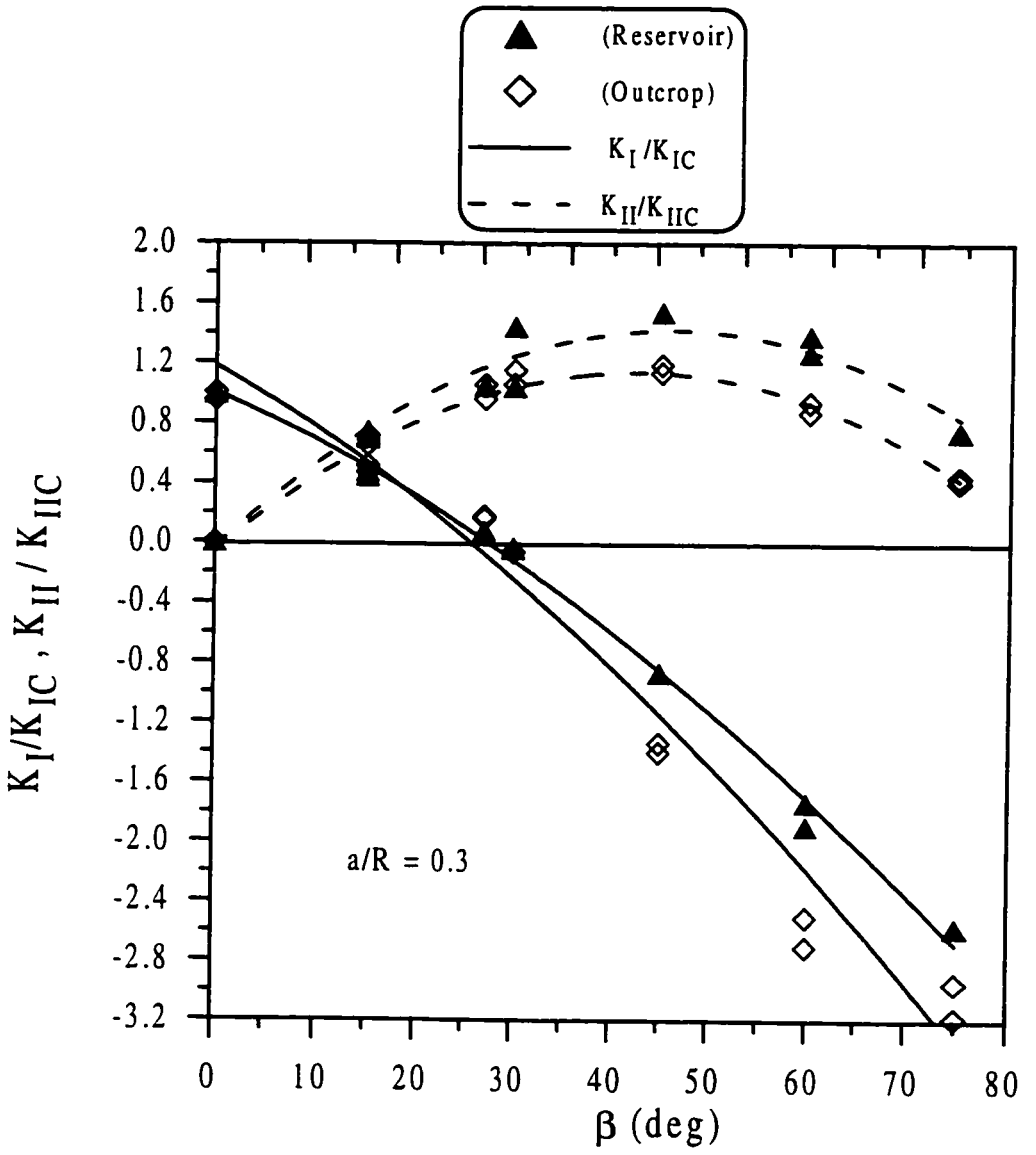

Figure 5.18: Normalized Mixed Mode I-II Fracture Toughness Variation for Straight Notched Outcrop and Reservoir Specimens at Ambient Conditions.

5.3.2 *In-situ* Conditions

Notched Brazilian disks from outcrop and from reservoir cores were tested for mode-I and mixed mode I-II fracture toughness study. The disks were 99 ± 1 mm in diameter and 23 ± 1 mm in thickness. The crack to radius ratio (a/R) was maintained at 0.3 in order to compare the results with the specimens tested under ambient conditions. Initially, it was proposed to study the fracture toughness variation under the combined influence of temperature and pressure. Unfortunately, the application of confining pressure after heating the sample was not successfully accomplished. During the sample heating stage, the "O" rings in the triaxial chamber became soft and broke upon the application of confining pressure resulting in leakage of oil from the cell. Quite a large number of trials were made after which it was decided to split the temperature and the pressure application program and to study their influence on the fracture toughness independent of each other.

5.3.2.1 Effect of Confining Pressure

Mode-I Results

The effect of confining pressure on mode-I fracture toughness was investigated by diametrically loading the hydrostaticaly confined straight notched Brazilian disk specimens. The dimensions of the specimens are described in the previous section. To study the variation in fracture toughness from ambient to a confining pressure of 28 MPa (4000 psi), a few specimens were tested by varying the confining pressure from 0

to 28 MPa with an increment of 7 MPa. On the contrary, most of the reservoir specimens were tested under mode-I under a confining pressure of 28 MPa only because of the limited number of specimens available from each lithology.

Figure 5.19 shows the load-displacement curves for the outcrop specimens tested under confining pressures of 0, 7, 14, 21, and 28 MPa. It was observed that the failure load increases as the confining pressure increases. Moreover, the load-deformation curves shifted to the right as the pressure increases and hence the deformation at failure increases with increasing confining pressure. It is, therefore, argued that the specimens at higher confining pressure behave in a more ductile way compared to those at low confining pressure. Similar response was observed by Vasarhelyi (1997) for an anisotropic rock under three point bending. The variation of fracture toughness with confining pressure is presented in Figure 5.20. The fracture toughness increases from an average value of 0.42 MPa $(m)^{1/2}$ for the specimens tested under ambient conditions to 1.57 MPa $(m)^{1/2}$ for those tested under a confining pressure of 28 MPa, representing an increase of 256%. The fracture toughness increased to almost 4 times. A straight line was used to fit the data with a coefficient of determination (R^2) of 0.99.

For the reservoir specimens, mode-I fracture toughness variation is presented in Figure 5.21, in which the results from outcrop specimens are also superimposed. The increase in the fracture toughness value at a confining pressure of 28 MPa over the ambient conditions was between 169 and 270% with the exception of three

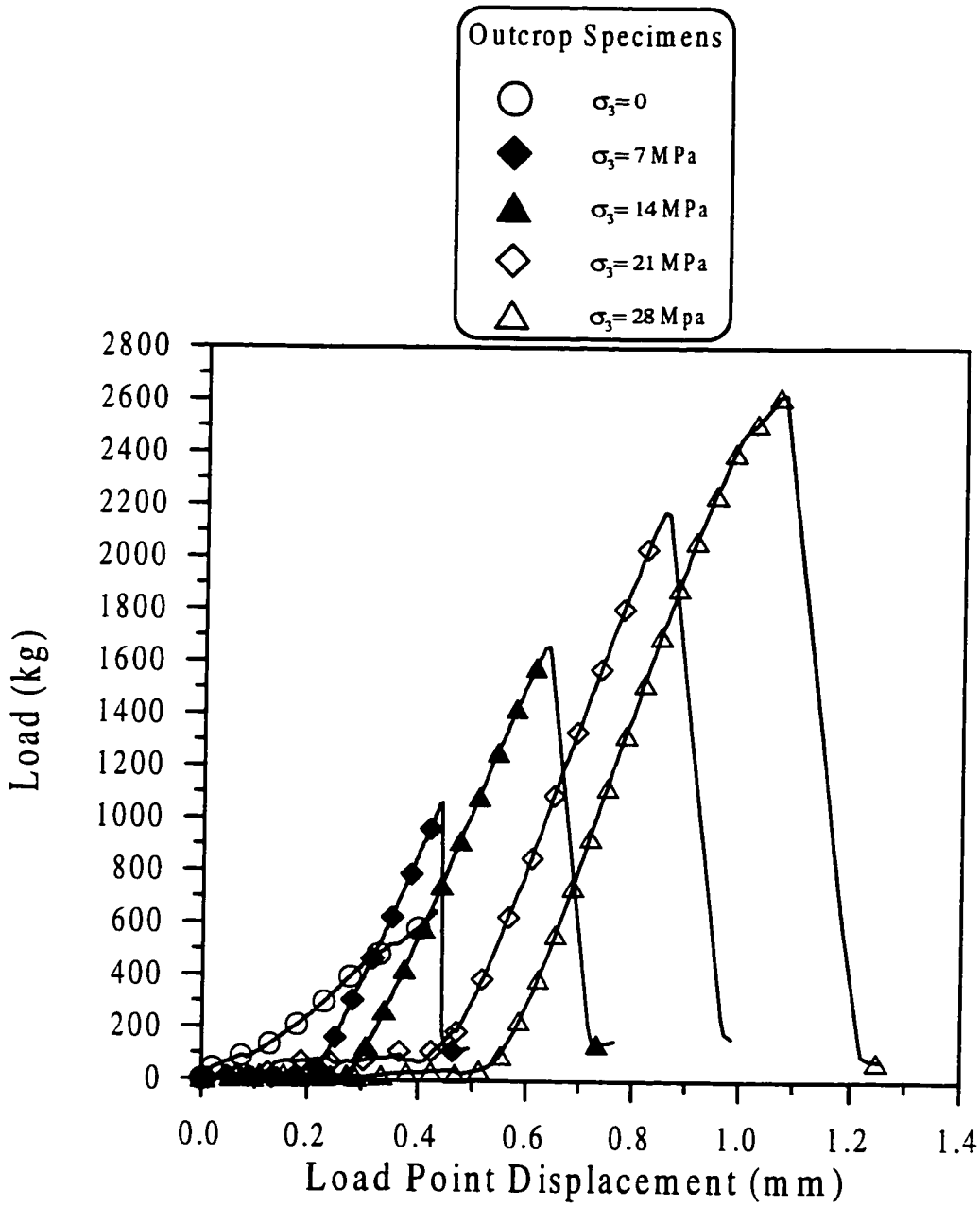

Figure 5.19: Load-Displacement Response of Straight Notched Brazilian Disk Specimens under Different Confining Pressures ($\beta = 0$).

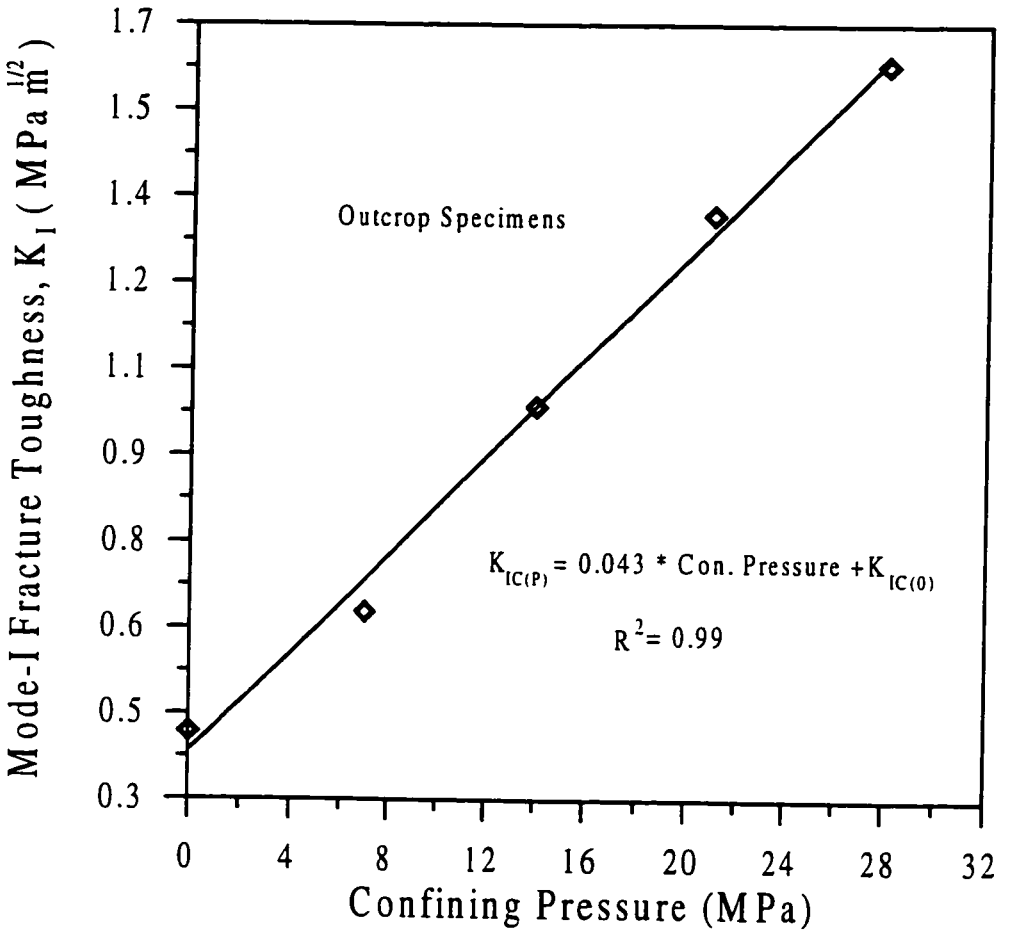

Figure 5.20: Effect of Confining Pressure on Mode-I Fracture Toughness.

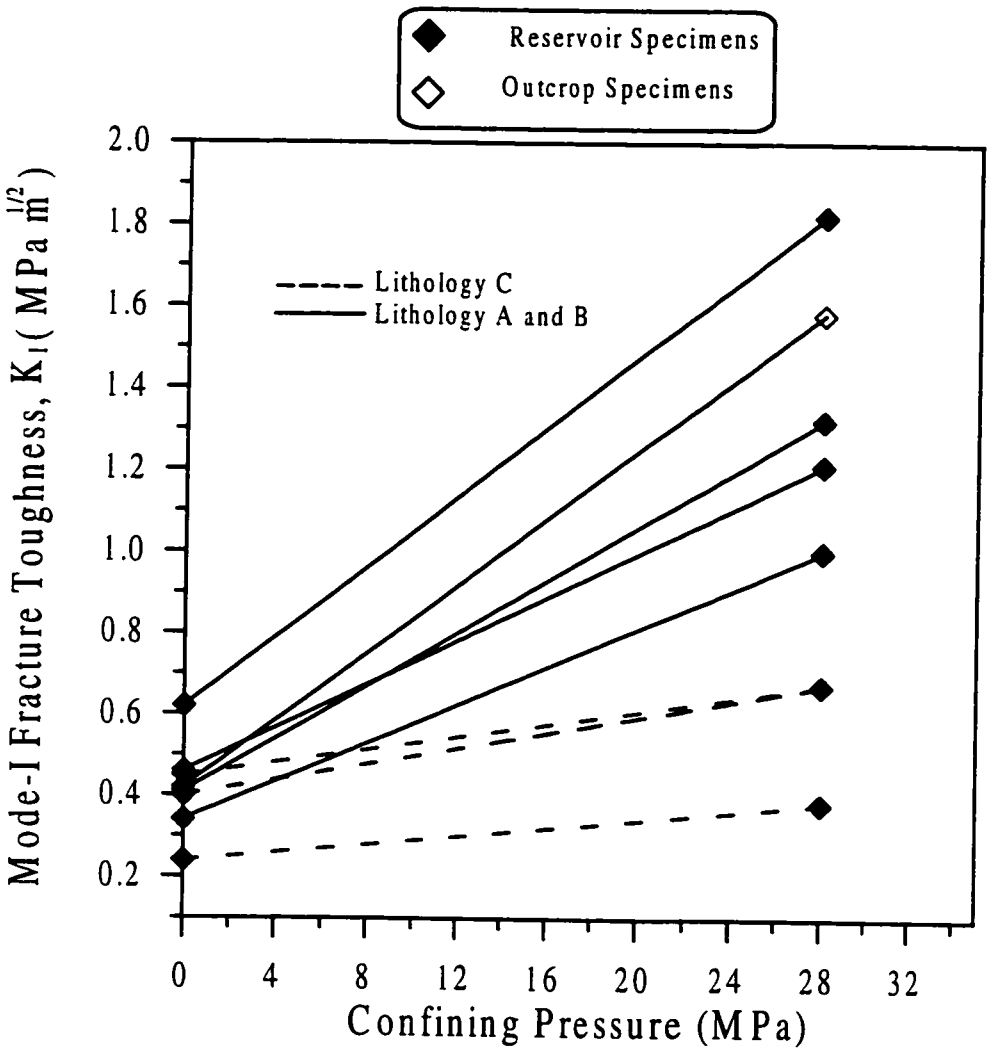

Figure 5.21: Effect of Confining Pressure on Mode-I Fracture Toughness for Reservoir Specimens.

specimens (from Lithology C) for which fracture toughness increased by only 50%. It was observed for those samples that they contain some impurities of anhydrite. The specimens failed at the interface of anhydrite and rock rather than along the notched line as is usually expected.

As a comparison to the above results, Schmidt and Huddle (1977) conducted fracture toughness testing of Indiana limestone under mode-I condition using a single edge notched beam in direct tension. Their results indicate that there was a significant increase in the fracture toughness value with increasing the confining pressure. Recently, Vasarhelyi (1997) studied the fracture toughness behavior of an anisotropic gneiss using a single edge cracked beam under three point bend configuration and concluded the same results. Abou-Sayed (1978) and Muller (1986) have reported the similar trend of fracture toughness variation with confining pressure.

It is believed that rock behaves in a more ductile manner under high confining pressures than at low or no confining pressure conditions. Increased fracture toughness at high confining pressure has been attributed to the relatively increased amount of energy required to create new surfaces in a ductile materials. Moreover, the high confining pressure results in a negative stress intensity factor at the crack tip causing an increase in the fracture toughness value with increasing confining pressure. Furthermore, the increase in confining pressure also reduces the size of the FPZ.

Effect of Specimen Size

Disk specimens 98 mm and 84 mm in diameter from outcrop were tested in mode-I at ambient conditions and under a confining pressure of 28 MPa. The fracture toughness

results are shown in Figure 5.22. The fracture toughness for 84 mm disk increases by 253% due to the application of 28 MPa confining pressure whereas for the 98 mm disks the increase is 244%.

Mixed Mode I-II Results

Mixed mode I-II fracture toughness testing under simulated reservoir simulated confining was conducted using both outcrop and reservoir specimens. The fracture toughness results obtained were compared to study the effect of both specimen origin and the testing conditions. Moreover, the effect of specimen size (i.e., diameter) on mixed mode I-II fracture toughness was also investigated. Brazilian disk specimens with a central straight notch were used in this investigation. The crack to radius ratio (a/R) was maintained at a value of 0.3. The crack orientation with respect to the loading direction was varied from 0 to 75 degrees. The samples were subjected to a confining pressure of 28 MPa (4000 psi) and then diametrally loaded to failure.

Results of Outcrop Specimens

Straight notched Brazilian disks from the outcrop with a diameter of 98 mm were used. The thickness of the specimens was chosen as 22 mm. Typical load-deformation curves for the outcrop specimens are shown in Figure 5.23. It was observed that all samples undergo a large amount of deformation without any significant increase in the load in the initial stage of testing. Moreover, the load-displacement behavior is no more pure elastic as was observed for the samples tested at ambient conditions. As can be seen in the plot, the load did not drop to zero after the specimens failed; the phenomenon observed for the specimens tested under ambient conditions. This

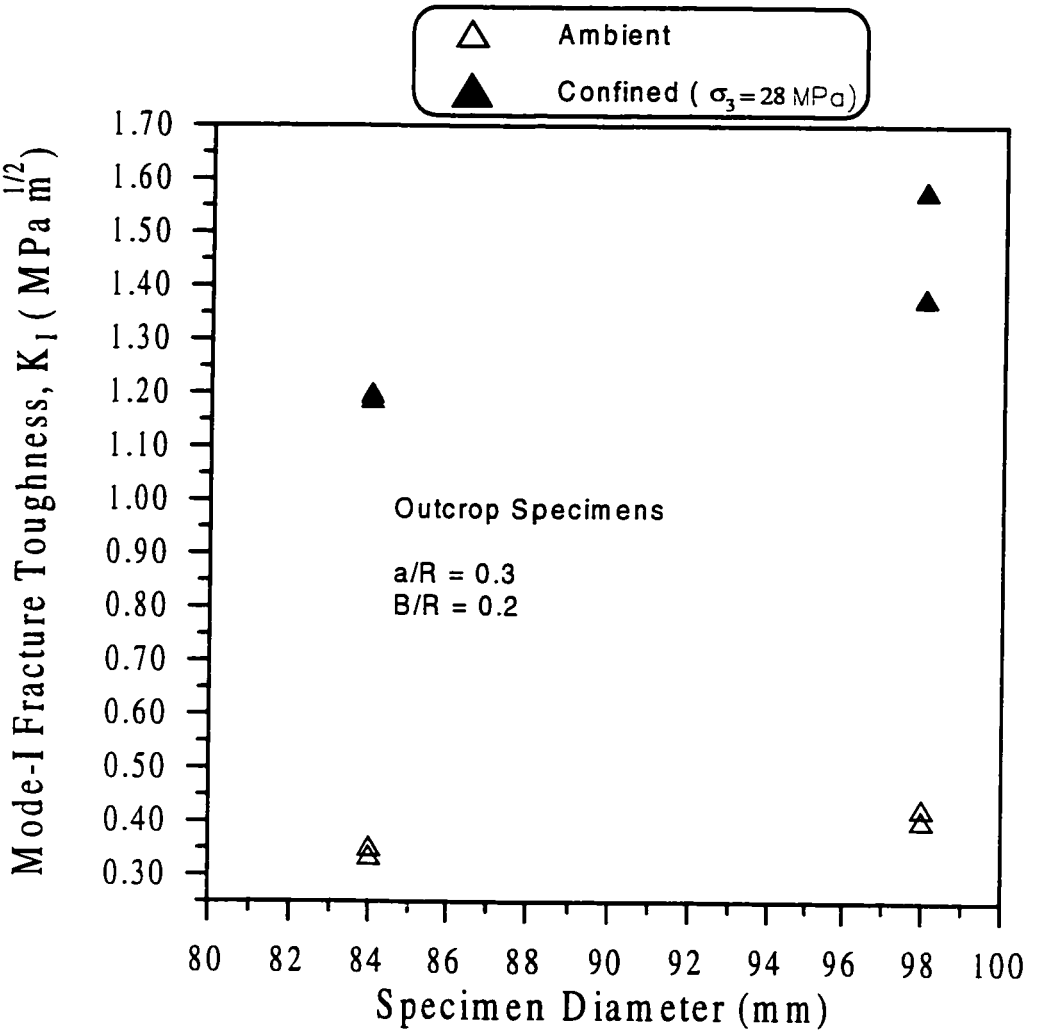

Figure 5.22: Effect of Specimen Diameter on Mode-I Fracture Toughness at Ambient and under Confining Pressure Conditions for Straight Notched Brazilian Disks.

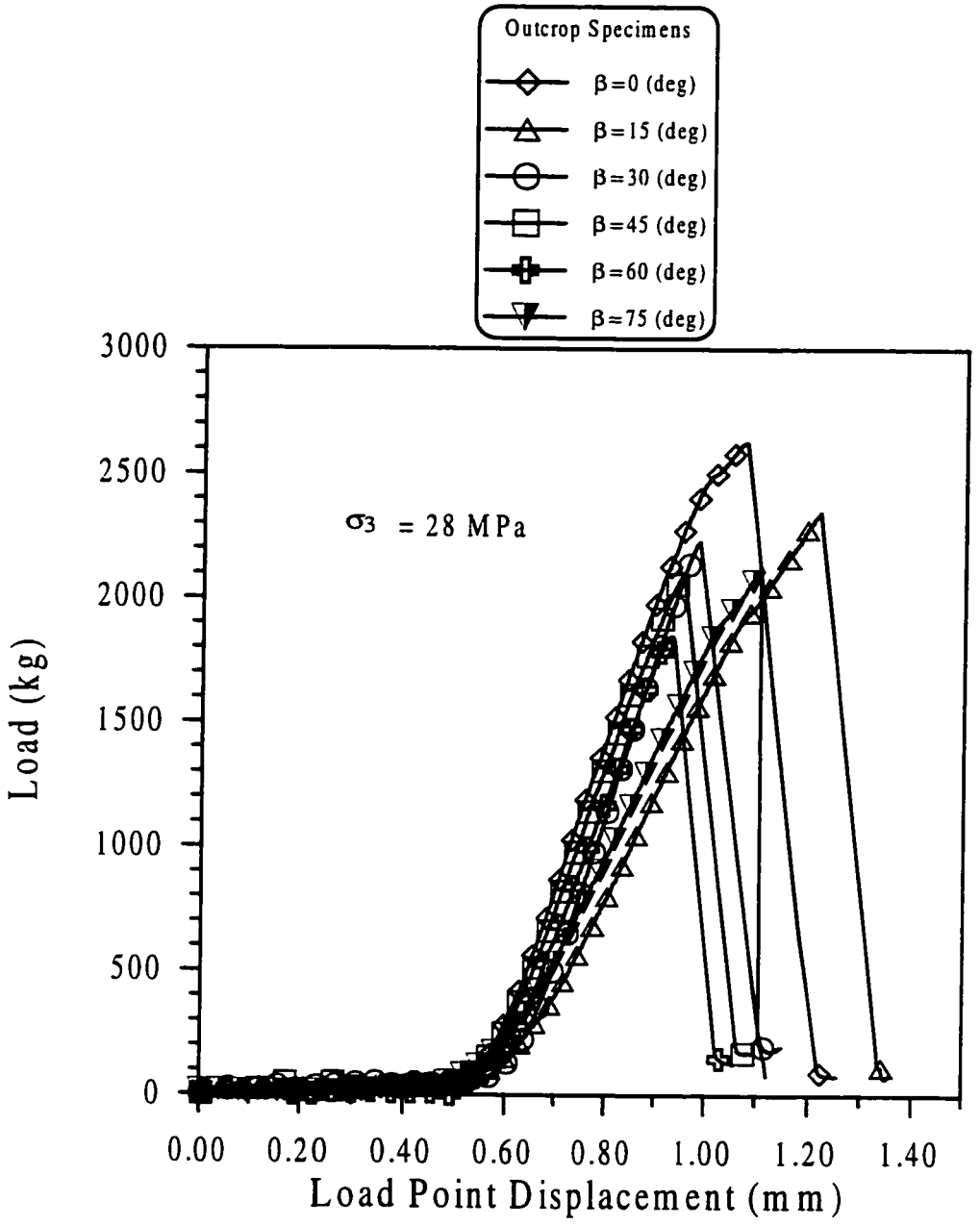

Figure 5.23: Load-Displacement Curves for Straight Notched Brazilian Disk Specimens for Mixed Mode I-II Loading under Confining Pressure.

behavior was attributed to the presence of confinement which held the two broken pieces together even after failure.

Mixed mode I-II fracture toughness results are plotted in Figure 5.24. Pure mode-I fracture toughness (K_{IC}) was 1.58 MPa $m^{1/2}$ and pure mode-II fracture toughness (K_{IIC}) was found to be 2.18 MPa $m^{1/2}$ and was achieved at a crack inclination angle of about 29 degrees. The fracture toughness results for the specimens tested under ambient and confining pressure are presented in Table 5.10 and plotted in Figure 5.25 for comparison. Pure mode-I and pure mode-II fracture toughness for the triaxially confined specimens increased by an amount of 265% and 137%, respectively, over the values obtained for ambient conditions. This led to the conclusion that mode-I fracture toughness is more sensitive to the confining pressure as compared to the mode-II component. The ratio of pure mode-II to pure mode-I (K_{IIC}/K_{IC}) was 1.39 for confined specimens as compared to a value of 2.14 for unconfined specimens representing a reduction of 54%.

Effect of Specimen Size

Effort was made to investigate the effect of specimen size when tested in a triaxially confined environment. For this purpose, notched Brazilian disks from outcrop with a diameter of 84 mm and normalized crack (a/R = 0.4) were used. The thickness to diameter ratio (B/D) was the same as that for the 98 mm specimens (i.e., 0.2), which resulted in a thickness of 17 mm. The specimens were tested in mixed mode I-II with a crack inclination of 0 to 75 degrees and the results were compared with those of the 98 mm diameter specimens. Mixed mode I-II fracture results for 84 and 98 mm disk

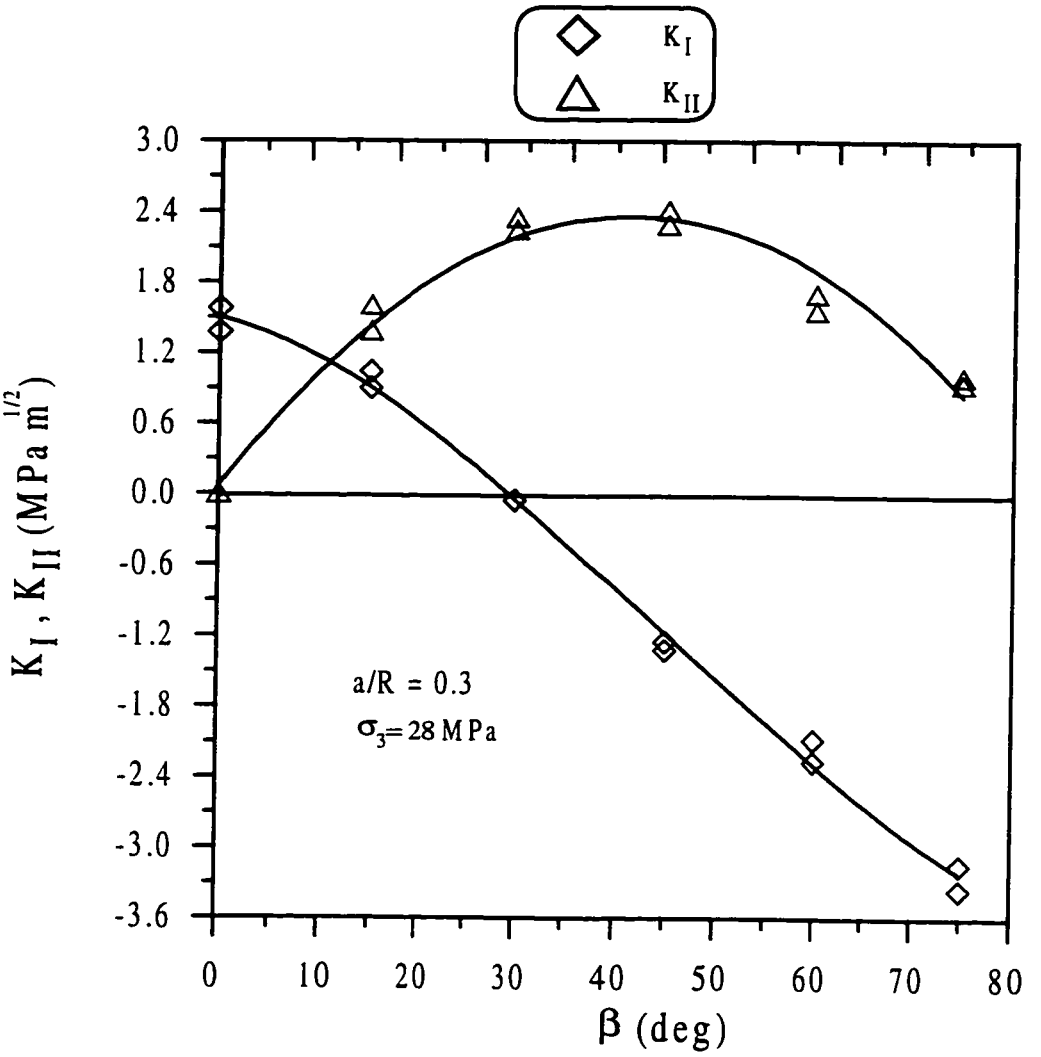

Figure 5.24: Mixed Mode I-II Fracture Toughness Variation for Outcrop Straight Notched Brazilian Disk Specimens under Confining Pressure.

Table 5.10: Summary of Mixed Mode Fracture Toughness Results for Outcrop Specimens at Ambient and under Confining Pressure.

At Ambient Conditions

β (deg)	B (mm)	D (mm)	*2a* (mm)	*2a/D*	P (kg)	K_I Mpa $(m)^{1/2}$	K_{II} Mpa $(m)^{1/2}$	K_I/K_{IC}	K_{II}/K_{IIC}
0	19	84	34	0	309	0.35	0.00	0.87	0.00
15	18	84	35	0	327	0.29	0.44	0.71	0.65
30	18	83	34	0	391	-0.01	0.80	-0.02	1.17
45	18	84	35	0	337	-0.41	0.68	-1.03	1.00
60	19	84	34	0	335	-0.75	0.49	-1.88	0.71
75	18	83	35	0	350	-1.15	0.29	-2.89	0.43
0	17	84	34	0	318	0.40	0.00	1.00	0.00
15	19	84	34	0	310	0.26	0.41	0.65	0.60
30	17	84	34	0	422	-0.01	0.90	-0.02	1.33
45	18	84	34	0	317	-0.39	0.65	-0.99	0.96
60	17	83	34	0	324	-0.82	0.53	-2.06	0.78
75	18	84	34	0	372	-1.20	0.30	-2.99	0.45

Under Reservoir Confining Pressure(σ_3 = 28 MPa)

β (deg)	B (mm)	D (mm)	*2a* (mm)	*2a/D*	P (kg)	K_I Mpa $(m)^{1/2}$	K_{II} Mpa $(m)^{1/2}$	K_I/K_{IC}	K_{II}/K_{IIC}
0	22.5	98.5	29	0.29	2626	1.58	0.00	1.00	0.00
15	22	98	29	0.30	2346	1.04	1.61	0.66	0.71
30	23	99	29	0.29	2227	-0.06	2.35	-0.04	1.05
45	22.5	98	29	0.30	2092	-1.32	2.42	-0.84	1.07
60	22	98.5	29	0.29	1846	-2.27	1.71	-1.44	0.76
75	23	98	29	0.30	2123	-3.35	1.01	-2.12	0.45
0	22	98	29	0.30	2321	1.43	0.00	0.91	0.00
15	23	98.5	29	0.29	2130	0.90	1.39	0.57	0.62
30	22.5	97	29	0.30	2039	-0.06	2.25	-0.04	1.00
45	22	98	29	0.30	1942	-1.25	2.30	-0.79	1.02
60	22	98	29	0.30	1684	-2.08	1.57	-1.32	0.70
75	22	98.5	29	0.29	1913	-3.15	0.95	-1.99	0.42

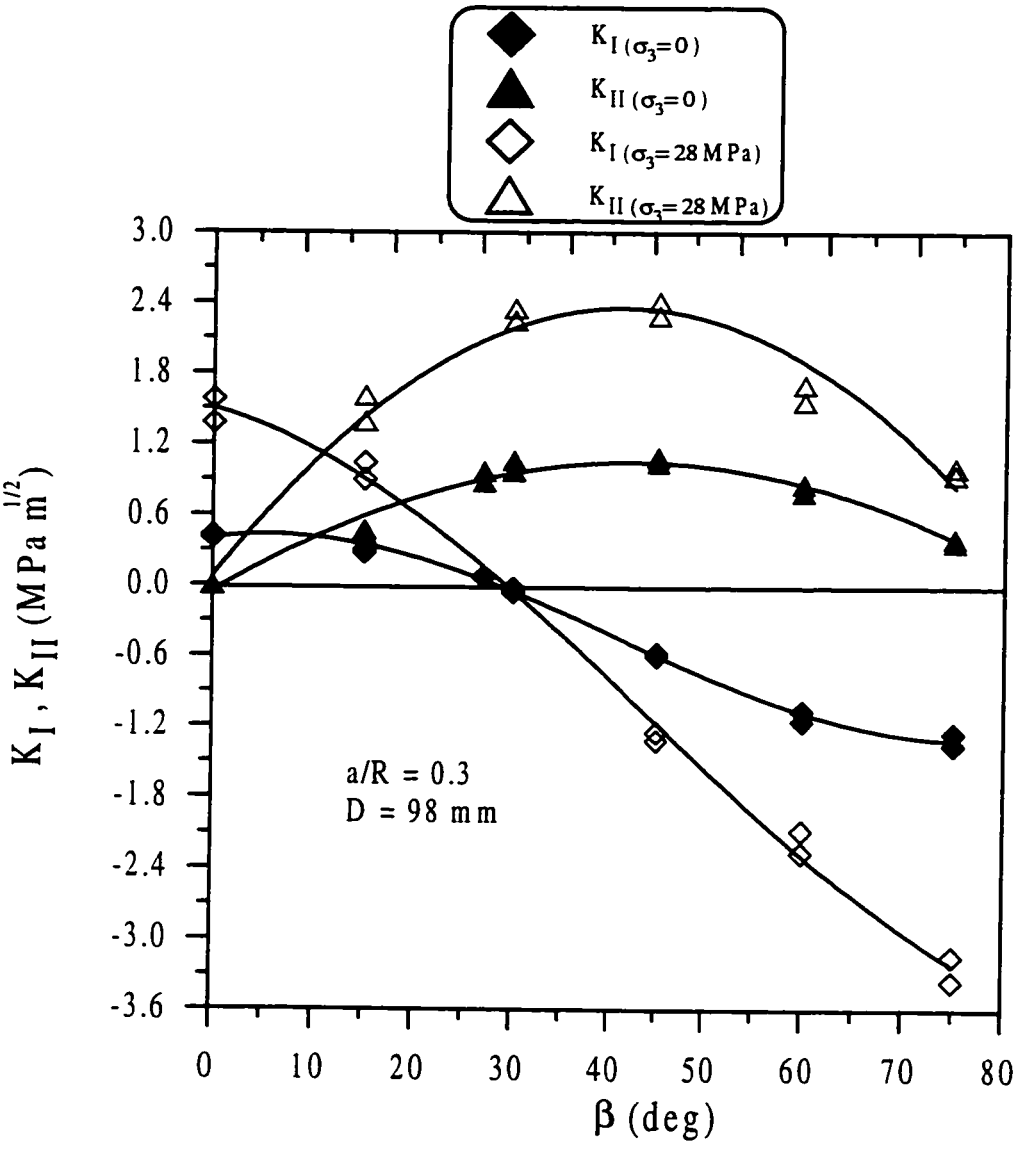

Figure 5.25: Comparison of Mixed Mode I-II Fracture Toughness Variation for Straight Notched Outcrop Brazilian Disk Specimens at Ambient and under Confining Pressure.

specimens are also plotted in Figure 5.26. Pure mode-I (K_{IC}) and pure mode-II (K_{IIC}) values for 84 mm diameter were found to be 1.19 and 1.49 MPa $m^{1/2}$, respectively; compared to the corresponding values of 1.58 and 2.18 MPa $m^{1/2}$ for 98 mm diameter disk specimens. The ratio of pure mode-II to pure mode-I (K_{IIC}/K_{IC}) for 84 mm diameter disk specimens was found to be 1.24 compared to 1.38 for 98 mm disks. This ratio for two specimens differs by 11% whereas it was found to be 14% for ambient conditions.

Results of Reservoir Specimens

For the reservoir specimens tested under a confining pressure of 28 MPa (4000 psi), the results of mixed mode I-II fracture toughness are shown in Figure 5.27 (see Table 5.11 for summary). Pure mode-I (K_{IC}) and pure mode-II (K_{IIC}) were found to be 1.32 and 2.18 MPa $m^{1/2}$, respectively; compared to corresponding values of 0.41 and 0.5 MPa $m^{1/2}$ at ambient conditions The mixed mode I-II fracture toughness results were compared with those obtained at ambient conditions, the variation for the two types of testing environments is presented in Figure 5.28. A tremendous increase in both mode-I and mode-II fracture toughness values was observed over the ambient conditions. Pure mode-I and mode-II fracture toughness values for the specimens tested under reservoir confining pressure were increased by 220% and 336% respectively. The ratio of Pure mode-II to pure mode-I (K_{IIC}/K_{IC}) was found to be 1.65 compared to 2.34 for the same specimens tested under ambient conditions.

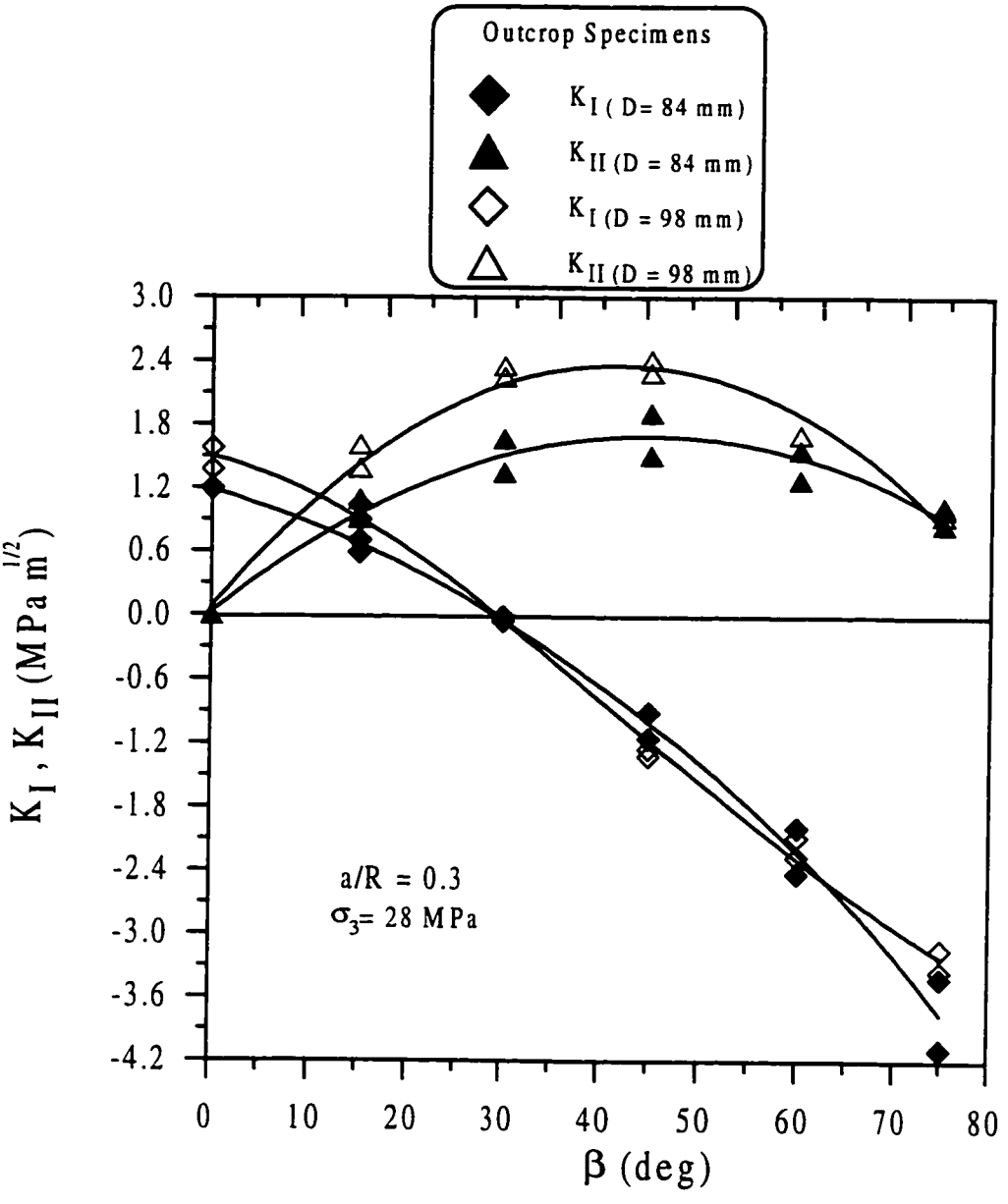

Figure 5.26: Effect of Specimen Size on Mixed Mode I-II Fracture Toughness for Straight Notched Brazilian Disks under Confining Pressure.

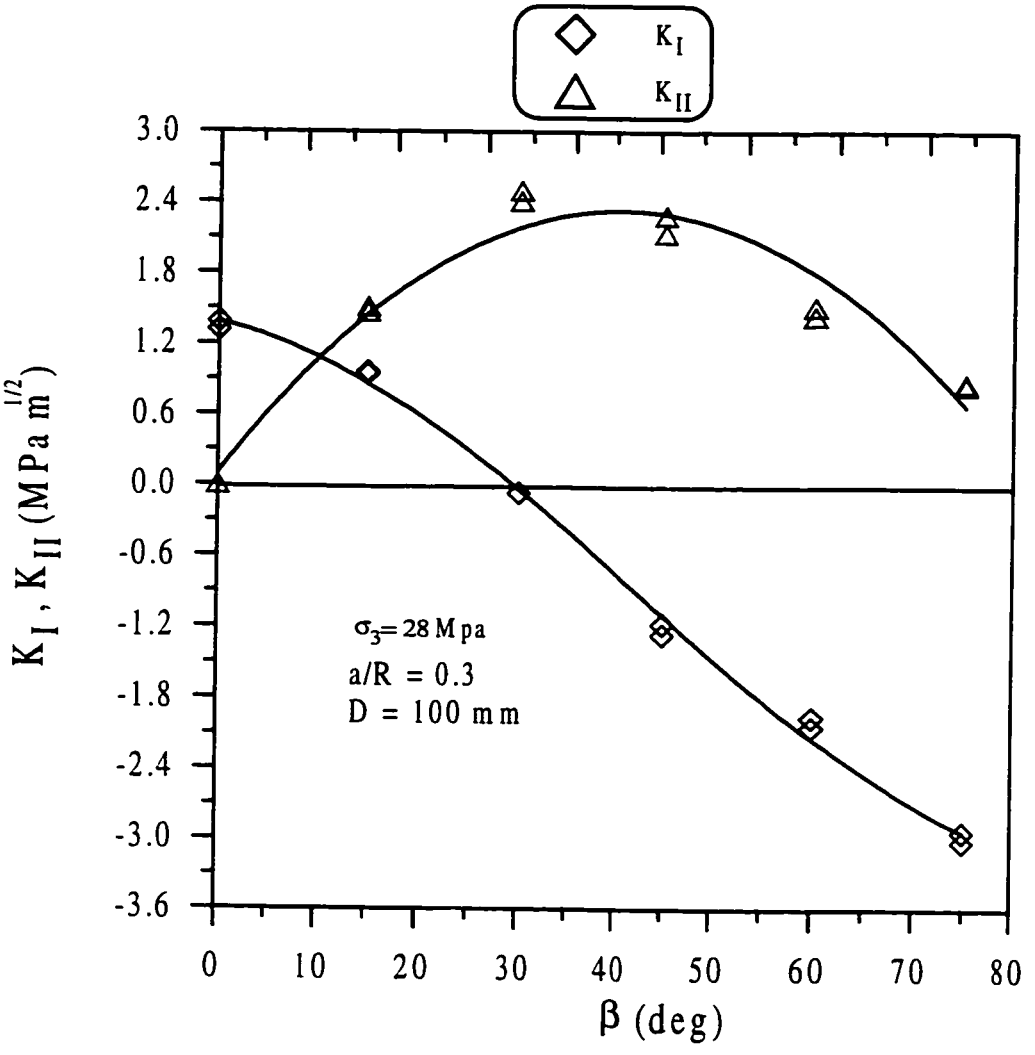

Figure 5.27: Mixed Mode I-II Fracture Toughness Variation for Straight Notched Reservoir Brazilian Disk Specimens under Confining Pressure.

Table 5.11: Summary of Mixed mode I-II Fracture Toughness Results for Reservoir Specimens under Reservoir Confining Pressure of 28 MPa.

β (deg)	B (mm)	D (mm)	*2a* (mm)	*2a/D*	P (kg)	K_I Mpa $(m)^{1/2}$	K_{II} Mpa $(m)^{1/2}$	K_I/K_{IC}	K_{II}/K_{IIC}
0	24	101	33	0.33	2247	1.32	0.00	1.00	0.00
15	23	101	31	0.31	2227	0.94	1.47	0.72	0.68
30	23	101	32	0.32	2280	-0.07	2.50	-0.05	1.15
45	23	100	32	0.32	1983	-1.27	2.29	-0.96	1.05
60	23	101	32	0.32	1628	-1.96	1.44	-1.49	0.66
75	23	100	32	0.32	1863	-3.02	0.87	-2.29	0.40
0	22.5	100	31	0.31	2261	1.38	0.00	1.05	0.00
15	22.5	101	32	0.32	2189	0.96	1.52	0.73	0.70
30	23	100	32	0.32	2178	-0.07	2.41	-0.05	1.11
45	23	101	32	0.32	1868	-1.18	2.14	-0.90	0.98
60	23	101	31	0.31	1725	-2.05	1.52	-1.55	0.70
75	23	101	32	0.32	1829	-2.94	0.86	-2.23	0.39

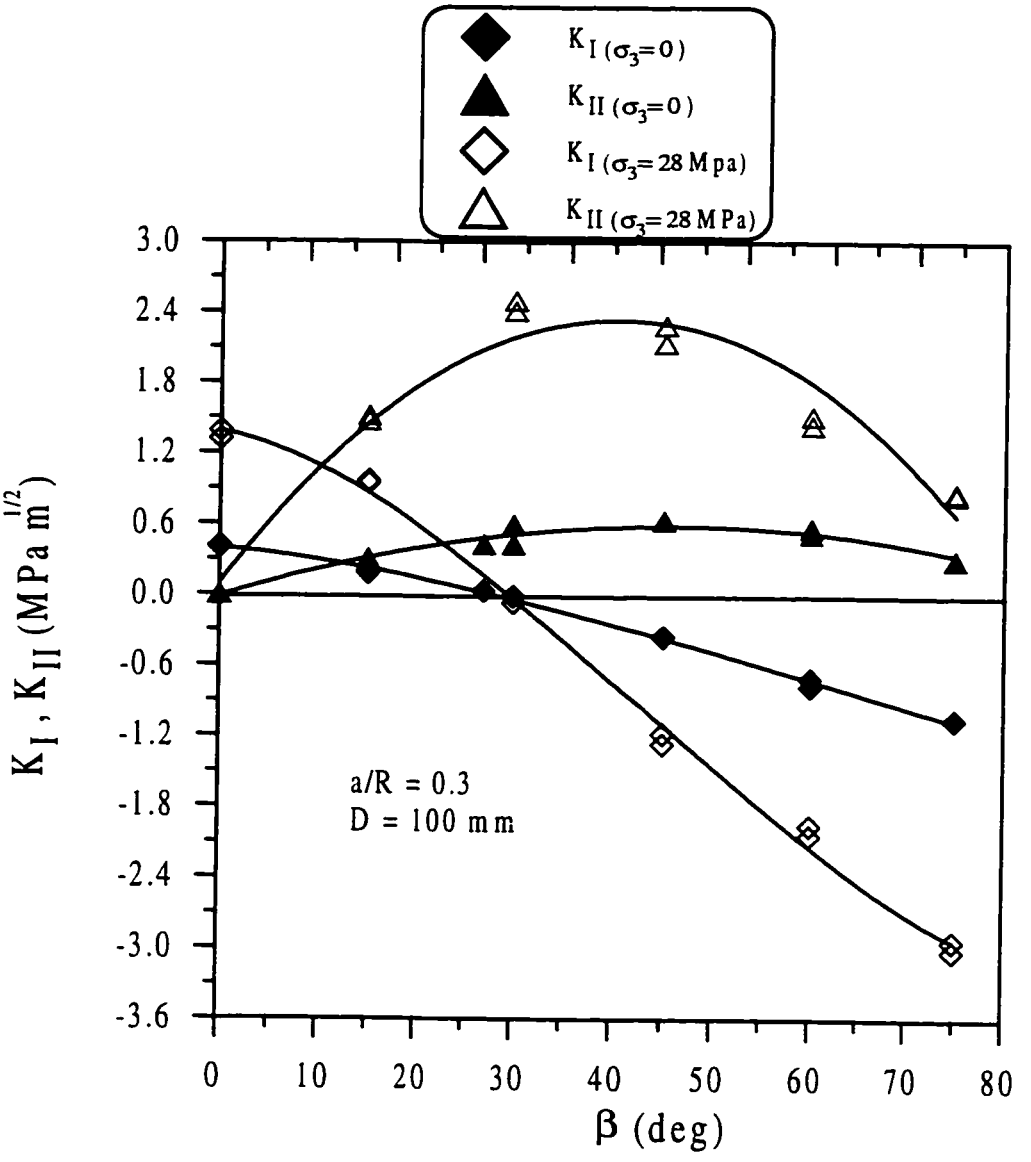

Figure 5.28: Comparison of Mixed Mode I-II Fracture Toughness Variation for Straight Notched Reservoir Brazilian Disk Specimens at Ambient and under Confining Pressure.

Comparison of Results for Outcrop and Reservoir Specimens

It was proposed to test the outcrop and reservoir specimens under simulated reservoir conditions in order to investigate whether the outcrop specimens could be used to determine the *in-situ* fracture behavior of specimens from the reservoir. For this purpose, the mixed mode I-II fracture toughness results for outcrop and reservoir specimens tested under confining pressure are compared. The results are shown in Figure 5.29. The results are in extremely good agreement with each other. Although both specimens showed a remarkable incompatibility in mixed mode I-II fracture results at ambient conditions, that incongruity was not seen for the case of triaxially confined conditions and the results were remarkably coherent. When specimens are tested under simulated pressure conditions, the microcracks in the reservoir specimens tend to close due to high compressive stresses. Due to this closure of microcrcaks, specimens become stronger and, hence, a higher fracture toughness was observed.

Figure 5.30 and Figure 5.31, respectively, show the variation of normalized mode-I and mode-II fracture toughness values for the outcrop and reservoir specimens under confined conditions. A straight line was used to best fit the data. Comparison of the normalized mode-I and mode-II fracture toughness under ambient and confined conditions is presented in Figure 5.32 and Figure 5.33, respectively.

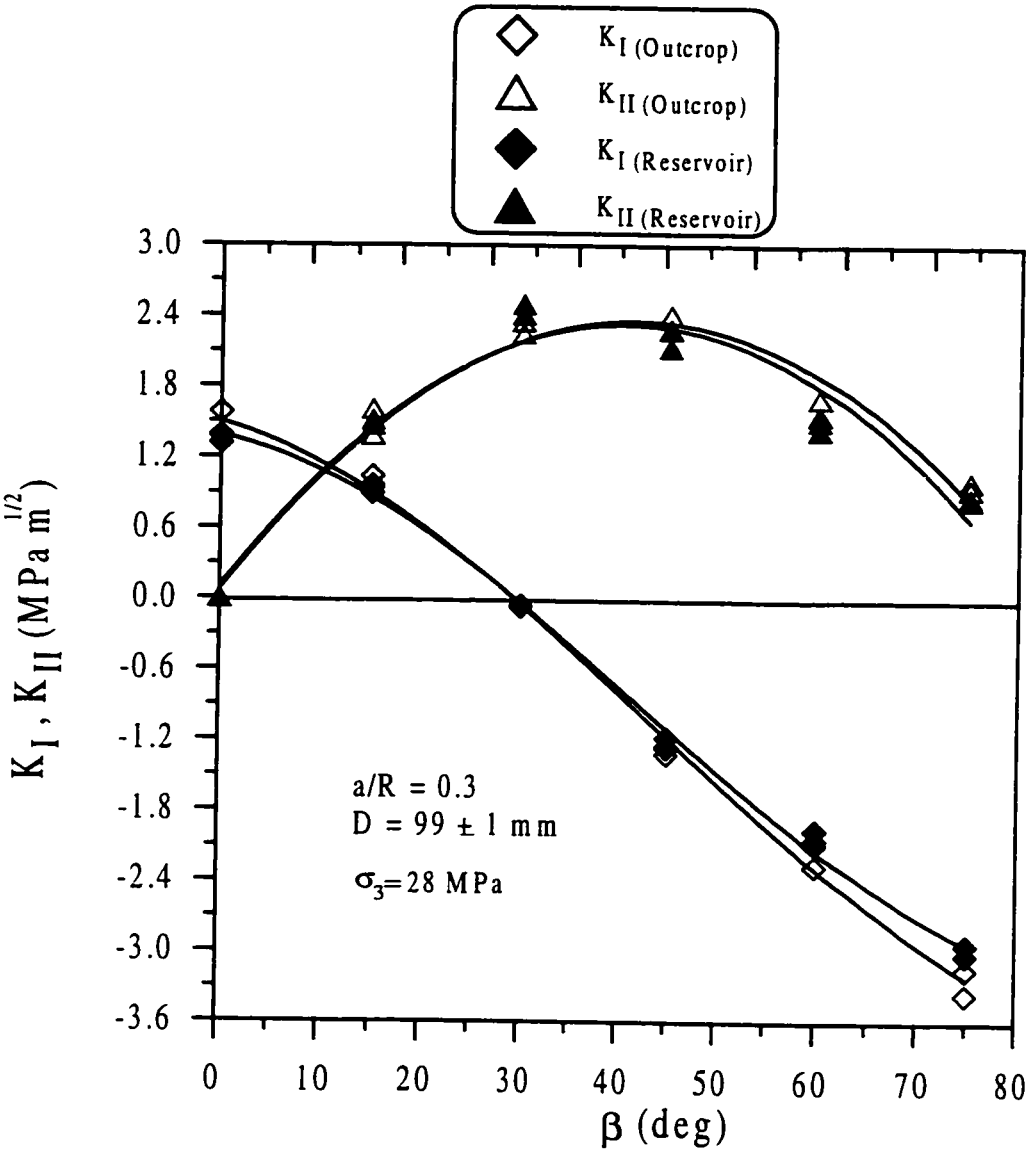

Figure 5.29: Comparison of Mixed Mode I-II Fracture Toughness Variation for Outcrop and Reservior Straight Notched Brazilian Disk Specimens under Confining Pressure.

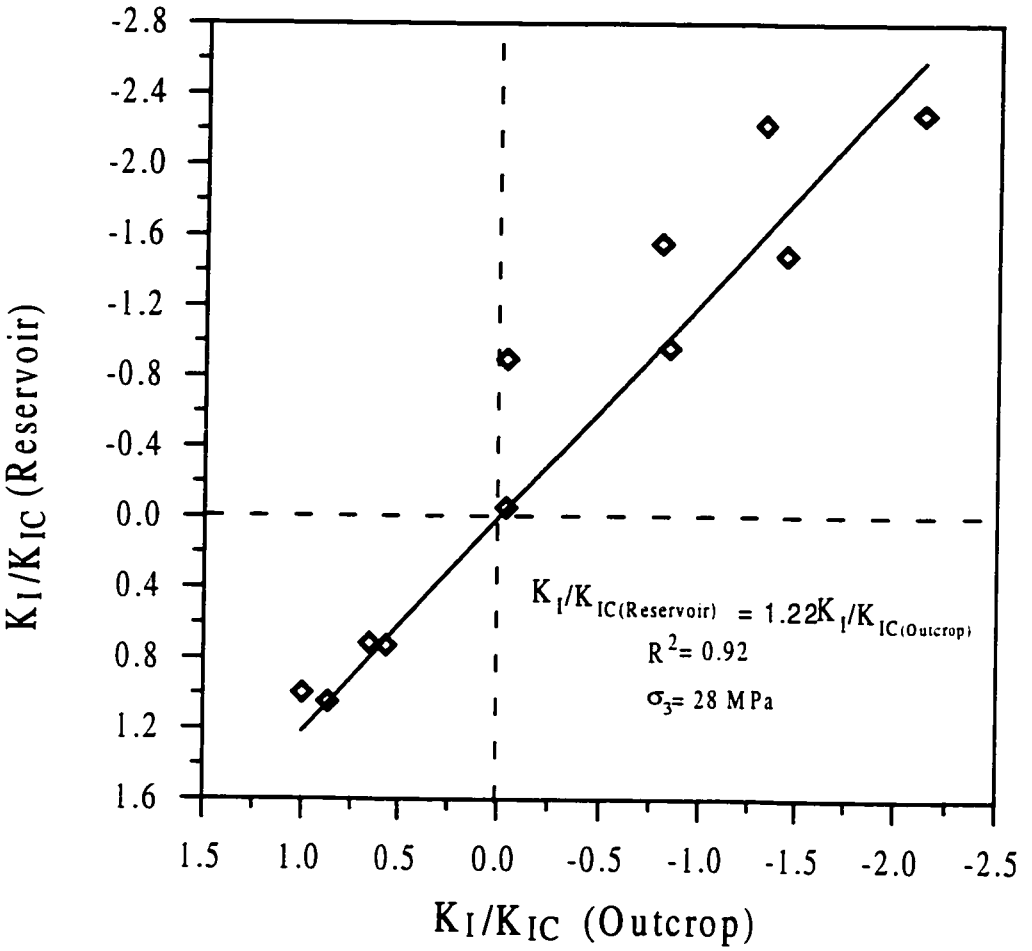

Figure 5.30: Comparison of Normalized Mode-I Fracture Toughness for Outcrop and Reservoir Straight Notched Brazilian Disk Specimens under Confining Pressure.

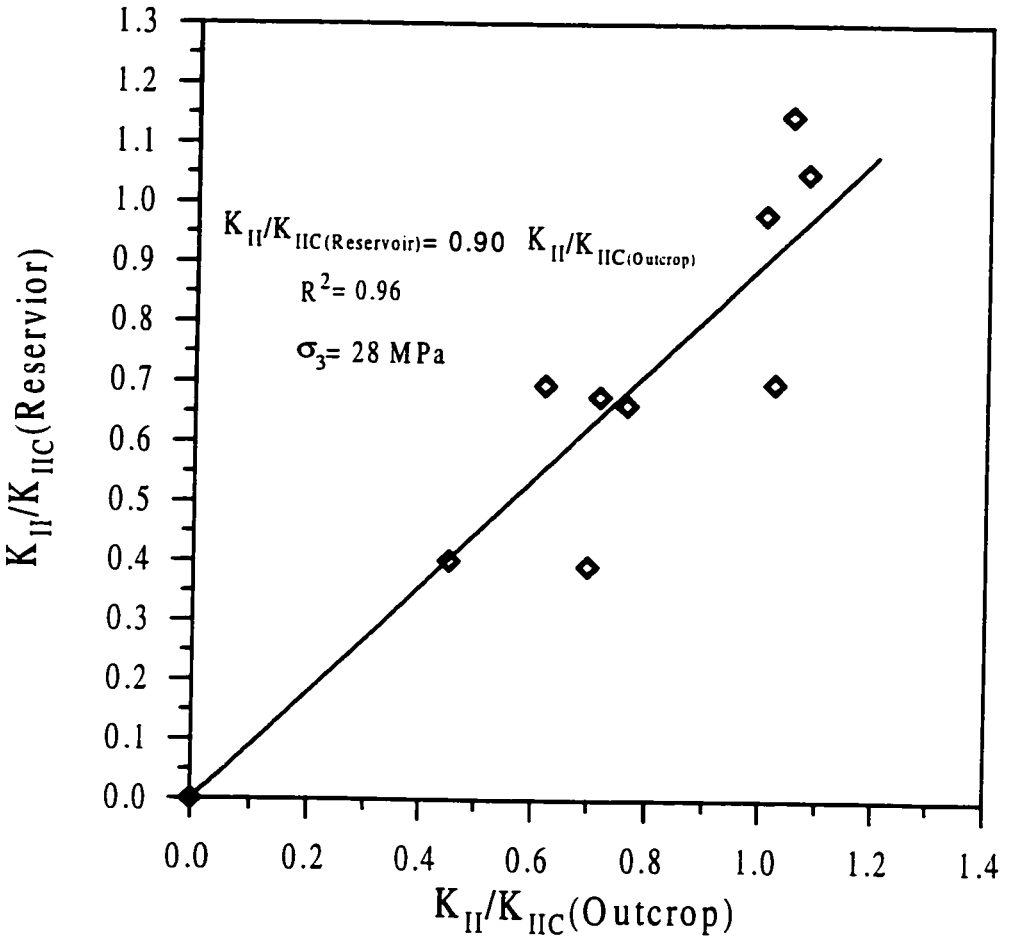

Figure 5.31: Comparison of Normalized Mode-II Fracture Toughness for Outcrop and Reservoir Straight Notched Brazilian Disk Specimens under Confining Pressure.

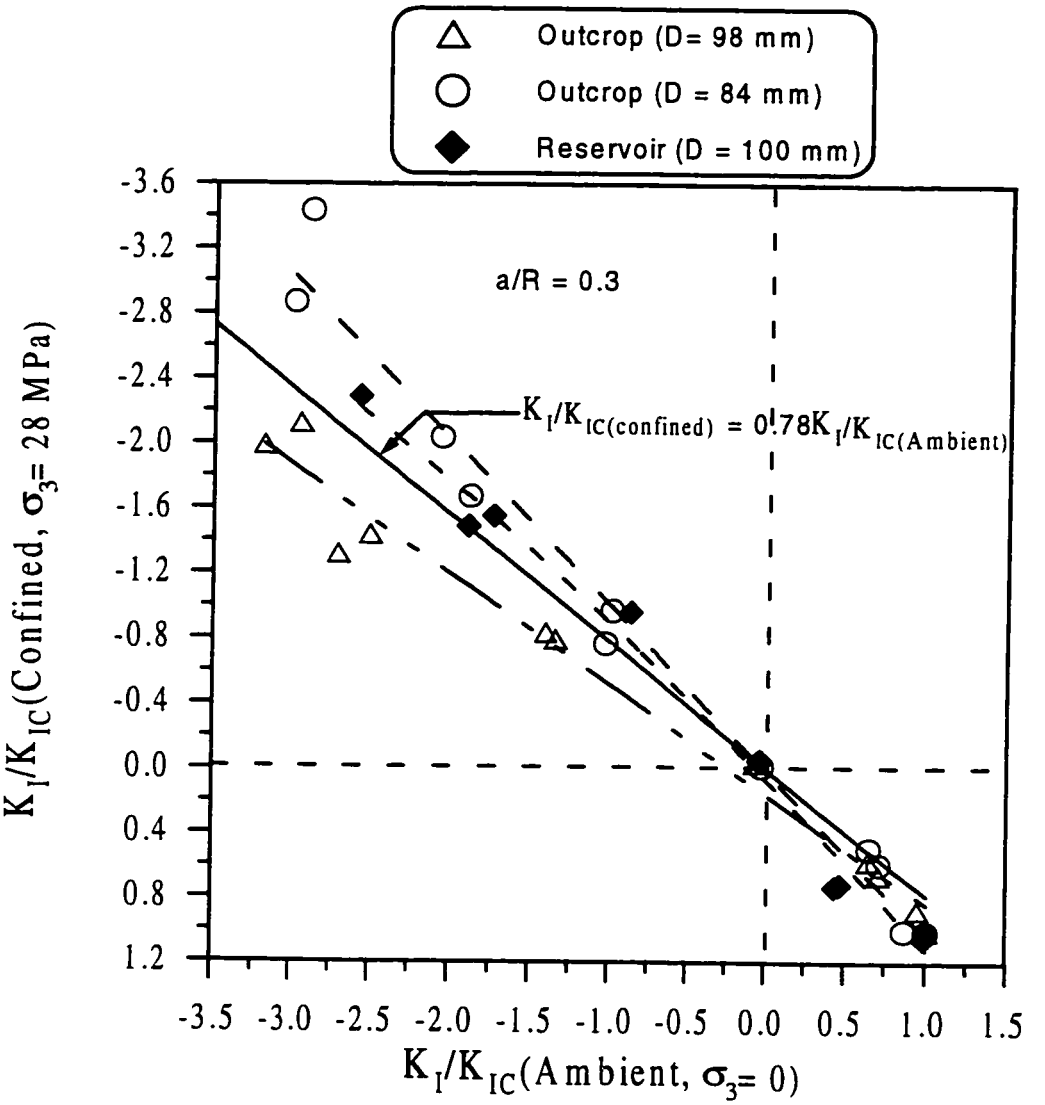

Figure 5.32: Comparison of Normalized Mode-I Fracture Toughness at Ambient and Under Confining Pressure for Straight Notched Outcrop and Reservior Brazilian Disk Specimens.

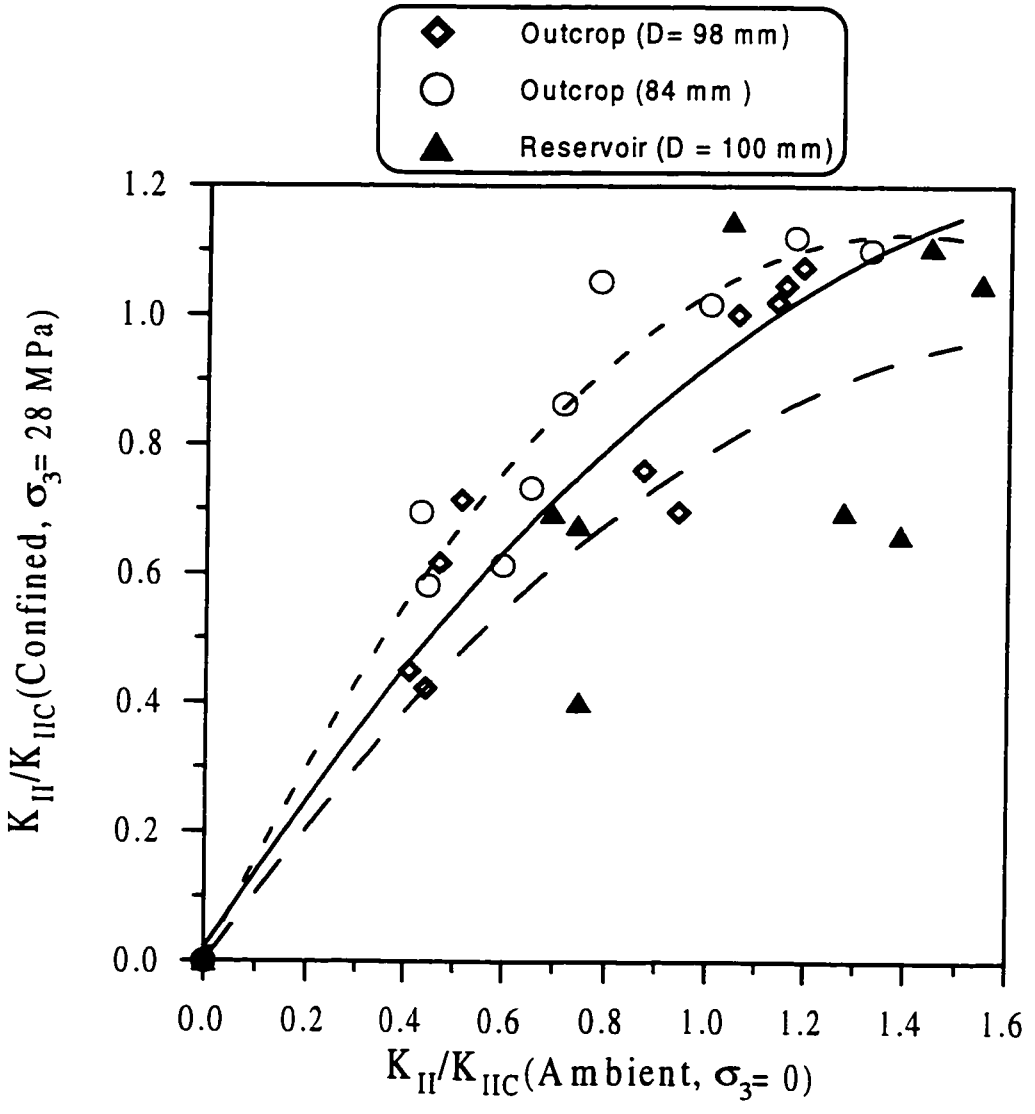

Figure 5.33: Comparison of Normalized Mode-II Fracture Toughness at Ambient and under Confining Pressure for Straight Notched Outcrop and Reservior Brazilian Disk Specimens.

5.3.2.2 Effect of Temperature

Fracture toughness variation with temperature is studied by conducting mode-I as well as mixed mode I-II tests on both outcrop and reservoir notched Brazilian Disk specimens. The results are compared to those obtained at ambient conditions as describe in the following sections.

Mode-I Results

The effect of temperature on mode-I fracture toughness was investigated using notched Brazilian disks from outcrop and reservoir specimens. The crack to radius ratio (a/R) was chosen as 0.3. The diameter and thickness of specimens were 99 ± 1 mm and 23 ± 1 mm, respectively. Figure 5.34 shows some typical load-deformation curves of such specimens under different temperatures. It can be seen that the effect of temperature on load-deformation response is insignificant upto a temperature of around 50 °C. However, the specimen tested at a temperature of 116 °C behaved in a more ductile fashion. This is probably due to the viscous nature of the material at the microscopic level at higher temperatures which not only results in excessive deformation but also in higher failure loads due to the resistance offered along the failure plane.

The variation in the mode-I fracture toughness is shown in Figure 5.35. It can be seen that the fracture toughness at the reservoir temperature (i.e., 116 °C) is 25% higher than the value obtained at ambient conditions. Similar findings have also been reported in the literature although some testing methods other than notched Brazilian

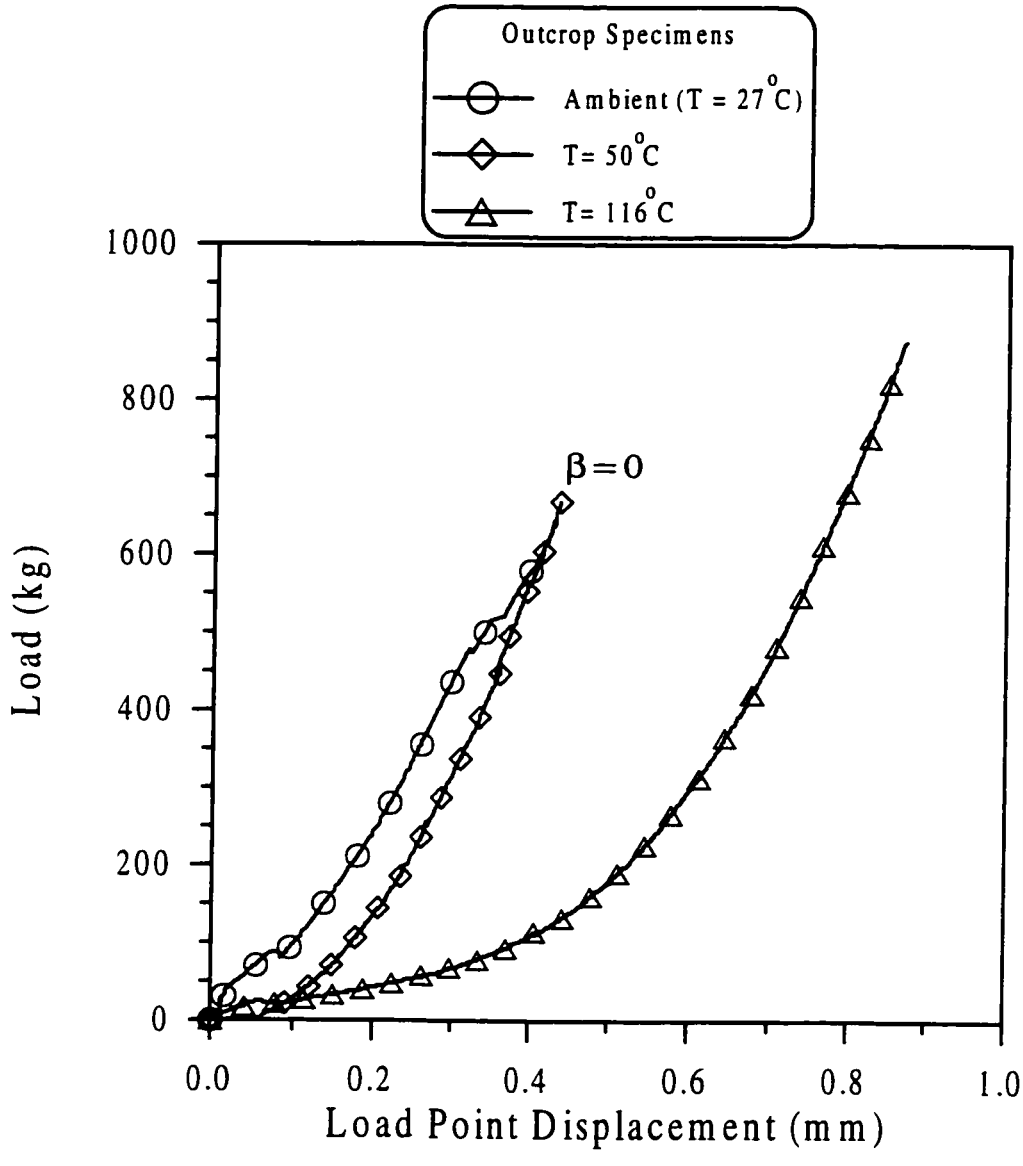

Figure 5.34: Comparison of Load-Displacement Response of Straight Notched Brazilian Disk Specimens under Different Temperatures.

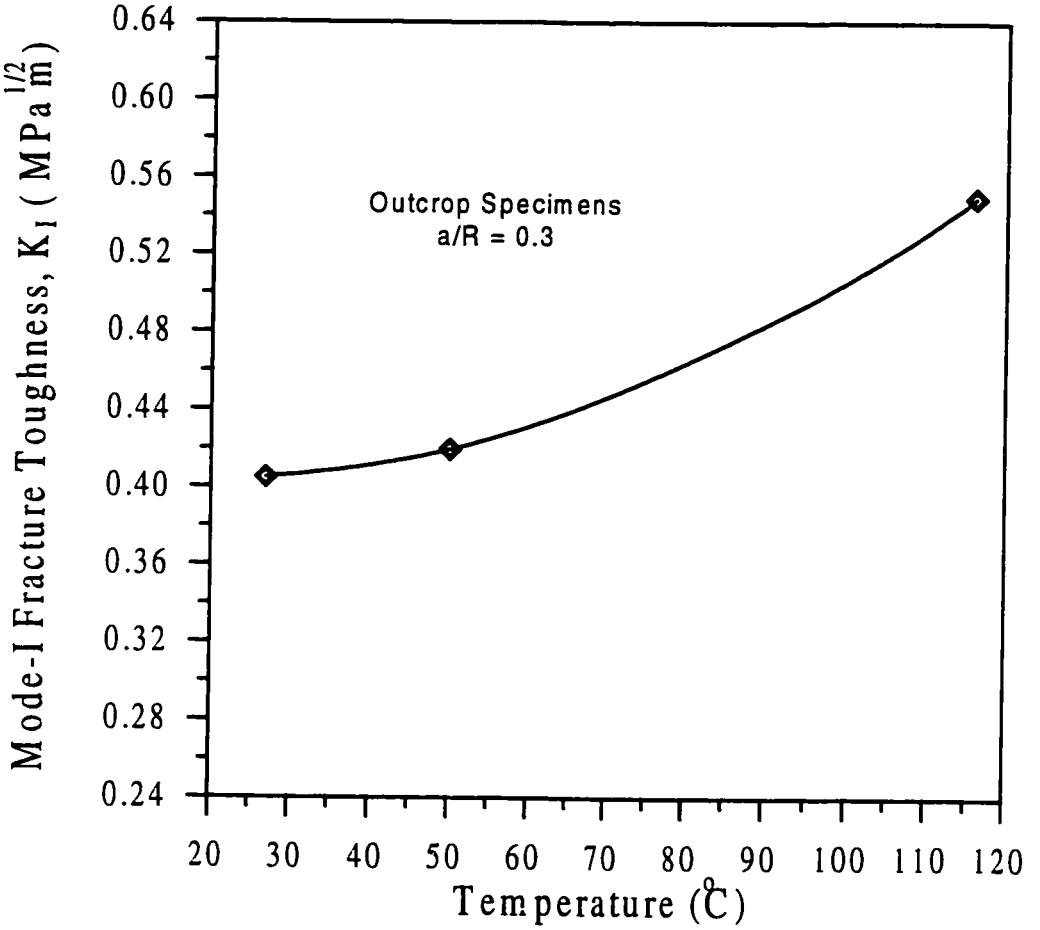

Figure 5.35: Effect of Temperature on Mode-I Fracture Toughness for Straight Notcherd Brazilian Disk Specimens.

disks were used in those investigation. Whittaker *et al.* (1982) has summarized those findings. They mentioned that the fracture toughness variation with temperature is material dependent and concluded that the fracture toughness for rocks generally increases slightly at low temperatures (20 °C - 100 °C).

Mixed Mode I-II Results

The effect of reservoir temperature (116 °C) on mixed mode I-II fracture toughness was investigated by using Brazilian disks with straight notch from outcrop. The disks were 98 mm in diameter and 22 mm thick. The normalized crack ratio (a/R) of 0.3 was used. Typical load-displacement curves are shown in Figure 5.36. It was observed that there was no significant increase in the load in the initial stage of loading and the curves were flatter in this region. The ductile behavior was believed to be the result of plastic "flow" of the rock material. Once this region of ductile deformation was over, the specimens started developing resistance against deformation and the load-displacement curves were becoming rather steeper.

The mixed mode I-II fracture toughness results for the specimens tested under both reservoir temperature and ambient conditions are shown in Figure 5.37. A small increases in pure mode-I (K_{IC}) fracture toughness value was observed over the value of 0.42 MPa $(m)^{1/2}$ for ambient conditions. The fracture toughness of 0.52 MPa $(m)^{1/2}$ was observed for the specimens tested at 116 °C. Pure mode-II (K_{IIC}) was 1.00 MPa $(m)^{1/2}$ and the ratio of K_{IIC}/K_{IC} was observed to be 1.92 compared to the value 2.14 for ambient conditions. Moreover, the fracture toughness values showed more variation at higher crack inclination angles than at smaller inclinations. At higher crack

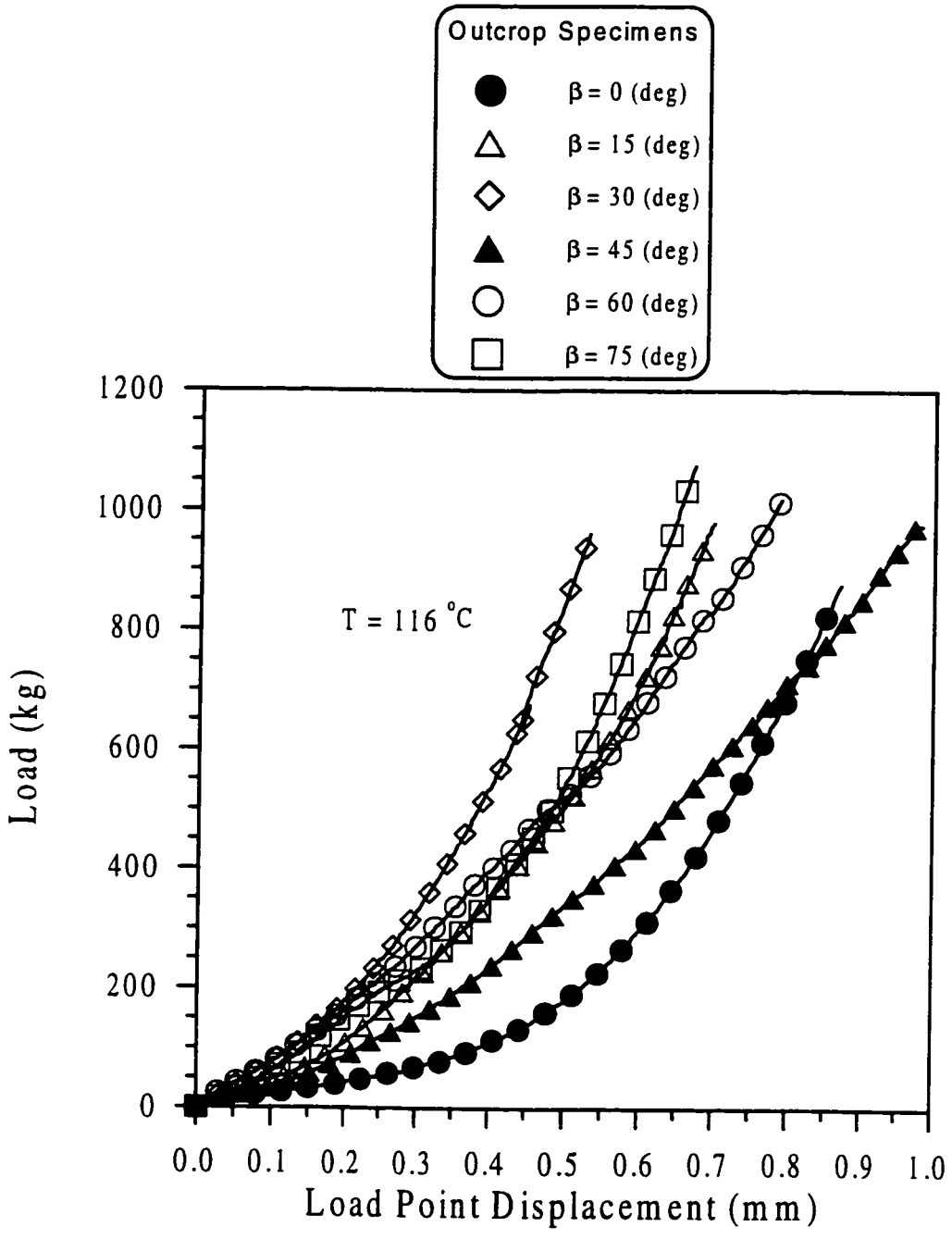

Figure 5.36: Load-Displacement Curves for Straight Notched Brazilian Disk Specimens under Mixed Mode I-II Loading at Reservoir Temperature.

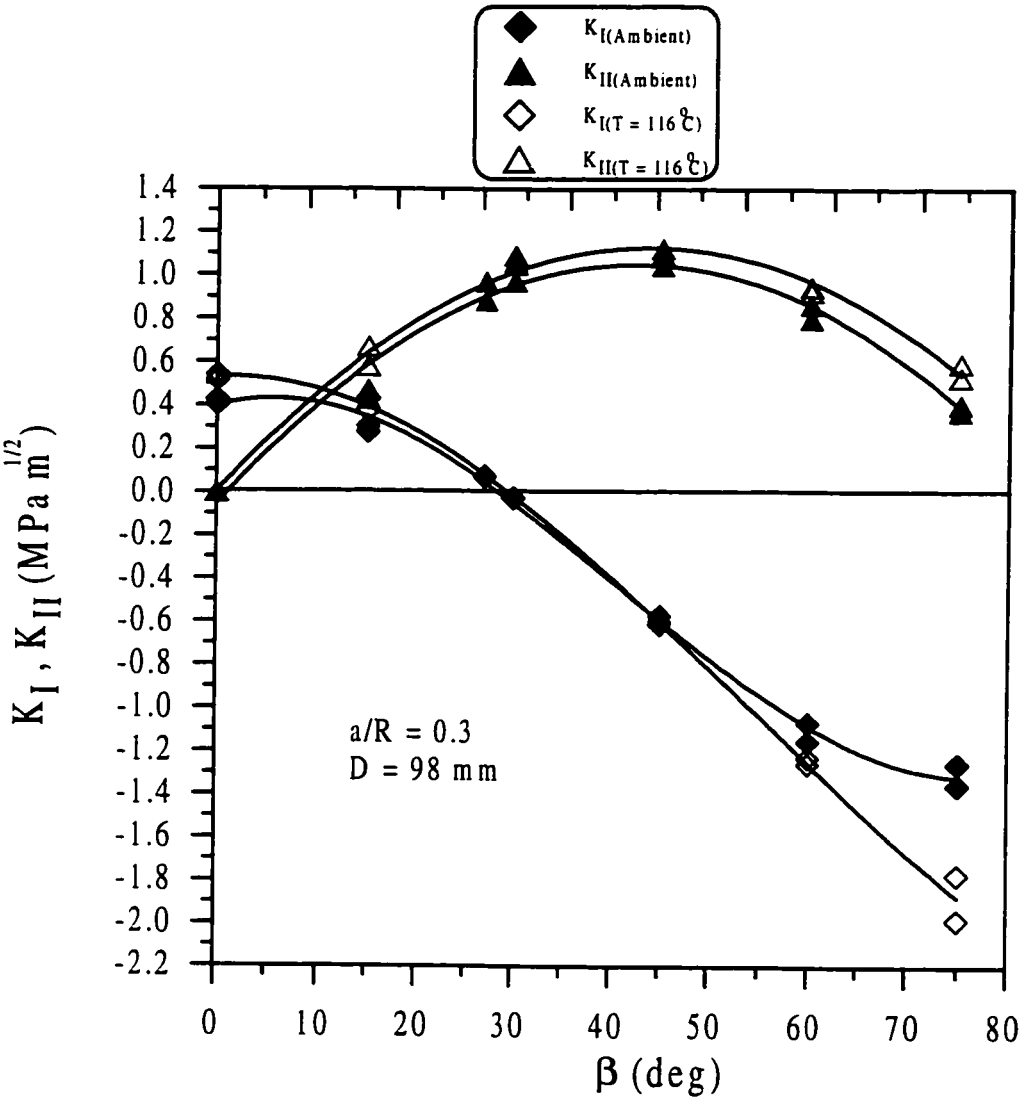

Figure 5.37: Comparison of Mixed Mode I-II Fracture Toughness for Straight Notched Outcrop Brazilian Disk Specimens at Ambient and Reservoir Temperature Conditions.

inclinations, the plastic deformation at the crack tip offered more resistance to the two sliding parts of the disk resulting in an increased load at failure.

Recognizing the fact that the fracture toughness variation with temperature is material dependent, and keeping in mind that both the outcrop and bulk of reservoir specimens used in this investigation had the same mineralogical composition, it was decided to conduct only pure mode-I and mode-II tests on reservoir specimens. Further, the limited number of reservoir specimens further dictates this idea. The pure mode-I (K_{IC}) and pure mode-II (K_{IIC}) values for reservoir specimens were found to be 0.51 and 0.56 MPa $m^{1/2}$, respectively, compared to the corresponding values of 0.40 and 0.50 MPa $m^{1/2}$, respectively, for ambient condition. The ratio of pure mode-II and pure mode-I (K_{IC}/K_{IIC}) was 0.91 as compared to a value of 1.25 at ambient conditions.

Load-displacement curves for the samples tested under ambient and simulated reservoir conditions of temperature and pressure are shown in Figure 5.38. The ductile phenomenon in the samples tested at reservoir temperature can be more clearly seen in this Figure.

5 .4 Crack Opening

For the Brazilian disk and the semicircular specimens tested under ambient conditions, crack extension was also monitored during testing. Figure 5.39 shows a typical crack opening response over the range of crack inclination angles for the outcrop Brazilian disk specimens. It was observed that the crack opened for the crack

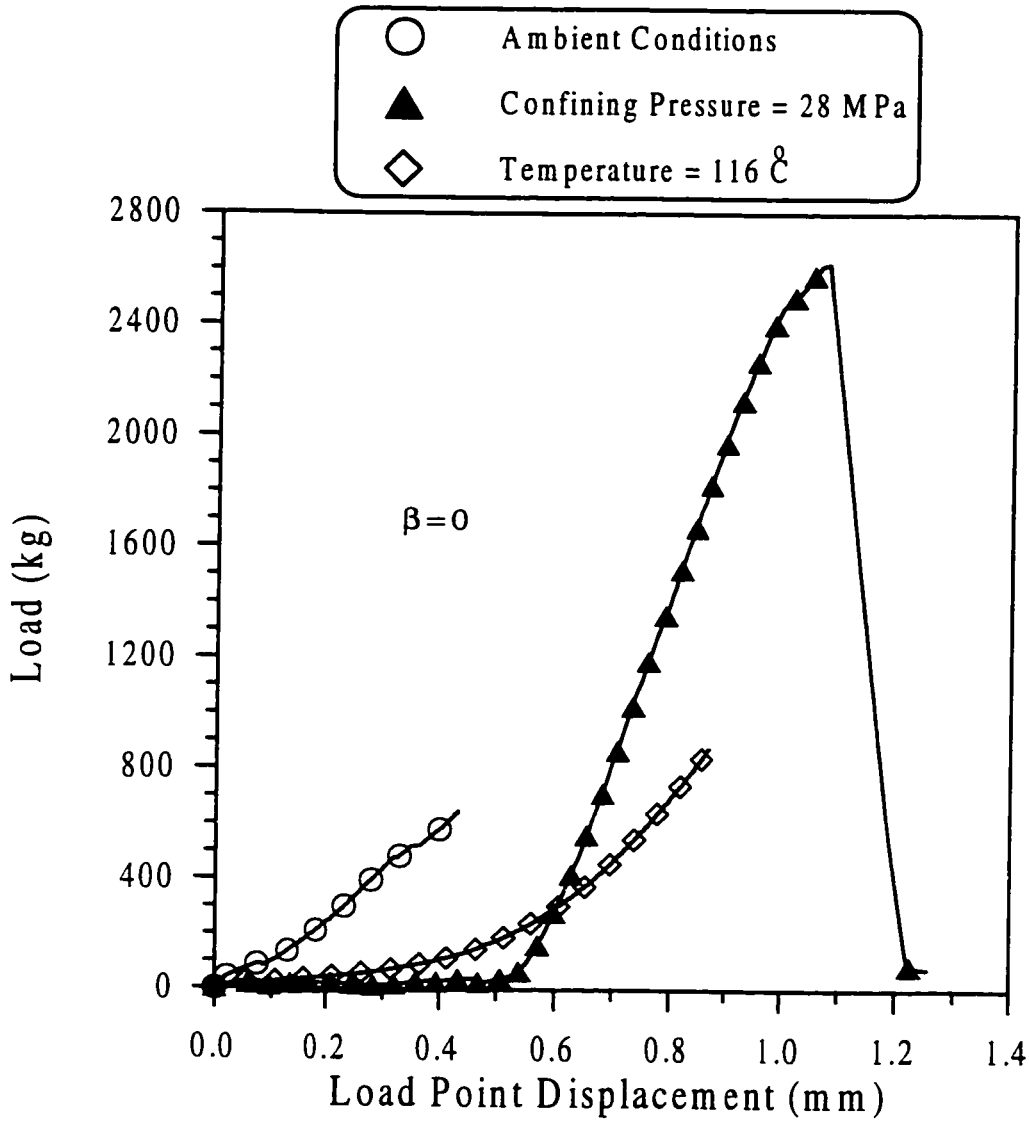

Figure 5.38: Comparison of Load-Displacement Response of Straight Notched Brazilian Disk Specimens at Ambient and Simulated Reservior Temperature and Confining Pressure Conditions.

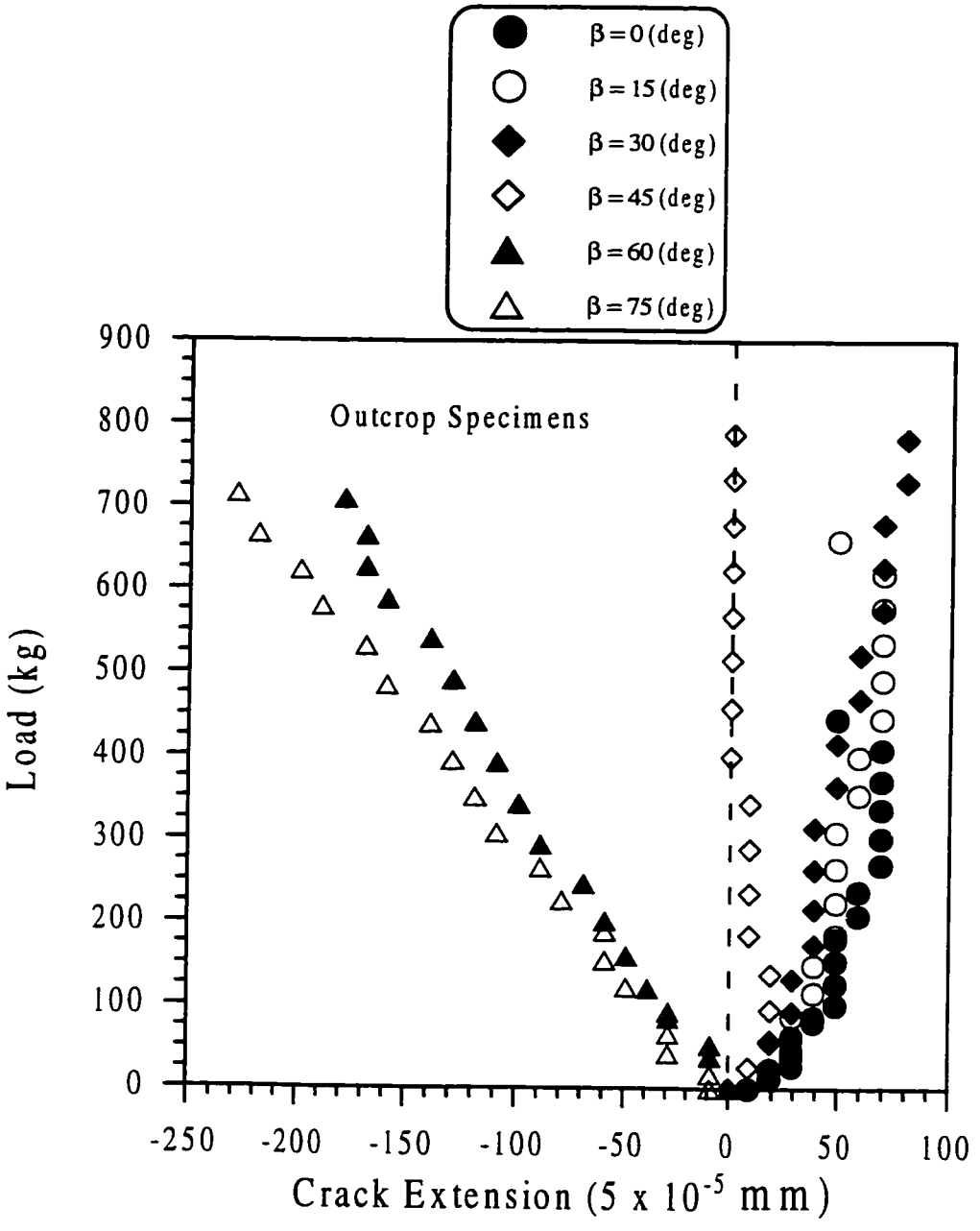

Figure 5.39: Crack Extension in Mixed Mode I-II Loading for Straight Notched Brazilian Disk Specimens at Ambient Conditions.

inclination of upto 30 degrees. This is mainly because mode-I crack tip stress is tensile in nature and this causes the crack to open. For a crack inclination of more than 30 degrees, mode-I stress becomes compressive thereby causing the crack to close. However, the effect of this compressive nature of stress was not significant for the samples tested upto an inclination of 45 degrees. Samples tested at a crack inclination of more than 45 degrees experienced an increased amount of compressive force at the crack tip and the mode-I component of fracture toughness reduces further. The crack closure becomes more pronounced under crack inclination higher than 45 degrees as can be seen in the plot for the samples tested for the crack inclination of 60 and 75 degrees.

Crack extension phenomenon for semicircular specimens is shown in Figure 5.40. It was observed that the crack opened for all the specimens in this case, contrary to the notched Brazilian disks specimens. Crack extensometer was attached to the bottom of the semicircular specimen at the crack mouth. Due to three point bend loading configuration, crack opening was expected irrespective of the crack inclination with respect to the loading direction. Therefore, it is believed that the crack closure would not come into picture even if the samples were tested for the crack inclination higher than those used in the present work. Crack opening was more significant for smaller crack inclinations than those at higher inclinations.

The maximum crack extension for the notched Brazilian and semicircular disk specimens is plotted against the crack inclinations in Figure 5.41. The maximum crack closure was observed for the notched Brazilian disk tested at a crack inclination of 75

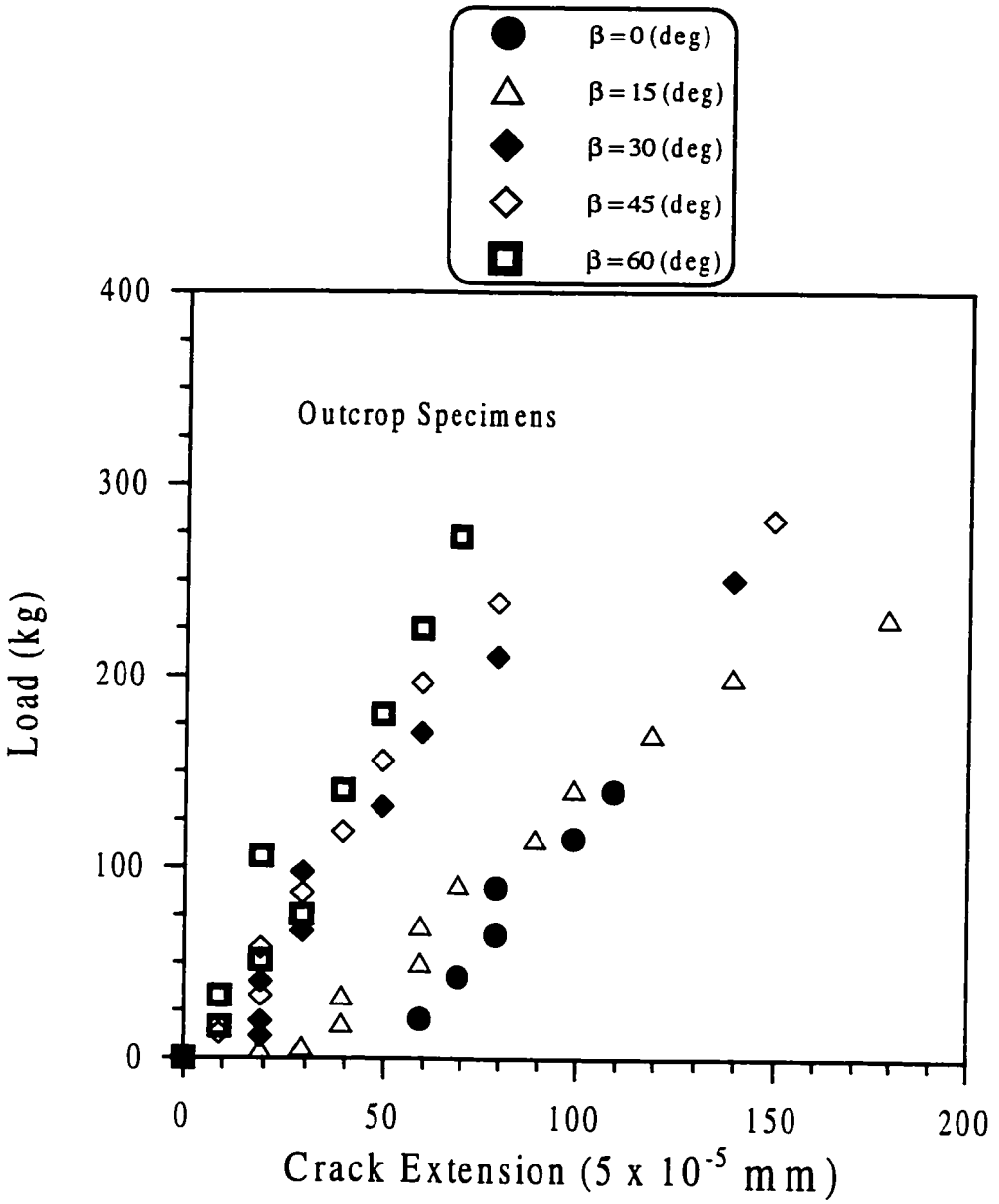

Figure 5.40: Crack Extension in Mixed Mode I-II Loading for Semicircular Specimens at Ambient Conditions.

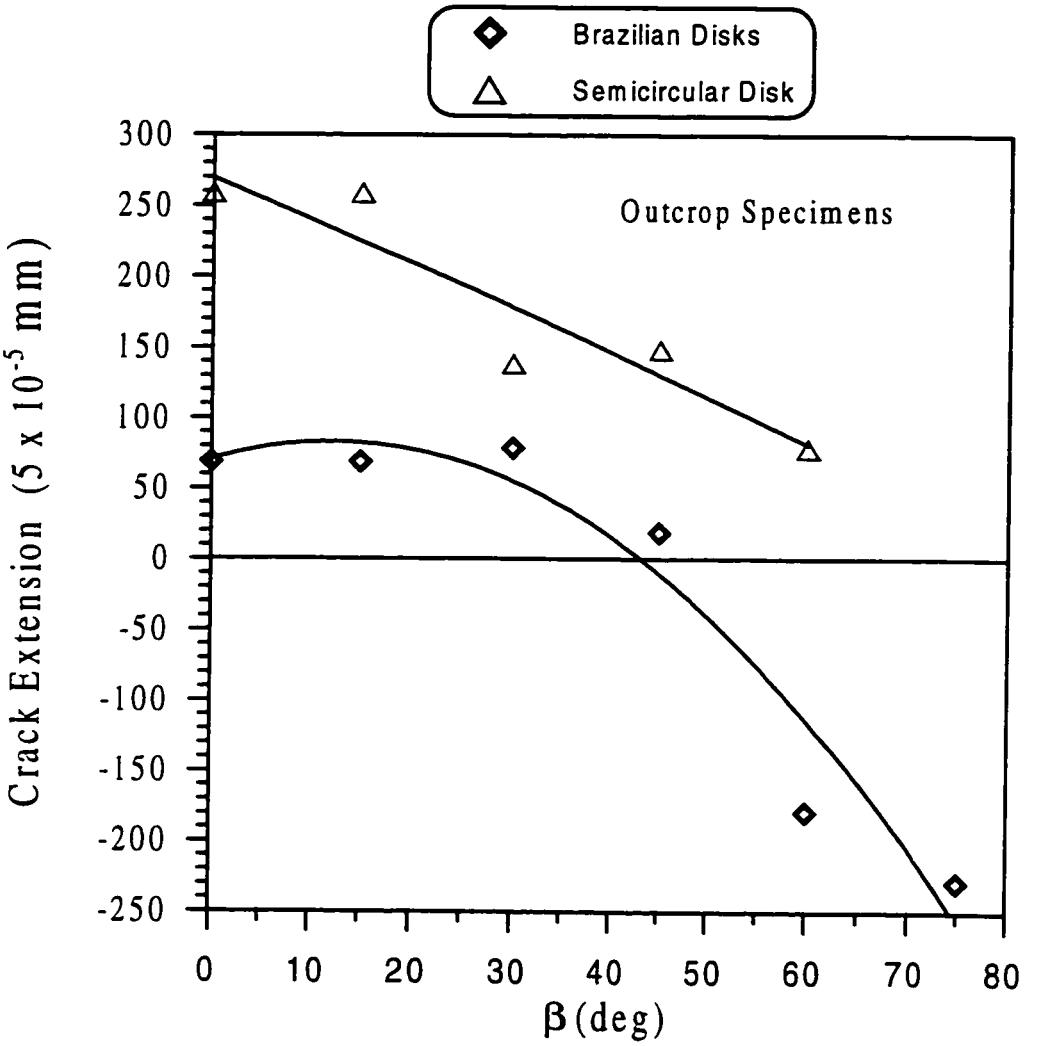

Figure 5.41: Comparison of Maximum Crack Extension under Mixed Mode I-II Loading for Straight Notched Brazilian and Semicircular Disk Specimens at Ambient Conditions.

degrees. The amount of this closure is around 0.12 mm. Since the width of the notch was twice (i.e., 0.25 mm) the maximum observed crack closure, it can be inferred that the two notched surfaces would have not come into contact before the specimen had failed.

5 .5 Crack Propagation

In addition to the stress intensity factor, another important factor in the mixed mode I-II fracture toughness study is the point and angle of crack initiation as well as its subsequent propagation. Notched Brazilian and semicircular disk specimens tested under mixed mode I-II were also investigated for crack propagation.

5 .5 .1 Crack Initiation Point and Angle

The pre-existing notches in the Brazilian disks remained open during the diametral compression and the cracks extend generally from their tips. When the externally applied load increases beyond a certain value, the cracks initiated at the tip (except for specimen at 75 degrees inclination) of the notches and propagated very rapidly in a brittle fashion towards the points on the boundary of the disk where the load was applied. When the propagating crack reached the upper and lower boundaries of the samples, it failed and broke into two pieces, as shown in Figure 5.42. The common boundary was formed between two pieces along the plane of the preexisting crack and two secondary cracks initiating from the notch tip. Moreover, it can be clearly seen in the Figure that except for the specimen tested at a crack inclination of 75 degrees,

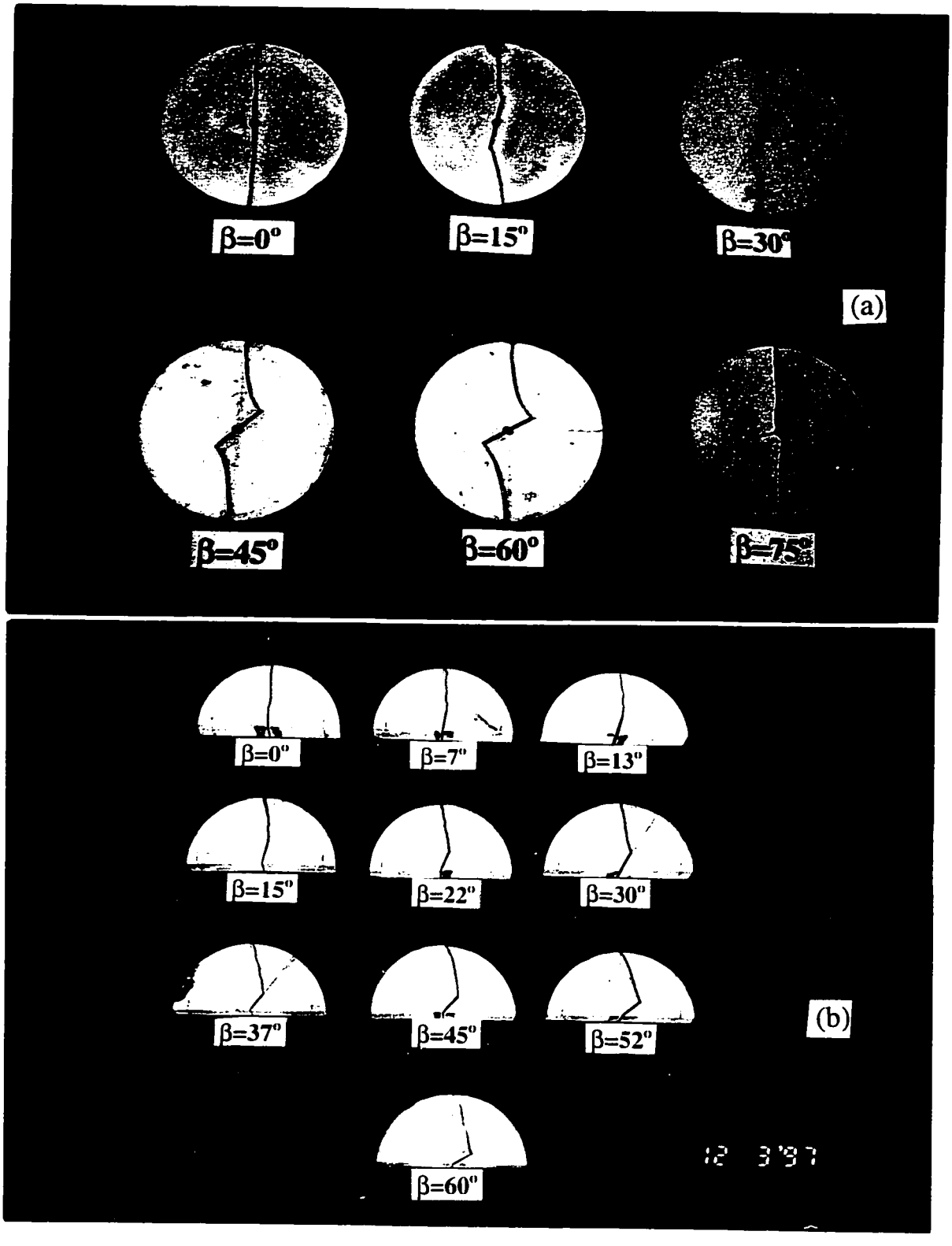

Figure 5.42: Rock Specimens after Failure (a) Notched Brazilian Disks, (b) Semicircular Disks.

crack initiation takes place form the notch tip. This phenomenon was common for all types of specimens tested under ambient and simulated reservoir conditions. However, for the specimens prepared from lithology C and tested under confined condition, failure occurred at the intersection of rock and anhydrite present therein.

When the crack starts extending upon failure of the specimen, the crack extension or deviation occurred at an angle θ from the plane of the original crack. The crack extension angle, θ , can easily be determined with the help of a protractor by joining the two broken pieces along the common failure surface. The crack extension angle for the notched Brazilian disk specimens has been plotted in Figure 5.43 against the crack orientation angle (β). The results are also compared with the theoretical analysis of crack propagation under mixed mode I-II loading condition based on the maximum tangential stress (i.e. σ-criterion). As seen in the plot, the crack propagation seems to be independent of not only the specimen size but also the testing conditions. The crack initiation angle for two types of disks (i.e. 98 mm and 84 mm diameter) tested under confined conditions was observed to be in the same range as that of the ambient conditions. The same trend was observed for the reservoir specimens tested under both ambient and simulated reservoir conditions. The experimental results fall close to the line for which $\rho/a = 0.1$, where ρ/a is a measure of the degree of crack tip sharpness and is the ratio of the radius of curvature at the crack tip to half of the crack length. For an ideally sharp crack tip $\rho/a = 0$. The crack initiation was observed to be more sensitive towards the degree of crack sharpness at small crack orientations with

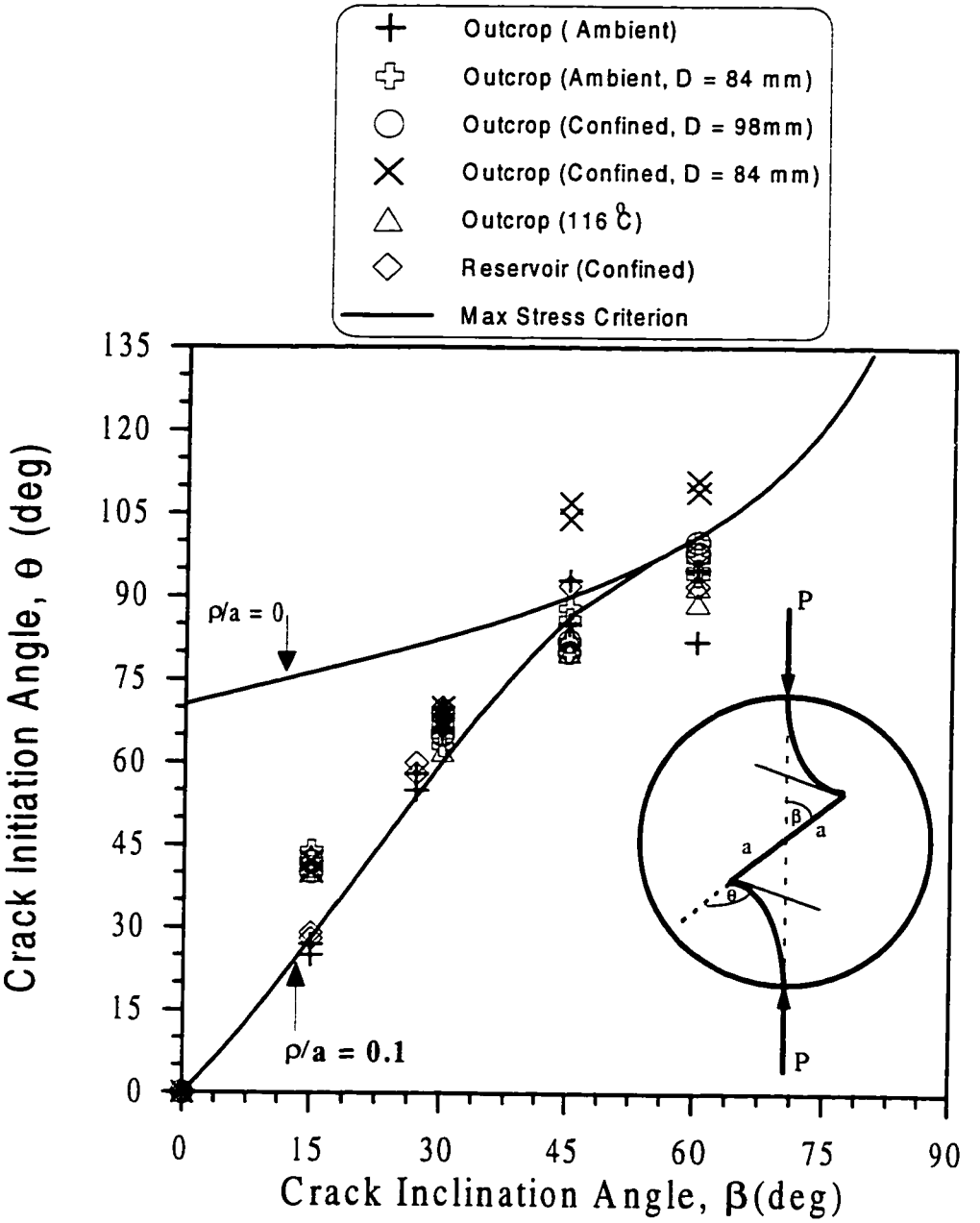

Figure 5.43: Variation of Crack Initiation Angle as a Function of Crack Inclination Angle under Mixed Mode I-II Loading for Straight Notched Brazilian Disk Specimens.

respect to the loading plane. At larger crack orientations ($\beta > 30$), the degree of crack sharpness has insignificant effect on the crack initiation angle.

5.5.2 Crack Propagation Path

The failure path of Brazilian disks for the mixed mode I-II condition was also studied. To precisely trace the crack propagation path, one of the two broken pieces of the specimens tested for each crack inclination was placed on white paper and the failure path and the perimeter of the piece was traced on the paper with a sharp pencil. A transparent plastic sheet was then placed over the paper to trace the failure path and the crack orientation on to the sheet. A graph paper was then placed under the sheet and the coordinates along the failure trajectory were carefully recorded. These coordinates were then plotted to get the failure trajectory for the specimens tested under different crack orientations and the results are shown in Figure 5.44. The same results have been plotted in Figure 5.45 by combining all cases. Again, from the failure trajectory, it can be seen that for all specimens, the crack initiated from the notch tip except for the specimens tested at a crack inclination of 75 degrees.

Apart from the experimental failure trajectories, some theoretical criteria of crack initiation and propagation have been reported in the literature. One of these criteria is the maximum tangential stress criterion (Chapter 2). To investigate how closely this criterion predicts the failure path in mixed mode I-II loading, experimental failure trajectories were superimposed over the theoretical stress contours. The results are shown in Figure 5.46 for the tangential stress. The results in the Figure show that

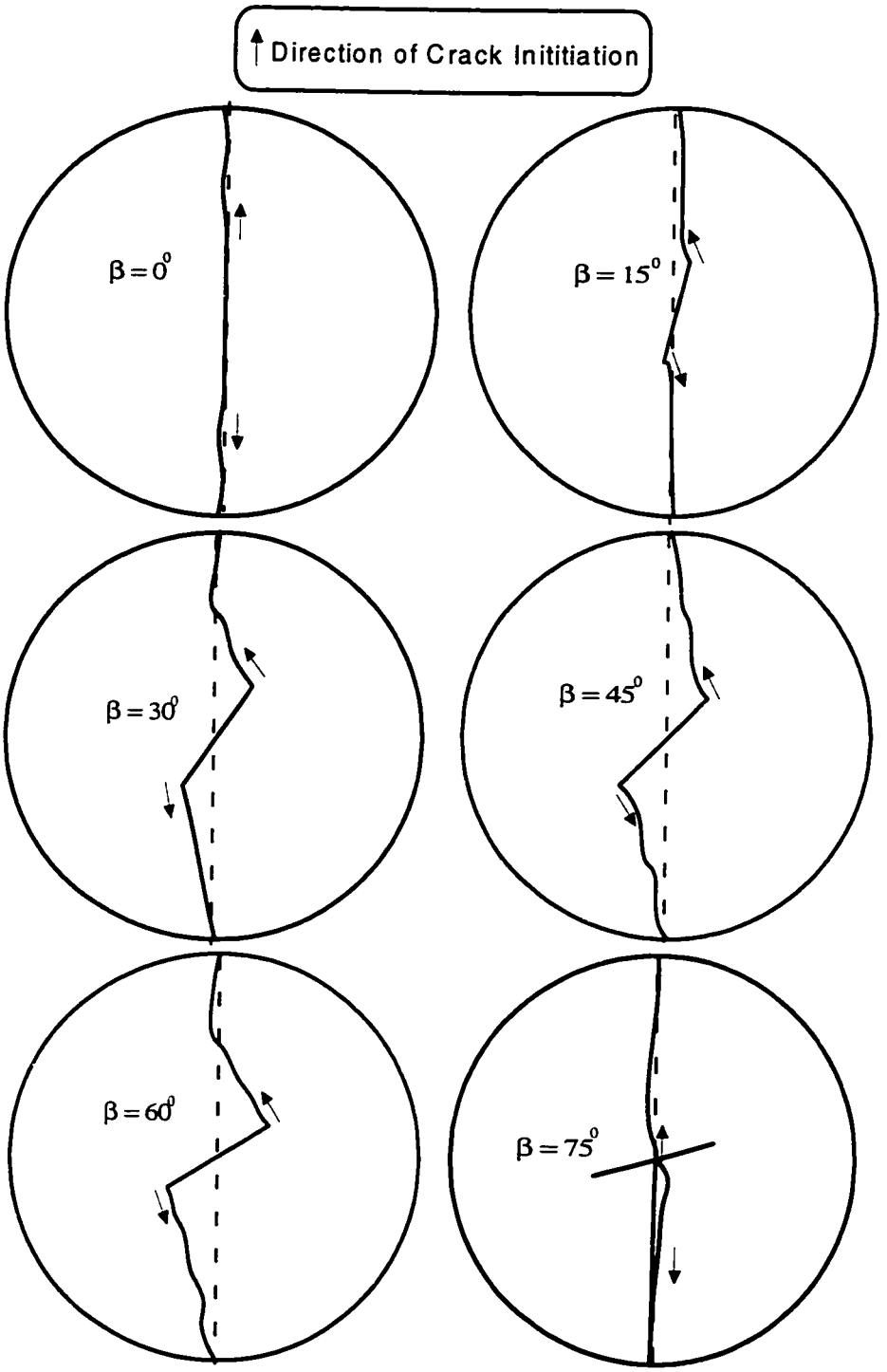

Figure 5.44: Experimental Failure Trajectoies for Straight Notched Brazilian Disk Specimens under Mixed Mode I-II Loading.

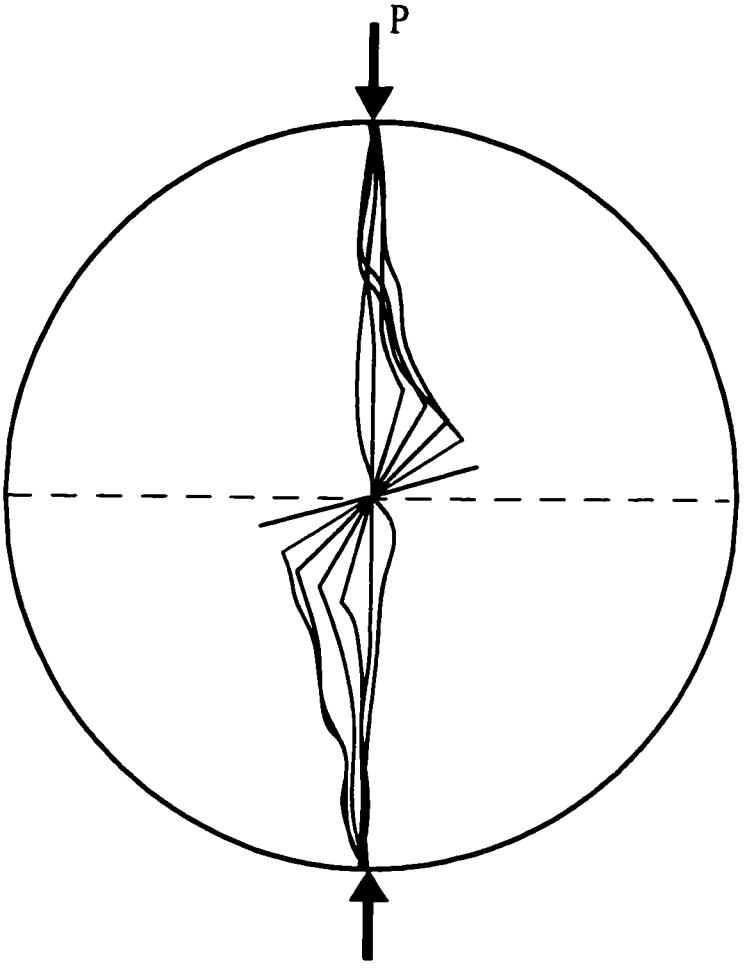

Figure 5.45: Combined Failre Trajectories for Straight Notched Brazilian Disk Specimens under Mixed Mode I-II loading.

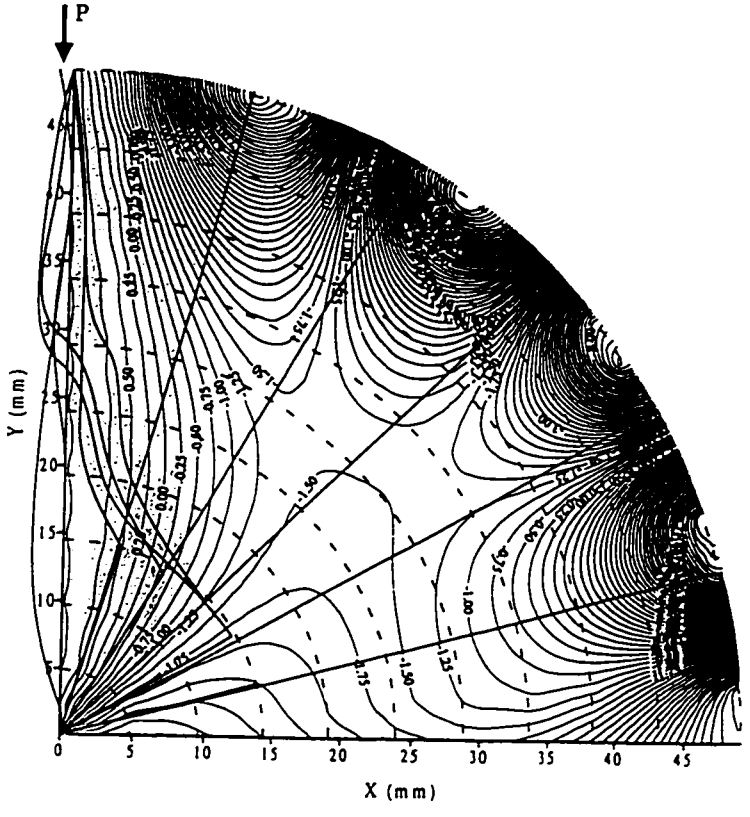

Figure 5.46: Failure Trajectories Superimposed on Normalized Tangential Stress Contours.

for pure mode-I, the crack propagates in its own plane under the influence of maximum (i.e., positive) tangential stress. For the specimens tested under mixed mode I-II, the cracks generally start originating from the tip. After initiation, they sharply enter into the zone where the tangential stress is tensile or positive in nature and then follow a path which is nearly perpendicular to the tangential stress in that region. However, for higher inclination (i.e., at 75 degrees), since the tangential stress becomes excessively compressive, it causes the crack to close. In this case, the crack could not start from the tip; rather it started in the tensile zone along the loading direction.

The crack propagation paths superimposed on shear stresses are shown in Figure 5.47. It can be seen that the stresses are almost in plane with the crack orientations. Due to these orientations and the fact that shear stresses only cause the two parts to slide over each other, it is concluded that they do not play any significant role in the crack propagation in mixed mode I-II.

In summary, it can be stated that the crack propagation in mixed mode I-II is predicted well by the theoretical approach in the range of crack inclinations such that the crack closure is not considerable. However, at larger inclinations, due to crack closure under compressive stresses, the maximum tangential stress criterion fails to predict the direction of crack propagation.

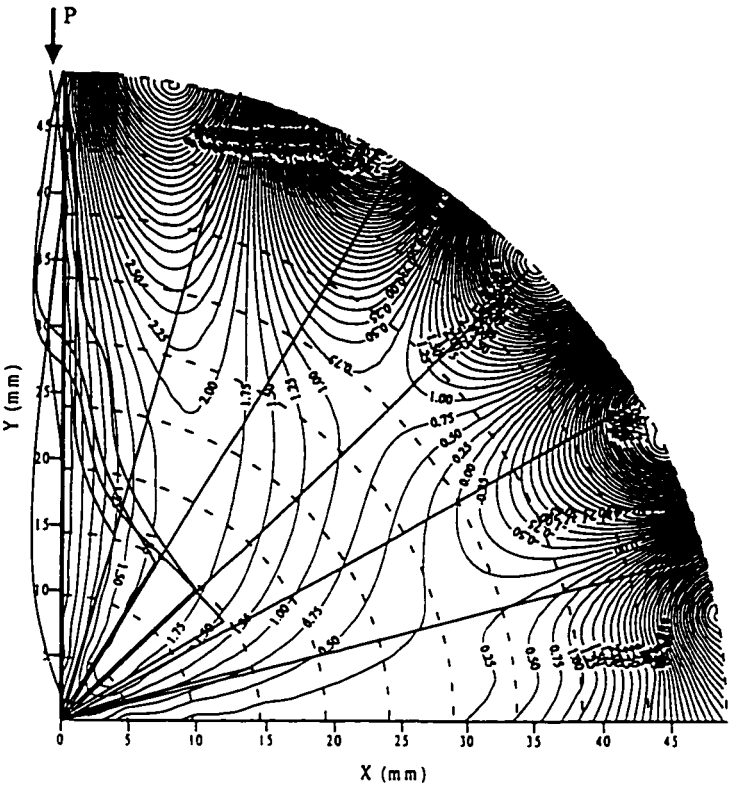

Figure 5.47: Failure Trajectories Superimposed on Normalized Shear Stress Contours.

5.6 Fracture Toughness Envelope

Although fracture propagation under mode-I is the most common type of fracture toughness study, nevertheless, many practical situations involve crack propagation in a mixed mode; particularly under mode I-II. Due to this mixed mode failure pattern, in addition to mode-I, fracture toughness under mode-II becomes important to be considered. When Brazilian disks with an inclined central notch are tested under diametral compression, a variety of mixed mode I-II fracture cases are obtained. For a particular material, a fracture locus or envelope can be obtained by plotting normalized mode-I and mode-II results. The envelope obtained could be used as a failure criterion in fracture toughness study for a particular material and testing condition in a way similar to the use of Mohr Columb strength envelope.

Normalized mode-I and mode-II fracture toughness results have been shown in Figure 5.48. The fracture loci, based on failure criteria mentioned earlier (Chapter 3), have also been plotted for comparison purpose. Since the existing theoretical work holds good only in the positive region and cannot predict the fracture behavior in the negative zone, the data points falling only in positive or crack opening region have been shown. It can be seen that the σ_{max}-criterion and S_{min}-criterion fit the experimental data well as compared to the G_{max}-criterion. However, no unique theoretical fracture criterion is best in predicting the experimental data for all cases. Similar results have been reported by other researchers, as mentioned earlier. Due to the poor prediction of experimental data by existing theoretical fracture theories, other

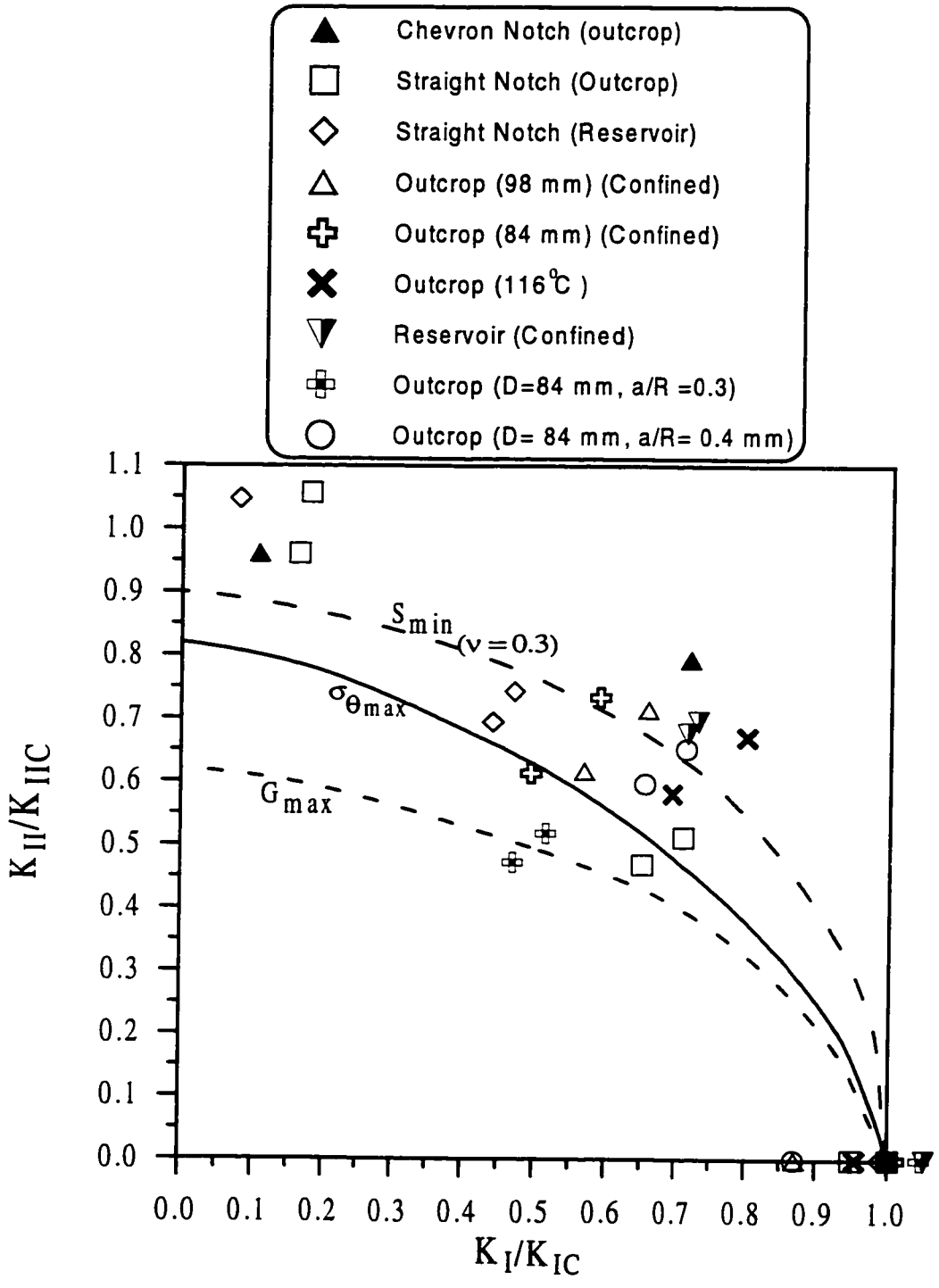

Figure 5.48 : Comparison of Mixed Mode FractureToughness Results for Notched Brazilian Disk Specimens with Thereotical Fracture Toughness Envelopes.

alternative is to use some mathematical or statistical functions which can satisfactorily fit the experimental results.

The fracture toughness data for mixed mode I-II in the positive region for both reservoir and outcrop specimens tested under different conditions is shown in Figure 5.49. Two type of regression functions using Equation 3.27 were used to best represent the scatter of the experimental results. Most of the data for ambient conditions lies close to the lower bound for which α was found to be 1.6, a value predicted by Awaji and Sato (1980) for graphite and plaster. The results for the specimens tested under reservoir simulated confining pressure and temperature showed a little bit different behavior and the results were fitted by a polynomial for which a value of 2.0 was observed for α. The regressions have the following form

$$\left(\frac{K_{II}}{K_{IIC}}\right)^{1.6}+\left(\frac{K_I}{K_{IC}}\right)^{1.6}=1 \quad \text{For ambient conditions} \tag{5.1}$$

$$\left(\frac{K_{II}}{K_{IIC}}\right)^{2}+\left(\frac{K_I}{K_{IC}}\right)^{2}=1 \quad \text{For confined conditions} \tag{5.2}$$

The experimental scatter for the data in the negative zone is shown in Figure 5.50. A second order polynomial was used to predict the experimental results which has the following form for ambient conditions:

$$\frac{K_{II}}{K_{IIC}}=-0.16\left(\frac{K_I}{K_{IC}}\right)^{2}-0.3\left(\frac{K_I}{K_{IC}}\right)+1.07 \tag{5.3}$$

For the tests conducted under reservoir simulated confining pressure, the equation has the following form:

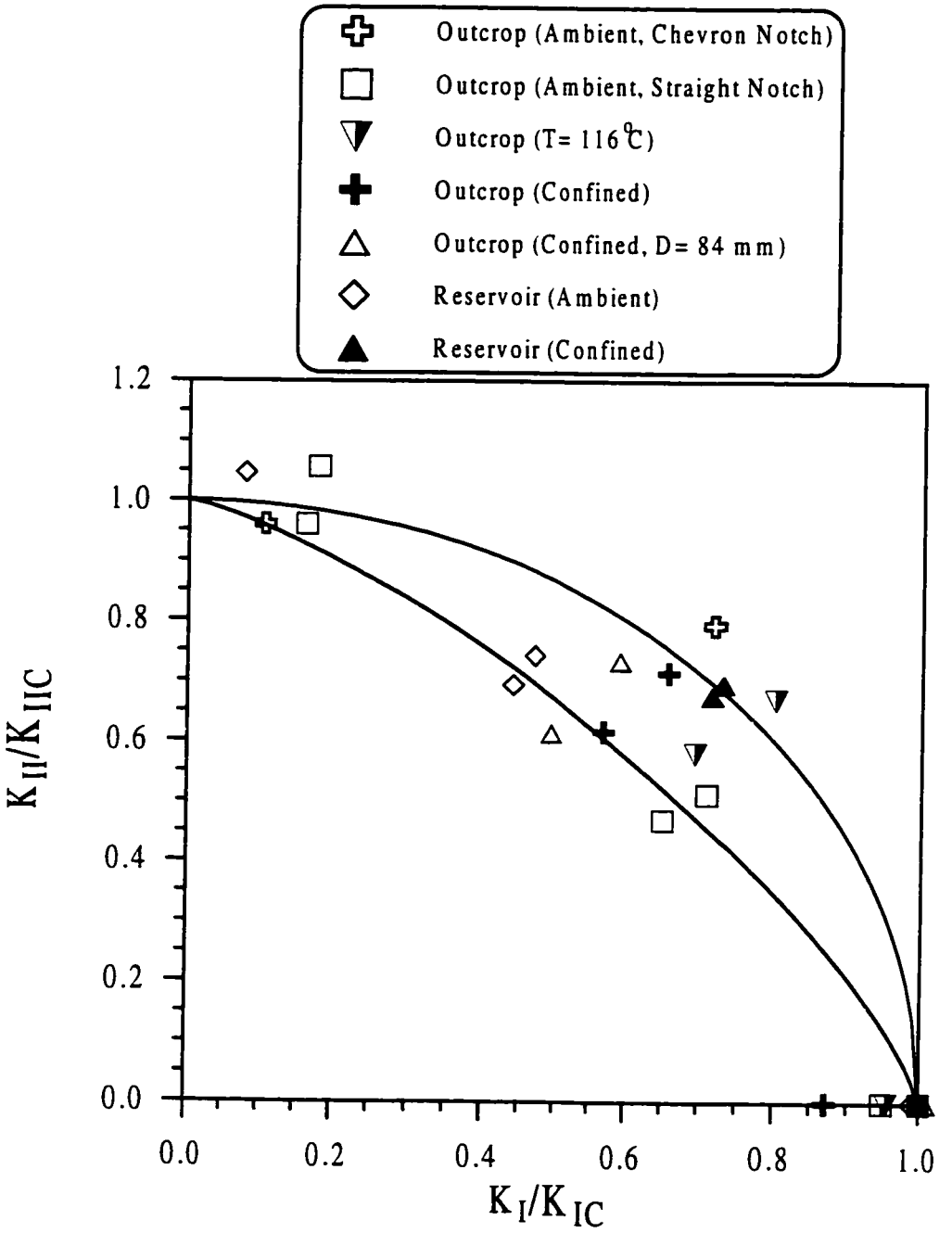

Figure 5.49: Proposed Mixed Mode I-II Fracture Toughness Envelope for Notched Brazilian Disk Specimens for Positive Fracture Tougghness Values.

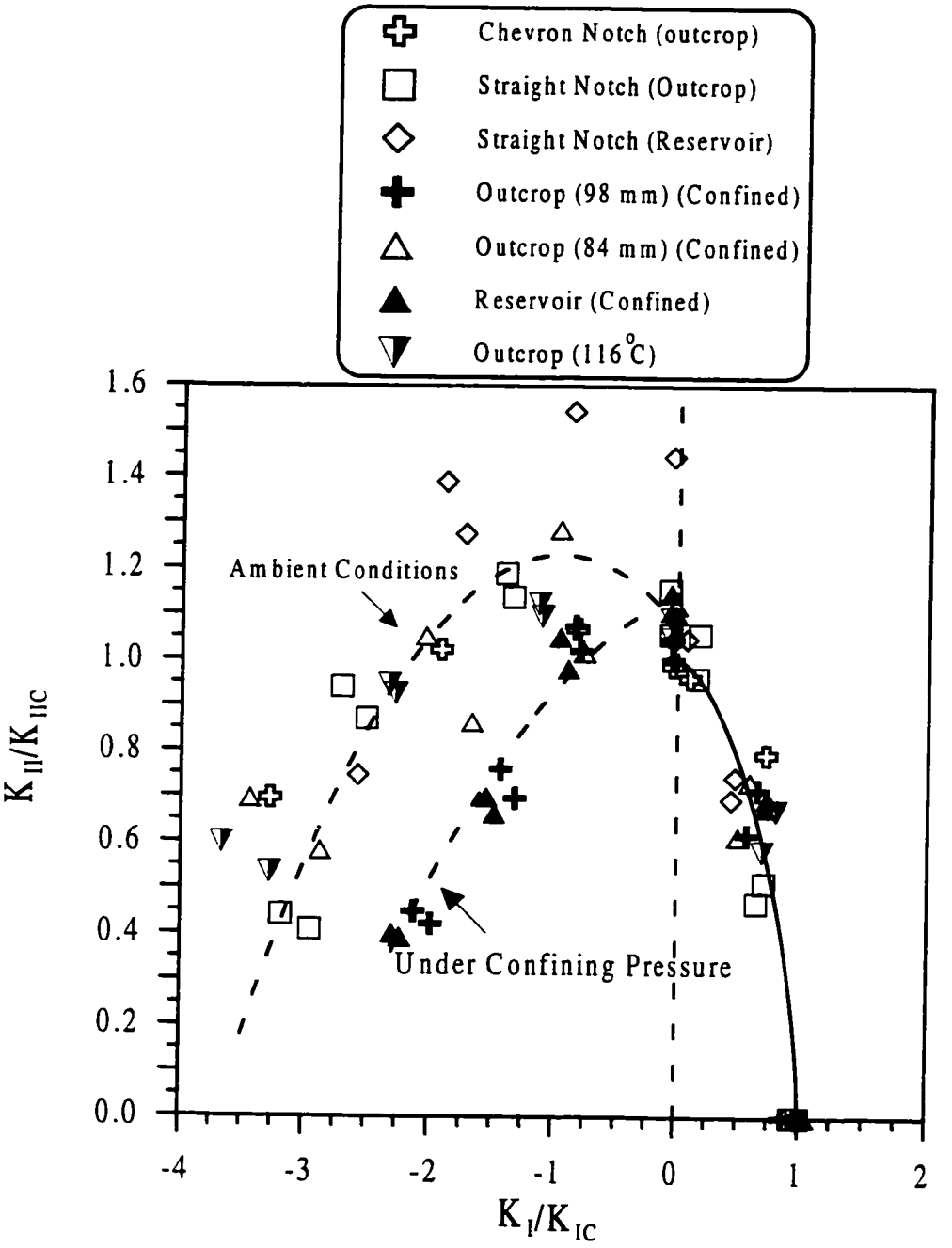

Figure 5.50: A Copmparison of Mixed Mode I-II Fracture Toughness Envelope under Different Testing Conditions for Notched Outcrop and Reservior Brazilian Disk Specimens.

$$\frac{K_{II}}{K_{IIC}} = -0.1\left(\frac{K_I}{K_{IC}}\right)^2 - 0.11\left(\frac{K_I}{K_{IC}}\right) + 1.15 \qquad (5.4)$$

It can be seen that the results for confined and ambient conditions fit into a relatively close bound in the positive zone; however, distinct regions of data exist in the negative side. Note that the results for the specimens tested under simulated reservoir temperature fall close to the data for ambient conditions in the negative zone revealing that the fracture toughness is not very much affected by the temperature used in this study. Moreover, it is also observed that the results for outcrop specimens at ambient conditions do not fall close to the fitted line indicating the different behavior of outcrop and reservoir specimens at ambient conditions. This behavior can be seen more clearly in Figure 5.51.

Contrary to the fracture behavior at ambient conditions, the results were found to be consistent for outcrop and reservoir specimens at simulated reservoir pressure, as shown in Figure 5.52. The data on the negative region was fitted by a second degree polynomial given in equation 5.4. Both the outcrop and the reservoir specimens exhibit similar behavior. The variation showed by outcrop specimens for which the diameter was 84 mm is due to the fact that they have relatively small fracture toughness values compared to the 98 mm diameter disk specimens.

5.7 SEM Results of Fractured Surfaces

The cracked surfaces of the Brazilian disks tested under mixed mode I-II loading were studied using Scanning Electron Microscope (SEM). The specimens were studied for

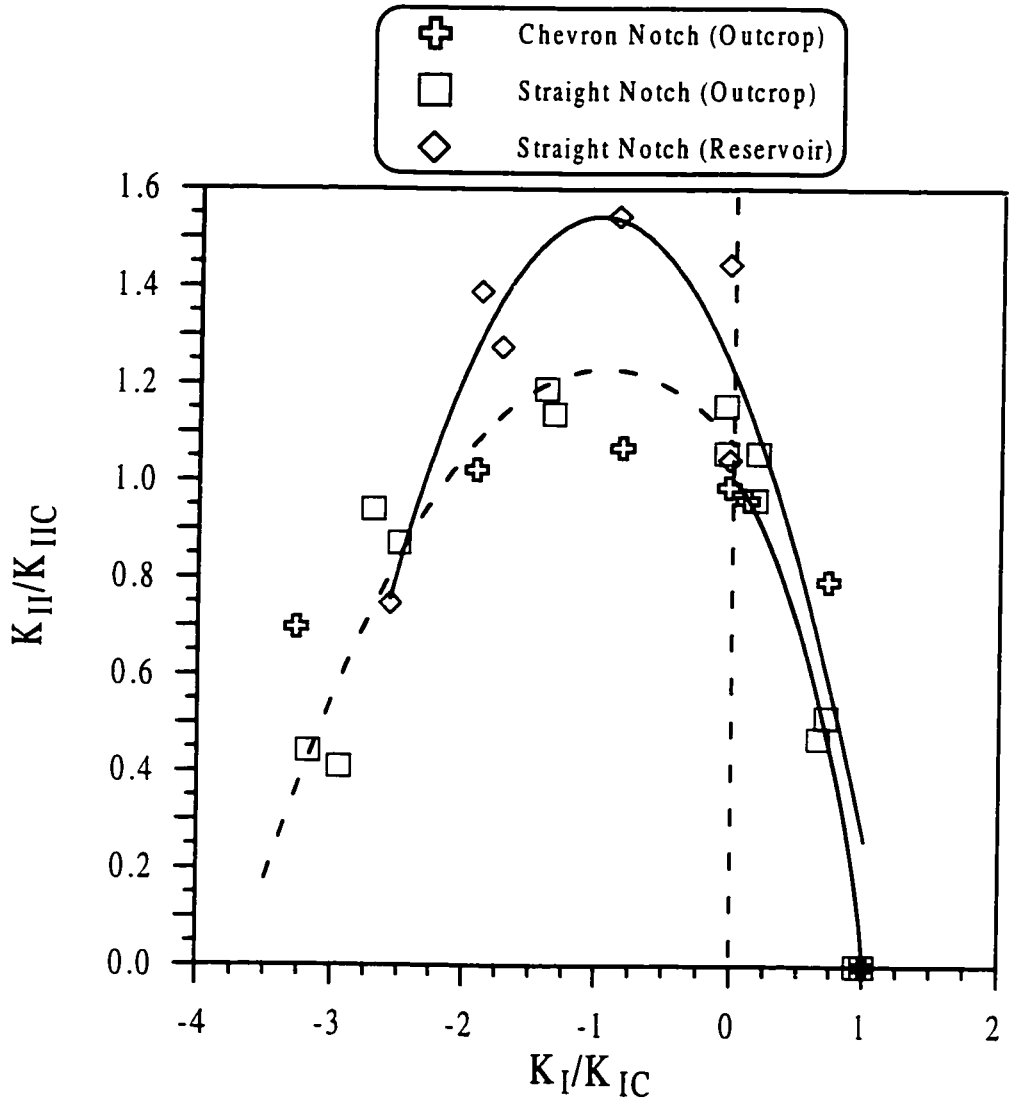

Figure 5.51: Mixed Mode I-II FractureToughness Envelope for Notched Outcrop and Reservoir Brazilian Disk Specimens at Ambient Conditions.

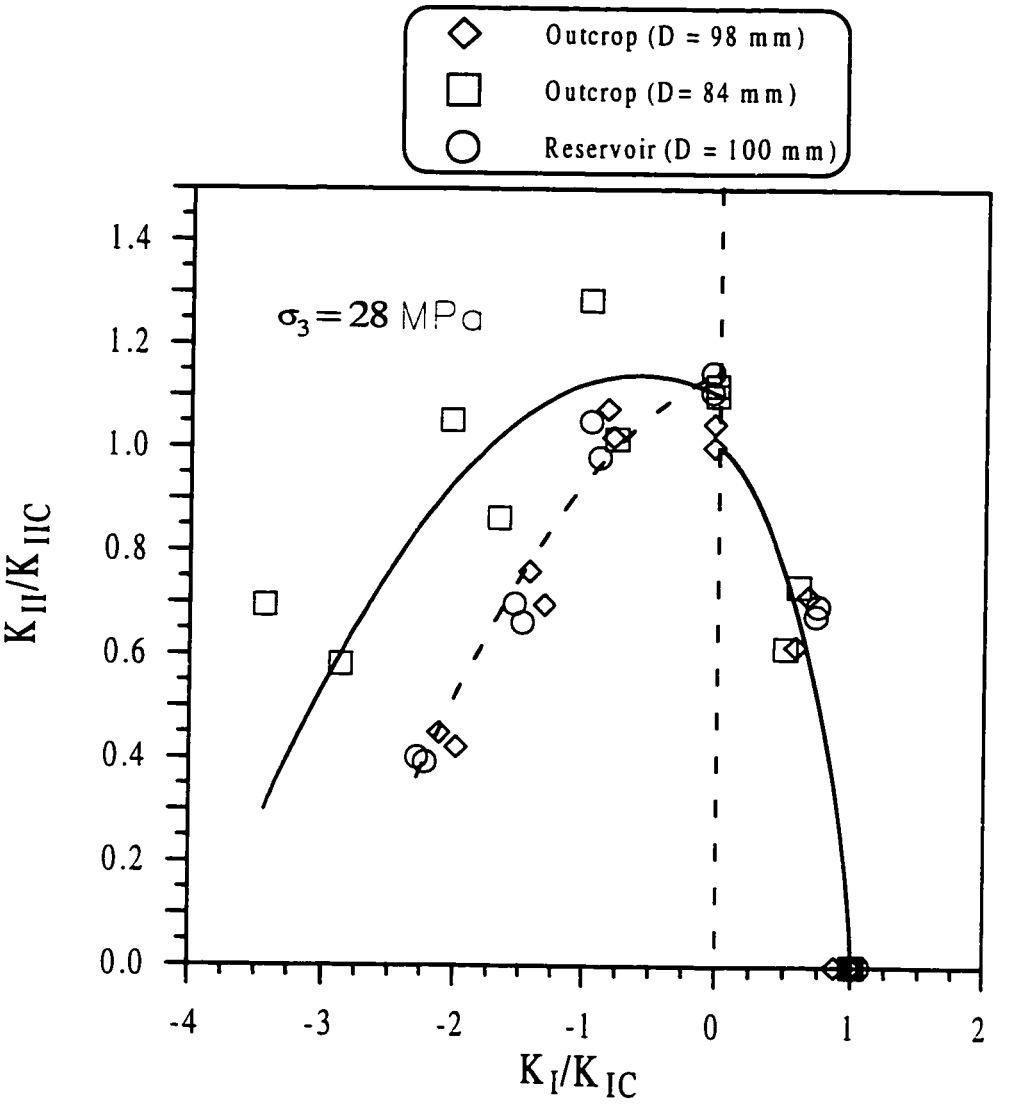

Figure 5.52: Mixed Mode I-II Fracture Toughness Envelope for Straight Notched Outcrop and Reservoir Brazilian Disk Specimens udern Reservoir Confining Pressure.

the crack orientations of 0, 15, 30, 45, 60 and 75 degrees. Figure 5.53 shows the SEM micrograph for the crack orientation of 0 and 15 degrees. For the crack orientation of 30 and 45 degrees, the micrographs are shown in Figure 5.54. Micrographs in both Figures show the coarse nature of the cracked surface representing failure occurring predominantly in the opening mode (i.e. insignificant sliding). Figure 5.55 shows the micrographs for the specimens tested at a crack orientation of 60 and 75 degrees. The nature of cracked surface for the sample tested at 60 degrees shows smaller granular appearance representing higher degree of abrasion and grain crushing. The sample tested at 75 degrees failed along the diametrical line coinciding with the loading direction (i.e. failure did not initiate from the crack tip). The micrograph for this sample appears to be the same as that tested at zero degree revealing that the failure surface was created under the influence of tensile stresses.

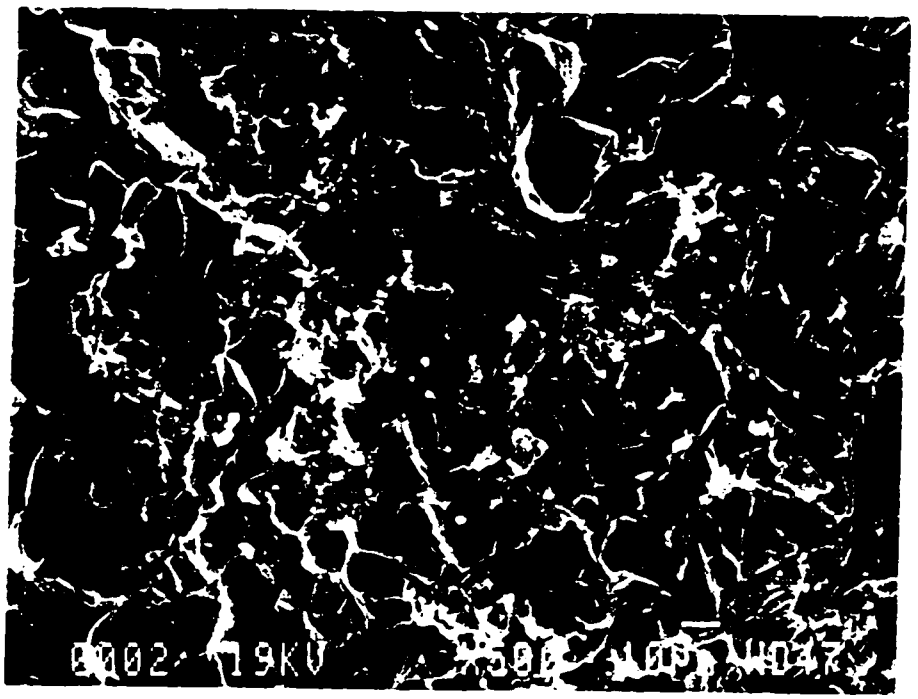

(a)

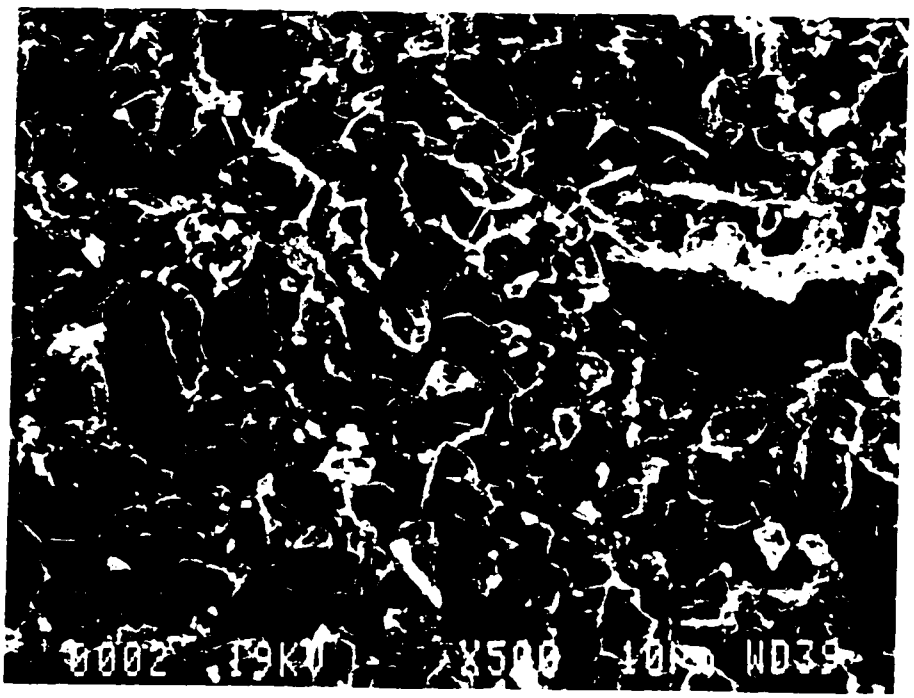

(b)

Figure 5.53: Scanning Electron Microscopic (SEM) Image of the Fractured Surface for Specimens tested at (a) $\beta = 0^{\circ}$, (b) $\beta = 15^{\circ}$.

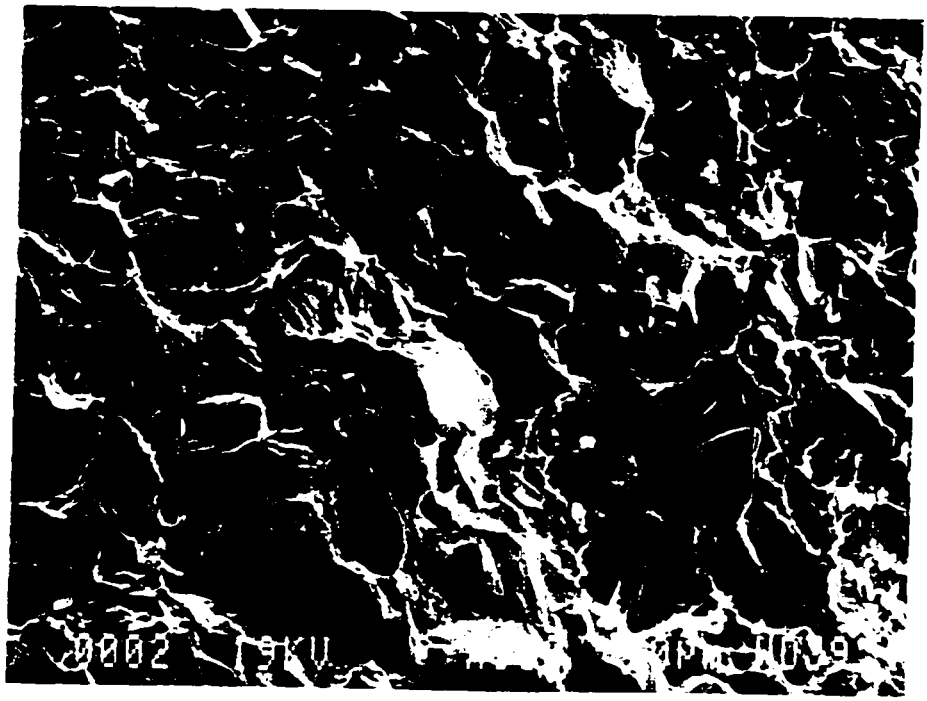

(a)

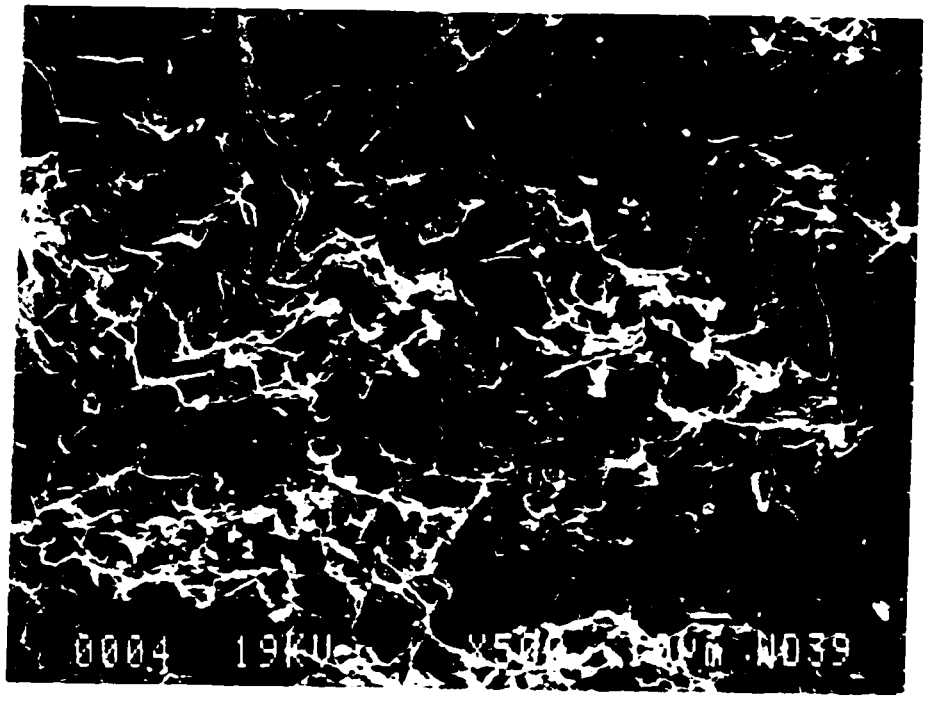

(b)

Figure 5.54: Scanning Electron Microscopic (SEM) Image of the Fractured Surface for Specimens Tested at (a) $\beta = 30^{\circ}$, (b) $\beta = 45^{\circ}$.

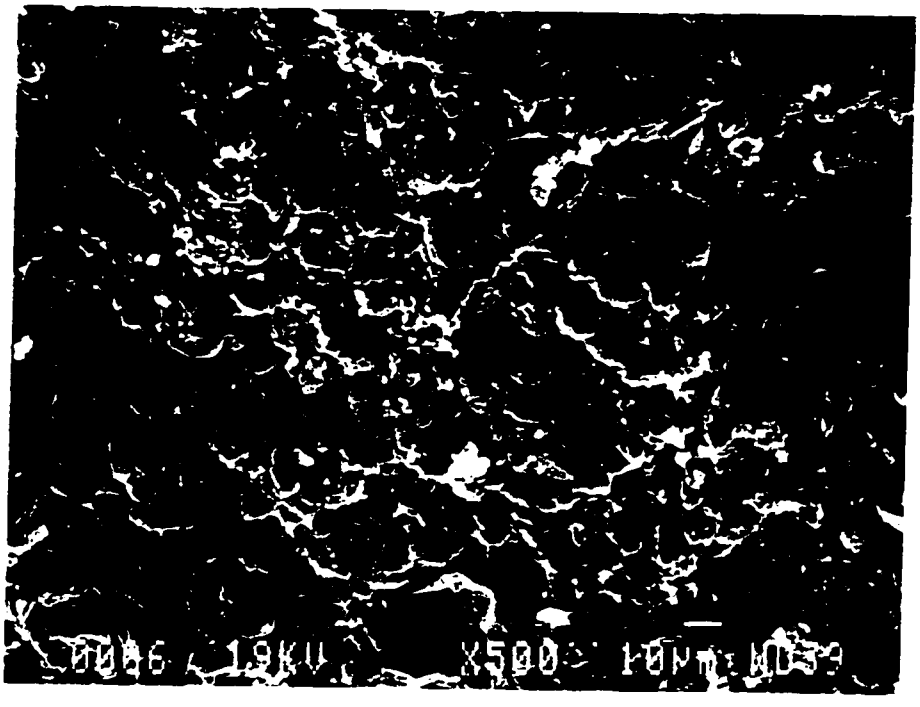

(a)

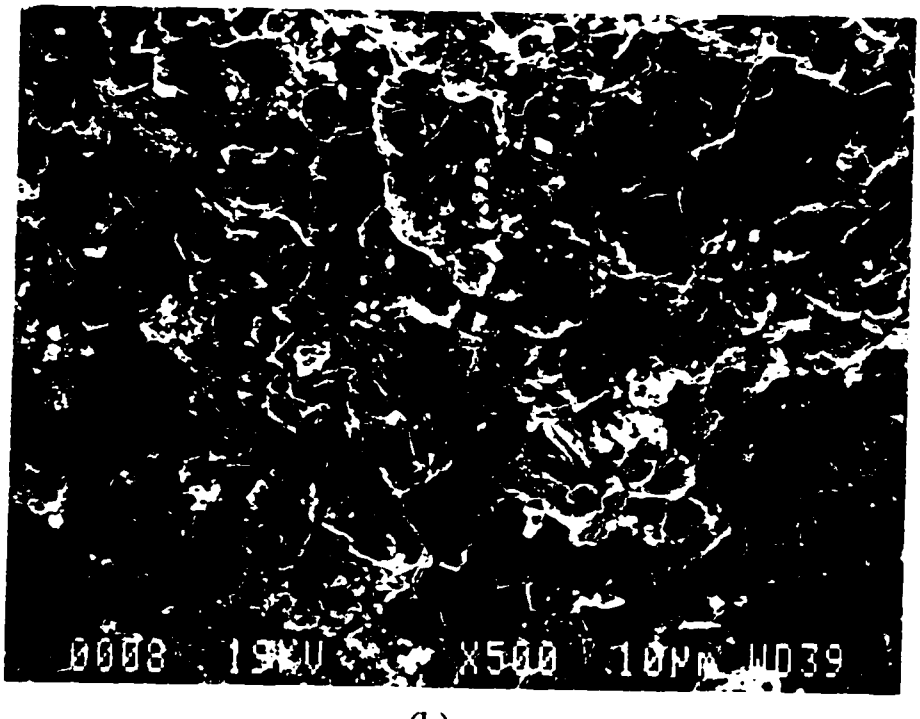

(b)

Figure 5.55: Scanning Electron Microscopic (SEM) Image of the Fractured Surface for Specimens Tested at (a) $\beta = 60°$, (b) $\beta = 75°$.

Chapter 6

Summary, Conclusions and Recommendations

6.1 Summary

This research work focused on the fracture toughness determination of a limestone rock formation in the Kingdom of Saudi Arabia (i.e., Khuff Formation). This sedimentary rock formation is buried at a depth of about 2 km in the Eastern Province and outcropped in the Central Province (Riyadh, Qassim). A large number of oil and gas fields of the Kingdom of Saudi Arabia are situated in this formation. Because of its prime importance to the oil and gas industry, its mechanical, hydraulic and strength properties have been of interest to both engineers and technologists.

Hydraulic fracturing is a well known technique to create fractures in deep-seated rock formations in order to enhance the oil or gas recovery from a reservoir of low permeability. The hydraulic fracturing of a reservoir formation is accomplished by first drilling a hole to the desired depth and then injecting a fluid under high pressure. This pressurized fluid (into the cracks and joints of the rock), causes the preexisting cracks to initiate and propagate further resulting in the increase of the surface area of the rock formation so as to achieve higher yield of oil or gas. The crack could

propagate under pure tensile fashion (mode-I) or under pure shear action (mode-II) or a combination of the two (mixed mode I-II). It has been reported that mode I-II is more commonly faced than the other two. How successfully this technique could be applied depends both on the properties of rock formation as well as on other factors such as the confining pressure, reservoir temperature, etc. The rock fracturing or fragmentation is studied by its fracture toughness which is a measure of the ease or difficulty of creating fractures. A usual way to study this problem is by conducting laboratory tests on the specimens from the field and obtaining results which can not only be a good data base for the whole formation, but can also be used in various fracture modeling tools. It has been reported that the fracture behavior of rocks in deep-seated formations, in addition to other factors, is very sensitive to the fracture toughness value of that rock material.

In the context to the applications of fracture toughness study to reservoir formation, two limitations come into picture. Firstly, the rock specimens from the deep-seated formations are not only very costly to obtain but their quality, sometimes, is also questionable. Secondly, the specimens can only be obtained in the form of cylindrical cores. Fortunately, the mathematical tools are available which, with the help of experimental results, can reasonably solve the fracture toughness behavior using centrally notched circular disk shape specimens called "Brazilian Disk". The problem of specimen quality could be partially solved by securing samples from the outcrop from the same geologic formation. Of course, reservoir conditions of

temperature and confining pressure should be incorporated to better understand the fracture toughness behavior of a deep-seated rock formation.

To study the fracture toughness of Khuff formation, reservoir as well as outcrop specimens from this formation were collected. Both outcrop and reservoir specimens were tested at ambient and simulated reservoir conditions of temperature and pressure to investigate if the outcrop specimens could be used to study the fracture toughness behavior of the reservoir rocks. The specimens were tested both under mode-I and mixed mode I-II loading conditions. The effective reservoir confining pressure of 28 MPa and a temperature of 116 ^{0}C were used to simulate the field conditions. The conclusions based on the lab-scaled results are presented in the following section.

6 .2 Conclusions

Based on the previously documented experimental work and the results obtained therefrom, following conclusions can be made.

1) Fracture toughness does not seem to be significantly effected by strain rate in the range of 0.005 to 0.1 mm/min. A strain rate of 0.1 mm/min is recommended as an upper limit for fracture toughness study. Strain rates higher than this limit are thought to cause rock specimen failure in a short interval of time and a representative load-deformation response may not be obtained in that case.
2) Both the notched Brazilian disk in diametrical compression and notched circular rod under three point bend resulted in a minimum crack length of 10 mm for valid

mode-I fracture toughness study. It can be concluded from the results that the minimum crack length criterion as adopted from what was recommended originally for metals may not be applied to rocks. Other studies reported in the literature also support this conclusion.

3) Keeping all the geometrical features (i.e., diameter, thickness, notch length) of the specimens same, mixed mode I-II fracture toughness results based on semicircular specimens are not comparable to Brazilian disk specimens. However, for pure mode-I fracture toughness study, semicircular specimens could be a better candidate.

4) Despite the fact that the fracture toughness value of the outcrop and the reservoir specimens was significantly different at ambient conditions, the values under confining pressure were very well matching. It is therefore concluded that the behavior of the reservoir specimens could be successively modeled by the outcrop specimens under simulated reservoir conditions.

5) Theoretically, the crack closure is predicted for the crack inclinations of around 21 to 30 degrees, but the measured crack opening suggests that the crack closure becomes significant only after a crack inclination of about 45 degrees.

6) The crack opening measurements revealed that the crack closure for the semicircular disk specimens is difficult to achieve even for a crack inclination of as high as 60 degrees.

7) The crack propagation in a notched Brazilian disk is best predicted by the maximum stress (σ_{max}) criterion

8) In the notched Brazilian disk specimens, the cracks initiated from the crack tip except for the specimens tested at a crack inclination of 75 degrees.

9) The crack initiation is independent of both the specimen origin and testing conditions. Although some specimens tested at higher inclination angles under confining pressure have showed some discrepancy, their behavior can not be generalized.

10) The trajectory of crack propagation seems to be independent of the testing environment.

11) The effect of temperature on the fracture toughness is negligible compared to that of the confining pressure.

6 .3 Recommendations

1) To better simulate the *in-situ* conditions, both the temperature and pressure should be incorporated simultaneously.

2) Some researchers have tried to compare the results based on different testing and loading configurations. Since the fracture toughness is dependent on both the material and the test conditions, it is recommended to conduct a comprehensive fracture toughness testing program on a synthetic rock for comparison and standardization purposes. This will help in establishing the guidelines for practical applications.

3) Minimum crack length requirements for valid fracture toughness testing seems to be dependent on material rather than the testing technique. However, further study is recommended to better understand this behavior.

4) Mixed mode I-II fracture toughness results seem to be dependent on the specimen diameter. Although larger specimens give values which are safer to be considered for practical purposes, an upper bound to the specimens size for which fracture toughness is constant, should be investigated however.

Nomenclature

θ	Crack initiation angle (degrees)with respect to crack original plane
ν	Poisson's ratio
σ_β	Tangential stress at the crack tip at an angle β from loading direction
σ_θ	Tangential stress at an angle θ from the crack tip
$\sigma_{\theta max}$	maximum tangential stress failure criterion
σ_r	Radial stress at an angle θ from the crack tip
$\sigma_{r\beta}$	Radial shear stress at the crack tip at an angle β from loading direction
$\sigma_{r\theta}$	Radial shear stress at an angle θ from the crack tip
σ_t	Tensile strength
2S	Support span for semicircular specimen
a	Notch length
β	Crack inclination angle (degrees)with respect to the loading direction
CCNBD	Cracked Chevron Notched Brazilian Disk
CSTBD	Cracked Straight Through Brazilian Disk
D	Diameter of the specimen
FPZ	Fracture Process Zone
G	Shear modulus
G_{max}	Maximum energy release rate
K_I	Mode-I stress intensity factor

K_{IC}	Pure mode-I stress intensity factor
K_{II}	Mode-0II stress intensity factor
K_{IIC}	Pure mode-II stress intensity factor
K_{III}	Mode-III stress intensity factor
LEFM	Linear Elastic Fracture Mechanics
N_I	Normalized mode-I stress intensity factor for notched Brazilian disk
N_{II}	Normalized Mode-II stress intensity farceur for notched Brazilian disk
P	Load at failure
R	Radius of the specimen
S	Support span for circular rod specimen
SEM	Scanning Electron Microscope
S_{min}	Minimum strain energy density
Y	Normalized stress intensity factor for semicircular specimen
Y'	Normalized stress intensity factor for circular rod specimen

References

Abou-Sayed, A. S. (1978), "An Experimental Technique for Measuring the Fracture Toughness of Rocks Under Downhole Stress Condition", *VDI-Berichte*, No. 13, pp. 819-824.

Andreev, G. E. (1995), "Brittle Failure of Rock Materials, Test Results and Constitutive Models", A. A. Balkema / Rotardam / Brookfiled, Netherland, pp. 149.

Ashmawi, N. M. (1990), *Fracture Modeling of Reinforced Beams in Mode-I Crack*, MS Thesis, King Fahd University of Petroleum & Minerals, Dhahran, Saudi Arabia.

Atkinson, C., Smelser, R. E. and Sanchez, J. (1982), "Combined Mode Fracture via the Cracked Brazilian Disk", *Intl. Journal of Fracture*, Vol. 18, pp. 279-291.

Awaji, H. and Sato, S. (1978), "Combined Mode Fracture Toughness Measurement by the Disk Test", *Journal of Engineering Materials and Technology*, Vol. 100, pp. 175-182.

Barker, L.M. (1977), "A Simplified Method for Measuring Plain-Strain Fracture Toughness", *Eng. Fract. Mech.*, Vol. 9, pp. 361-369.

Chong, K. P., Kuruppu, M. D. and Kuszmaul, J. S. (1987), "Fracture Toughness Determination of Layered Materials", *Eng. Frcat. Mech.*, Vol. 28, pp. 55-65.

Degiorgi, V. G., Matic, P., Baron, I., Lee, G. M. C. (1995), "An experimental and Computational Investigation of Crack Growth Initiation in Three Point Bend Fracture Specimens", *Eng. Fract. Mech.*, Vol. 50, pp. 1-9.

Erdogan, F. and Sih, G. C. (1963), "On the Crack Extension Path in Plates Under Plane Loading and Transverse Shear", *ASME J. Basic Eng.*, Vol. 85, pp. 519-527.

Fowell, R. J and Xu, C. (1994), "The Use of the Cracked Brazilian Disk Geometry for Rock Fracture Investigations", *Int. J. Rock Mechanics Min. Sci. & Geomech. Abstr.*, Vol. 31, No. 6, pp. 571-579.

Fowell, R. J. and Chen, J. F. (1990), "The Third Chevron Notch Rock Fracture Specimen- The Cracked Chevron-Notched Brazilian Disk", *Proc. 31st U.S. Symp. on Rock Mechanics*, pp.295-302.

Griffith, A. A. (1921), "The Phenomenon of Rupture and Flow in Solids", *Phill. Trans. R. Soc. London*, Series A, 221, pp. 163-198.

Guo, H., Aziz, N. I. and Schmidt, L. C. (1993), "Rock Fracture-toughness Determination by the Brazilian Test", *Engineering Geology*, Vol. 33, pp. 177-188.

Haberfield, C. M. and Johnston, I. W. (1990), "Determination of the Fracture Toughness of a Saturated Soft Rock", *Canadian Geotechnical Journal*, Vol. 27, pp. 276-284

Hefny, A. and Lo, K. Y. (1992), "The interpretation of Horizontal and Mixed Mode Fractures in Hydraulic Fracturing Tests in Rocks", *Can. Geotech. J.*, Vol. 29, pp. 902-917.

Huang, J. and Wang, S. (1985), "An Experimental Investigation Concerning the Comprehensive Fracture Toughness of Some Brittle Rocks", *Int. J. Rock Mech. Min. Sci. and Geomech. Abstr.*, Vol. 22, No. 2, pp. 99-104.

Hussain, M. A., Pu,. E. L. and Underwood, J. H. (1974), "Strain Energy Release Rate for a Crack Under Combined Mode-I and Mode-II", *ASTM STP* 560, pp. 2-28.

Ingraffea, A. R. (1981), "Mixed Mode Fracture Initiation in Indiana Limestone and Westerly Granite, *Proc. 22nd US Symp. on Rock Mechanics*, Cambridge, MA., pp. 186-191.

I.S.R.M (Co-ordinator: F. Ouchterlony). (1988), "Suggested Methods for Determining the Fracture Toughness of Rock", *Int. J. Rock Mech. Min. Sci. and Geomech. Abstr.*, Vol. 25, pp. 71-96.

Irwin, G. R. (1957), "Analysis of Stress and Strains Near the End of Crack Traversing a Plate", *Journal of Applied Mech.*, Vol. 24 Sept., pp 361-364.

Kanninen, M. F. and Popelar, C. H. (1985), *Advanced Fracture Mechanics*, Oxford Engineering Science Series, Vol.15, Oxford University Press, New York.

Kenner, V. H., Advani, S. H., and Richard, T. G. (1982), "A Study of Fracture Toughness for an Anisotropic Shale.", *Proc. 23rd US Symp. on Rock Mech.*, The University of California, Berkeley, California, R.E. Goodman & F.E Heuez, (Eds.), pp 471-479.

Kobayashi, R., Matsuki, N. and Otsuka, N. (1986), "Size Effect in the Fracture Toughness of Ogino Tuff", *Int. J. Rock Mech. Min. Sci & Geomech. Abstr.*, Vol. 23, No. 1, pp. 13-18.

Laqueche, H., Rousseau, A. and Valentin, G. (1986), "Crack Propagation Under Mode-I and II Loading in Slate Schist", *Int. J. Rock Mech. Min. Sci. & Geomech. Abstr.*, Vol. 23, No. 5, pp. 347-354.

Lim, I. L., Johnston, I. W. and Choi, S. K. (1993), "Stress Intensity Factors For Semicircular Specimens Under Three-Point Bending", *Eng. Fract. Mech.*, Vol. 44, No. 3, pp. 363-382.

Lim, I. L., Johnston, I. W. and Choi, S. K. (1994-a), "Assessment of Mixed Mode Fracture Toughness Testing Methods for Rock." *Int. J. Rock Mech. Min. Sci. & Geomech. Abstr.*, Vol. 31, No. 3, pp. 265-272.

Lim, I. L., Johnston, I. W., Choi, S. K. and Boland, J. N. (1994-b), "Fracture Testing of a Soft Rock with Semicircular Specimens Under Three Point Bending-Part 1", *Int. J.Rock Mech. Min. Sci & Geomech. Abstr.*, Vol. 31, No. 3, pp. 185-197.

Lim, I. L., Johnston, I. W., Choi, S.K and Boland, J. N. (1994-c), "Fracture Testing of a Soft Rock with Semicircular Specimens Under Three Point Bending-Part 2 Mixed Mode", *Int. J .Rock Mech. Min. Sci & Geomech. Abstr.*, Vol. 31, No. 3, pp. 199-212.

Lubtz, J. F., Shah, S. P. and Dowding, C. H. (1987), "The Fracture Process Zone in Granites: Evidence and Effects", *Int. J. Rock Mech. Min. Sci. & Geomech. Abstr.*, Vol. 24, pp. 235-246.

Matsuki, K., Nozuyama, Y. and Takahashi, H. (1988), "Size Effect in Fracture Testing of Rocks Using a Boring Core", *Proc., Spring Meeting*, Mining and Metallurgical Institute, Japan, pp. 193-194.

Muller, W. (1986), "Brittle Crack Growth in Rock", *PAGEOPH*, Vol. 124, No.4/5, pp. 694-709.

Orowan, E. (1952), "Fatigue and Fracture of Metals", *Proc. of 1950 Conf. at M.I.T.*, John Wiley, N.Y., 139.

Ouchterlony, F. (1981), "Extension of Compliance and Stress Intensity Formulas for the Single Edge Cracked Round Bar in Bending", *ASTM STP 745*, pp. 237-256.

Sanchez, J. (1979), *Application of the Disk Test to Mode-I-II Fracture Toughness Analysis,* M.S Thesis, Engineering Department, University of Pittsburgh, Pittsburgh, U.S.A

Schmidt, R. A. (1976), "Fracture-toughness Testing of Limestone", *Exp. Mech.*, Vol. 16, pp. 161-167.

Schmidt, R. A. and Huddle, C. W. (1977), "Effect of Confining Pressure on Fracture Toughness of Indiana Limestone", *Int. J. Rock Mech. Min. Sci & Geomech. Abstr.*, Vol. 14, pp. 289-293.

Schmidt, R. A. and Lutz, T. J. (1979), "K_{IC} and J_{IC} of Westerly Granite - Effects of Thickness and In-Plane Dimensions", *ASTM STP* 678, pp. 166-182.

Schmidt, R.A. (1980), "A Micorcrack model and its Significance to Hydraulic Fracturing and Fracture Toughness Testing", *Pro. 21st US symp. On Rock Mech.*, pp. 581-590.

Shah, S. P. and Mcgarryy, F. J. (1971), "Griffith Fracture Criterion and Concrete", *Journal of the Eng. Mech. Division*, ASCE Proceedings, Vol. 97, pp 1663-1676.

Shetty, D. K. and Rosenfield, A. R. (1987), "Fracture Toughness of Ceramics Measured by a Chevron Notched Diametral Compression Brazilian Disk Test", *Eng. Fract. Mech.*, Vol. 26, pp. 825-840.

Shetty, D. K. and Rosenfield, A. R. (1985), "Fracture Toughness of Ceramics Measured by a Chevron-Notch Diametral-Compression Test", *J. Am. Ceram. Soc.*, Vol. 65, No.11, pp. 566-572.

Shlyapobersky, J. (1985), "Energy Analysis of Hydraulic Fracturing", *Proc. 26th U.S. Symp. On Rock Mech.*, Rapid City SD, pp. 539-548.

Sih, G. C. and Cha, B. C. K. (1974), "A Fracture Criteria for Three Dimensional Problems", *Eng. Fract. Mech.*, Vol. 6, pp. 699-723.

Sih, G. C. (1974), "Strain Energy Density Factor Applied to Mixed Mode Crack Problems" *International Journal of Fracture*, Vol. 10, pp. 305-321.

Singh, D. and Shetty, D. K. (1989), "Fracture Toughness of Polycrystalline Ceramic in Combined Mode-I-II Loading", *Journal of American Ceramic Society*, Vol. 72, pp. 78-84.

Singh, R. N. and Pathan, A. G. (1988), "Fracture Toughness of Some British Rocks by Diametral Compression of Disks", *Min. Sci. Techn.*, Vol. 6, pp. 179-190.

Singh, R. N. and Sun, G. X. (1990), "A Numerical and Experimental Investigation for Determining Fracture Toughness of Welsh Limestone", *Min. Sci. Tech.*, Vol. 10, pp. 61-70.

Sun, Z.Q. (1983), *Fracture Mechanics and Tribology of Rocks and rock Joints*, PhD Thesis, Lulea University, Sweden.

Sun, G.X. (1990), *Application of Fracture Mechanics to Mine Design*, PhD Thesis, Dept. of Mining Engineering, University of Nottingham, England.

Thallak, S., Holder, J. and Gray, K. E. (1993), "The Pressure Dependence of Apparent Hydrofracture Toughness" *Int. J .Rock Mech. Min. Sci & Geomech. Abstr.*, Vol. 30, No. 7, pp. 831-835.

Thiercelin, M. and Rogiers, J .C. (1986), "Toughness Determination with the Modified Ring Test", *Proc. 27th U.S. Symp. on Rock Mechanics*, pp. 615-622.

Tirosh, J. and Catz, E. (1981), "Mixed Mode Fracture Angle and Fracture Locus of Materials Subjected to Compressive Loading", *Eng. Fract. Mech.*, Vol. 14, pp. 27-38.

Twiss, R. J. and Moores, E. M. (1992), *Structural Geology*, W.H Freeman and Company Publishers, New York.

Vasarhelyi, B. (1997), "Influence of Pressure on the Crack Propagation Under Mode-I Loading in Anisotropic Gneiss", *Rock Mech. and Rock Eng.*, Vol. 30, No. 1, pp. 59-64.

Yareman, S. Y. and Krestin, G. S. (1966), "Determination of the Modulus of Cohesion of Brittle Materials by Compression Testing of Disks with a Crack", *Soviet Material Science*, Vol. 2, pp. 10-14.

Whittaker, B. N., Singh, R. N. and Sun, G. (1992), "*Rock Fracture Mechanics; Principles, Design and Applications*", Developments in Geotechnical Engineering, Elsevier Publishers, Netherland.

Xediakis, G. S., Samaras, I.S., Zacharopoulos, D.A. and Papakaliatakis, G.E. (1997), "Trajectories of Unstably Growing Cracks in Mixed Mode I-II Loading of marble Beams", *Rock mechanics and Rock Engineering*, Vol. 30, No. 1, pp.19-33.

Yi, X. P. (1987), *Fracture toughness and Crack Growth in Short Rod Specimens of Rocks*, Licentia Thesis, Division of Rock Mechanics, Lulea University, Sweden.

Vita

- Khaqan Khan
- Born in Azad Kashmir, Pakistan
- Received Bachelor of Engineering Degree in Civil Engineering from N.E.D University of Engineering and Technology, Karachi, Pakistan in December, 1993.
- Worked as a Senior Instructor in Polytechnic Institute, Rawalakot (Azad Kashmir), Pakistan.
- Completed Master of Science Degree Requirements at King Fahd University of Petroleum and Minerals, Dhahran, Saudi Arabia in April 1998.

IMAGE EVALUATION
TEST TARGET (QA-3)

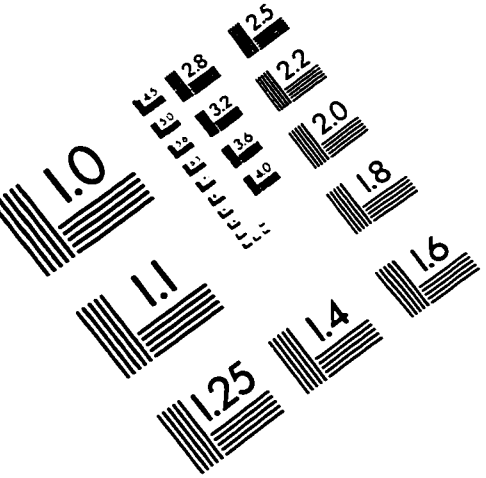

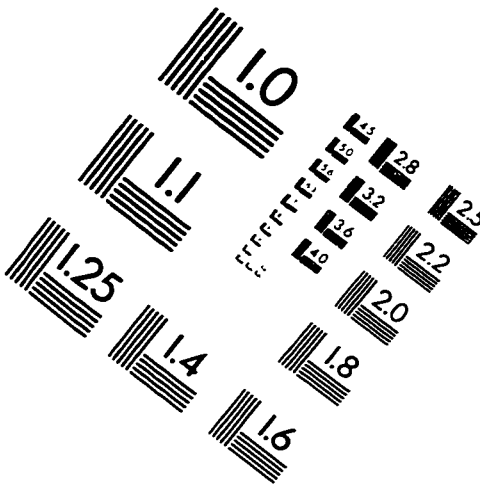

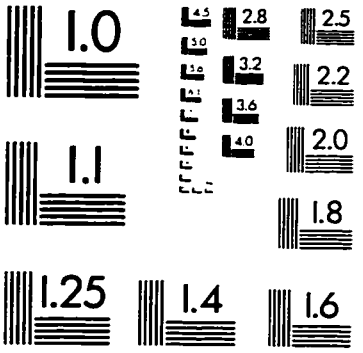

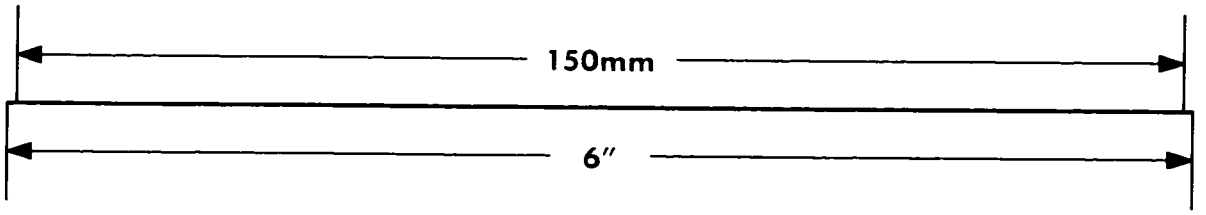

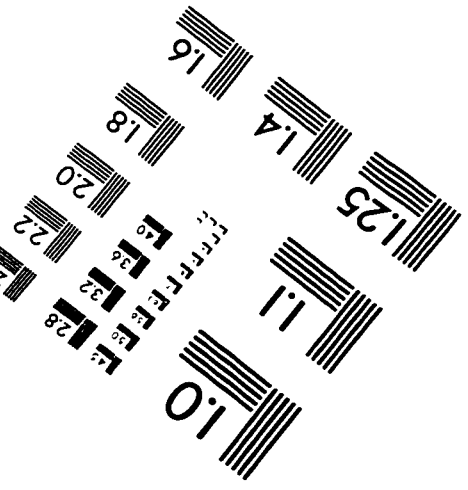

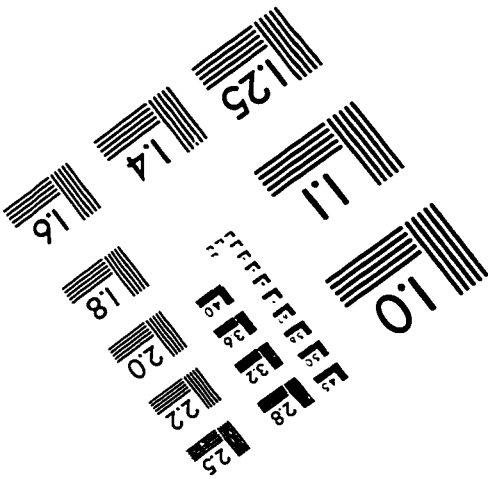

APPLIED IMAGE, Inc
1653 East Main Street
Rochester, NY 14609 USA
Phone: 716/482-0300
Fax: 716/288-5989